



**MARIA JORGE
PRATAS DE MELO
PINTO**

**FORMULAÇÃO DE BIODIESEL
BIODIESEL FUEL FORMULATION**

Tese apresentada à Universidade de Aveiro para cumprimento dos requisitos necessários à obtenção do grau de Doutor em Engenharia de Química, realizada sob a orientação científica do Professor Doutor João Manuel da Costa Araújo Pereira Coutinho, Professor Associado com Agregação do Departamento de Química da Universidade de Aveiro e Co-orientação de Doutora Sílvia Maria Carriço dos Santos Monteiro, Professora Adjunta do Departamento de Engenharia do Ambiente da Escola Superior de Tecnologia e Gestão, do Instituto Politécnico de Leiria.

Apoio financeiro do POCTI no âmbito do III Quadro Comunitário de Apoio. Co-financiamento do POPH/FSE.



O doutorando agradece o apoio financeiro da FCT no âmbito do III Quadro Comunitário de Apoio (SFRH/BD/28258/2006)



Aos amores da minha vida: Duarte e Ilídio.

o júri

presidente

Doutor Paulo Jorge de Melo Matias Faria de Vila Real
professor catedrático da Universidade de Aveiro

Doutor João Manuel da Costa e Araújo Pereira Coutinho
professor associado com agregação da Universidade de Aveiro

Doutor Luís Manuel das Neves Belchior Faia dos Santos
professor associado da Faculdade de Ciências da Universidade do Porto

Doutor Abel Gomes Martins Ferreira
professor auxiliar Faculdade de Ciências e Tecnologia da Universidade de Coimbra

Doutor Nelson Simões Oliveira
professor adjunto da Escola Superior de Tecnologia e Gestão do Instituto Politécnico de Leiria

Doutora Sílvia Maria Carriço dos Santos Monteiro
professora adjunta da Escola Superior de Tecnologia e Gestão do Instituto Politécnico de Leiria

Doutora Mariana Belo Oliveira
estagiária de pós doutoramento da Universidade de Aveiro

agradecimentos

Agradeço à Fundação para a Ciência e a Tecnologia a bolsa de doutoramento atribuída e os subsídios para participação em congressos, que permitiram o desenvolvimento deste trabalho.

O meu obrigada muito especial vai para o meu Orientador, João Coutinho, que ao longo destes anos me foi abrindo portas neste PATH da investigação... obrigada pelo apoio, pelo incentivo, pela disponibilidade e pelos conhecimentos transmitidos. Agradeço orgulhosamente pela oportunidade em trabalhar consigo neste maravilhoso grupo.

A Sílvia Monteiro, mais que Co-Orientadora, foi uma amiga muito próxima que eu ganhei. Obrigada por teres acreditado em mim, acreditado neste projeto e contribuído de forma tão activa para a escalada até ao cume desta montanha.

À Marina Reis da empresa Sovena, com que discuti pormenores técnicos que ajudaram a desatar certos nós deste trabalho, agradeço pela sua simpatia, amizade e disponibilidade para avaliar as minhas produções de biodiesel.

Bom, ao fim de 4 anos e meio de doutoramento, 2 anos e meio de mestrado, 1 ano de estágio curricular e 1 semestre de projeto, achava que já fazia parte da mobília... afinal fazia (e faço) parte de uma família chamada PATH que foi crescendo, crescendo... agradeço a herança que recebi do agora chamado "JurasicPATH"! Obrigada amigos, vão ficar sempre no meu coração: Tó Zé, Ana Dias, Ana Caço, Nuno, Nelson, Carla, Fatima.

Pessoalmente quero agradecer aos colegas que estiveram sempre presentes, com quem partilhei as alegrias e tristezas desta longa jornada: Mara, Pedro, Mariana, Sónia, Catarina, Rita, Rute, Marta, Luciana, Bernd, Jorge, Samuel, Ana Filipa, Catarina V., Mayra... em particular aos que acompanharam a minha gravidez com a proximidade de uma família...

Um agradecimento especial à Mariana e ao Samuel que guiaram este trabalho quando me ausentei para a maternidade. À Mariana também pela amizade, pela proximidade e pela cumplicidade.

Fica também uma palavra de gratidão aos alunos de mestrado e projecto que acompanhei ao longo destes anos: a Marise, o Ricardo, a Mi, a Vanda e o Rui, que contribuíram para o enriquecimento desta tese.

Agradeço ao Departamento de Química pela enriquecedora experiência de docência, e aos meus alunos pela forma que me motivaram, uns mais que outros, para fazer mais e melhor.

Agradeço também aos colegas da empresa EGEO Solventes, na pessoa do Eng. Vitor Leitão, que me receberam na equipa como se sempre dela tivesse feito parte. Obrigada por tudo, especialmente pela compreensão na fase final de preparação desta tese.

Neste agradecimento não posso deixar de fora a minha família e amigos, por estarem sempre por perto e por me apoiarem incondicionalmente. Em especial aos meus pais que me deram a possibilidade de chegar até aqui.

Um agradecimento sem tamanho mensurável vai para os meus segundos pais, obrigada por tudo, especialmente pela forma como cuidam do meu tesouro.

Aos amores da minha vida: Duarte e Ilídio, nem me atrevo a agradecer, serão sempre o meu porto de abrigo...

palavras-chave

Biodiesel, Propriedades Termodinâmicas, Densidade, Viscosidade, Modelação, Esteres Etilícos e Metílicos de Ácidos Gordos.

resumo

O consumo de energia a nível mundial aumenta a cada dia, de forma inversa aos recursos fósseis que decrescem de dia para dia. O sector dos transportes é o maior consumidor deste recurso. Face ao actual cenário urge encontrar uma solução renovável e sustentável que permita não só, diminuir a nossa dependência de combustíveis fósseis mas fundamentalmente promover a sua substituição por energias de fontes renováveis. O biodiesel apresenta-se na vanguarda das alternativas aos combustíveis derivados do petróleo, para o sector dos transportes, sendo considerado uma importante opção a curto prazo, uma vez que o seu preço pode ser competitivo com o diesel convencional, e para a sua utilização o motor de combustão não necessita de alterações. O biodiesel é uma mistura líquida, não tóxica, biodegradável de ésteres de ácidos gordos, sem teor de enxofre ou compostos aromáticos, apresenta boa lubrificidade, alto número de cetano, e origina emissões gasosas mais limpas.

O presente trabalho contribui para um melhor conhecimento da dependência das propriedades termofísicas do biodiesel com a sua composição. A publicação de novos dados permitirá o desenvolvimento de modelos mais fiáveis na previsão do comportamento do biodiesel.

As propriedades densidade e viscosidade são o espelho da composição do biodiesel, uma vez que dependem directamente da matéria prima que lhe deu origem, mais do que do processo de produção. Neste trabalho os dados medidos de densidade e viscosidade de biodiesel foram testados com vários modelos e inclusivamente foram propostos novos modelos ajustados para esta família de compostos. Os dados medidos abrangem uma ampla gama de temperaturas e no caso da densidade também foram medidos dados a alta pressão de biodiesel e de alguns ésteres metílico puros.

Neste trabalho também são apresentados dados experimentais para o equilíbrio de fases sólido-líquido de biodiesel e equilíbrio de fases líquido-líquido de alguns sistemas importantes para a produção de biodiesel. Ambos os tipos de equilíbrio foram descritos por modelos desenvolvidos no nosso laboratório.

Uma importância especial é dado aqui a propriedades que dependem do perfil de ácidos gordos da matéria-prima além de densidade e viscosidade; o índice de iodo e temperature limite de filtrabilidade são aqui avaliados com base nas considerações das normas.

Os ácidos gordos livres são um sub-produto de refinação de óleo alimentar, que são removidos na desodoração, no processo de purificação do óleo. A catálise enzimática é aqui abordada como alternativa para a conversão destes ácidos gordos livres em biodiesel. Estudou-se a capacidade da lipase da *Candida antarctica* (Novozym 435) para promover a esterificação de ácidos gordos livres com metanol ou etanol, utilizando metodologia de superfície de resposta com planeamento experimental. Avaliou-se a influência de diversas variáveis no rendimento da reacção.

keywords

Biodiesel Fuel, Thermodynamic Properties, Density, Viscosity, Modelling, Fatty Acid Ethyl and Methyl Esters.

abstract

World energy consumption rises every day and, inversely, fossil fuel resources are dwindling day by day. Transportation sector is the bigger consumer of oil. Faced with the actual scenario a renewable and sustainable alternative is needed, not just to decrease our dependence of petroleum but also to base our power in a renewable source. Biodiesel is at the forefront of the alternatives to petroleum based fuels in the transportation sector, being considered an important short-time option since its price can be competitive with conventional diesel and no motor changes are required. Biodiesel consists on a liquid blend of, non toxic, biodegradable fatty acid esters, with non sulfur and aromatic content, good lubricity, high cetane number, nontoxic character of their exhaust emissions and cleaner burning.

Aiming at tuning biodiesel to optimize the fuel composition, the present work contributes for a better knowledge of the dependence of thermophysical properties of biodiesel on their composition. New data is required to help in the development of reliable models to predict biodiesel behavior.

Density and viscosity data are a mirror of biodiesel composition, as both depend on the raw material, more than the production process. New data of density and viscosity were measured and respective models were tested and compared, and new adjusted parameters proposed for this family of compounds. The measured data include a wide range of temperatures and in the case of density data were also measured at high pressure for biodiesel and some pure methyl esters.

This work also reports experimental data for the solid-liquid-phase equilibria of biodiesel and, liquid-liquid equilibria of some important systems in biodiesel production. Both type of equilibria were described with models developed in our laboratory.

A special importance is here given to properties that depend on fatty acid profile of raw material besides density and viscosity; the iodine value, and cold filter plugging point are here evaluated based on norm considerations.

Free Fatty Acids (FFA) are a by-product in edible oil refining, that are removed in the deodorizing step on oil purification. Enzymatic catalysis is here studied as an alternative to convert this by-product into biodiesel. The ability of immobilized lipase from *Candida antarctica* (Novozym 435) to catalyze the esterification of FFA with methanol and ethanol were evaluated using response surface methodology with an experimental design. Influence of several variables were evaluated in the yield of reaction.

Index

GENERAL CONTEXT.....	1
Work Aims and Motivations	3
Document Organization.....	4
GENERAL INTRODUCTION	7
SECTION 1 THERMODYNAMIC PROPERTIES AND PHASE EQUILIBRIA	27
• CHAPTER 1 DENSITY AND VISCOSITY	33
Densities and Viscosities of Fatty Acid Methyl and Ethyl Esters	39
Densities and Viscosities of Minority Fatty Acid Methyl and Ethyl Esters Present in Biodiesel	63
Biodiesel Density: Experimental Measurements and Prediction Models	81
High-Pressure Biodiesel Density: Experimental Measurements, Correlation and CPA EoS Modeling	103
Evaluation of predictive models for the Viscosity of biodiesel.....	133
• CHAPTER 2 LOW TEMPERATURE BEHAVIOUR	157
Measurement and Modelling of Biodiesel Cold Flow Properties.....	161
• CHAPTER 3 BIODIESEL PROPERTIES VS COMPOSITION.....	183
Dependency of the Biodiesel Properties on its Composition	185

• CHAPTER 4 WATER SOLUBILITY IN BIODIESELS AND FATTY ACIDS	205
Description of the mutual solubilities of fatty acids and water with the CPA EoS.....	209
Another look at the water solubility in biodiesels: Further experimental measurements and prediction with the CPA EoS	239
SECTION 2 ENZYMATIC SYNTHESIS OF BIODIESEL	259
Enzymatic Biodiesel Production using Novozyme 435 as a catalyst	263
GENERAL CONCLUSIONS.....	289
IDEAS TO THE FUTURE	293
BIBLIOGRAPHY	295
APPENDIX A	301

General Context

With the depletion of oil resources as well as the negative environmental impact associated with the use of fossil fuels, there is a renewed interest in alternative energy sources. Since the world reserves of fossil fuels and raw materials are limited, active research interest has been focusing in nonpetroleum, renewable, and nonpolluting fuels. Biofuels are one of the most important alternative source of energy for the foreseeable future and can still form the basis of sustainable development in terms of socioeconomic and environmental concerns. Biodiesel appears to be a promising future energy sources.¹

Work Aims and Motivations

Biodiesel derived from oil crops is a potential renewable and carbon neutral alternative to petroleum fuels. Chemically, biodiesel is a monoalkyl ester of long chain fatty acids derived from renewable feed stock like vegetable oils and animal fats. It is obtained by the transesterification reaction between oil or fat and a monohydric alcohol in presence of a catalyst. Biodiesel has to fulfill quality standards which are compiled in the norm that specify minimum or maximum requirements and test methods to evaluate biodiesel quality. In Europe the biodiesel fuel standards are compiled in the norm CEN EN 14214, and in USA in the norm ASTM D6751. Some of these properties depend on the raw materials used on the biodiesel fuel production and as a consequence on the fatty acid esters profile of biodiesel fuel. Differences in chemical and physical properties among biodiesel fuels can be explained largely by the fuels' fatty acid content.

For technical reasons, political and economic production of biodiesel obeying the required quality standards cannot be made from one single oil but only from mixtures of oils. The main goal of this work is to develop relations between the oils composition and the final characteristics of the biodiesel which indicate the most appropriated formulation for a biodiesel fuel. Nevertheless, the environmental conditions can limit biodiesel utilization, as some specific norm parameters differ between regions and seasons (winter and summer).

This work was motivated by the lack of information on the thermophysical properties of biodiesel fuel and their dependency on the fuel composition. Unlike diesel fuels, biodiesels are composed by a limited number of compounds, which allows the study of the properties of each individual compound and the development of relationships between them and the fuel properties. It was thus necessary to study the thermophysical properties of the components of biodiesel, namely methyl and ethyl esters of long saturated and unsaturated alkyl chains (C8-C22). In this work the focus was on the densities and viscosities of the biodiesel fuels and their components. These properties were measured not just at temperatures set in the norms, but in a wide range of temperatures from 278K to 363K. Concerning the density the influence of pressure has been also studied.

Some biodiesel specifications involve biodiesel performances at low temperature, but there is little information about the low-temperature behavior of biodiesel fuels. To overcome this limitation, the liquid- and solid- phase composition as well as fractions at temperatures below the cloud point were studied.

Mutual solubilities of fatty acid with water and solubility of water in biodiesel were studied due to their importance in biodiesel production and purification. Measurements were done to help the development of models to describe the phase equilibria with water.

The possibility of using residual fatty acids, obtained in the process of deodorization of edible oils as raw material in fatty acid ester production was also studied. Given the limitations of both basic and acid catalysis on this process, enzymatic catalysis was attempted in this work using a commercial lipase from Novozymes.

Document Organization

During these last four years of investigation in Biodiesel Fuels several articles were produced and published in several international journals. Developed work will be presented through a collection of all produced papers. They are compiled in chapters according to their subjects and in the following order:

Section 1: Thermodynamic Properties and Phase Equilibria

Chapter 1 Density and viscosity

- 1.** Densities and Viscosities of Fatty Acid Methyl and Ethyl Esters.
- 2.** Densities and Viscosities of Fatty Acid Methyl and Ethyl Esters of Minority Components of Biodiesel.
- 3.** Biodiesel Density: Experimental Measurements and Prediction Models.
- 4.** High-Pressure Densities: Measuring and Modeling.
- 5.** Evaluation of predictive models for the viscosity of biodiesel.

Chapter 2 Low temperature behavior

- 6.** Measurements and Modelling of Biodiesel Cold Flow Properties.

Chapter 3 Biodiesel Properties vs Composition

- 7.** Influence of esters profile in biodiesel properties.

Chapter 4 Water solubility in biodiesels and fatty acids

- 8.** Description of the mutual solubilities of fatty acids and water with the CPA EoS
- 9.** Another look at the water solubility in biodiesels: Further experimental measurements and prediction with the CPA EoS.

Section 2: Enzymatic Synthesis of Biodiesel

- 10.** Enzymatic Biodiesel Fuel Production.

The bibliographic references of each paper are presented in the end of the respective paper; the general bibliography appears at the end of the document.

General Introduction

The world energy demand is on the rise. Worldwide energy consumption is projected to grow by 53 percent between 2008 and 2035, with much of the increase driven by strong economic growth in the developing nations especially China and India. In European Union (EU) energy consumption is expected to level out in future but world energy consumption will continue to grow due to global population growth and economic catching up as shown in Figure 1.¹

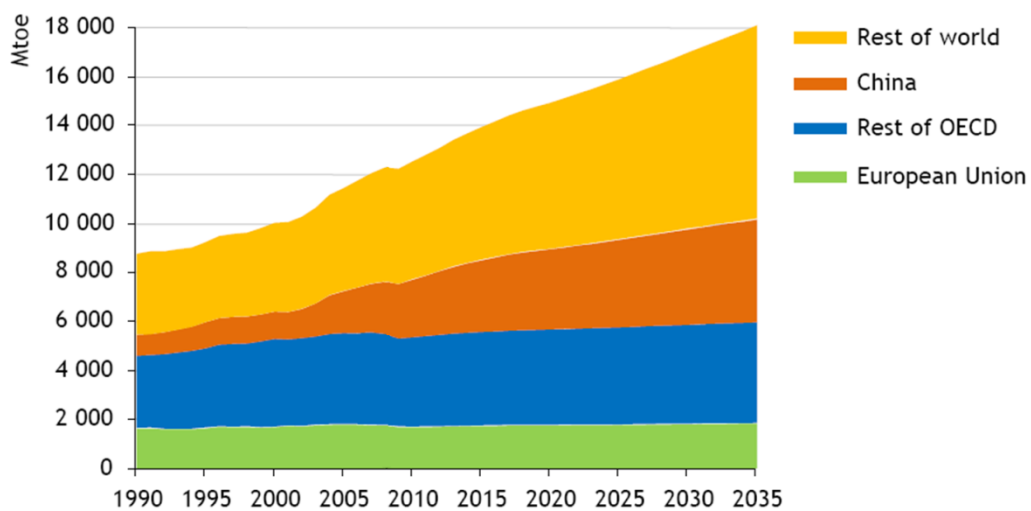


Figure 1- World energy demand.¹(Mtoe - Million tonnes of oil equivalent)

The EU energy mix is slowly changing. Fossil fuels still represent up to 80% of the energy mix today. In a “business as usual” scenario, the share may still be 70% by 2030, but renewable sources are expected to account for an increasing proportion (Figure2).^{2,3}

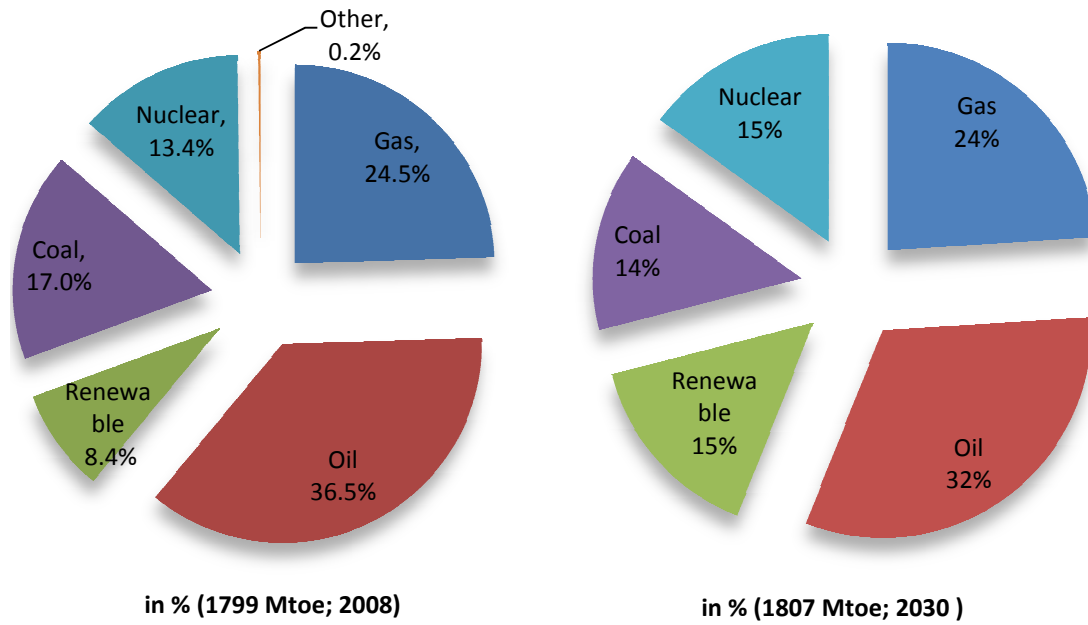


Figure 2- EU gross inland consumption in 2008 and a prediction for 2030.^{2,3}

Energy powers our society and economy. Transport and industry consume more than half of the total final energy in the EU, while a quarter of final energy is consumed by households (Figure 3).

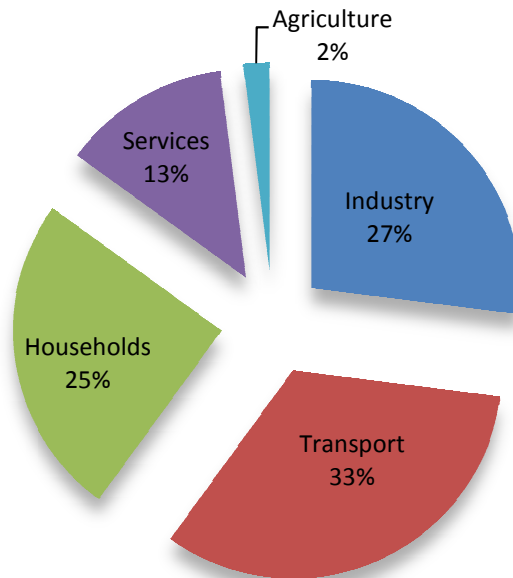


Figure 3- Final energy consumption in European Union, distributed by sectors (2008).²

The fossil fuel resources are dwindling day by day. Oil is becoming increasingly scarce and soon will not be able to meet the numerous demands, arising mainly from the transport sector. Decline of available oil reserves and more stringent environmental regulations have motivated the global interest in other energy sources. But there are other ways of fueling our cars??? That question has already been answered: *“The use of vegetable oils for engine fuels may seem insignificant today. But such oils may become in the course of time as important as the petroleum and coal tar products of the present time“*. This sentence could be pronounced today, but I am quoting Rudolf Diesel which had such a visionary idea in 1900. The concept of using alternative, renewable energy was demonstrated by the German engineer at World Exhibition in Paris, the first diesel engine using peanut oil as fuel. The engine was built for petroleum and was used with the vegetable oil without any change. In this case also, the consumption experiments resulted in heat utilization identical to petroleum.⁴

The extremely low cost of mineral oils and their abundant supply made research and development activities on vegetable oil not seriously pursued. These activities only received attention recently when it was realized that petroleum fuels were dwindling fast and environment-friendly renewable substitutes ought to be identified.

Faced with the energy crisis and environmental degradation, due to the massive use of fossil energy sources, biodiesel became an attractive alternative to diesel fuel.

In 2001, the European Commission adopted a policy to promote biofuels for transport, and a number of targets were set. The integrated energy and climate change strategy agreed at the end of 2008 foresees the share of renewable (such as biofuels) in total fuel consumption rising to at least 10 % by 2020, percentage in energy value.⁵

Biodiesel production has increased exponentially in the last decade; from worldwide negligible productions in 1990 its production reached over 2500 million tons in 2008 being biodiesel the most used biofuel in Europe.⁶

Biofuels are a renewable source of energy that may be described as 'carbon neutral' as shown in Figure 4.

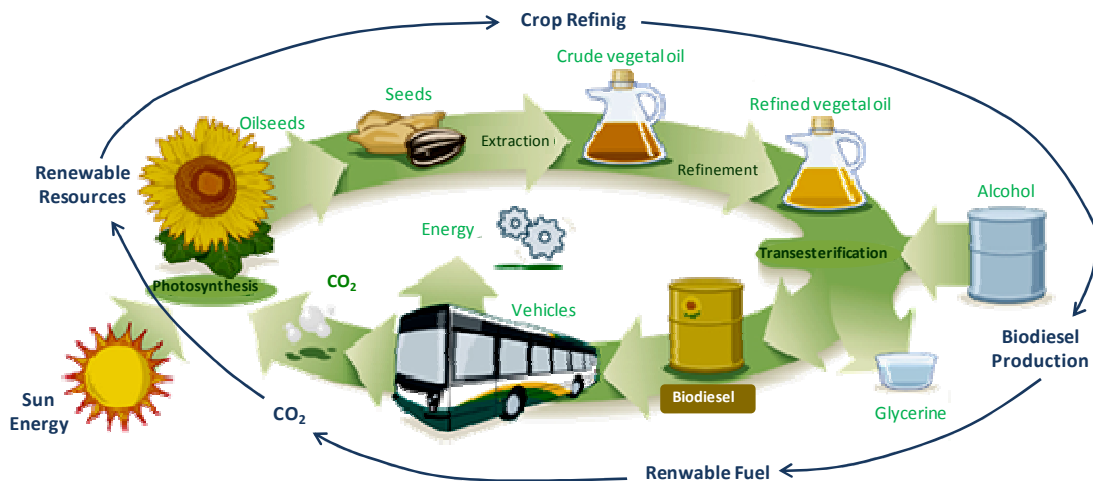


Figure 4- Biodiesel cycle.⁷

Biodiesel fuel is seen as an alternative to the conventional petroleum based fuels in the transportation sector, being considered as an important short-time option as its prices can be similar to petroleum based fuels and no motor changes are required, reducing the dependency on fossil fuels and controlling green house gases emissions.⁴ Biodiesel fuel advantages and applications are well established as described.^{4,8-14}

As a fuel it offers many benefits such as ready availability, portability, renewability, domestic origin, lower sulfur and aromatic content, biodegradability, better ignition quality, inherent lubricity, higher cetane number, positive energy balance, higher density, greater safety, nontoxic character of their exhaust emissions and cleaner burning.¹⁵⁻¹⁸

Gasoline and diesel come in the category of non-renewable fuel and will last for a limited period of time. Another important point is that carbon contained in the fossil fuel deposits was removed from the atmosphere millions of years ago and has been locked up within Earth's crust ever since. When this fossil carbon is put back into the atmosphere as a result of burning fossil fuels, it represents a new input of carbon into the modern atmosphere. These non-renewable fuels also emit pollutants in the form of oxides of nitrogen, oxides of sulphur, carbon dioxide, carbon monoxide, lead, hydrocarbons, etc. during their processing and use.¹⁹ Table 1 presents a brief description of advantages and disadvantages of the use of biodiesel fuels.

Table 1- Advantages and disadvantages of biodiesel fuels. ^{4, 11, 19-20}

Advantages	Disadvantages
◆Mitigation of greenhouse gas emissions, considered carbon neutral.	◆Biodiesel gels in cold weather, problems at low temperatures
◆Renewable, biodegradable, non toxic	◆Higher NOx Emissions
◆Reduce CO, hydrocarbons and particles in exhaust emission; do not contain Sulfur (reduction of air pollution and related public health risks)	◆Competition between food and Biodiesel, food shortages and increased food price
◆Higher cetane number than standard diesel	◆Lower calorific power than standard diesel
◆Easily blended with standard diesel	◆Biodiesel has around 11% less energy content compared to standard petroleum diesel
◆Higher lubricity	
◆Useable in standard diesel engines with little or no engine or fuel system modification (in contrast to other “eco-fuels” such as hydrogen)	◆Affect biodiversity as countries will sacrifice their rainforests to build more oil plantations (non-sustainable biofuel production)
◆Safer to handle and store due to higher flash point than petro-diesel	◆Susceptible to water contamination and bacteriological growth
◆Reduce dependence on foreign petroleum, improve energy security and energy independence, benefiting “domestic” economy	◆Biodiesel degrades the rubber seals in engines previous than 1996

Having on view the various pro’s and con’s presented in Table 1, no wonder the number of studies related to biodiesel has grown exponentially in recent years, as shown in the Figure 5.

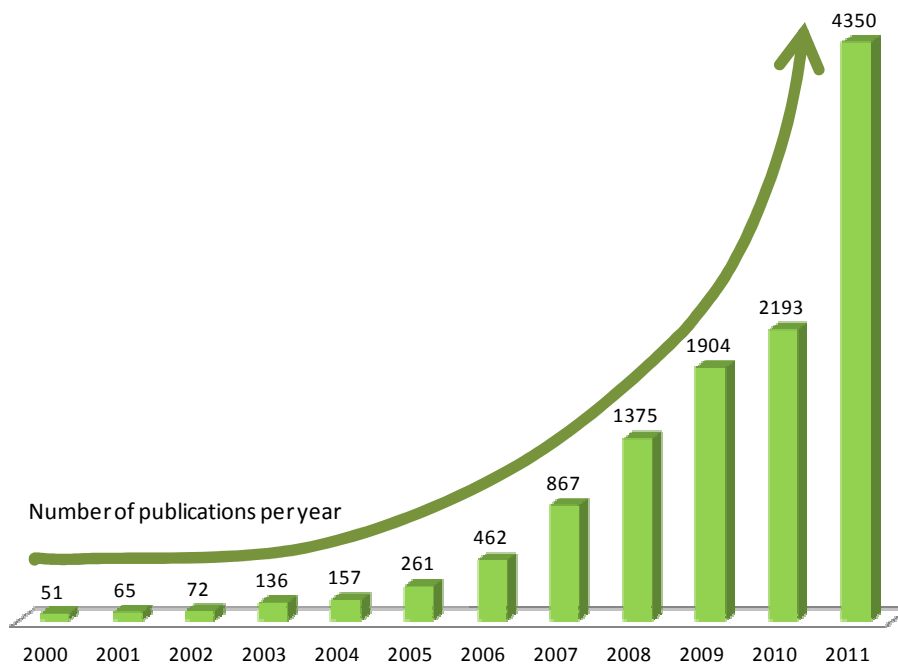


Figure 5- Exponential increase of publication number per year since 2000 related to “biodiesel” theme (based on a search in ISI Web of Knowledge with papers, abstracts and patents included).

Biodiesel refers to the pure fuel before blending with neat diesel fuel, namely B100. Biodiesel blends are denoted as “BXX” with “XX” representing the percentage of biodiesel contained in the blend e.g., B20 is 20% of biodiesel, 80% of petroleum diesel.

Use of biodiesel can greatly benefit the environment by reducing emissions. Using biodiesel instead of conventional diesel reduces emissions such as the overall life cycle of carbon dioxide (CO₂) emissions, particulate matter, carbon monoxide, sulfur oxides (SO_x), volatile organic compounds (VOCs), and unburned hydrocarbons. However, while reducing the aforementioned types of emissions, nitrogen oxides (NO_x) emissions, mostly NO and NO₂, are increased. NO_x is formed at high temperature in the combustion chamber when oxygen and nitrogen combination occurs. This type of NO_x is generally formed during fuel combustion such as gas or diesel. Nevertheless the combustion of biodiesel needs more energy (as oxygen represents in mass 11% of biodiesel) and consequently higher temperatures that promote the increase of NO_x.²¹

Figure 6 shows the impact that biodiesel-diesel blends have on emissions. Photography was taken one minute after start the light, as 4 minutes late in diesel lamp it was impossible to see the flame.

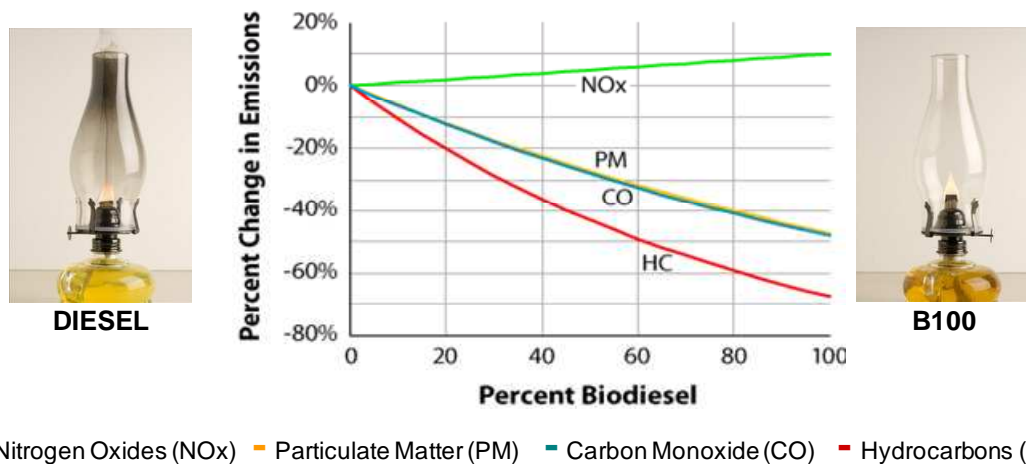


Figure 6- Variation in emissions when substitutes diesel fuel by biodiesel.²¹

As already mentioned chemically the biodiesel is a fuel comprised of mono-alkyl esters of long chain fatty acids derived from vegetable oils, animal fats, or mixtures of them. It is usually produced by the transesterification reaction of triglycerides with a short chain alcohol, generally methanol or ethanol, in presence of a catalyst, leading to the formation of mixtures of fatty acid methyl esters (FAMES) or fatty acid ethyl esters (FAEEs) respectively.^{4, 14} The stoichiometry requires 3 mol of alcohol and 1 mol of triglyceride to give 3 mol of fatty acid esters and 1 mol of glycerine, as shown in Figure 7, where R₁, R₂ and R₃ are alkyl chains derived from fatty acids, which most common are presented in Table 2, R₄ is the alcohol alkyl chain.^{19 22 23}

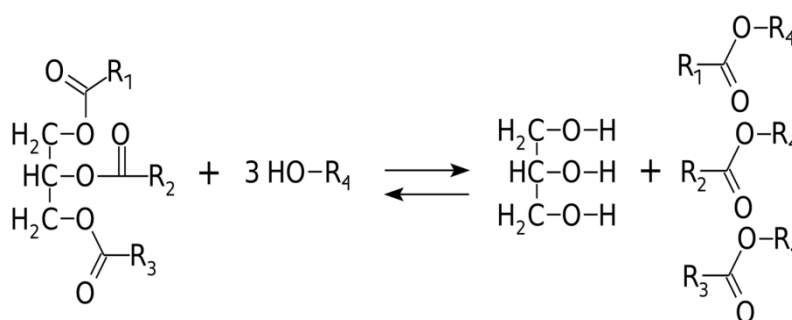


Figure 7- Transesterification reaction for biodiesel production.

The transesterification reaction consists of a sequence of reversible reactions that occurs in three different steps, in the presence of an alcohol (A). In the first step, triglycerides (TG) are converted to diglycerides (DG) which get converted to

monoglycerides (MG) in the next step. In the third and last step monoglycerides are converted to glycerol (G). A mole of esters is liberated at each step, normally namely fatty acid methyl esters (FAME). Thus three FAMEs are obtained from one triglycerides molecule.¹⁹ Equation [1] to [3] summarizes the reaction of transesterification.



where k_1 to k_6 are the constant rate involved in the kinetics of reactions in biodiesel development. The reactions are reversible, although the equilibrium lies towards the production of fatty acid esters and glycerol. Figure 8 shows the concentration profiles of all components until equilibrium is reached, based in reactions described.

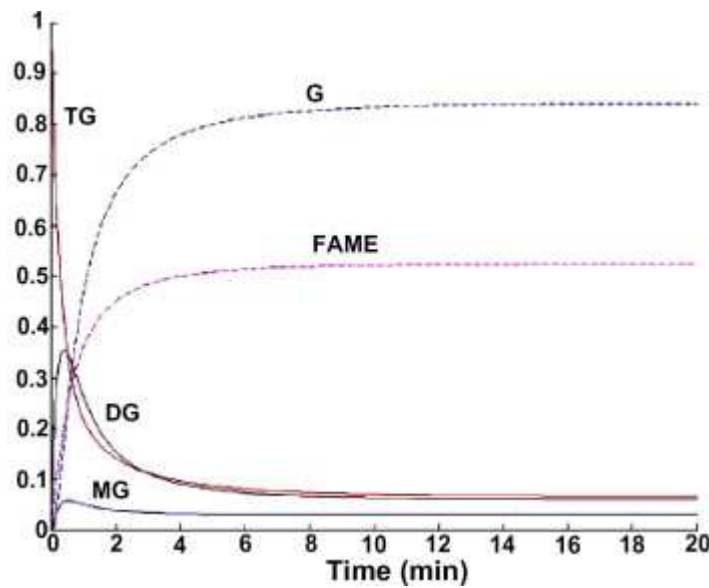


Figure 8- Simulated concentration profile of glycerol (G), tri-glyceride (TG), di-glyceride (DG), mono-glyceride (MG) and fatty acid methyl ester (FAME) during transesterification.¹⁹

The transesterification can be performed using alkaline, acid, or enzymatic catalysts. At industrial scale alkaline catalysis reaction is worldwide used; while acid and

enzymatic catalysis have little or no expression. The acid catalysis is slower and requires higher temperatures; while the enzymatic catalysis suffers from the enzymes being too expensive.²⁴

There are also two noncatalyzed transesterification processes, namely BIOX process and supercritical alcohol process. The BIOX process developed in Canada uses inert co-solvents that generate an oil-rich one-phase system and with 99% of yield in seconds at ambient temperature.²⁵ The supercritical methanol reacts with the oil as a single phase reaction, the process involves much simpler purification of products, has lower reaction time.²⁶

In alkaline catalysis of biodiesel several factors affect the transesterification reaction as the type of catalyst, the alcohol/oil molar ratio, temperature, the reagents purity, the amount of free fatty acids, the alcohol used and the mixing, as this is a two phase reaction.^{23,27}

Methanol is the preferred alcohol due to its low cost, physical and chemical advantages in the process.²³ Nevertheless, ethanol can prevail in regions where it is less expensive than methanol, due to its easier production and accessibility²⁸, and higher chain alcohols have as well been suggested.^{29,30} Moreover, the process is easy to control and biodiesel purification easier with methanol than with heavier alcohols.³¹ An excess of alcohol is necessary in order to displace the transesterification reaction towards product creation.²³ After the reaction is complete, two major products form: glycerin and biodiesel. The glycerin phase is denser than the biodiesel phase and the two can be gravity separated.

The basic catalyst is typically sodium hydroxide or potassium hydroxide. As alkali-catalyzed systems are very sensitive to both water and free fatty acid (FFA) content, the glycerides and alcohol must be substantially anhydrous because the water promotes a secondary reaction, saponification, which produces soaps, thus consuming the catalyst and reducing the catalyst efficiency, as well as causing an increase in viscosity, and difficulty in separations.²³ Figure 9 shows a flow chart of alkaline catalysis of biodiesel.

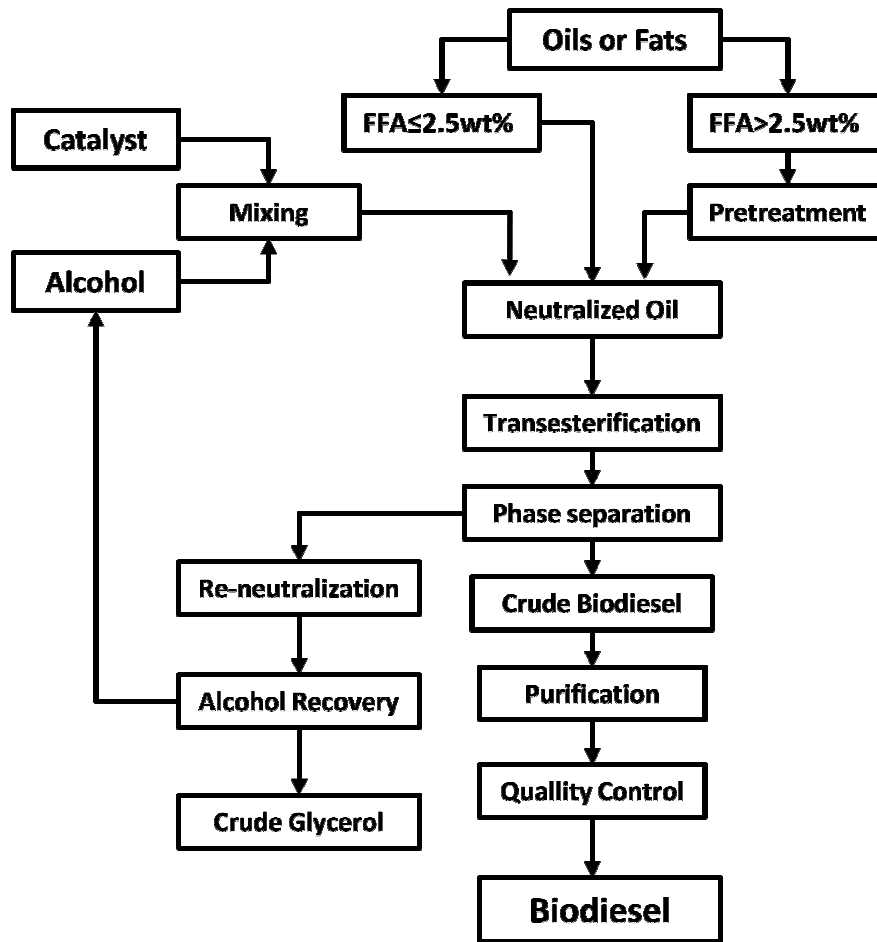


Figure 9 – Flow chart of biodiesel alkaline transesterification.³²

The typical industrial biodiesel production and purification process is sketched in Figure 10 and can be described as follows: the reaction takes place in a multiphase reactor where an oil reacts with an alcohol, in presence of an alkaline catalyst, to form fatty acid esters and glycerol.³³ The glycerol formed separates from the oil phase and at the outlet of the reactor two liquid phases co-exist: one rich in glycerol and the other in fatty acid esters. The unreacted alcohol is distributed between these two liquid phases²³ (Figure 10 (1)). After the reactor, the glycerol rich phase is sent to the alcohol recovery section where it is recovered by distillation and recycled into the reactor of the transesterification section. The glycerol-rich stream coming from the distillation process is then evaporated to decrease its water content and to meet the specifications for sale in the glycerol market (Figure 10 (2)). The fatty acid ester stream leaving the transesterification reactor is washed with acidified water to neutralize the catalyst and to convert any existing soaps into free fatty acids. The raffinate current is composed of water saturated biodiesel while the extract is a low pH aqueous solution containing the

polar compounds. The washed methyl ester product is finally dried to reduce the water content to an acceptable value by the biodiesel required standards (Figure 10 (3)).

The removal of excess alcohol from the fatty acid ester stream leaving the transesterification reactor can be performed by flash evaporation or distillation.^{23,33} Distillation is the most used method and the recovered alcohol is re-used in the transesterification process.

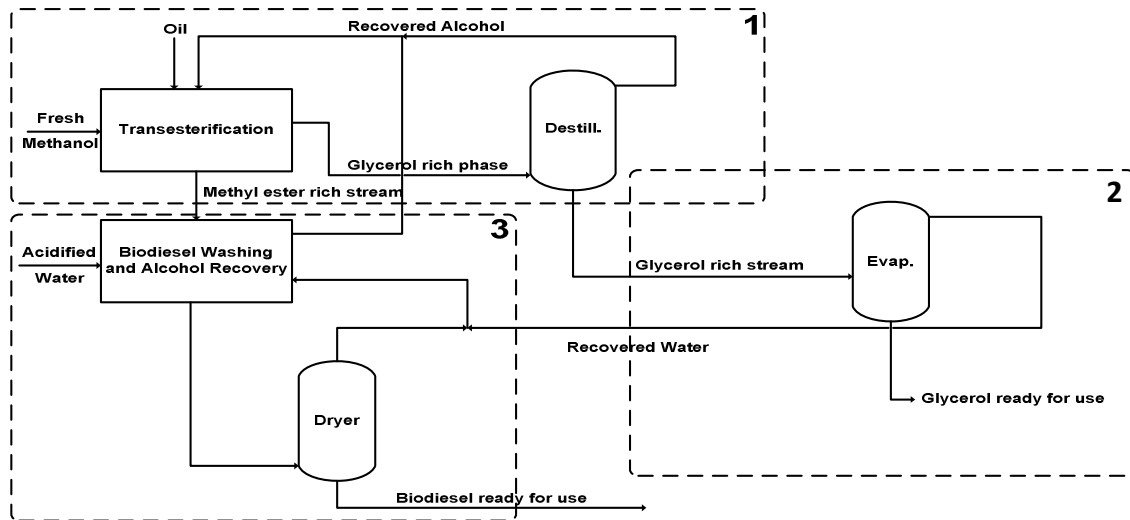
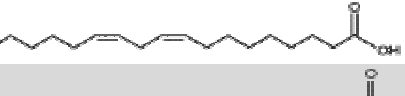
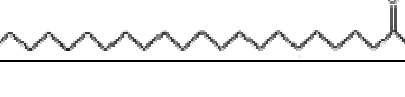


Figure 10. Simplified flow sheet of an industrial biodiesel production and purification process.³⁴

The main components of biodiesel fuel are palmitate, stearate, oleate and linoleate esters.³⁵ However, and depending on the raw materials used, a larger range of esters can be present.³⁶ Table 2 resumes names, CAS n°, and molecular information about corresponding fatty acid presents in vegetal oils.

Table 2- Structure of corresponding fatty acid present in vegetal oils.²⁰

Common Name	Formal Name	CAS. No.	Abbreviation	Molecular Formula	Molecular Weight	Molecular Structure *
Lauric acid	Dodecanoic acid	143-07-7	12:0	C ₁₂ H ₂₄ O ₂	200.32	
Myristic acid	Tetradecanoic acid	544-63-8	14:0	C ₁₄ H ₂₈ O ₂	228.38	
Myristoleic acid	<i>cis</i> -9-Tetradecenoic acid	544-64-9	14:1	C ₁₄ H ₂₆ O ₂	226.26	
Palmitic acid	Hexadecanoic acid	57-10-3	16:0	C ₁₆ H ₃₂ O ₂	256.43	
Palmitoleic acid	<i>cis</i> -9-Hexadecanoic acid	373-49-9	16:1	C ₁₆ H ₃₀ O ₂	254.42	
Stearic acid	Octadecanoic acid	57-11-4	18:0	C ₁₈ H ₃₆ O ₂	284.48	
Oleic acid	<i>cis</i> -9-Octadecenoic acid	112-80-1	18:1	C ₁₈ H ₃₄ O ₂	282.47	
Linoleic acid	<i>cis</i> -9,12-Octadecadienoic acid	60-33-3	18:2	C ₁₈ H ₃₂ O ₂	280.46	
Linolenic acid	<i>cis</i> -9,12,15-Octadecatrienoic acid	463-40-1	18:3	C ₁₈ H ₃₀ O ₂	278.44	
Arachidic acid	Eicosanoic acid	506-30-9	20:0	C ₂₀ H ₄₀ O ₂	312.54	
Gondoic acid	<i>cis</i> -11-Eicosenoic acid	5561-99-9	20:1	C ₂₀ H ₃₈ O ₂	310.53	
Behenic acid	Docosanoic acid	112-85-6	22:0	C ₂₂ H ₄₄ O ₂	340.6	
Erucic acid	<i>cis</i> -13-Docosenoic acid	112-86-7	22:1	C ₂₂ H ₄₂ O ₂	338.58	
Lignoceric acid	Tetracosanoic acid	557-59-5	24:0	C ₂₄ H ₄₈ O ₂	368.63	

*molecules with unsaturation(s) presents a non linear structure

Table 3 presents the normal mean composition of common vegetal oils used in biodiesel production.

Table 3 – Major fatty acids in some of the main oils and fats used for biodiesel production.²⁰

Fatty Acid	Camelina	Canola	Coconut	Corn	Jatropha	Palm	Rapeseed	Safflower	Soy	Sunflower	Tallow	Yellow Grease														
Common Name	Abbrev.	mean	dev	mean	Dev	mean	Dev	mean	Dev	mean	Dev	mean	Dev	mean	Dev	mean	Dev	mean	Dev	mean	Dev	mean	Dev			
Capriotic	6:0				0.6	0.3																				
Caprylic	8:0				6.8	1.9																		0.1		
Capric	10:0			0.1		5.4	1.1																	0.1		
Lauric	12:0	0.4				47.7	5.4				0.1	0.2	0.3	0.3	0.1	0.1		0.1	0.2	0.1	0.3	0.2	0.1	0.2	0.6	
Tridecyllic	13:0																									
Myristic	14:0	2.7	3.6			18.5	1.3				0.3	0.5	1.1	0.5	0.0	0.0	0.1	0.1	0.1	0.2	0.1	0.1	2.6	0.7	0.8	0.6
Myristoleic	14:1																						0.3	0.2		
Pentadanoic	15:0																						0.6	0.3	0.1	
Pentadecenoic	15:1																						0.1			
Palmitic	16:0	6.1	1.5	4.2	1.0	9.1	1.7	11.5	1.7	14.9	2.1	42.5	3.2	4.2	1.1	8.2	1.7	11.6	2.0	6.4	1.8	24.3	2.8	16.5	5.6	
Palmitoleic	16:1			0.3	0.3	0.1	0.2	0.2	0.2	1.0	0.5	0.2	0.1	0.1	0.1	0.1	0.1	0.2	0.3	0.1	0.1	2.6	1.0	0.9	1.1	
Hexadecadienoic	16:2																									
Hexadecatrienoic	16:3																									
Heptadecanoic	17:0			0.1						0.1		0.1		0.1				0.1	0.1	0.1		1.4	0.2	0.1	0.1	
Heptadecenoic	17:1			0.1			0.1															0.6	0.3	0.1		
Stearic	18:0	2.8	0.4	2.0	0.4	2.7	0.7	1.9	0.3	6.1	1.7	4.2	1.1	1.6	0.7	2.5	1.0	3.9	0.8	3.6	1.1	18.2	4.5	7.1	3.9	
Oleic	18:1	16.8	3.0	60.4	2.9	6.8	2.1	26.6	2.2	40.4	6.7	41.3	2.9	59.5	7.8	14.2	3.2	23.7	2.4	21.7	5.3	42.2	4.1	44.6	9.3	
Linoleic	18:2	17.0	2.3	21.2	1.8	2.1	1.4	58.7	2.8	36.2	6.1	9.5	1.8	21.5	2.8	74.3	8.3	53.8	3.5	66.3	7.6	4.4	2.9	25.1	10.3	
Linolenic	18:3	35.6	3.4	9.6	2.1	0.1	0.1	0.6	0.4	0.3	0.2	0.3	0.1	8.4	1.3	0.1	0.1	5.9	2.6	1.5	2.6	0.9	0.7	1.1	1.1	
Stearidonic	18:4																					0.4		0.5		
Arachidic	20:0	1.4	1.3	0.7	0.3	0.1	0.1	0.3	0.2	0.2	0.1	0.3	0.1	0.4	0.5	0.1	0.1	0.3	0.3	0.3	0.3	0.2	0.2	0.1	0.3	0.1
Gondoic	20:1	14.4	2.8	1.5	0.2	0.0		0.1		0.1		0.1	0.1	2.1	3.0			0.3	0.1	0.2	0.2	0.6	0.2	0.5	0.1	
Eicosadienic	20:2	1.5	0.2	0.1										0.1												
Eicosatrienoic	20:3	0.8																								
Eicosatetraenoic	20:4																									
Eicosapentaenoic	20:5																									
Behenic	22:0	0.9	0.6	0.3	0.1			0.1	0.1	0.2	0.1	0.1		0.3	0.3			0.3	0.2	0.6	0.4	0.1	0.1	0.4	0.2	
Erucic	22:1	3.1	0.8	0.5	0.2	0.0	0.0	0.1	0.1	0.1	0.1	0.0		0.5	0.5			0.1	0.1	0.1	0.1	0.1		0.1	0.1	
Docosatetraenoic	22:4					0.0																				
Docosapentaenoic	22:5																									
Docosahexaenoic	22:6																									
Lignoceric	24:0	0.7	0.5	0.2	0.1	0.0		0.1	0.1	2.6	3.5	0.1		0.1				0.1	0.1	0.2	0.2			0.2	0.2	
Nervonic	24:1	0.2		0.2		1.0				0.1				0.1	0.1			0.3	0.6					4.4		
Other/Unknown		1.0		2.2				0.3		1.2	1.1	0.9	0.9	4.3	4.4	0.8	0.8	4.1	4.7	0.1		2.0	1.2			
Total		104.1		101.2		101.1		100.2		102.7		101.2		99.9		99.5		100.8		101.2		100.0		103.1		
		Dominant species in FAME Composition											Other major species (>= 10%) in FAME composition													

The biodiesel fuel has to fulfill a number of quality standards. In Europe the biodiesel fuel standards are compiled in the norm CEN EN 14214³⁷, and in USA in the norm ASTM D6751³⁸. The norms specify the requirements and test methods for biodiesel fuel to be used in diesel engines, in order to increase the biodiesel fuel quality and its acceptance among consumers. Table 4 presents the European followed norm. American requirements are presented in Appendix A.

Table 4- CEN EN 14214:2003 requirements and test methods for biodiesels.³⁷

Property	Unit	Limits		Test method
		Minimum	Maximum	
Ester content	% (m/m)	96.5		EN 14103
Density @ 15°C	kg/m ³	860	900	EN ISO 3675 EN ISO 12185
Viscosity @ 40°C	mm ² /s	3.50	5.00	EN ISO 3104 ISO 3105
Flash point	°C	120		EN ISSO 3679
Sulfur content	mg/kg		10.0	EN ISSO 20846 EN ISSO 20884
Carbon residue (on 10% distillation residue)	% (m/m)		0.30	EN ISO 10370
Cetane number		51.0		EN ISO 5165
Sulphated ash content	% (m/m)		0.02	ISO 3987
Water content	mg/kg		500	EN ISO 12937
Total contamination	mg/kg		24	EN 12662
Copper strip corrosion (3hr at 50°C)	rating	CLASS 1	CLASS 1	EN ISO 2160
Oxidation stability, 110°C	hours	6.0		EN 14112
Acid value	mg KOH/g		0.50	EN 14104
Iodine value	g iodine/100g		120	EN 14111
Linolenic acid methyl ester	% (m/m)		12.0	EN 14103
Polyunsaturated (>= 4 double bonds) methyl esters	% (m/m)		1	
Methanol content	% (m/m)		0.20	EN 14110
Monoglyceride content	% (m/m)		0.80	EN 14105
Diglyceride content	% (m/m)		0.20	EN 14105
Triglyceride content	% (m/m)		0.20	EN 14105
Free glycerol	% (m/m)		0.02	EN 14105 EN 14106
Total glycerol	% (m/m)		0.25	EN 14105
Group I metals (Na ⁺ , K ⁺)	mg/kg		5.0	EN 14108 EN 14109
Group II metals (Ca ⁺ , Mg ⁺)	mg/kg		5.0	prEN14538
Phosphorus content	mg/kg		10.0	EN 14107
CFPP	°C	Grade A to F		EN 116

There are biodiesel properties that directly depend on the raw materials composition while others have more dependence on the production process. Knowing the profile fatty acid esters in biodiesel is of great importance as it controls some of its properties as described in Table 4.³⁶

Table 5 – Properties dependency raw materials or production process.^{4 39 40 41}

Property	Depend on		Obs.
	raw material	production process	
Ester content		+++	
Density @ 15°C	+++		
Viscosity @ 40°C	++	++	Presence of small quantity of contaminants increases viscosity
Flash point	++	+	Methanol residues decrease this parameter
Water content		+++	Promote hydrolysis reactions, corrosion problems and possibility of bacteriological growth
Oxidation stability, 110°C	++	++	Affects the stability of biodiesel during storage and distribution; additives are used to improve this parameter
Acid value	+	++	Promote corrosion in motors and increase speed of degradation
Iodine value	+++		Depend on unsaturation degree; promote polymerization and hydrolysis processes
Linolenic acid methyl ester	+++		Decrease oxidative stability and increase iodine value
Polyunsaturated >= 4 double bonds	+++		
Methanol content		+++	Decrease flash point, viscosity and density; corrosion on aluminum and zinc parts
Monoglyceride content		+++	Incomplete reaction
Diglyceride content		+++	Promote deposition in injectors and cylinder
Triglyceride content		+++	
Free glycerol		+++	Crystallization
Total glycerol		+++	Increase Viscosity
Group I metals (Na⁺, K⁺)		+++	Promote deposits and catalysed polymerisation reaction
Group II metals (Ca⁺, Mg⁺)		+++	
CFPP	++	+	

At **Section 1** Thermodynamic Properties are discussed. Viscosities and densities are two of the main properties evaluated in this work which will depend on the raw materials used on the biodiesel fuel production and in consequence on the profile of methyl or ethyl esters of the biodiesel fuel.³⁶

Density data are relevant because injection systems, pumps and injectors must deliver the amount of fuel precisely adjusted to provide a proper combustion.⁴² Boudy and Seers^{43,44} showed that the fuel density is the main property that influences the amount of mass injected. The viscosity is required not only for the design of pipes, fittings and equipment to be used in industry of oil and fuel⁴⁵, but also for monitoring the quality of fuel itself to be used in diesel engines. A viscous fuel, causing a poorer atomization, which is the first step of combustion, is responsible for premature injector cooking and poor fuel combustion.^{43,46}

Many studies have been devoted to the measurement and prediction of the density and viscosity of biodiesel fuel as function of temperature. Being able to predict those properties is of high relevance for the correct formulation of an adequate blend of raw materials that optimize the cost of biodiesel fuel production while allowing the fuel to meet the required quality standards.

Inside **Section 1** the work addressing the low temperature behavior and phase equilibria of biodiesel are also presented. The biodiesel cold flow performance depends both on the oil and alcohol used in the transesterification. A biodiesel with a large concentration of saturated fatty acid esters, although less vulnerable to oxidation and displaying better combustion properties, has a worst performance at low temperatures because of its tendency to crystallize.⁴⁷ This work reports experimental data for the solid-liquid-phase equilibria of biodiesel modelled with the UNIQUAC model.

In the biodiesel production process, the fatty esters rich current coming from the reactor is saturated with glycerol, alcohol, catalyst and unreacted soaps. This current is washed in a liquid-liquid extractor in counter current with acidified water to neutralize the catalyst and to convert soaps to free fatty acids. The raffinate current is composed of water saturated biodiesel while the extract is a low pH aqueous solution containing the polar compounds³³. The design and optimization of the purification of biodiesel with water requires a model that can describe the water solubility in biodiesel and mutual solubility of fatty acid + water systems. In this work new experimental data was successfully modelled with the Cubic-Plus-Association EoS.

In fact, in process operation and optimization the use of predictive models for biodiesel fuel properties could be a most useful tool.

Biodiesels with different profile are synthesized and evaluated in this work; specifically fatty acid methyl esters of soybean, rapeseed, palm oils and their mixtures (binary and ternary) and also, sunflower. The properties that depend on fatty acid profile of raw material which are studied are namely density, viscosity, iodine value, and cold filter plugging point (CFPP).

In **Section 2** enzymatic catalysis is addressed. Free Fatty Acids (FFA) are a by-product in edible oil refining, that are removed in the deodorizing step on oil purification. The deodorization is carried not just in edible oils but also in some cases before alkaline catalysis in biodiesel production. Enzymatic catalysis is here studied as an alternative to convert this by-product into biodiesel.

Section 1

**Thermodynamic
Properties and
Phase Equilibria**

General Context

Density and Viscosity are an important biodiesel parameter, with impact on fuel quality. Predicting these properties is of high relevance for a correct formulation of an adequate blend of raw materials that optimize the cost of biodiesel fuel production while allowing the produced fuel to meet the required quality standards.

For the higher FAEEs and FAMEs, the density and viscosity data for a wide range of temperatures available in the literature, are either scarce or contradictory, limiting their use in the development and testing of models to predict those properties for biodiesels.

To address this limitation, in this work densities and viscosities of ethyl esters and methyl esters, present in biodiesel ranging in alkyl chain from C8 to C18, were measured at atmospheric pressure and temperatures from 273.15K to 363.15K, and are reported in Paper 1. Some of the minor components of biodiesel have received little attention in the past but they may have a non negligible influence on the biodiesel fuel properties and, depending on the raw material used, these components can be present in a significant concentration. In Paper 2 new density and viscosity data for the minority components of biodiesel fuel such as methyl palmitoleate, methyl linolenate, methyl arachidate, methyl gadoleate, methyl behenate, methyl erucate, methyl lignocerate, ethyl linoleate, ethyl linolenate, and ethyl arachidate, at atmospheric pressure and temperatures from 273.15K to 363.15K are presented.

In both these works, a comparison with the experimental data available and its critical evaluation is performed. Correlations of these experimental data using the equations on which the multicomponent models are based, a linear correlation of the densities with temperature and the Vogel Tamman Fluch (VTF) equation for the viscosities were carried and reported. The densities and viscosities of the pure ethyl and methyl esters here measured were also used to evaluate the performance of three predictive models. The group contribution method GCVOL⁴⁸ was evaluated for the prediction of densities while the models of Ceriani et al.^{45,49} and Marrero and Gani^{50,51} were evaluated for the viscosity. The behavior of these models is compared against the data for the compounds studied.

The capacity to correctly predict biodiesel densities is of major relevance for a correct formulation of an adequate blend of raw materials aiming at producing biodiesel according to the required quality standards^{52,53} with the lowest production costs.

There are three main types of methods exist for estimating liquid densities of pure compounds. The first type are the methods based on the corresponding states theory, such as the Rackett equation and the Spencer and Danner method.^{16,36,44,54-56}

These methods have, however, some disadvantages such as the requirement of critical properties and since they often use experimental data adjusted parameters, they have a limited predictive ability. The second type of methods is based on mixing rules, such as Kay's⁵⁷, that allow the estimation of a mixture density provide that the composition of the fuel and the densities of the pure compounds are known. They are only applicable to simple mixtures with a near ideal behavior. Finally, the third type is group contribution models that only requires the chemical structure of the desired molecule to be known to estimate the thermophysical properties, such as liquid densities. The group contribution method GCVOL⁴⁸ is a predictive model that was shown in previous works to be able to provide pure fatty acid methyl esters (FAMES) densities descriptions within 1% deviation.

In the work presented in Paper 3, new experimental density data was reported for ten biodiesel samples, for which a detailed composition is presented. They were produced from different vegetable oils or oil blends, in our laboratory. The data covers the temperature range from 278.15K to 373.15K at atmospheric pressure. Correlations for the temperature dependency of the experimental data are reported and the isobaric expansivities estimated. In this paper a comparison between Mixing Rules based in different concentration units (molar, volumetric and mass fraction) are presented but the aim is the comparison of the predictive capabilities of GCVOL model as well as extended CGVOL for the estimation of the density of several biodiesel. A revised version of the GCVOL model is also proposed and evaluated.

These data, along with other data collected from literature, are used to carry out a critical evaluation of biodiesel density predictive models.

Knowledge and description of biodiesel densities as a function of pressure and temperature are required for a proper design and optimization of common rail engines injection systems, in order to a precisely adjusted amount of fuel be delivered to provide

a proper combustion while minimizing NO_x emissions⁴². However, in spite of its importance, little attention has been given to high pressure densities of biodiesels and measurements and predictions of that property have been restricted to ambient conditions. After reporting experimental data for the atmospheric pressure temperature dependence of density for several fatty acid methyl and ethyl esters for different biodiesels^{53,52}, and studying the best models to predict the densities of biodiesel⁵⁸, new experimental high pressure density data were carried out for several of these pure compounds and biodiesels. In Paper 4 new high pressure density data is reported in this work for three fatty acid methyl esters and seven biodiesels, in the temperature range 283K to 333K and from atmospheric pressure up to 45 MPa. Experimental densities were correlated using the modified Tait-Tammann equation⁵⁹ and thermodynamic properties such as isothermal compressibilities and isobaric expansion coefficients were as well calculated and evaluated, on the temperature and pressure ranges studied. Empirical models, like the modified Tait-Tammann equation, are the most commonly used to correlate high pressure density experimental data. In this work, a different and completely predictive approach was also applied, that consisted on the use of the Cubic-Plus-Association equation of state (CPA EoS) to describe the experimental data. In previous works⁶⁰⁻⁶² the CPA EoS was shown to be the most appropriate model to be applied to biodiesel production and purification processes. A discussion about the most appropriate CPA pure compound parameters for esters is also presented.

There is still a lack of viscosity data of biodiesel blends and biodiesel-diesel over the whole composition range at different operational conditions of pressure and temperature. In this regard, the use of theoretical approaches to estimate the viscosity of biodiesel systems is of great practical interest and is presented in Paper 5.

A number of works has presented predictive models and empirical equations with adjustable parameters for the viscosity of fatty acid esters. By knowing the viscosity of fatty acid esters, it is possible to determine the viscosity of biodiesel using the mixing rule suggested by Grunberg-Nissan or Hind⁶³. Moreover there is a possibility to optimize its properties by simply changing the composition of fatty acid esters. The predictive capabilities of three models developed by Ceriani *et al.*⁶⁴, Krisnangkura *et al.*⁶⁵, and Yuan *et al.*⁵⁵ for the estimation of the viscosity of several biodiesel and their blends with diesel fuels were compared. A revised version of the Yuan model is also proposed and evaluated.

Besides density and viscosity there are other properties of biodiesel that can be directly related to the chemical composition of the raw material. Iodine index, CP (pour point) and CFPP (cold filter plugging point) were studied and evaluated based on norms considerations.

- **Chapter 1**
Density and
Viscosity

My direct contribution for Published Papers

In first Chapter five published articles are presented, all related to new data for density and viscosity of biodiesel produced by myself from different oil sources, as well for pure components present in biodiesel fuel. All data were measured with a Viscometer Anton Parr Strabinger, in a wide range of temperatures. I was responsible for experimental measurements of density and viscosity of biodiesel and pure compounds, as well as the density modelling. High pressure density was measured on different equipment at University of Vigo and the modeling with CPA was also carried by me in collaboration with Mariana Belo. Viscosity modelling was made by Samuel Freitas.

Experimental section

Biodiesel Synthesis

Eight biodiesel samples, studied in this work, were synthesized at our laboratory by a transesterification reaction of the vegetal oils: Soybean (S), Rapeseed (R), and Palm (P), and their respective binary and ternary mixtures: Soybean+Rapeseed (SR), Rapeseed+Palm (RP), Soybean+Palm (SP), and Soybean+Rapeseed +Palm (SRP) and Sunflower (Sf). Transesterification reaction for all biodiesel samples was performed under specific conditions: the molar ratio of oil/methanol used was 1:5 with 0.5% sodium hydroxide by weight of oil as catalyst, the reaction was performed at 55 °C during 24 h under methanol reflux and the reaction time chosen was adopted for convenience in order to guarantee a complete reaction conversion of one liter of oil. Raw glycerol was removed in two steps, the first after 3 h reaction and then after 24 h reaction in a separating funnel. Figure 11 shows the biodiesel production.

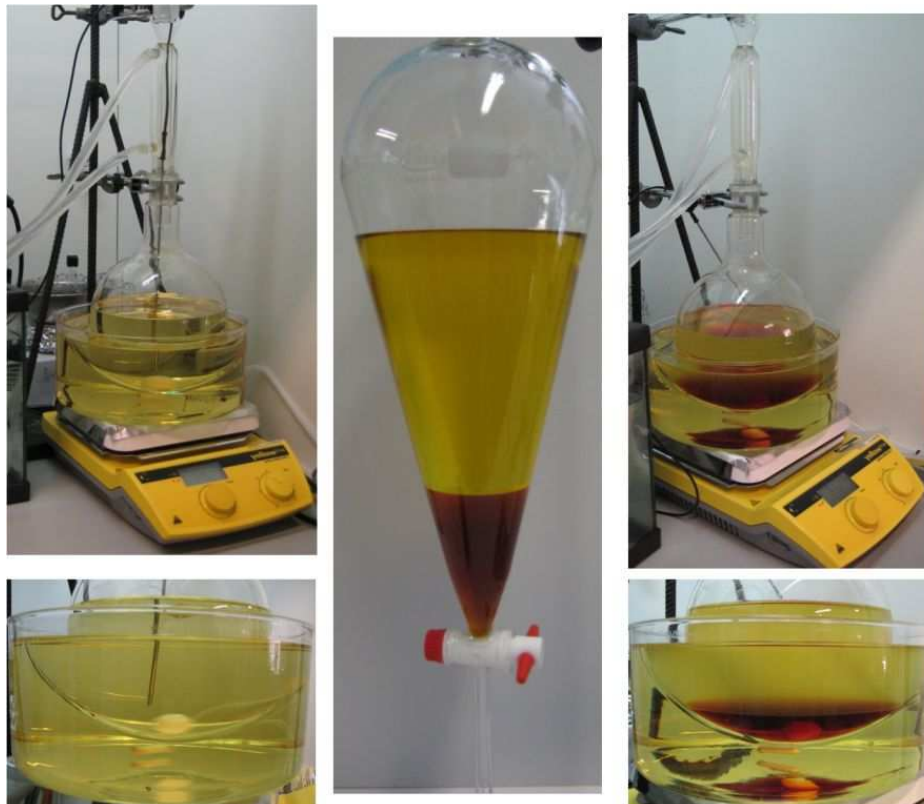


Figure 11- Experimental assembly of biodiesel production.

Biodiesel was purified by washing with hot distilled water until a neutral pH was achieved. The biodiesel was then dried until the EN ISO 12937 limit for water was reached (less than 500 ppm of water). The water content was checked by Karl- Fischer titration.

It is necessary to present here additional information about biodiesel synthesis, as the procedure was adjusted during the work after testing several variables. For a correct characterization of biodiesel it is necessary to obtain close to 100% conversion on the reaction. This prevents the contamination of intermediate species as mono-, di-, and tri-glycerides in the biodiesel with important impacts on the fuel properties.

There are a lot of publications that report biodiesel productions in shorter times (3-4 hours of synthesis). In the beginning of the present work this method was also followed but at some point we realized that the biodiesels did not possess a good quality level, as the yield was less than 90%. The presence of intermediate species in biodiesel influences dramatically their thermodynamic properties. Viscosities data were measured in these conditions and were used as training set to test the model developed by Ceriani et al.⁵⁶ for the estimation of viscosity of fatty compounds and biodiesel esters as a function of the temperature and also to investigate the influence of small concentrations of intermediate compounds of transesterification reaction in the viscosity of biodiesels.⁵⁷

The conditions to produce biodiesel were tuned until conversion reaction obtained presented yields of more than 96%. Therefore the reaction time was increased to a limit value to guarantee a complete reaction conversion.

Biodiesel Characterization

Biodiesel was characterized by GC-FID following the British Standard EN14103 from EN 142144 to know the alkyl esters composition of the samples. A Varian CP-3800 with a flame ionization detector in a split injection system with a Select™ Biodiesel for FAME Column, (30 m x 0.32 mm x 0.25 μm), was used to discriminate between all methyl esters in analysis inclusively the polyunsaturated ones. The column temperature was set at 120°C and then programmed to increase up to 250 °C, at 4 °C/min. Detector and injector were set at 250°C. The carrier gas was helium with a flow rate of 2 mL/min. Methyl heptadecanoate was used as internal standard.

Densities and Viscosities of Fatty Acid Methyl and Ethyl Esters

Journal of Chemistry & Engineering Data **2010**, 55, 3983–3990.

DOI: 10.1021/je100042c

Densities and Viscosities of Fatty Acid Methyl and Ethyl Esters

Maria Jorge Pratas, Samuel Freitas, Mariana B. Oliveira, Sílvia C. Monteiro[#],

Álvaro S. Lima[§], João A.P. Coutinho

CICECO, Chemistry Department, University of Aveiro, Campus de Santiago, 3810–193

Aveiro, Portugal;

[#]Polytechnic Institute of Leiria, Leiria, Morro do Lena – Alto Vieiro, 2411-901 Leiria,

Portugal;

[§] Universidade Tiradentes, Av. Murilo Dantas 300, Farolândia, Aracaju-SE, Brasil.

Abstract

To develop reliable models for the densities and viscosities of biodiesel fuel reliable data for the pure fatty acid esters are required. Densities and viscosities were measured for seven ethyl esters and eight methyl esters, at atmospheric pressure and temperatures from (273.15 to 363.15) K. A critical assessment of the measured data against the data previously available in the literature was carried out. It is shown that the data here reported presents deviations of less than 0.15 % for densities and less than 5 % for viscosities. Correlations for the densities and viscosities with temperature are proposed. The densities and viscosities of the pure ethyl and methyl esters here reported were used to evaluate three predictive models. The GCVOL group contribution method is shown to be able to predict densities for these compounds within 1 %. The methods of Ceriani and Meirelles (CM) and of Marrero and Gani (MG) were applied to the viscosity data. It is shown that only the first of these methods is able to provide a fair description of the viscosities of fatty acid esters.

Keywords: Density, Viscosity, Methyl and Ethyl Esters, Biodiesel Fuel.

Introduction

In consequence of environmental, economical and also political turmoil, caused by the excessive use and dependency of conventional petroleum based fuels the attention of several countries has been addressed towards the development of alternative fuels from renewable resources.^{1,2}

Among those alternatives, biodiesel fuel, along with bioethanol fuel, is in the forefront of the substitutes to petroleum based fuels in the transportation sector, being considered as an important short-time option as its prices can be similar to petroleum based fuels and no motor changes are required.³

Biodiesel is a fuel comprised of mono-alkyl esters of long chain fatty acids derived from vegetable oils, animal fats, or mixtures of them. It is produced by the transesterification of triglycerides with a short chain alcohol, usually methanol or ethanol, in presence of a catalyst, leading to the formation of mixtures of fatty acid methyl esters (FAMES) or fatty acid ethyl esters (FAEEs) respectively.^{3,4} The main components of biodiesel fuel are palmitate, stearate, oleate and linoleate esters.⁵ However, and depending on the raw materials used, a larger range of esters can be present.⁶

The biodiesel fuel has to fulfill a number of quality standards. In Europe the biodiesel fuel standards are compiled in the Norm CEN EN 14214⁷, and in United States of America in the Norm ASTM D6751⁸. Norms specify minimum requirements and test methods for biodiesel fuel to be used in diesel engines and for heating purposes, in order to increase the biodiesel fuel quality and its acceptance among consumers. Viscosities and densities are two of the main properties evaluated which will depend on the raw materials used on the biodiesel fuel production and in consequence on the profile of methyl or ethyl esters of the biodiesel fuel.⁶

Density data are relevant because injection systems, pumps and injectors must deliver the amount of fuel precisely adjusted to provide proper combustion.⁹ Boudy and Seers show that fuel density is the main property that influences the amount of mass injected.^{10,11} The viscosity is required not only for the design of pipes, fittings and equipment to be used in industry of oil and fuel¹², but also for monitoring the quality of fuel itself to be used in diesel engines. A viscous fuel, causing a poorer atomization,

which is the first step of combustion, is responsible for premature injector cooking and poor fuel combustion.^{10, 13}

Many studies have been devoted to the measurement and prediction of the density and viscosity of biodiesel fuel as function of temperature. Being able to predict those properties is of high relevance for the correct formulation of an adequate blend of raw materials that optimize the cost of biodiesel fuel production while allowing the fuel to meet the required quality standards. In fact, in process operation and optimization the use of correlative and predictive models for biodiesel fuel properties could be a most useful tool.

Several models have been proposed in the literature to calculate biodiesel fuel density. The most important among them rely on the accurate knowledge of the properties of the pure compounds. Tat and Van Gerpen¹⁴ and Clements¹⁵ used a linear mixing rule of pure densities based on the empirical equation proposed by Janarthanan¹⁵. Huber¹⁶ et al. also use density mixing rule to develop preliminary thermodynamic model for biodiesel fuel. Similarly for the viscosities the approaches proposed by Krisnangkura et al.¹⁷ and Yuan et al.¹⁸ allow the estimation of the viscosity of biodiesel fuel using the Grunberg-Nissan equation that requires accurate values of the viscosities of pure FAME's or FAEE's¹⁹.

For the higher FAEEs and FAMEs, the density and viscosity data for a wide range of temperatures available in the literature are sometimes scarce or contradictory, limiting the use of these models to predict those properties for biodiesels.

To address this limitation, in this work densities and viscosities of seven ethyl esters and eight methyl esters, from C8 to C18, were measured at atmospheric pressure and temperatures from (273.15 to 363.15) K. A comparison with the experimental data available and its critical evaluation is performed. Correlations of these experimental data using the equations on which the multicomponent models are based, a linear correlation of the densities with temperature and the Vogel Tamman Fluch (VTF) equation for the viscosities were carried and reported.

The densities and viscosities of the pure ethyl and methyl esters here measured were also used to evaluate the performance of three predictive models. The group contribution method GCVOL²⁰ was evaluated for the prediction of densities while the models of Ceriani et al.¹² and Marrero and Gani^{21,22} were evaluated for the viscosity.

Experimental Section

Materials and Procedure. Seven ethyl ester and eight methyl esters were used in this study. Table 1 reports the name, purity, supplier, and CAS number of each compound used in this study. Compounds purity was confirmed by GC-FID.

Table 1. Methyl and Ethyl Esters Studied in this Work.

Compound	Common Name	Purity m/m%	Source	CAS
Octanoic acid, ethyl ester	Ethyl Caprylate	99	Aldrich	106-32-1
Decanoic acid, ethyl ester	Ethyl Caprate	99	Fluka	110-38-3
Dodecanoic acid, ethyl ester	Ethyl Laurate	99	Sigma	106-33-2
Tetradecanoic acid, ethyl ester	Ethyl Myristate	99	Aldrich	124-06-1
Hexadecanoic acid, ethyl ester	Ethyl Palmitate	99	Sigma	628-97-7
Octadecanoic acid, ethyl ester	Ethyl Stearate	99	Fluka	111-61-5
(Z)-9-Octadecenoic acid, ethyl ester	Ethyl Oleate	98	Aldrich	111-62-6
Octanoic acid, methyl ester	Methyl Caprylate	99	Fluka	111-11-5
Decanoic acid, methyl ester	Methyl Caprate	99	Acros Org.	110-42-9
Dodecanoic acid, methyl ester	Methyl Laurate	98	Sigma	111-82-0
Tetradecanoic acid, methyl ester	Methyl Myristate	98	SAFC	124-10-7
Hexadecanoic acid, methyl ester	Methyl Palmitate	99	SAFC	112-39-0
Octadecanoic acid, methyl ester	Methyl Stearate	99	Fluka	112-61-8
(Z)-9-Octadecenoic acid, methyl ester	Methyl Oleate	99	Aldrich	112-62-9
(Z,Z)-9,12-Octadecadienoic acid, methyl ester	Methyl Linoleate	99	Sigma	112-63-0

Experimental Measurements. Measurements of viscosity and density were performed in the temperature range of (273.15 to 363.15) K at atmospheric pressure using an automated SVM 3000 Anton Paar rotational Stabinger viscometer-densimeter. The viscometer is based on a tube filled with the sample in which floats a hollow measuring rotor.

Due to its low density, the rotor is centered in the heavier liquid by buoyancy forces. Consequently, a measuring gap is formed between the rotor and the tube. The rotor is forced to rotate by shear stresses in the liquid and is guided axially by a built-in permanent magnet, which interacts with a soft iron ring. The rotating magnetic field delivers the speed signal and induces Eddy currents in the surrounding copper casing. These Eddy currents are proportional to the speed of the rotor and exert a retarding torque on the rotor. Two different torques influence the speed of the measuring rotor, and at the equilibrium, the two torques are equal and the viscosity can be traced back to a single speed measurement. The SVM 3000 uses Peltier elements for fast and efficient thermostability. The temperature uncertainty is 0.02 K from (288.15 to 378.15) K. The absolute uncertainty of the density is $0.0005 \text{ g}\cdot\text{cm}^{-3}$ and the relative uncertainty of the dynamic viscosity obtained is less than 1.5 % for the standard fluid SHL120 (SH Calibration Service GmbH), in the range of the studied temperatures. The repeatability of the equipment was measured with temperature and presents a maximum standard deviation relative value of 0.15 % in the studied viscosity range for the same temperature range. Also the reproducibility of the equipment was evaluated with time and presents a maximum of 0.25 %.²³ Further details about the equipment and method can be found elsewhere.²⁴ This viscometer was previously tested for other compounds and presented a very good reproducibility.²⁵

Results and Discussion

Density

The experimental data obtained are reported in Tables 2 and 3. For methyl myristate, palmitate, and stearate, and ethyl palmitate and stearate the measurements were only carried at temperatures above the melting point of these compounds.

Table 2. Experimental Density, in $\text{kg}\cdot\text{m}^{-3}$, for Ethyl Esters.

T / K	Ethyl						
	Caprylate	Caprate	Laurate	Myristate	Palmitate	Stearate	Oleate
278.15	880.2						881.5
283.15	875.9	872.5	870.3	868.7			877.9
288.15	871.6	868.4	866.4	864.8			874.1
293.15	867.3	864.3	862.4	861.0			870.5
298.15	863.0	860.2	858.5	857.2			866.9
303.15	858.7	856.2	854.6	853.4	852.6		863.2
308.15	854.4	852.1	850.7	849.6	848.9		859.5
313.15	850.0	848.0	846.8	845.8	845.2	844.8	855.8
318.15	845.7	843.9	842.9	842.0	841.5	841.1	852.2
323.15	841.4	839.8	839.0	838.2	837.9	837.5	848.5
328.15	837.1	835.7	835.1	834.5	834.2	833.9	844.9
333.15	832.8	831.6	831.1	830.7	830.5	830.3	841.2
338.15	828.4	827.5	827.2	826.9	826.9	826.7	837.6
343.15	824.1	823.4	823.3	823.1	823.2	823.1	834.0
348.15	819.7	819.2	819.4	819.4	819.5	819.5	830.3
353.15	815.3	815.1	815.4	815.6	815.9	815.9	826.7
358.15	810.8				812.2	812.3	823.1
363.15	806.4				808.6	808.7	819.5

Table 3. Experimental Density, in $\text{kg}\cdot\text{m}^{-3}$, for Methyl Esters.

T / K	Methyl							
	Caprylate	Caprate	Laurate	Myristate	Palmitate	Stearate	Oleate	Linoleate
278.15		884.7						897.2
283.15	885.9	880.6	877.7				881.4	893.5
288.15	881.5	876.4	873.7				877.7	889.9
293.15	877.1	872.3	869.8				874.1	886.2
298.15	872.8	868.2	865.8	863.7			870.4	882.5
303.15	868.4	864.1	861.8	859.9			866.8	878.8
308.15	864.0	860.0	857.9	856.0	854.5		863.1	875.2
313.15	859.6	856.0	853.9	852.2	850.8	849.8	859.5	871.5
318.15	855.2	851.9	850.0	848.4	847.0	846.1	855.9	867.9
323.15	850.8	847.8	846.1	844.6	843.3	842.5	852.3	864.3
328.15	846.4	843.6	842.1	840.8	839.6	838.9	848.7	860.7
333.15	841.9	839.5	838.1	837.0	835.8	835.3	845.1	857.0
338.15	837.5	835.3	834.2	833.1	832.1	831.7	841.5	853.4
343.15	833.0	831.2	830.2	829.3	828.4	828.1	837.9	849.8
348.15	828.5	827.0	826.2	825.5	824.7	824.5	834.3	846.1
353.15	824.0	822.9	822.3	821.8	821.0	820.9	830.7	842.5
358.15		818.7			817.3	817.3		838.7
363.15		814.5			813.6	813.7		835.1

Data shows that the density of FAMEs decreases with increasing alkyl chain length, and increases with the level of unsaturation, the same happening with FAEEs. Surprisingly the FAMEs present a higher value for density than the corresponding FAEEs with the same number of carbon atoms in acid side chain. This difference is higher than what would be expected from the addition of a methylene (CH_2) group to the molecule. This results from a change in the ordering of the molecules in the liquid state akin to what can be observed in the crystal structures of methyl stearate and ethyl stearate.²⁶ It was also previously observed for other light esters that the addition of CH_2 group in to the alcohol moiety induces a lower molecular packing efficiency decreasing density.²⁷

Figures 1 and 2 present the relative deviations between this work's experimental data and density data available in the literature as function of temperature for FAEEs and FAMEs, respectively. This comparison shows a good agreement with relative average deviation of lower than 0.10 % for FAEEs and lower than 0.15 % for FAMEs, with exception methyl stearate measured by Gaikward and Subrahmanyam²⁸, that presents a deviation below 0.25 % and methyl palmitate measured by Ott et al.²⁹ that present a relative deviation of -0.25 %. The density values for methyl palmitate reported in this work were repeated using samples from various suppliers with a good agreement among them and with the data previously reported in the literature by other authors for this compound.^{28, 30-32}

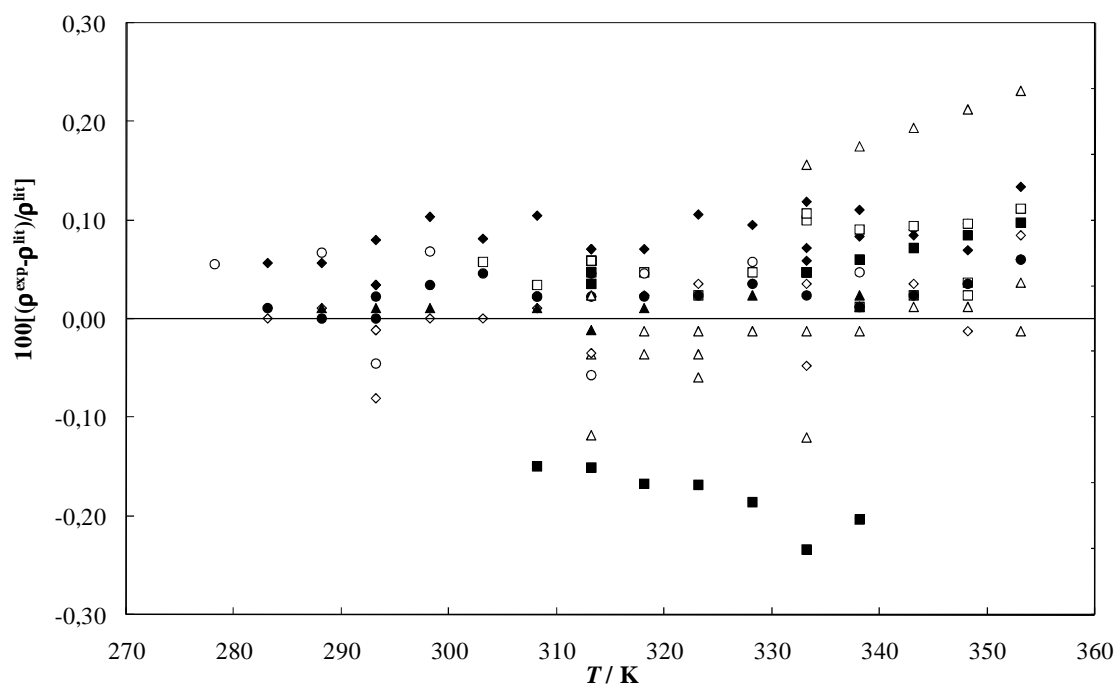


Figure 1. Relative deviations for methyl esters density data available in the literature^{28-32, 34-39} as function of temperature: ●, methyl caprylate, ◇, methyl caprate, ◆, methyl laurate, □, methyl myristate, ■, methyl palmitate, △ methyl stearate, ▲, methyl oleate and ○, methyl linoleate. Zero line is this work's experimental data.

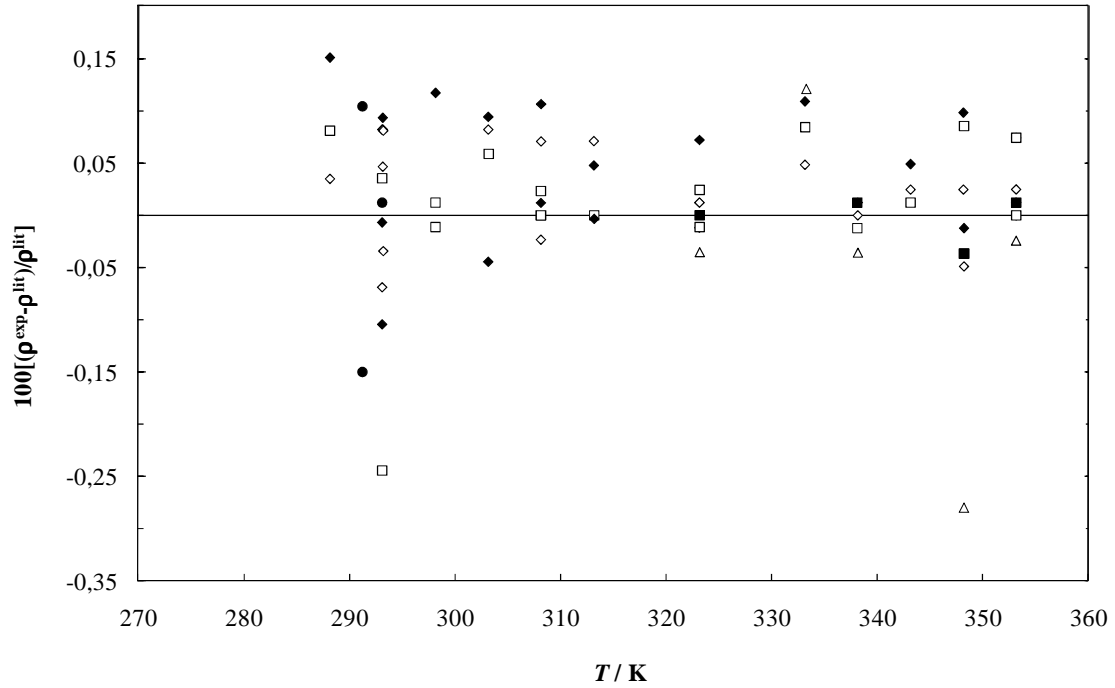


Figure 2. Relative deviations for ethyl esters density data available in the literature^{32, 35, 40-47} as function of temperature: ●, ethyl caprylate, ◇, ethyl caprate, ◆, ethyl laurate, □, ethyl myristate, ■, ethyl palmitate, and △ ethyl stearate. Zero line is this work's experimental data.

The experimental density data here measured were correlated using a linear temperature dependency using an optimization algorithm based on the least-squares method,

$$\rho / \text{kg} \cdot \text{m}^{-3} = b \cdot T / \text{K} + a \quad (1)$$

And the parameter values along with their confidence limits are reported in Table 4. These correlations can be used for the estimation of the densities of biodiesels using the Janarthanan et al.¹⁵ approach.

Table 4. Density Correlation Constants for Pure Methyl and Ethyl Esters over the Temperature Range (278.15 to 363.15) K, and Corresponding 95 % Confidence Limits.

	$b / \text{kg}\cdot\text{m}^{-3}\cdot\text{K}^{-1}$	\pm	$t \cdot s_b$	$a / \text{kg}\cdot\text{m}^{-3}$	\pm	$t \cdot s_A$
Ethyl Caprylate	-0.8668	\pm	0.0021	1121.4		0.7
Ethyl Caprate	-0.8194	\pm	0.0013	1104.5	\pm	0.4
Ethyl Laurate	-0.7832	\pm	0.0009	1092.0	\pm	0.3
Ethyl Myristate	-0.7576	\pm	0.0014	1083.1	\pm	0.4
Ethyl Palmitate	-0.7334	\pm	0.0011	1077.9	\pm	0.3
Ethyl Stearate	-0.7209	\pm	0.0012	1070.5	\pm	0.4
Ethyl Oleate	-0.7209	\pm	0.0013	1084.5	\pm	0.4
Methyl Caprylate	-0.8832	\pm	0.0027	1136.1	\pm	0.8
Methyl Caprate	-0.8244	\pm	0.0018	1114.0	\pm	0.6
Methyl Laurate	-0.7912	\pm	0.0009	1101.7	\pm	0.3
Methyl Myristate	-0.7629	\pm	0.0017	1091.1	\pm	0.5
Methyl Palmitate	-0.7438	\pm	0.0015	1083.7	\pm	0.5
Methyl Stearate	-0.7209	\pm	0.0012	1075.5	\pm	0.4
Methyl Oleate	-0.7236	\pm	0.0015	1086.2	\pm	0.5
Methyl Linoleate	-0.7294	\pm	0.0012	1100.0	\pm	0.4

s - standard deviation

The GCVOL model²⁰ was used to predict the densities of the compounds studied in this work. The results reported in Figure 3 show that the densities of FAMEs can be predicted within an uncertainty of ± 0.5 % with exception of methyl linoleate due to a poor model description of the unsaturation effect on the densities. In Figure 4 the deviations for the FAEE's are reported. Due to the different effect of the introduction of a methylene group in the acid or alcohol moieties discussed above a group contribution model cannot produce an adequate description of the densities and an overestimation of between 1 and 1.5 % of the experimental densities is obtained. Again a problem associated to the unsaturation is observed although in this case it contributes to minimize the model deviations.

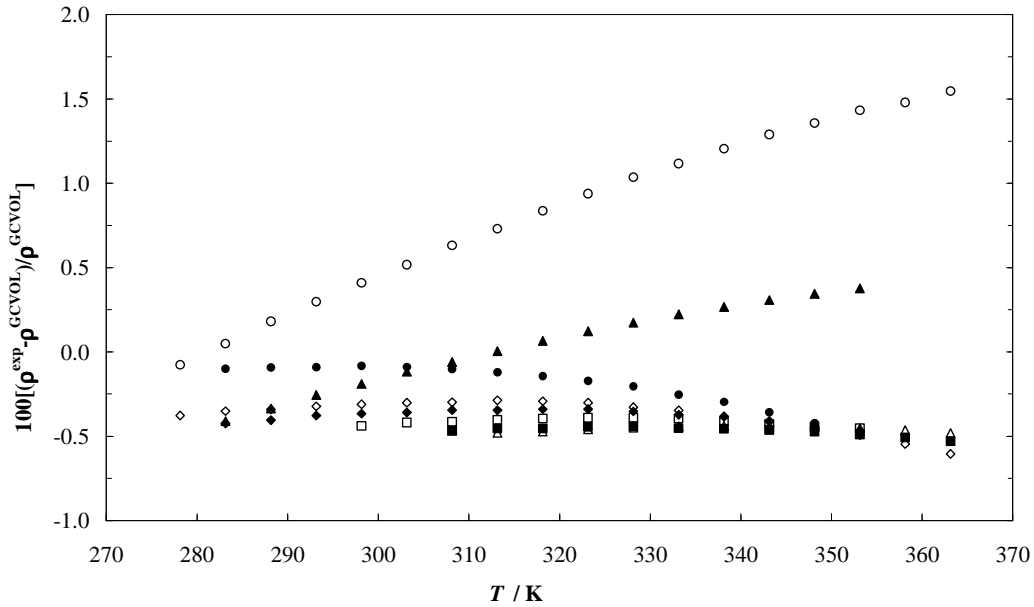


Figure 3. Relative deviations between density of methyl esters predicted by GCVOL and this work's experimental data as function of temperature: ●, methyl caprylate, ◇, methyl caprate, ◆, methyl laurate, □, methyl myristate, ■, methyl palmitate, △ methyl stearate, ▲, methyl oleate and ○, and methyl linoleate.

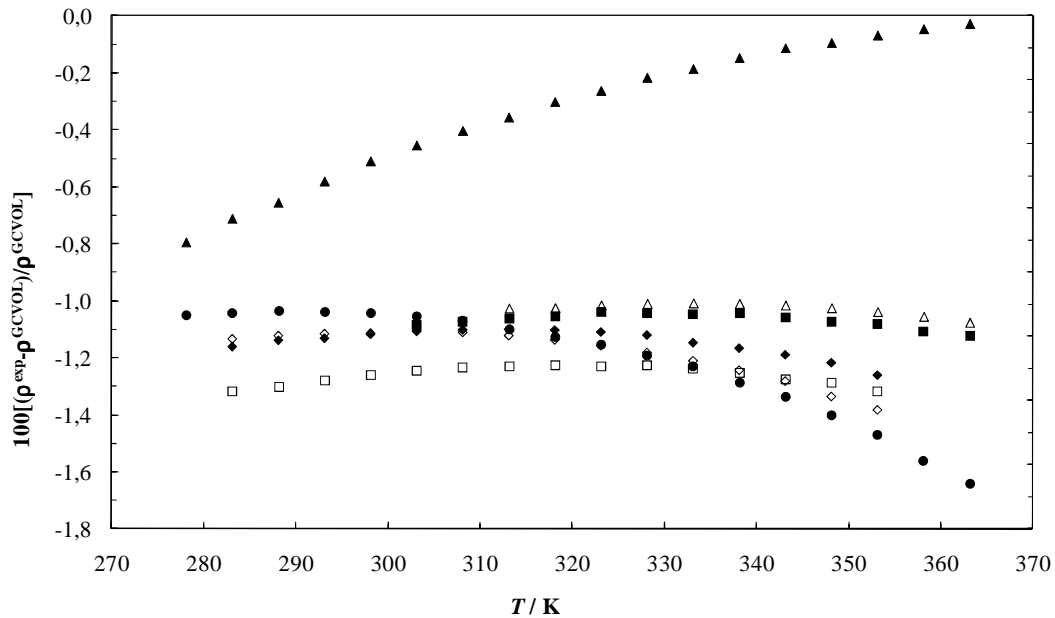


Figure 4. Relative deviations between density of ethyl esters predicted by GCVOL and this work's experimental data as function of temperature: ●, ethyl caprylate, ◇, ethyl caprate, ◆, ethyl laurate, □, ethyl myristate, ■, ethyl palmitate, △ ethyl stearate, ▲, and ethyl oleate.

The isobaric expansivity coefficient at constant pressure (α_p) is defined as

$$\alpha_p = -\left(\frac{\partial \ln \rho}{\partial T}\right)_p \quad (2)$$

In the studied temperature range the logarithm of density exhibits a linear behavior with temperature. The value of α_p will thus be a constant for the studied compounds within the temperature range investigated. The isobaric expansivities estimated from the experimental data are reported in Table 5. It is observed that α_p decreases with the increment of carbons in alkyl acid side chain and also decreases with unsaturation level for both ethyl and methyl esters. The isobaric expansivities are identical for the FAMEs and FAEEs within the experimental uncertainty of the data here reported.

Table 5. Isobaric Expansivities, α_p , for the Studied Fatty Acid Esters, and Corresponding 95 % Confident Limits.

	$\alpha_p \cdot 10^3 / \text{K}^{-1}$	\pm	$t \cdot s_{\alpha_p} \cdot 10^3$
Ethyl Caprylate	1.028	\pm	0.009
Ethyl Caprate	0.971	\pm	0.007
Ethyl Laurate	0.929	\pm	0.005
Ethyl Myristate	0.900	\pm	0.003
Ethyl Palmitate	0.883	\pm	0.003
Ethyl Stearate	0.872	\pm	0.003
Ethyl Oleate	0.859	\pm	0.003
Methyl Caprylate	1.033	\pm	0.009
Methyl Caprate	0.971	\pm	0.008
Methyl Laurate	0.931	\pm	0.005
Methyl Myristate	0.905	\pm	0.004
Methyl Palmitate	0.892	\pm	0.003
Methyl Stearate	0.867	\pm	0.003
Methyl Oleate	0.845	\pm	0.003
Methyl Linoleate	0.842	\pm	0.004

s - standard deviation

Viscosity

The experimental data of viscosity of the ethyl and methyl esters here studied are reported in Tables 6 and 7 respectively. As expected the viscosity of all esters increases with the ester chain length and decreases with its level of unsaturation. The ethyl esters also present a higher viscosity than the corresponding methyl ester of the equivalent fatty acid.

Table 6. Experimental Viscosities, in mPa•s, for Fatty Acid Ethyl Esters.

<i>T</i> / K	Ethyl					
	Caprate	Laurate	Myristate	Palmitate	Stearate	Oleate
278.15						10.9040
283.15	2.8960	4.3353	6.2601			9.2553
288.15	2.5882	3.8135	5.4303			7.9421
293.15	2.3263	3.3797	4.7492			6.8906
298.15	2.1029	3.0152	4.1880			6.0236
303.15	1.9111	2.7073	3.7207	5.0107		5.3094
308.15	1.7453	2.4455	3.3278	4.4399		4.7156
313.15	1.6000	2.2198	2.9928	3.9558	5.0823	4.2137
318.15	1.4729	2.0240	2.7056	3.5472	4.5285	3.7876
323.15	1.3599	1.8531	2.4579	3.1973	4.0574	3.4247
328.15	1.2594	1.7037	2.2423	2.8969	3.6535	3.1102
333.15	1.1695	1.5703	2.0549	2.6373	3.3073	2.8367
338.15	1.0892	1.4529	1.8891	2.4121	3.0072	2.5988
343.15	1.0171	1.3486	1.7432	2.2140	2.7439	2.3901
348.15	0.9516	1.2543	1.6139	2.0391	2.5153	2.2065
353.15	0.8929	1.1708	1.4986	1.8842	2.3132	2.0434
358.15				1.7464	2.1355	1.8978
363.15				1.6233	1.9777	1.7683

Table 7. Experimental Viscosities, in mPa*s, for Fatty Acid Methyl Esters.

<i>T</i> / K	Methyl							
	Caprylate	Caprate	Laurate	Myristate	Palmitate	Stearate	Oleate	Linoleate
278.15		2.9888						7.4664
283.15	1.7103	2.6543	4.0678				8.6987	6.4658
288.15	1.5593	2.3733	3.5771				7.4518	5.6550
293.15	1.4275	2.1360	3.1668				6.4499	4.9822
298.15	1.3127	1.9335	2.8237	3.9821			5.6336	4.4275
303.15	1.2120	1.7601	2.5356	3.5430			4.9612	3.9615
308.15	1.1233	1.6091	2.2893	3.1651	4.2122		4.4012	3.5666
313.15	1.0444	1.4773	2.0776	2.8447	3.7551	4.9862	3.9303	3.2270
318.15	0.97334	1.3613	1.8944	2.5709	3.3682	4.4348	3.5306	2.9358
323.15	0.90926	1.2589	1.7347	2.3343	3.0378	3.9645	3.1892	2.6822
328.15	0.85178	1.1675	1.5948	2.1295	2.7540	3.5684	2.8944	2.4605
333.15	0.79980	1.0864	1.4714	1.9498	2.5083	3.2252	2.6377	2.2660
338.15	0.75279	1.0133	1.3621	1.7932	2.2947	2.9293	2.4160	2.0934
343.15	0.71014	0.94770	1.2651	1.6549	2.1073	2.6724	2.2216	1.9403
348.15	0.67130	0.88860	1.1781	1.5321	1.9421	2.4477	2.0499	1.8038
353.15	0.63589	0.83420	1.1002	1.4233	1.7960	2.2504	1.8974	1.6816
358.15		0.78595			1.6659	2.0762		
363.15		0.74207			1.5499	1.9217		

The experimental data here measured was compared with viscosity data previously reported in the literature for the same systems. The relative deviations for the FAMES and FAEEs are presented in Figures 7 and 8. For the FAMES the deviations are within ± 4 % of the literature data with exception of the data by Meirelles et al.³³ at high temperatures that show large deviations when compared with both our data and data from other authors. For the FAEEs the data available is far more scarce but in spite of being more than 50 years old it is in good agreement with the viscosities here reported with relative deviations of less than 1 %.

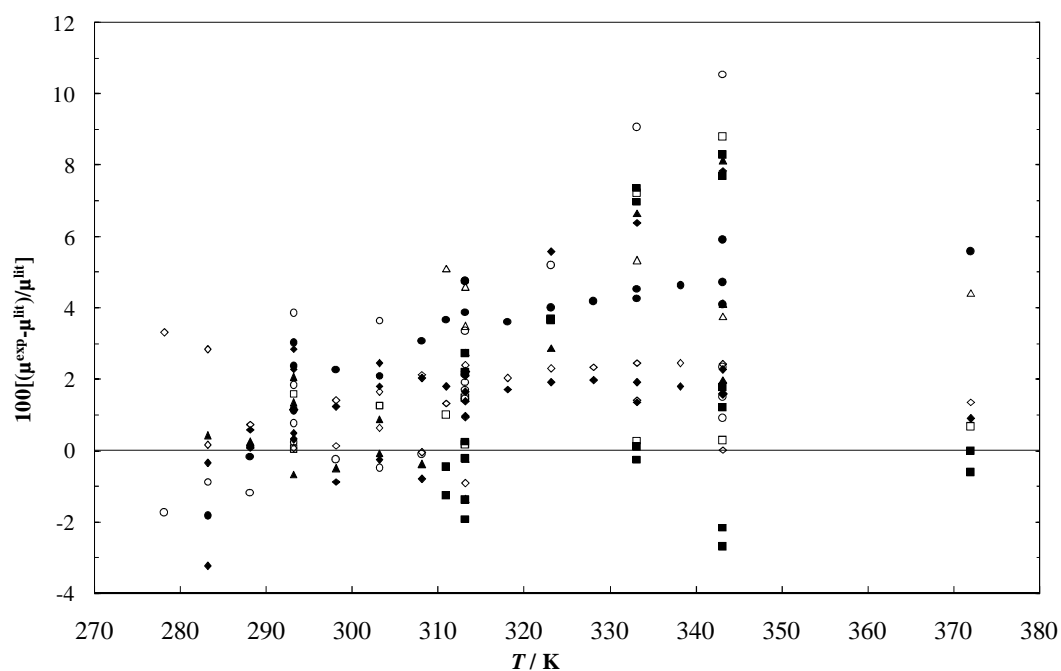


Figure 5. Relative deviation of methyl esters dynamic viscosity vs Temperature: ●, methyl caprylate, ◇, methyl caprate, ◆, methyl laurate, □, methyl myristate, ■, methyl palmitate, △ methyl stearate, ▲, methyl oleate, and ○, methyl linoleate.^{30,31, 36, 41, 48} Zero line is this work's experimental data.

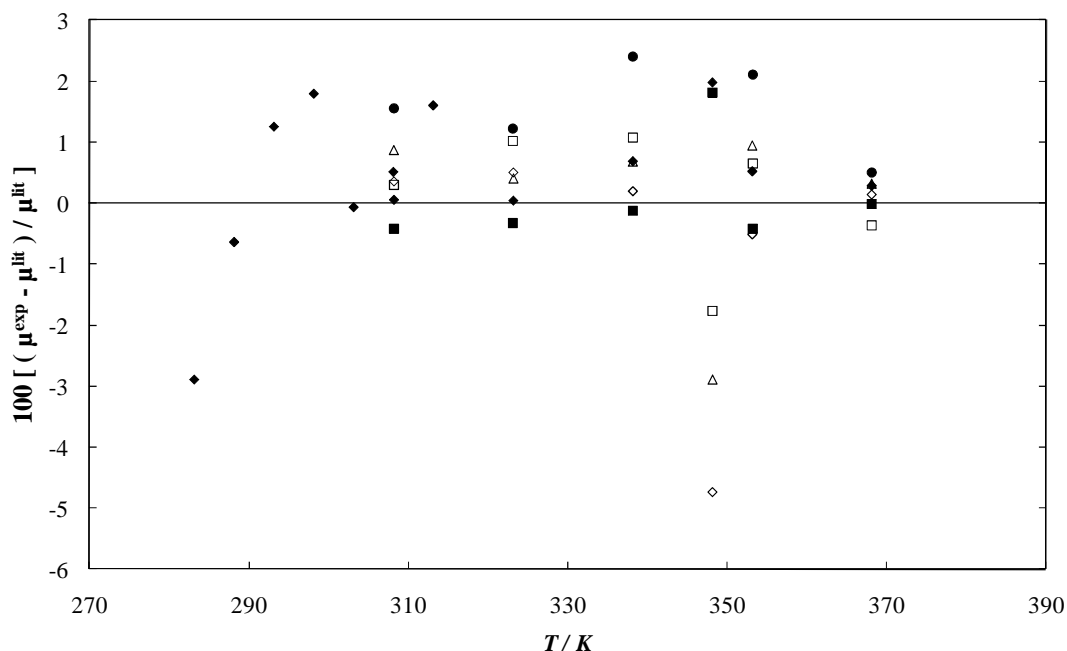


Figure 6. Relative deviation of ethyl esters Viscosity vs Temperature: ●, ethyl caprylate, ◇, ethyl caprate, ◆, ethyl laurate, □, ethyl myristate, ■, ethyl palmitate, and △ ethyl stearate.^{32, 41, 48} Zero line is this work's experimental data.

The experimental viscosities here measured were correlated using the Vogel-Tammann-Fulcher (VTF) equation:

$$\mu/mPa \cdot s = \exp\left(A + \frac{B}{(T/K - T_0)}\right) \quad (3)$$

Where A, B and T_0 are fitting parameters whose values were estimated using an optimization algorithm based on the least-squares method. The parameter values along with their uncertainty and the average absolute deviations (AAD %) of the correlation are reported in Table 8. As can be seen the VTF equation provides a very good description of the experimental data.

Table 8. Viscosity Correlation Constants for Pure Ethyl and Methyl Esters over the Temperature Range (278.15 to 363.15) K, and Corresponding 95 % Confident Limits.

	A	$t \cdot s_A$	B / K	$t \cdot s_B$	T_0 / K	$t \cdot s_{T_0}$	AAD(%)
Ethyl Caprylate	-3.58	0.055	926.963	28.2	63.493	3.8	0.078
Ethyl Caprate	-3.42	0.086	883.295	39.8	85.943	5.2	0.10
Ethyl Laurate	-3.15	0.073	818.076	30.5	105.827	3.9	0.096
Ethyl Myristate	-2.97	0.058	793.873	22.7	117.701	2.8	0.084
Ethyl Palmitate	-3.00	0.053	854.539	22.0	117.650	2.6	0.046
Ethyl Stearate	-3.04	0.025	920.174	10.8	115.962	1.3	0.010
Ethyl Oleate	-2.65	0.040	759.323	15.5	127.32	1.9	0.11
Methyl Caprylate	-3.48	0.054	859.303	26.1	68.948	3.7	0.046
Methyl Caprate	-3.32	0.070	814.674	30.7	93.317	4.2	0.13
Methyl Laurate	-3.09	0.054	767.388	21.4	112.267	2.8	0.075
Methyl Myristate	-3.12	0.036	837.282	15.2	112.358	1.9	0.019
Methyl Palmitate	-2.81	0.056	746.528	22.5	132.676	2.9	0.049
Methyl Stearate	-2.98	0.034	876.221	14.7	122.303	1.8	0.015
Methyl Oleate	-2.70	0.043	748.184	16.0	129.249	2.0	0.070
Methyl Linoleate	-2.62	0.068	733.236	26.3	119.641	3.4	0.12

s -standard deviation

$$* AAD = \frac{1}{N_p} \sum_{i=1}^{N_p} ABS \left[\frac{(exp_i - lit_i)}{lit_i} \right] \times 100$$

The measured data were also used to test two predictive viscosity models. The Ceriani and Meirelles³³(CM) and the Marrero and Gani^{21,22} (MG) group contribution models were used to estimate the dynamic viscosity of the fatty acid esters as a function of temperature. The average deviations of viscosity between the measured data and those estimated by CM and MG are shown in Table 9.

Table 9. Average Deviation between the Measured Viscosity of Pure Ethyl and Methyl Esters over the Temperature Range (278.15 to 363.15) K and those Estimated by CM and MG Models.

	CM (%)	MG (%)
Ethyl Caprylate	14.8	16.4
Ethyl Caprate	13.0	18.6
Ethyl Laurate	3.35	18.9
Ethyl Myristate	6.47	20.8
Ethyl Palmitate	7.32	19.8
Ethyl Stearate	12.4	54.6
Ethyl Oleate	8.68	24.8
Methyl Caprylate	4.67	6.27
Methyl Caprate	4.24	7.40
Methyl Laurate	3.66	7.85
Methyl Myristate	2.03	8.64
Methyl Palmitate	2.72	10.1
Methyl Stearate	4.88	10.3
Methyl Oleate	3.61	20.4
Methyl Linoleate	9.50	25.5

The CM method predicts the experimental data here measured with a global deviation of 4.53 % for FAMES with maximum deviations of 9.50 % while for FAEEs the average deviations are of 7.92 % with maximum deviations of 14.8 %.

The MG method is far less accurate with average deviations of 12.0 % and 23.5 % for FAMEs and FAEEs respectively and maximum deviations of 25.5 % and 54.6 %. While the CM method provides a good description of the viscosities the deviations for the FAEEs are clearly superior than for FAMEs, meaning that the inclusion of a methyl group affects the viscosities differently depending on its location as also observed for the densities. Moreover this model also provides poor estimates for the viscosities of unsaturated esters at high temperatures. This may be related with the use of Ceriani et al.³³ data on the estimation of the model parameters that, as discussed above, present large deviations from the data of other authors.

Conclusions

New experimental data for the density and viscosity of pure saturated and unsaturated methyl and ethyl esters in the temperature range (273 to 363) K and at atmospheric pressure are presented. An extensive critical review of the data available for these systems was carried out to identify spurious or poor quality data among the often conflicting data previously available in the literature.

The experimental data here reported were used to test predictive models for these properties. The liquid densities were compared with GCVOL model predictions to show that it is able to describe the FAMEs with deviations smaller than 1 %. However, larger deviations were found for the correlation of FAEEs densities and GCVOL model predicted values, presenting a maximum deviation from the experimental data of 1.5 %.

The Ceriani and Meirelles method is shown to be superior to the Marrero and Gani method with viscosity predictions with an average deviation of 4.53 % for FAMEs and 7.92 % for FAEEs.

Literature Cited

- (1). Leder, F.; Shapiro, J. N., This time it's different - An inevitable decline in world petroleum production will keep oil product prices high, causing military conflicts and shifting wealth and power from democracies to authoritarian regimes. *Energy Policy* **2008**, *36*, 2850-2852.
- (2). Hallock, J. L.; Tharakan, P. J.; Hall, C. A. S.; Jefferson, M.; Wu, W., Forecasting the limits to the availability and diversity of global conventional oil supply. *Energy* **2004**, *29*, 1673-1696.
- (3). Knothe, G.; Gerpen, J. V.; Krahl, J., Eds. *The Biodiesel Handbook*. 2005, AOCS Press, Champaign, Illinois.
- (4). Ashok Pandey, *Handbook of Plant-based Biofuels*. 2009: CRC Press Taylor & Francis Group.
- (5). Knothe, G., "Designer" Biodiesel: Optimizing fatty ester composition to improve fuel properties. *Energy Fuels* **2008**, *22*, 1358-1364.
- (6). Blangino, E.; Riveros, A. F.; Romano, S. D., Numerical expressions for viscosity, surface tension and density of biodiesel: analysis and experimental validation. *Phys. Chem. Liq.* **2008**, *46*, 527 - 547.
- (7). BS, *EN 14214 Automotive fuels - Fatty acid methyl esters (FAME) for diesel engines - Requirements and test methods*. 2009.
- (8). ASTM, *D6751 - 09 Standard Specification for Biodiesel Fuel Blend Stock (B100) for Middle Distillate Fuels*. 2009.
- (9). Dzida, M.; Prusakiewicz, P., The effect of temperature and pressure on the physicochemical properties of petroleum diesel oil and biodiesel fuel. *Fuel* **2008**, *87*, 1941-1948.
- (10). Frédéric Boudy; Seers, P., Impact of physical properties of biodiesel on the injection process in a common-rail direct injection system. *Energy Convers. Manage.* **2009**, *50*, 2905-2912.
- (11). Baroutian, S.; Aroua, M. K.; Raman, A. A. A.; Sulaiman, N. M. N., Density of palm oil-based methyl ester. *J. Chem. Eng. Data* **2008**, *53*, 877-880.
- (12). Goncalves, C. B.; Ceriani, R.; Rabelo, J.; Maffia, M. C.; Meirelles, A. J. A., Viscosities of Fatty Mixtures: Experimental Data and Prediction. *J. Chem. Eng. Data* **2007**, *52*, 2000-2006.
- (13). Ejim, C. E.; Fleck, B. A.; Amirfazli, A., Analytical study for atomization of biodiesels and their blends in a typical injector: Surface tension and viscosity effects. *Fuel* **2007**, *86*, 1534-1544.
- (14). Tat, M. E.; Van Gerpen, J. H., The specific gravity of biodiesel and its blends with diesel fuel. *J. Am. Oil Chem. Soc.* **2000**, *77*, 115-119.
- (15). Clements, L. D., *Blending rules for formulating biodiesel fuel*, in *Liquid Fuels and Industrial Products from Renewable Resources—Proceedings of the Third Liquid Fuel Conference* 1996, Nashville, TN.
- (16). Huber, M. L.; Lemmon, E. W.; Kazakov, A.; Ou, L. S.; Bruno, T. J., Model for the Thermodynamic Properties of a Biodiesel Fuel. *Energy Fuels* **2009**, *23*, 3790-3797.
- (17). Krisnangkura, K.; Yimsuwan, T.; Pairintra, R., An empirical approach in predicting biodiesel viscosity at various temperatures. *Fuel* **2006**, *85*, 107-113.

- (18). Yuan, W.; Hansen, A. C.; Zhang, Q., Predicting the temperature dependent viscosity of biodiesel fuels. *Fuel* **2009**, *88*, 1120-1126.
- (19). Allen, C. A. W.; Watts, K. C.; Ackman, R. G.; Pegg, M. J., Predicting the viscosity of biodiesel fuels from their fatty acid ester composition. *Fuel* **1999**, *78*, 1319-1326.
- (20). Elbro, H. S.; Fredenslund, A.; Rasmussen, P., Group Contribution Method for the Prediction of Liquid Densities as a Function of Temperature for Solvents, Oligomers, and Polymers. *Ind. Eng. Chem. Res.* **1991**, *30*, 2576-2582.
- (21). Marrero, J.; Gani, R., Group-contribution based estimation of pure component properties. *Fluid Phase Equilib.* **2001**, *183*, 183-208.
- (22). Conte, E.; Martinho, A.; Matos, H. A.; Gani, R., Combined Group-Contribution and Atom Connectivity Index-Based Methods for Estimation of Surface Tension and Viscosity. *Ind. Eng. Chem. Res.* **2008**, *47*, 7940-7954.
- (23). Ellison, S. L. R.; Rosslein, M.; Williams, A., *Quantifying Uncertainty in Analytical Measurement*. Second ed. 2000: Eurachem / CITAC.
- (24). Paredes, X.; Fandino, O.; Comunas, M. J. P.; Pensado, A. S.; Fernandez, J., Study of the effects of pressure on the viscosity and density of diisodecyl phthalate. *J. Chem. Thermodyn.* **2009**, *41*, 1007-1015.
- (25). Carvalho, P. J.; Regueira, T.; Santos, L. M. N. B. F.; Fernandez, J.; Coutinho, J. A. P., Effect of Water on the Viscosities and Densities of 1-Butyl-3-methylimidazolium Dicyanamide and 1-Butyl-3-methylimidazolium Tricyanomethane at Atmospheric Pressure. *J. Chem. Eng. Data* **2010**, *55*, 645-652.
- (26). Dorset, D. L., *Crystallography of the polymethylene chain*. 2005, New York: Oxford Science Press Inc.
- (27). Gardas, R. L.; Johnson, I.; Vaz, D. M. D.; Fonseca, I. M. A.; Ferreira, A. G. M., PVT property measurements for some aliphatic esters from (298 to 393) K and up to 35 MPa. *J. Chem. Eng. Data* **2007**, *52*, 737-751.
- (28). Subrahmanyam, V. R.; Gaikwad, B. R., Physical properties of n-Saturated Higher Fatty Alcohols in Liquid State. *J. Indian Chem. Soc.* **1988**, *65*, 266-268.
- (29). Ott, L. S.; Huber, M. L.; Bruno, T. J., Density and Speed of Sound Measurements on Five Fatty Acid Methyl Esters at 83 kPa and Temperatures from (278.15 to 338.15) K. *J. Chem. Eng. Data* **2008**, *53*, 2412-2416.
- (30). Bonhorst, C. W.; Althouse, P. M.; Triebold, H. O., Esters of Naturally Occurring Fatty Acids - Physical Properties of Methyl, Propyl, And Isopropyl Esters of C-6 to C-18 Saturated Fatty Acids *Ind. Eng. Chem.* **1948**, *40*, 2379-2384.
- (31). Gouw, T. H.; Vlugter, J. C., Physical Properties of Fatty Acid Methyl Esters .I. Density + Molar Volume. *J. Am. Oil Chem. Soc.* **1964**, *41*, 142-145.
- (32). Gros, A. T.; Feuge, R. O., Surface and Interfacial Tensions, Viscosities, and Other Physical Properties of Some n-Aliphatic Acids and their Methyl and Ethyl Esters. *J. Am. Oil Chem. Soc.* **1952**, *29*, 313.
- (33). Ceriani, R.; Goncalves, C. B.; Rabelo, J.; Caruso, M.; Cunha, A. C. C.; Cavaleri, F. W.; Batista, E. A. C.; Meirelles, A. J. A., Group Contribution Model for Predicting Viscosity of Fatty Compounds. *J. Chem. Eng. Data* **2007**, *52*, 965-972.
- (34). Boelhouwer, J. W. M.; Nederbragt, G. W.; Verberg, G., Viscosity data of organic liquids *Appl. Sci. Res.* **1950**, *2*, 249-268.
- (35). Liew, K. Y.; Seng, C. E., Molal Volumes of Some N-Fatty Acids and Their Methyl and Ethyl-Esters. *J. Am. Oil Chem. Soc.* **1992**, *69*, 734-740.

- (36). Liew, K. Y.; Seng, C. E.; Oh, L. L., Viscosities and Densities of the Methyl-Esters of Some N-Alkanoic Acids. *J. Am. Oil Chem. Soc.* **1992**, *69*, 155-158.
- (37). Postigo, M. A.; Garcia, P. H.; Ortega, J.; Tardajos, G., Excess Molar Volumes of Binary-Mixtures Containing a Methyl-Ester (Ethanoate to Tetradecanoate) with Odd N-Alkanes at 298.15-K. *J. Chem. Eng. Data* **1995**, *40*, 283-289.
- (38). Knegtel, J. T.; Boelhouwer, C.; Tels, M.; Waterman, H. I., Shifting of the Double Bond in Methyl Oleate during Hydrogenation. *J. Am. Oil Chem. Soc.* **1957**, *34*, 336-337.
- (39). Wheeler, D. H.; Riemenschneider, R. W., The Preparation and Properties of Highyl Purified Methyl Oleate. *Oil Soap* **1939**, *16*, 207-209.
- (40). Liao, W. R.; Tang, M.; Chen, Y. P., Densities and viscosities of butyl acrylate plus 1-butanol and ethyl laurate plus 1-butanol at 293.15, 303.15, and 313.15 K. *J. Chem. Eng. Data* **1998**, *43*, 826-829.
- (41). Shigley, J.; Bonhorst, C.; Liang, P.; Althouse, P.; Triebold, H., Physical characterization of a) a series of ethyl esters and b) a series of ethanoate esters. *J. Am. Oil Chem. Soc.* **1955**, *32*, 213-215.
- (42). Hwu, W. H.; Cheng, J. S.; Cheng, K. W.; Chen, Y. P., Vapor-liquid equilibrium of carbon dioxide with ethyl caproate, ethyl caprylate and ethyl caprate at elevated pressures. *J. Supercrit. Fluid* **2004**, *28*, 1-9.
- (43). Sobotka, H.; Kahn, J., Determination of solubility of sparingly soluble liquids in water. *J. Am. Chem. Soc.* **1931**, *53*, 2935-2938.
- (44). Baker, W. O.; Smyth, C. P., The possibility of molecular rotation in the solid forms of cetyl alcohol and three long-chain ethyl esters. *J. Am. Chem. Soc.* **1938**, *60*, 1229-1236.
- (45). Francesconi, R.; Comelli, F., Excess molar enthalpies of binary mixtures containing acetic or propionic acid plus eight ethyl alkanoates at 298.15 K. *Thermochim Acta* **1998**, *322*, 63-68.
- (46). Lide, D.; Frederikse, H., *Handbook of chemistry and physics*. 80th ed. Boca Raton. 1999, FL: CRC Press.
- (47). Ruhoff, J. R.; Reid, E. E., A group of isomeric esters. *J. Am. Chem. Soc.* **1933**, *55*, 3825-3828.
- (48). Knothe, G.; Steidley, K. R., Kinematic viscosity of biodiesel components (fatty acid alkyl esters) and related compounds at low temperatures. *Fuel* **2007**, *86*, 2560-2567.

***Densities and Viscosities of Minority Fatty Acid Methyl and Ethyl
Esters Present in Biodiesel***

Journal of Chemical & Engineering Data, **2011**, 56, 2175-2180.

DOI: 10.1021/je1012235.

Densities and Viscosities of Minority Fatty Acid Methyl and Ethyl Esters Present in Biodiesel

Maria Jorge Pratas, Samuel Freitas, Mariana B. Oliveira, Sílvia C. Monteiro[#],

Álvaro S. Lima[§], João A.P. Coutinho

CICECO, Chemistry Department, University of Aveiro, Campus de Santiago, 3810–193
Aveiro, Portugal;

[#]Polytechnic Institute of Leiria, Leiria, Morro do Lena – Alto Vieiro, 2411-901 Leiria,
Portugal;

[§] Universidade Tiradentes, Av. Murilo Dantas 300, Farolândia, Aracaju-SE, Brasil.

Abstract

Biodiesel has several known components in their composition. The majority components are well described in literature but minority components are poorly characterized. These are however required to develop reliable models to predict the biodiesel behavior. This work considers minor components of biodiesel: the polyunsaturated compounds (in C18), the mono unsaturated (in C16, C20 and C22) and the long chain saturated esters. In this work densities and viscosities of pure fatty acid esters minor components of biodiesel fuel were measured (three ethyl esters and seven methyl esters), at atmospheric pressure and temperatures from (273.15 to 373.15) K. Correlations for the densities and viscosities with temperature are proposed. Three predictive models were evaluated in the prediction of densities and viscosities of the pure ethyl and methyl esters here reported. The GCVOL group contribution method is shown to be able to predict densities for these compounds within 1.5 %. The methods of Ceriani et al. (CM) and of Marrero et al. (MG) were applied to the viscosity data. The first show a better predictive capacity to provide a fair description of the viscosities of the minority esters here studied.

Keywords: Biodiesel, Density, Fatty Acid Methyl Esters, Fatty Acid Ethyl Esters, Viscosity.

Introduction

Nowadays, biodiesel fuel is seen as an alternative to the conventional petroleum based fuels, reducing the dependency on fossil fuels and controlling green house gases emissions.¹ Biodiesel fuel advantages and applications are well established.²⁻⁹ This biofuel is comprised of mono-alkyl esters of fatty acids derived from vegetable oils, animal fats, or mixtures of them. It is usually produced by the transesterification reaction of triglycerides with a short chain alcohol, usually methanol or ethanol, in presence of a catalyst, leading to the formation of mixtures of fatty acid methyl esters (FAMES) or fatty acid ethyl esters (FAEEs), respectively.^{7, 9} The main components of biodiesel fuel depend on the raw materials used and, consequently, a wide range of esters can be present.¹⁰ Knowing the profile of methyl or ethyl esters in biodiesel is of great importance as it controls its main properties.¹⁰

The fuel density influences the amount of mass injected at the injection systems, pumps and injectors.¹¹⁻¹² An amount of fuel precisely adjusted is necessary to provide proper combustion.¹³ Combustion is initialized through atomization of the fuel. The use of a viscous fuel leads to a poor atomization which is responsible of premature injector cooking and poor fuel combustion.^{11, 14}

Densities and viscosities data are well established for the more important biodiesel compounds, however some of the minor components have received little attention in the past. However, they may have a non negligible influence on the biodiesel fuel properties and, depending on the raw material used, these components can be present in a significant concentration.

The main goal of this work is to present new density and viscosity data for the minority components of biodiesel fuel such as methyl palmitoleate, methyl linolenate, methyl arachidate, methyl gadoleate, methyl behenate, methyl erucate, methyl lignocerate, ethyl linoleate, ethyl linolenate, and ethyl arachidate, at atmospheric pressure and temperatures from (273.15 to 363.15) K. Some of these esters can be found in biodiesel fuel from peanut, rapeseed or canola oils.⁹

Among the studied esters, density data with temperature has been found only for methyl linolenate. Ott et al.¹⁵ compiled the available density data. Besides the seven points reported by them only Gouw and Vlугter¹⁶ measured two other data points, in

1964. For the other esters some isolated density data were obtained from the compound's supplier.

As experimental measurements are time consuming and expensive, especially for these minority biodiesel esters components, new models are necessary to predict these properties.

Several models have been proposed in the literature to estimate biodiesel fuel density and viscosity. The most important among them rely on the accurate knowledge of the properties of the pure compounds.¹⁷ However, the scarcity of density and viscosity data available in the literature restricts the use of these models to predict properties for biodiesel fuel. In a previous work¹⁷, the densities and viscosities of common pure methyl and ethyl esters were measured and used to evaluate the performance of three predictive models. For prediction of density the group contribution method GCVOL¹⁸ model was evaluated while the models of Ceriani et al.¹⁹ and Marrero et al.²⁰ were tested for the viscosity. The behavior of these models is here compared against the data for the compounds here studied.

Experimental Section

Materials and Procedure. Three ethyl ester and seven methyl esters were used in this study. Table 1 reports the name, purity, supplier, and CAS number of each compound used in this study. Compound purity was confirmed by gas chromatography/flame ionization detection (GC-FID).

Experimental Measurements. Measurements of viscosity and density were performed in the temperature range of (273.15 to 373.15) K, or above melting point for saturated compounds, at atmospheric pressure using an automated SVM 3000 Anton Paar rotational Stabinger viscometer-densimeter. The viscometer is based on a tube filled with the sample in which floats a hollow measuring rotor. Because of its low density, the rotor is centered in the heavier liquid by buoyancy forces. Consequently, a measuring gap is formed between the rotor and the tube. The rotor is forced to rotate by shear stresses in the liquid and is guided axially by a built-in permanent magnet, which interacts with a soft iron ring. The rotating magnetic field delivers the speed signal and induces Eddy currents in the surrounding copper casing. These eddy currents are

proportional to the speed of the rotor and exert a retarding torque on the rotor. Two different torques influence the speed of the measuring rotor, and at the equilibrium, the two torques are equal and the viscosity can be traced back to a single speed measurement. The SVM 3000 uses Peltier elements for fast and efficient thermostability. The temperature uncertainty is 0.02 K from (288.15 to 378.15) K. The absolute uncertainty of the density is $0.0005 \text{ g}\cdot\text{cm}^{-3}$ and the relative uncertainty of the dynamic viscosity obtained is less than 0.5 % for the standard fluid SHL120 (SH Calibration Service GmbH), in the range of the studied temperatures. Further details about the equipment and method can be found elsewhere.²¹ This viscometer was previously tested for other compounds and presented a very good reproducibility.^{17, 22}

Results and Discussion

Density. The experimental data obtained are reported in Table 2. For ethyl and methyl arachidate, methyl behenate, and methyl lignocerate the measurements were only carried out at temperatures above the melting point of these compounds.

Table 2. Experimental Density, in kg · m⁻³, for Ethyl and Methyl Esters

<i>T</i> / K	Ethyl			Methyl						
	Linoleate	Linolenate	Arachidate	Palmitoleate	Linolenate	Arachidate	Gadoleate	Behenate	Erucate	Lignocerate
278.15	893.8	904.6		880.4	913.2		884.8		881.6	
283.15	890.0	900.8		876.6	909.5		881.1		877.9	
288.15	886.3	897.0		872.8	905.7		877.5		874.3	
293.15	882.6	893.3		869.0	901.9		873.8		870.7	
298.15	878.8	889.5		865.2	898.2		870.2		867.1	
303.15	875.2	885.8		861.4	894.5		866.6		863.6	
308.15	871.5	882.0		857.6	890.7		863		860.0	
313.15	867.8	878.3		853.8	887.0		859.5		856.5	
318.15	864.2	874.6	841.2	850.0	883.3		855.9		853.0	
323.15	860.6	870.9	837.7	846.3	879.6	842.3	852.3		849.4	
328.15	856.9	867.2	834.1	842.5	876.0	838.7	848.8		845.9	
333.15	853.3	863.5	830.5	838.7	872.3	834.9	845.2	834.5	842.4	
338.15	849.7	859.9	827.0	834.9	868.6	831.4	841.7	831.0	839.0	830.5
343.15	846.0	856.2	823.5	831.1	864.9	827.8	838.2	827.5	835.5	827.1
348.15	842.4	852.5	820.0	827.3	861.2	824.3	834.6	824.1	832.0	823.7
353.15	838.8	848.9	816.6	823.5	857.6	820.8	831.1	820.6	828.6	820.3
358.15	835.2	845.3	813.2	819.8	853.9	817.3	827.6	817.2	825.1	816.9
363.15	831.6	841.6	809.7	816.0	850.3	813.8	824.1	813.7	821.7	813.5
368.15		838.0	806.1			810.4	820.7	810.3		810.1
373.15		834.5	802.4			807.0	817.3	806.9		806.8

In Figure 1 deviations from experimental values and available data were presented. Methyl linolenate is the only compound for which data is available in a wide temperature range¹⁵ presenting a deviation of 0.3 % against the experimental data here reported. For some of the other compounds only the supplier data were available to compare with measured data²³. A few isolated points for erucate methyl ester¹⁶ and linoleate ethyl ester²⁴ were also identified. The relative deviations of these data are less than 2%.

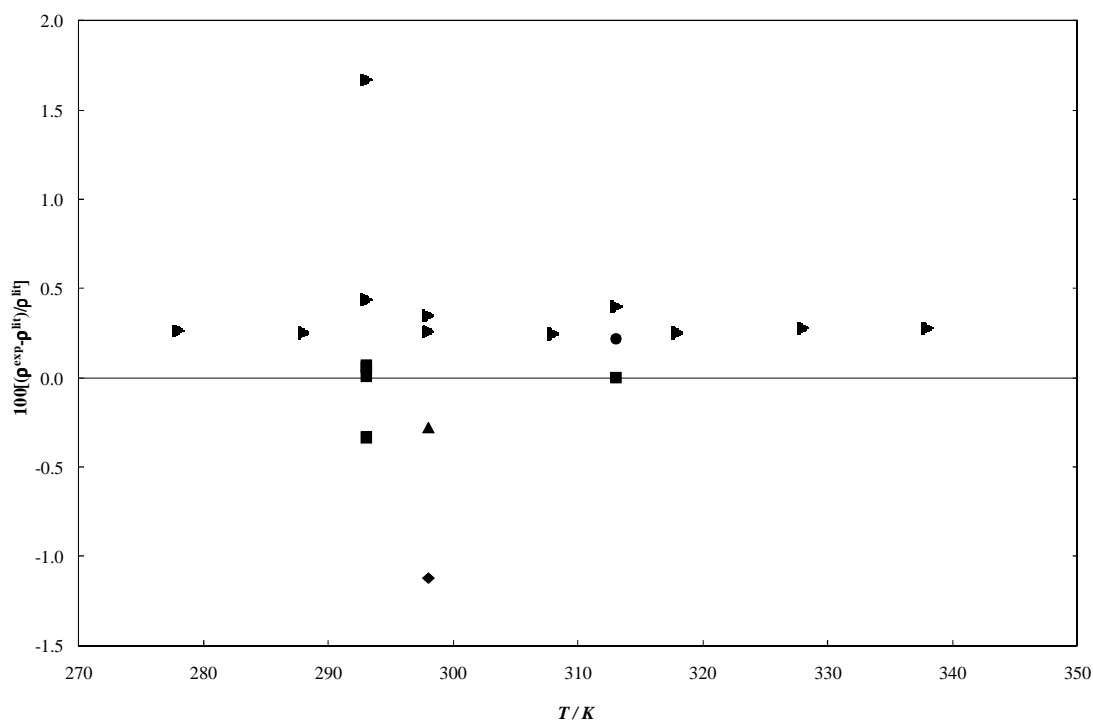


Figure 1. Relative deviation of methyl and esters density data available in the literature^{15-16, 23-24} as a function of temperature: ●, ethyl linoleate; ▲, ethyl linolenate; ◆, methyl palmitoleate; ▶, methyl linolenate; and ■, methyl erucate. Zero line is this work's experimental data.

A linear temperature dependency using an optimized algorithm based on the least-squares method was used to correlate the experimental density data measured, and the parameter values along with their confidence limits are reported in Table 3. This approach was already adopted previously for common pure methyl and ethyl esters.¹⁷

$$\rho/\text{kg} \cdot \text{m}^{-3} = b \cdot T/\text{K} + a \quad (1)$$

Table 3. Density Linear Temperature Correlation Constants (Equation 1) for Pure Methyl and Ethyl Esters over the Temperature Range (278.15 to 373.15) K, and Corresponding 95 % Confidence Limits

	$b / \text{kg} \cdot \text{m}^{-3} \cdot \text{K}^{-1}$	$\pm t \cdot s_b$	$a / \text{kg} \cdot \text{m}^{-3}$	$\pm t \cdot s_A$	t	AAD %
Ethyl Linoleate	-0.7307	0.002	1096.8	0.7	2.1	0.01
Ethyl Linolenate	-0.7406	0.003	1109.7	0.7	2.1	0.08
Ethyl Arachidate	-0.7015	0.004	1064.3	1.3	2.4	0.01
Methyl Palmitoleate	-0.7577	0.001	1091.1	0.2	2.1	0.003
Methyl Linolenate	-0.7401	0.002	1118.9	0.6	2.4	0.009
Methyl Arachidate	-0.7117	0.002	1070.2	0.8	2.1	0.24
Methyl Gadoleate	-0.7133	0.001	1082.2	0.2	2.4	0.09
Methyl Behenate	-0.6900	0.003	1064.3	0.9	2.1	0.004
Methyl Erucate	-0.7038	0.003	1077.0	1.0	2.1	0.01
Methyl Lignocerate	-0.6783	0.002	1059.9	0.8	2.2	0.006

s - standard deviation

A number of models to describe the density can be found in literature, often based on the Racket equation^{12, 25-27}, but since they require experimental data adjusted parameters they are not predictive.

The group contribution method GCVOL model¹⁸ was here used to predict the molar volumes and the densities of the compounds studied in this work. Figures 2 and 3 show GCVOL deviations on the density property predicted for FAEEs and FAMEs, respectively, where unsaturated esters are represented by full symbols and saturated by empty symbols. The results reported that the densities of FAME and FAEE can be predicted within a deviation of ± 1.5 %, with exception of linolenate esters for higher temperatures due to a poor model description of the poliunsaturation effect on the densities.

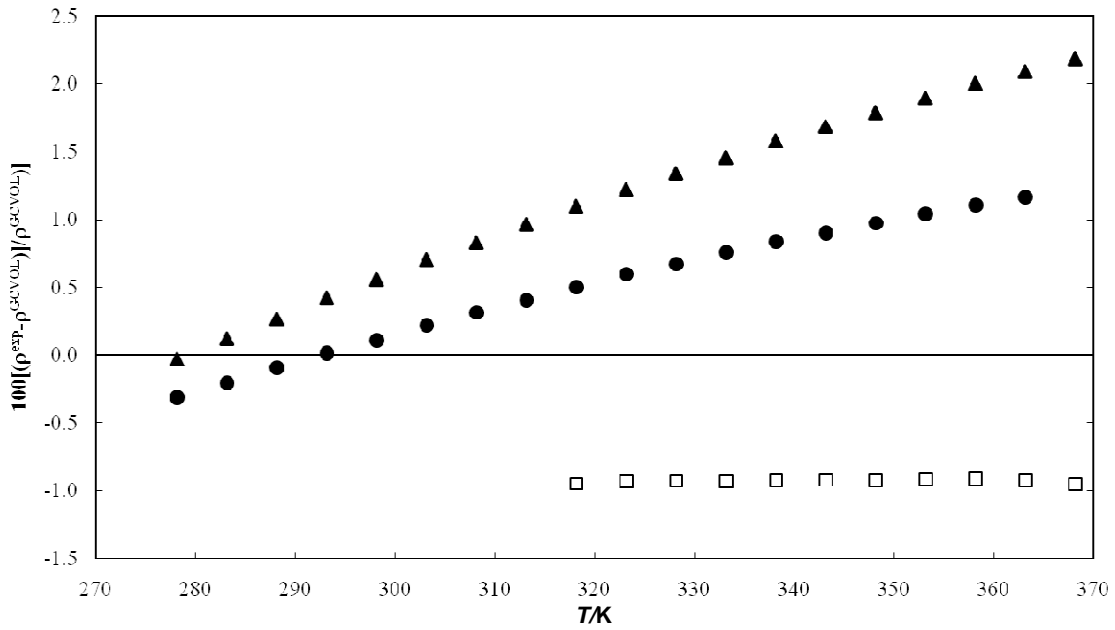


Figure 2. Relative deviations between density of ethyl esters predicted by GCVOL and this work's experimental data as function of temperature: ●, ethyl linoleate; ▲, ethyl linolenate; and □, ethyl arachidate.

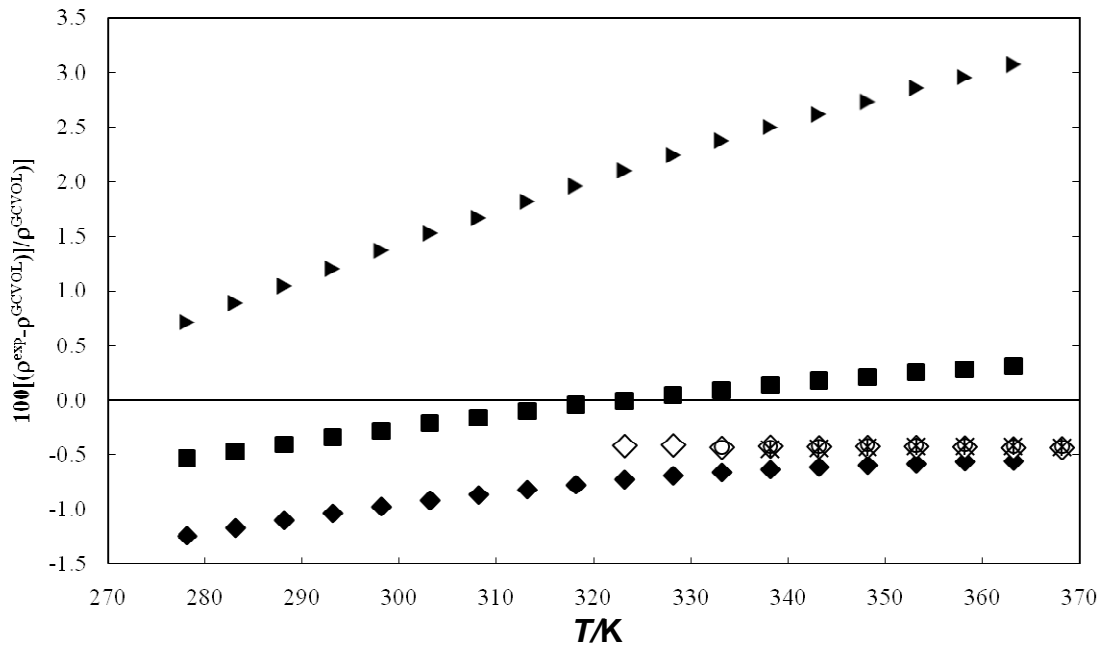


Figure 3. Relative deviations between density of methyl esters predicted by GCVOL and this work's experimental data as function of temperature: ◆, methyl palmitoleate; ►, methyl linolenate; ◇, methyl arachidate; ★, methyl gadoleate; ○, methyl behenate; ■, methyl erucate; and *, methyl lignoceric.

The isobaric expansivity coefficient at constant pressure (α_p) is defined as

$$\alpha_p = -\left(\frac{\partial \ln \rho}{\partial T}\right)_p \quad (2)$$

The logarithm of density exhibits a linear behavior with temperature in the studied temperature range. The isobaric expansivities estimated from the experimental data are reported in Table 4.

Table 4. Isobaric Expansivities, α_p , for the Studied Fatty Acid Esters, and Corresponding 95 % Confidence Limits

	$\alpha_p \cdot 10^3 / \text{K}^{-1} \pm t \cdot s(\alpha_p) \cdot 10^3$	
Ethyl Linoleate	0.847	0.002
Ethyl Linolenate	0.850	0.002
Ethyl Arachidate	0.854	0.003
Methyl Palmitoleate	0.894	0.005
Methyl Linolenate	0.840	0.002
Methyl Arachidate	0.860	0.002
Methyl Gadoleate	0.836	0.001
Methyl Behenate	0.841	0.001
Methyl Erucate	0.827	0.001
Methyl Lignocerate	0.829	0.001

s - standard deviation

Viscosity

The experimental data of viscosity of several minority esters here studied are reported in Table 5. As observed in a previous work¹⁷ the viscosity of all esters increases with the ester chain length and decreases with the level of unsaturation.

Table 5. Experimental Viscosities, in mPa · s, for Fatty Acid Ethyl and Methyl Esters

<i>T</i> / K	Ethyl			Methyl						
	Linoleate	Linolenate	Arachidate	Palmitoleate	Linolenate	Arachidate	Gadoleate	Behenate	Erucate	Lignocerate
278.15	8.1875	6.2820		6.1685	6.3612		14.340		18.087	
283.15	7.0842	5.5379		5.3667	5.6183		11.975		14.943	
288.15	6.1652	4.9210		4.6617	5.0032		10.131		12.556	
293.15	5.4231	4.4014		4.1075	4.4844		8.6667		10.657	
298.15	4.8073	3.9606		3.6471	4.0429		7.4879		9.1414	
303.15	4.3074	3.5831		3.2886	3.6665		6.5284		7.9069	
308.15	3.8539	3.2578		2.9430	3.3405		5.7379		6.9171	
313.15	3.4060	2.9750		2.6162	2.9253		5.0803		5.9575	
318.15	3.1608	2.7281	5.6573	2.4218	2.6750		4.5289		5.4021	
323.15	2.8291	2.5114	4.9733	2.1751	2.4725	4.8319	4.0624		4.7602	
328.15	2.6411	2.3204	4.5070	2.0304	2.3030	4.3226	3.6649		4.3306	
333.15	2.4287	2.1511	4.0577	1.8697	2.1234	3.8888	3.3231	4.7493	3.9100	
338.15	2.2414	2.0004	3.6714	1.7275	1.9659	3.5170	3.0278	4.2736	3.5480	5.1392
343.15	2.0753	1.8658	3.3373	1.5945	1.8165	3.1964	2.7709	3.8657	3.2344	4.6279
348.15	1.9270	1.7450	3.0462	1.4822	1.6878	2.9177	2.5461	3.5133	2.9609	4.1894
353.15	1.7727	1.6362	2.7799	1.3656	1.5827	2.6745	2.3484	3.2066	2.7070	3.8102
358.15	1.6757	1.5382	2.5690	1.2898	1.4877	2.4612	2.1736	2.9392	2.5097	3.4797
363.15	1.5685	1.4491	2.3716	1.2070	1.4021	2.2726	2.0186	2.7087	2.3223	3.1895
368.15		1.3684	2.1961		1.3272	2.1066	1.8807	2.5020		2.9327
373.15		1.2950	2.0395		1.2527	1.9591	1.7576	2.3169		2.7066

To better ascertain the experimental data of viscosity here measured, these were compared with literature data as shown in Figure 4. Unfortunately the comparison limited due to the lack of viscosity data in literature for the esters here studied. Only viscosities of four FAMES and one FAEE²⁸⁻³¹ were found and used on this comparison. The relative deviations observed reached a maximum deviation of 15 % against the data by Meirelles et al.¹⁹ as discussed in a previous work¹⁷ these deviations must be due to experimental problems on the data reported by the authors.

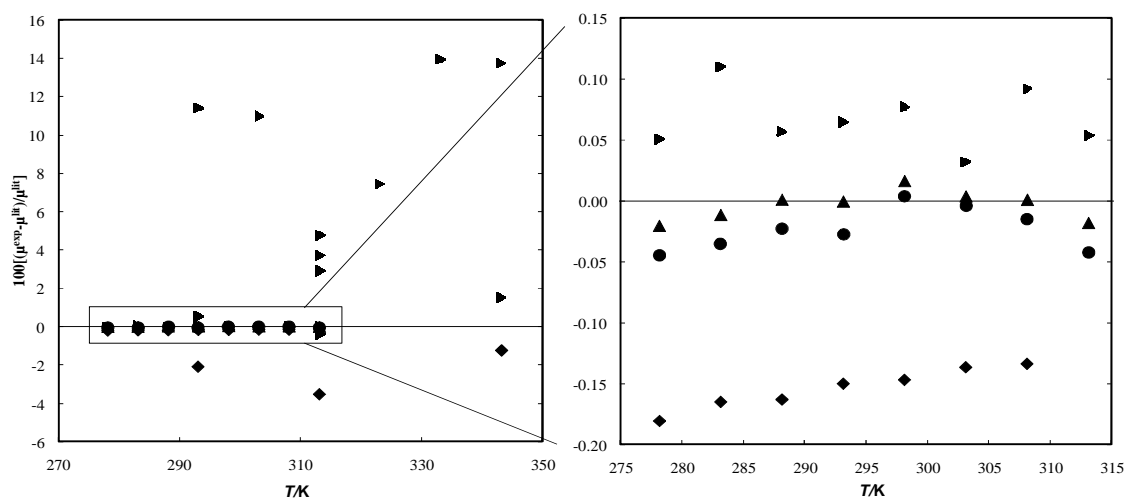


Figure 4. Relative deviation of methyl and esters dynamic viscosity data available in the literature²⁸⁻³¹ as a function of temperature: ●, ethyl linoleate; ▲, ethyl linolenate; ◆, methyl palmitoleate; ►, methyl linolenate; and, ■, methyl erucate. Zero line is this work's experimental data.

The Vogel Tammann-Fulcher equation (3) was used to describe the experimental viscosities as a function of temperature.

$$\mu/\text{mPa}\cdot\text{s} = \exp\left(A + \frac{B}{(T/\text{K} - T_0)}\right) \quad (3)$$

where A, B and T_0 are fitting parameters whose values were estimated using an optimization algorithm based on the least-squares method. The values of the parameters in conjunction with their uncertainty and the average absolute deviations (AAD %) of the correlation are reported in Table 6. The results show that the VTF equation provides a good description of the experimental data of viscosity with a maximum value of AAD of 0.52 %.

Table 6. Vogel Tammann-Fulcher Equation Constants for Pure Ethyl and Methyl Esters over the Temperature Range (278.15 to 373.15) K, and Corresponding 95 % Confidence Limits

	A	±	t. s_A	B / K	±	t. s_B	T_0 / K	±	t. s_{T_0}	AAD* (%)
Ethyl Linoleate	-2.54		0.23	715.05		88.3	124.13		11.7	0.49
Ethyl Linolenate	-2.67		0.46	795.17		202	101.67		24.5	0.053
Ethyl Arachidate	-2.90		0.23	906.95		92.0	122.33		12.0	0.22
Methyl Palmitoleate	-2.87		0.35	748.28		159	118.44		19.8	0.52
Methyl Linolenate	-3.00		0.12	904.38		48.4	91.88		6.42	0.74
Methyl Arachidate	-2.72		0.02	806.47		7.20	135.35		0.938	0.0070
Methyl Gadoleate	-2.54		0.02	733.80		7.22	137.19		0.877	0.071
Methyl Behenate	-2.53		0.15	768.64		52.3	145.06		6.17	0.036
Methyl Erucate	-2.41		0.12	715.39		52.4	143.27		6.26	0.38
Methyl Lignocerate	-2.87		0.022	951.53		9.76	127.00		1.32	0.021

s -standard deviation

$$* AAD = \frac{1}{N_p} \sum_{i=1}^{N_p} ABS \left[\frac{(exp_i - calc_i)}{calc_i} \right] \times 100$$

The Ceriani et al.¹⁹ (CM) and the Marrero et al.³² (MG) group contribution models were evaluated against the viscosity data here measured. The deviations between the experimental and predicted viscosities are shown in Table 7. The CM model presented an overall deviation of 11.9 % for all minority esters studied with the maximum deviations of 21.7 % for ethyl linolenate and 25.9 % for methyl linolenate respectively. These deviations denote some limitations of CM model in predicting viscosity of the unsaturated esters. The MG method is much less accurate with an overall AAD of 25.7 %, and large deviations for all minority esters.

Table 7. Absolute Average Deviation between the Measured Viscosity of Pure Ethyl and Methyl Esters over the Temperature Range (278.15 to 373.15) K and those Estimated by CM and MG Models

	CM (%)	MG (%)
Ethyl Linoleate	7.84	29.5
Ethyl Linolenate	21.7	31.0
Ethyl Arachidate	17.3	23.5
Methyl Palmitoleate	5.95	24.1
Methyl Linolenate	25.9	18.4
Methyl Arachidate	11.8	13.4
Methyl Gadoleate	9.30	25.9
Methyl Behenate	18.2	44.3
Methyl Erucate	0.250	27.5
Methyl Lignocerate	0.270	19.5
Overall AAD	11.9	25.7

Conclusions

New experimental data for the densities and viscosities of pure saturated and unsaturated methyl and ethyl esters from minority biodiesel fuel composition, in the temperature range (273 to 363) K and at atmospheric pressure are presented. New correlations of the density and viscosity dependency with temperature are also proposed. The experimental data here reported were used to test density and viscosity predictive models.

The GCVOL model predictions were compared with the experimental liquid densities to show that it is able to describe the FAMES and FAEEs densities with deviations smaller than 1 % for saturated compounds and 2 % for unsaturated.

The Ceriani et al. method showed to be superior to the Marrero et al. method in terms of predictive ability for viscosities, presenting an overall average deviation of 11.9 % for all minority esters here studied.

Literature Cited

- (1) Ma, F. R.; Hanna, M. A. Biodiesel production: a review. *Bioresour. Technol.* **1999**, *70*, 1-15.
- (2) Demirbas, A. Political, economic and environmental impacts of biofuels: A review. *Appl. Energy* **2009**, *86*, S108-S117.
- (3) Demirbas, M. F.; Balat, M. Recent advances on the production and utilization trends of bio-fuels: A global perspective. *Energy Convers. Manage.* **2006**, *47*, 2371-2381.
- (4) Pinzi, S.; Garcia, I. L.; Lopez-Gimenez, F. J.; de Castro, M. D. L.; Dorado, G.; Dorado, M. P. The Ideal Vegetable Oil-based Biodiesel Composition: A Review of Social, Economical and Technical Implications. *Energy Fuels* **2009**, *23*, 2325-2341.
- (5) Fukuda, H.; Kondo, A.; Noda, H. Biodiesel fuel production by transesterification of oils. *J. Biosci. Bioeng.* **2001**, *92*, 405-416.
- (6) Karaosmanoglu, F. Vegetable oil fuels: A review. *Energy Sources* **1999**, *21*, 221-231.
- (7) Ashok Pandey *Handbook of Plant-based Biofuels*; CRC Press Taylor & Francis Group: Boca Raton, 2009.
- (8) Demirbas, A. *Biodiesel: A Realistic Fuel Alternative for Diesel Engines*; Springer-Verlag London Limited: Turkey, 2008.
- (9) Knothe, G.; Gerpen, J. V.; Krahl, J. *The Biodiesel Handbook*; AOCS Press: Illinois, 2005.
- (10) Blangino, E.; Riveros, A. F.; Romano, S. D. Numerical expressions for viscosity, surface tension and density of biodiesel: analysis and experimental validation. *Phys. Chem. Liq.* **2008**, *46*, 527 - 547.
- (11) Boudy, F.; Seers, P. Impact of physical properties of biodiesel on the injection process in a common-rail direct injection system. *Energy Convers. Manage.* **2009**, *50*, 2905-2912.
- (12) Baroutian, S.; Aroua, M. K.; Raman, A. A. A.; Sulaiman, N. M. N. Density of palm oil-based methyl ester. *J. Chem. Eng. Data* **2008**, *53*, 877-880.
- (13) Dzida, M.; Prusakiewicz, P. The effect of temperature and pressure on the physicochemical properties of petroleum diesel oil and biodiesel fuel. *Fuel* **2008**, *87*, 1941-1948.
- (14) Ejim, C. E.; Fleck, B. A.; Amirfazli, A. Analytical study for atomization of biodiesels and their blends in a typical injector: Surface tension and viscosity effects. *Fuel* **2007**, *86*, 1534-1544.
- (15) Ott, L. S.; Huber, M. L.; Bruno, T. J. Density and Speed of Sound Measurements on Five Fatty Acid Methyl Esters at 83 kPa and Temperatures from (278.15 to 338.15) K. *J. Chem. Eng. Data* **2008**, *53*, 2412-2416.
- (16) Gouw, T.; Vlugter, J. Physical properties of fatty acid methyl esters. I. density and molar volume. *J. Am. Oil Chem. Soc.* **1964**, *41*, 142-145.
- (17) Pratas, M. J.; Freitas, S.; Oliveira, M. B.; Monteiro, S. C.; Lima, A. S.; Coutinho, J. A. P. Densities and Viscosities of Fatty Acid Methyl and Ethyl Esters. *J. Chem. Eng. Data* **2010**, *55*, 3983-3990.
- (18) Elbro, H. S.; Fredenslund, A.; Rasmussen, P. Group Contribution Method for the Prediction of Liquid Densities as a Function of Temperature for Solvents, Oligomers, and Polymers. *Ind. Eng. Chem. Res.* **1991**, *30*, 2576-2582.

- (19) Ceriani, R.; Goncalves, C. B.; Rabelo, J.; Caruso, M.; Cunha, A. C. C.; Cavaleri, F. W.; Batista, E. A. C.; Meirelles, A. J. A. Group Contribution Model for Predicting Viscosity of Fatty Compounds. *J. Chem. Eng. Data* **2007**, *52*, 965-972.
- (20) Marrero, J.; Gani, R. Group-contribution based estimation of pure component properties. *Fluid Phase Equilib.* **2001**, *183*, 183-208.
- (21) Paredes, X.; Fandino, O.; Comunas, M. J. P.; Pensado, A. S.; Fernandez, J. Study of the effects of pressure on the viscosity and density of diisodecyl phthalate. *J. Chem. Thermodyn.* **2009**, *41*, 1007-1015.
- (22) Carvalho, P. J.; Regueira, T.; Santos, L. M. N. B. F.; Fernandez, J.; Coutinho, J. A. P. Effect of Water on the Viscosities and Densities of 1-Butyl-3-methylimidazolium Dicyanamide and 1-Butyl-3-methylimidazolium Tricyanomethane at Atmospheric Pressure. *J. Chem. Eng. Data* **2010**, *55*, 645-652.
- (23) Sigma Aldrich, www.sigmaaldrich.com, 2010.
- (24) Smith, R. L.; Yamaguchi, T.; Sato, T.; Suzuki, H.; Arai, K. Volumetric behavior of ethyl acetate, ethyl octanoate, ethyl laurate, ethyl linoleate, and fish oil ethyl esters in the presence of supercritical CO₂. *J. Supercrit. Fluids* **1998**, *13*, 29-36.
- (25) Veny, H.; Baroutian, S.; Aroua, M. K.; Hasan, M.; Raman, A. A.; Sulaiman, N. M. N. Density of *Jatropha curcas* Seed Oil and its Methyl Esters: Measurement and Estimations. *Int. J. Thermophys.* **2009**, *30*, 529-541.
- (26) Blangino, E.; Riveros, A. F.; Romano, S. D. Numerical expressions for viscosity, surface tension and density of biodiesel: analysis and experimental validation. *Phys. Chem. Liq.* **2008**, *46*, 527-547.
- (27) Baroutian, S.; Aroua, M. K.; Raman, A. A. A.; Sulaiman, N. M. N. Densities of ethyl esters produced from different vegetable oils. *J. Chem. Eng. Data* **2008**, *53*, 2222-2225.
- (28) Yuan, W.; Hansen, A. C.; Zhang, Q. Predicting the temperature dependent viscosity of biodiesel fuels. *Fuel* **2009**, *88*, 1120-1126.
- (29) Knothe, G.; Steidley, K. R. Kinematic viscosity of biodiesel components (fatty acid alkyl esters) and related compounds at low temperatures. *Fuel* **2007**, *86*, 2560-2567.
- (30) Knothe, G. "Designer" Biodiesel: Optimizing Fatty Ester Composition to Improve Fuel Properties. *Energy Fuels* **2008**, *22*, 1358-1364.
- (31) Allen, C. A. W.; Watts, K. C.; Ackman, R. G.; Pegg, M. J. Predicting the viscosity of biodiesel fuels from their fatty acid ester composition. *Fuel* **1999**, *78*, 1319-1326.
- (32) Conte, E.; Martinho, A.; Matos, H. A.; Gani, R. Combined Group-Contribution and Atom Connectivity Index-Based Methods for Estimation of Surface Tension and Viscosity. *Ind. Eng. Chem. Res.* **2008**, *47*, 7940-7954.

***Biodiesel Density: Experimental Measurements and Prediction
Models***

Energy & Fuel, **2011**, 25, 2333-2340.

DOI:10.1021/ef2002124

Biodiesel Density: Experimental Measurements and Prediction Models

Maria Jorge Pratas, Samuel V.D. Freitas, Mariana B. Oliveira, Sílvia C. Monteiro[#],

Álvaro S. Lima[§] João A.P. Coutinho

CICECO, Chemistry Department, University of Aveiro, Campus de Santiago, 3810–193

Aveiro, Portugal;

[#]Polytechnic Institute of Leiria, Leiria, Morro do Lena – Alto Vieiro, 2411-901 Leiria,

Portugal;

[§] Universidade Tiradentes, Av. Murilo Dantas 300, Farolândia, Aracaju-SE, Brasil

Abstract

Density is an important biodiesel parameter with impact on fuel quality. Predicting density is of high relevance for a correct formulation of an adequate blend of raw materials that optimize the cost of biodiesel fuel production while allowing the produced fuel to meet the required quality standards. The aim of this work is to present new density data for different biodiesels and use the reported data to evaluate the predictive capability of models previously proposed to predict biodiesel or fatty acid methyl esters densities. Densities were measured here for ten biodiesel samples, for which detailed composition is reported, at atmospheric pressure and temperatures from 278.15 to 373.15 K. Density dependence with temperature correlations was proposed for the biodiesels and isobaric expansivities are presented. The new experimental data here presented were used, along with other literature data, to evaluate predictive density models such as those based on Kay's mixing rules and the GCVOL group contribution method. It is shown that Kay's mixing rules and a revised form of GCVOL model are able to predict biodiesels densities with average deviations of only 0.3%. A comparison between biodiesel densities produced from similar vegetable oils, by different authors, highlights the importance of knowing the detailed composition of the samples. An extension of GCVOL for high pressures is also proposed here. It is shown that it can predict the densities of biodiesel fuels with average deviations less than 0.4%.

Keywords: Biodiesel, Fatty Acid Methyl Esters, Density Prediction, Kay's mixing rules, GCVOL.

1. Introduction

Biodiesel is a promising alternative energy resource for diesel fuel, consisting of alkyl monoesters of fatty acids, obtained from vegetable oils or animal fats combined with a short chain alcohol. It has properties similar to ordinary diesel fuel made from crude oil and can be used in conventional diesel engines without any motorization transformation. Transesterification by alkaline catalysis is the most common process for producing biodiesel at industrial level. Biodiesel is more environmentally friendly, nontoxic and biodegradable compared to diesel fuel.¹⁻³

Biodiesel fuel has to fulfill a number of quality standards. In Europe, the biodiesel fuel standards are compiled in the Norm CEN EN 14214⁴ and in USA in the ASTM D6751⁵. Norms specify minimum requirements and test methods for biodiesel fuel to be used in diesel engines and for heating purposes, in order to increase the biodiesel fuel quality and its acceptance among consumers. Density is an important fuel property, because injection systems, pumps and injectors, must deliver an amount of fuel precisely adjusted to provide proper combustion.⁶ Boudy and Seers⁷ and Baroutian et al.⁸ show that fuel density is the main property that influences the amount of mass injected. Density data is also important in numerous unit operations in biodiesel production. Density data is required to be known to properly design reactors, distillation units and separation process, storage tanks and process piping.^{9,10} Density depends on the raw materials used for biodiesel fuel production and on the biodiesel methyl esters profile.¹¹ Following a previous work addressing biodiesels viscosity predictions¹², this work aims at evaluating the best predictive models for biodiesel densities and subsequent revision of them.

Rapeseed, soybean and palm oils are the most commonly used oils to produce biodiesel, although non edible oils, such as Jatropha, are becoming more important.⁹ The capacity to correctly predict biodiesel densities is of major relevance for a correct formulation of an adequate blend of raw materials aiming at producing biodiesel according to the required quality standards^{13,14} with the lowest production costs.

Three main types of methods exist for estimating liquid densities of pure compounds. The first types are the methods based on the corresponding states theory, such as the Rackett equation and the Spencer and Danner method.^{8,9,11,15-19} These methods have,

however, some disadvantages such as the requirement of critical properties and since they often use experimental data adjusted parameters, they have a limited predictive ability. The second type of methods is based on mixing rules, such as Kay's^{20,21} that allow the estimation of a mixture density provide that the composition of the fuel and the densities of the pure compounds are known. They are only applicable to simple mixtures with a near ideal behavior. Finally, group contribution models are another approach that only requires the chemical structure of the desired molecule to be known to estimate the thermophysical properties, such as liquid densities. The group contribution method GCVOL²² is a predictive model that was shown in previous works^{13,14} to be able to provide pure fatty acid methyl esters (FAMES) densities descriptions within 1% deviation.

There are several publications in the literature presenting density data for biodiesels in wide ranges of temperatures, but usually no information about biodiesels compositions is provided and thus this data cannot be used for model evaluation. The scarcity of biodiesel density data for which composition information is available, limits the use of these models to predict this property for biodiesel fuels.

In the present work, we report new experimental density data for ten biodiesel samples, for which a detailed composition is presented. They were produced from different vegetable oils or oil blends as reported below. The data cover the temperature range from 278.15 to 373.15 K at atmospheric pressure. Correlations for the temperature dependency of the experimental data are reported and the isobaric expansivities estimated.

These data, along with other data collected from literature, are used to carry out a critical evaluation of biodiesel density predictive models.

2. Experimental Section

2.1. Biodiesel samples synthesis

Ten biodiesel samples were studied in this work. Two of these samples were obtained from Portuguese biodiesel producers, namely Soy A and GP (Soybean+Rapeseed). Eight biodiesel samples were synthesized at our laboratory by a transesterification reaction of the vegetal oils: Soybean (S), Rapeseed (R), and Palm (P), and their

respective binary and ternary mixtures: Soybean+Rapeseed (SR), Rapeseed+Palm (RP), Soybean+Palm (SP), and Soybean+Rapeseed +Palm (SRP) and Sunflower (Sf). The molar ratio of oil/methanol used was 1:5 with 0.5% sodium hydroxide by weight of oil as catalyst. The reaction was performed at 55 °C during 24 h under methanol reflux. The reaction time chosen was adopted for convenience and to guarantee a complete reaction conversion. Raw glycerol was removed in two steps, the first after 3 h reaction and then after 24 h reaction in a separating funnel. Biodiesel was purified by washing with hot distilled water until a neutral pH was achieved. The biodiesel was then dried until the EN ISO 12937 limit for water was reached (less than 500 ppm of water). The water content was checked by Karl- Fischer titration.

Biodiesel was characterized by GC-FID following the British Standard EN14103 from EN 142144 to know the methyl esters composition of the samples.

2.2 Experimental Measurements

Density measurements were performed in the temperature range of 278.15 to 373.15 K and at atmospheric pressure using an automated SVM 3000 Anton Paar rotational Stabinger Viscometer. The apparatus was equipped with a vibrating U-tube densimeter. The absolute uncertainty of the density is 0.0005 kg·m⁻³. The SVM 3000 uses Peltier elements for fast and efficient thermostability. The temperature uncertainty is ±0.02 K from 288.15 to 378.15 K. The SVM was previously tested for other compounds and presented a very good reproducibility.^{13,23} The instrument was rinsed with ethanol three times and then pumped in a closed circuit at constant flow of the solvent during twenty minutes at 323 K. This cleaning cycle was repeated with acetone and then kept at 343 K for thirty minutes under a stream of air to ensure that the measurement cell was thoroughly cleaned and dried before the measurement of a new sample.

Capillary gas chromatography was used to determine the composition in methyl ester of biodiesel samples. A Varian CP-3800 with a flame ionization detector in a split injection system with a Select™ Biodiesel for FAME Column, (30 m x 0.32 mm x 0.25 µm), was used to discriminate between all methyl esters in analysis inclusively the polyunsaturated ones. The column temperature was set at 120°C and then programmed to increase up to 250 °C, at 4 °C/min. Detector and injector were set at 250°C. The carrier gas was helium with a flow rate of 2 mL/min.

3. Density models

3.1. Linear Mixing Rules

Kay's Mixing Rules^{20,21} are the simplest form of mixing rules by which mixture properties are obtained by summing the products of the component properties by weighting factors, which are usually the concentrations of the components in a mixture. For example,

$$\rho = \sum_i^m c_i \rho_i \quad \text{Eq. 1}$$

where c_i is the concentration and ρ_i is the density of component i .

The major drawback in the application of linear mixing rules is that they require the knowledge of the experimental densities of the pure components present on the mixture and assume that the mixture excess volumes are negligible. This may be not feasible for many real fluids because they are either composed by a large number of compounds or they have different natures and subsequently the excess volumes are non negligible. However biodiesels are simple mixtures composed, in general, by less than ten fatty acid esters all from the same family and consequently excess volumes are very small. In fact, they have been used before by several authors to predict biodiesels densities. Janarthanan and Clemments²⁴ first used this approach with molar fraction as weighting factors. Tat and Gerpen¹⁸ proposed the use of mass fractions as weighting factor. Nevertheless, the dimensionally correct way to use concentrations in Kay's mixing rules to predict densities would be as volumetric fractions. Recently, new accurate information about biodiesels fatty acid methyl esters composition was reported^{13,14} allowing the application of Kay's Mixing Rules to predict biodiesels density data

3.2. GCVOL Group Contribution Method

GCVOL is a group contribution method developed for the prediction of molar volumes of liquids. It is a completely predictive model based exclusively in the molecular structure of the compound. With this approach liquid densities, even for strongly polar solvents, can be predicted with an error of approximately 1% in the temperature range between melting temperature and the normal boiling point.²²

In previous works^{13,14} we have shown that good descriptions of fatty esters densities could be obtained with this model.

For the calculation of liquid densities the relation between molecular weight, MW_j , and molar volume, V_j , is used

$$\rho = \frac{\sum_j x_j MW_j}{\sum_j x_j V_j} \quad \text{Eq. 2}$$

Being x_j the molar fraction of the component j . The molar volume of a liquid j is calculated by the following equation

$$V = \sum_i n_i \Delta v_i \quad \text{Eq. 3}$$

where n_i is the number of group i , and the temperature dependency of molar group, Δv_i , in $\text{cm}^3 \cdot \text{mol}^{-1}$, is given by the following simple polynomial function

$$\Delta v_i = A_i + B_i \cdot T + C_i \cdot T^2 \quad \text{Eq. 4}$$

where T is the absolute temperature that can vary between the melting point and the normal boiling point when the model is used to predict densities of solvents. The A_i , B_i and C_i parameters were obtained from Elbro et al.²² The original GCVOL model presented 36 different group parameters for a variety of chemical classes, such as alkanes, aromatic, alkenes, alcohols, ketones, aldehydes, esters, ethers, chlorides, and siloxanes.

3.3. Extended GCVOL Group Contribution Method

Since the publication of GCVOL in 1991 other new groups were defined and new parameters for different functional groups were published. In 2003 an extension and revised version of GCVOL, with new parameters for all groups, was published.²⁵ This version of the GCVOL was also tested in this work.

3.4. Database for Biodiesels Densities

Although some biodiesel density data can be found in literature, information concerning the detailed biodiesel composition, other than just the oil used in the

biodiesel synthesis, is scarce. Densities in a range of temperature, instead of the standard value at 15 °C required by the EN 14214⁴, are also rare.

Detailed biodiesel composition is required for the application of the models here selected. The database used in this study, reported in Table 1, was collected from the literature and supplemented with the new experimental data for ten biodiesels measured in this work. The most important oils used in biodiesel production (soy, rapeseed and palm) were covered by this study, and mixtures of them as well as other vegetable oils (sunflower and two biodiesel samples from a Portuguese biodiesel producer) were also used. Literature soybean biodiesel density data were compiled even without information about esters composition, in order to compare density data from distinct oil crops of the same kind.

Table 1. Biodiesels used in this study.

Reference	Biodiesel	Oil Source	Temperature Range / K	Density Range / $\text{kg}\cdot\text{m}^{-3}$
Baroutian et al. ⁸	PalmS	Palm	288.15-363.15	821.5-875.9
Benjumea et al. ³⁰	PalmA	Palm	313.15-373.15	809.0-853.3
Hubber et al. ²⁸	SoyAB	Soybean	278-333	849.41-893.23
	SoyBB	Soybean	278-334	848.58-892.37
Tat and Van Gerpen ¹⁸	SoyTG	Soybean	273.15-373.15	831.40-897.60
Nogueira et al. ²⁹	SoyC	Soybean	293.15-373.15	828.0-885.8
	Cotton	Cottonseed	293.15-373.15	814.6-876.2
Veny et al. ⁹	Jatrop	Jatropha	288.15-363.15	825.67-880.32

4. Results and Discussion

New experimental density data for eight biodiesels synthesized in this work and for two industrial biodiesels are reported in Table 2. For palm oil biodiesel, measurements were only carried at temperatures above its cloud point. Table 3 reports the methyl esters compositions of the studied biodiesels.

Table 2. Experimental Density, in kg·m⁻³, for Methylic Biodiesel.

T / K	S	R	P	SR	RP	SP	SRP	Sf	GP	SoyA
278.15	894.6	893.3		893.2	889.5		890.4	894.8	891.8	
283.15	890.9	889.6		889.5	885.8	885.7	886.7	890.9	888.0	888.4
288.15	887.3	886.0	877.9	885.7	882.1	882.0	883.0	887.2	884.3	884.7
293.15	883.6	882.3	874.1	882.0	878.4	878.2	879.3	883.5	880.6	881.0
298.15	880.0	878.6	870.4	878.3	874.7	874.5	875.6	879.8	876.9	877.3
303.15	876.3	875.0	866.7	874.7	871.1	870.9	871.9	876.2	873.2	873.6
308.15	872.7	871.3	863.0	871.0	867.4	867.2	868.2	872.6	869.6	870.0
313.15	869.0	867.7	859.4	867.3	863.7	863.5	864.6	868.9	865.9	866.3
318.15	865.3	864.1	855.7	863.7	860.1	859.9	860.9	865.3	862.2	862.7
323.15	861.7	860.4	852.1	860.1	856.5	856.3	857.3	861.6	858.6	859.0
328.15	858.0	856.8	848.5	856.4	852.8	852.6	853.6	858.0	855.0	855.4
333.15	854.3	853.2	844.9	852.8	849.2	849.0	850.0	854.4	851.4	851.8
338.15	850.7	849.5	841.2	849.2	845.5	845.4	846.4	850.7	847.7	848.2
343.15	847.0	845.9	837.6	845.6	841.9	841.8	842.8	847.1	844.1	844.5
348.15	843.4	842.3	834.0	842.0	838.2	838.1	839.2	843.5	840.5	840.9
353.15	839.8	838.7	830.4	838.4	834.6	834.5	835.6	839.9	836.9	837.3
358.15	836.1	835.0	826.8	834.9	830.9	831.0	832.0	836.3	833.3	
363.15	832.5	831.4	823.2	831.3	827.3	827.4	828.4	832.8	829.8	

Table 3. Compositions of the Biodiesels studied, in mass percentage.

Methyl Esters	S	R	P	SR	PR	SP	SRP	Sf	GP	SoyA
C10		0.01	0.03		0.02	0.01	0.01			
C12		0.04	0.24	0.03	0.20	0.18	0.14	0.02	0.02	
C14	0.07	0.07	0.57	0.09	0.54	0.01	0.38	0.07	0.13	
C16	10.76	5.22	42.45	8.90	23.09	25.56	18.97	6.40	10.57	17.04
C16:1	0.07	0.20	0.13	0.15	0.17	0.11	0.14	0.09	0.13	
C18	3.94	1.62	4.02	2.76	3.02	4.04	3.28	4.22	2.66	3.73
C18:1	22.96	62.11	41.92	41.82	52.92	33.13	42.51	23.90	41.05	28.63
C18:2	53.53	21.07	9.80	37.51	15.47	31.72	27.93	64.16	36.67	50.45
C18:3	7.02	6.95	0.09	7.02	3.08	3.58	4.66	0.12	7.10	
C20	0.38	0.60	0.36	0.46	0.49	0.39	0.45	0.03	0.44	
C20:1	0.23	1.35	0.15	0.68	0.67	0.20	0.52	0.15	0.67	
C22	0.80	0.35	0.09	0.46	0.24	0.32	0.33	0.76	0.45	
C22:1	0.24	0.19	0.00	0.12	0.09	0.12	0.14	0.08	0.12	
C24		0.22	0.15			0.63	0.53			

The experimental data show that the biodiesels density decreases with increasing temperature and with the level of unsaturation of the FAMEs, as expected from previous works^{13,14} where the same behavior for pure compounds was observed.

The density data here measured were correlated using a linear temperature dependency using an optimization algorithm based on the least-squares method,

$$\rho / \text{kg} \cdot \text{m}^{-3} = b \cdot T / \text{K} + a \quad \text{Eq. 5}$$

and the parameter values along with their confidence limits are reported in Table 4. This approach was already adopted previously for several pure methyl and ethyl esters.^{13,14}

Table 4. Density Correlation Constants for Biodiesel Methyl Esters over the Temperature Range 278.15 to 363.15 K and Corresponding 95% Confidence Limits.

	b / kg·m⁻³·K⁻¹	±	t · s_b	a / kg·m⁻³	±	t · s_A
S	-0.731		0.001	1097.9		0.2
R	-0.728		0.001	1095.6		0.3
P	-0.728		0.002	1087.4		0.6
SR	-0.728		0.003	1095.4		0.9
RP	-0.731		0.001	1092.8		0.3
SP	-0.728		0.002	1091.7		0.7
SRP	-0.729		0.002	1093.0		0.7
Sf	-0.728		0.002	1097.0		0.7
GP	-0.729		0.002	1094.4		0.8
SoyA	-0.730		0.001	1094.8		0.4

s - standard deviation

The isobaric expansivity coefficient at constant pressure (α_p) is defined as

$$\alpha_p = - \left(\frac{\partial \ln \rho}{\partial T} \right)_p \quad \text{Eq. 6}$$

and was estimated from the measured data. In the temperature range investigated, the variation of α_p with temperature is below the precision of our data. The value of α_p reported is estimated at 298 K and will be here taken as a constant for the biodiesel fuels studied. The isobaric expansivities estimated for the different biodiesels are reported in Table 5. These values are similar to those for other biodiesel fuels previously reported in the literature and to the expansivities observed for pure fatty acid methyl esters.^{13,14} Though the α_p values obtained are statistically similar a trend with the unsaturation content of biodiesels is observed.

Table 5. Isobaric Expansivities, α_p , for the Studied Biodiesel Methyl Esters and Corresponding 95% Confident Limits at 298 K.

	$\alpha_p \cdot 10^3 / \text{K}^{-1}$	\pm	$t \cdot s_{\alpha_p} \cdot 10^3$
S	0.847		0.004
R	0.844		0.004
P	0.856		0.002
SR	0.844		0.002
RP	0.852		0.004
SP	0.851		0.002
SRP	0.849		0.002
Sf	0.843		0.002
GP	0.847		0.002
SoyA	0.846		0.002

s - standard deviation

To study the predictive ability of the various models investigated in this work, the relative deviations (RDs) for the predicted densities for each biodiesel were estimated according to Eq.7

$$RD = \frac{\rho_{calc_i} - \rho_{exp_i}}{\rho_{exp_i}} \times 100 \quad \text{Eq. 7}$$

where ρ is the density in $\text{kg} \cdot \text{m}^{-3}$. The average relative deviation (ARD) was calculated as a summation of the modulus of RD over N_p experimental data points. The overall average relative deviation (OARD) was calculated by Eq. 8

$$OARD = \frac{\sum_n ARD}{N_s} \quad \text{Eq. 8}$$

where N_s is the number of systems studied.

The ARDs for each biodiesel studied are reported in Table 6, while the RDs of the individual data points for the 18 biodiesel samples are shown in Figure 1 (A to C).

Table 6. Absolute Relative Deviations for the models tested. Bold numbers are the total group OARD.

	GCVOL			Kay Mixing Rules		
	Original	Extension	Revised	v	x	W
S	0.750	4.01	0.039	0.306	0.302	0.292
R	0.789	2.09	0.173	0.520	0.520	0.520
P	0.349	3.95	0.068	0.314	0.340	0.356
SR	0.594	2.84	0.093	0.318	0.312	0.305
RP	0.430	1.22	0.046	0.476	0.485	0.464
SP	1.00	0.537	0.509	0.254	0.256	0.247
SRP	0.964	1.02	0.416	0.318	0.328	0.310
Sf	0.776	4.16	0.043	0.328	0.324	0.319
GP	0.473	2.49	0.239	0.174	0.170	0.161
Soy C	1.07	4.52	0.319	0.553	0.551	0.537
Cotton	0.187	1.32	0.693	0.393	0.372	0.406
SoyA	0.515	1.72	0.036	0.375	0.306	0.305
PalmS	0.144	3.95	0.285	0.124	0.142	0.130
PalmA	0.470	4.74	0.792	0.312	0.330	0.363
SoyAB	0.555	0.393	0.097	0.168	0.169	0.408
SoyBB	0.624	0.178	0.103	0.362	0.361	0.600
SoyTG	0.851	9.05	0.385	0.500	0.507	0.253
Jatrop	0.321	0.127	0.228	0.084	0.090	0.086
OARD%	0.603	2.69	0.254	0.327	0.326	0.337

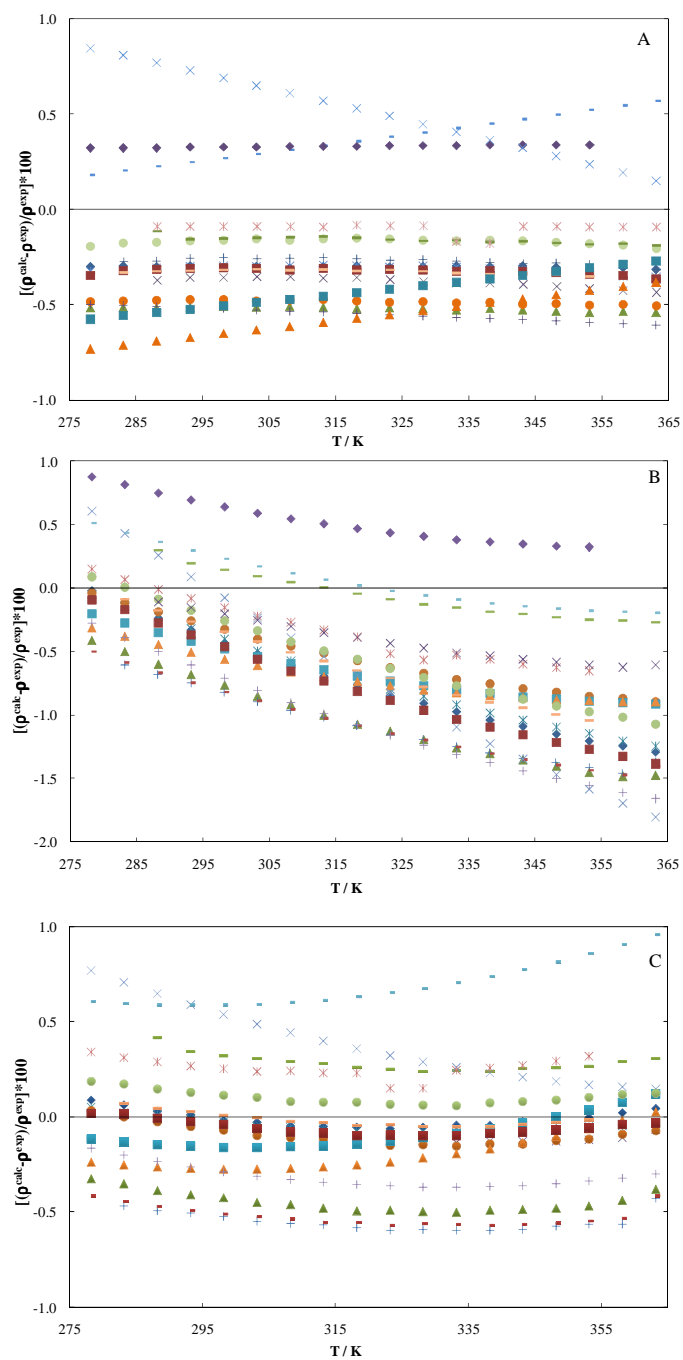


Figure 1. Relative deviations between experimental and predicted densities as function of temperature using A) Kay Mixing Rule with molar fraction as a concentration factor, B) original GCVOL model, and C) Revised GCVOL model for 18 biodiesel fuels. Zero line is experimental data. Legend: \times P, \blacklozenge S, \blacktriangle R, $*$ SR, \bullet PR, $+$ SP, $-$ SRP, $-$ PalmS, \blacksquare SoyBA²⁸, \blacktriangle SoyBB²⁸, \times SoyTG¹⁸, $*$ Jatrop⁹, \blacksquare Sf, \bullet GP, $+$ SoyC²⁹, $-$ Cotton²⁹, $-$ SoyA, and \blacklozenge Palma³⁰.

Three versions of the Kay's Mixing Rule, with mass, molar and volumetric fractions, were used to predict the biodiesels densities. Pure compound densities were obtained from our previous works^{13,14}. Detailed results are reported on Table 6 for all the biodiesel studied. Very good predictions were obtained with all the three approaches considered, with ARD of about 0.33%. No significant differences between the results obtained with the different versions of the Kay's Mixing Rule are observed, what may come as a surprise but that can easily be justified by the similarity of the compounds, in nature and size, present in the biodiesels, resulting on similar concentrations values wherever are the units adopted resulting in a marginal impact on the prediction (Figure 1A).

The two versions of GCVOL model were also used to predict biodiesels densities. Results for the relative deviations are reported for all the biodiesels studied in Table 6. To define the ester group, parameters for both the $-\text{COO}-$ and $-\text{CH}_2\text{COO}-$ groups were tested, and large deviations were reported when using the $-\text{CH}_2\text{COO}-$ group. Consequently, the $-\text{COO}-$ group was adopted in this work to describe the ester group. The results reported suggest that, the original version of GCVOL, with overall average deviations of 0.60% is far superior to the Extended GCVOL version with overall average deviations of 2.7%.

Results from previous works of ours^{13,14} and the ones shown in Figure 1B indicate that the GCVOL has a poor performance for unsaturated methyl esters and biodiesels with higher content of unsaturated esters, such as soybean biodiesel. The results suggest that the temperature dependency of the $-\text{CH}=\text{}$ parameter is not correct and can be improved.

New values for A_i , B_i and C_i for the double bond parameter ($-\text{CH}=\text{}$) were estimated based on the density data for fatty acid esters reported in previous works of ours^{13,14} and used to predict the densities of the biodiesels here studied. The new values for the $-\text{CH}=\text{}$ parameter here proposed, reported in Table 7, reduce the overall relative deviations of the GCVOL predictions from 0.60% to 0.25%. Figure 1C presents the relative deviations obtained by the revised GCVOL model as function of the temperature and it is shown that the deviations are now essentially temperature independent.

Table 7. Parameters used for the models tested: GCVOL, Extended GCVOL and new parameters proposed in this work.

	GCVOL				Extended GCVOL				Revised GCVOL
	CH2	CH3	CH=	COO	CH2	CH3	CH=	COO	CH=
A	12.52	18.96	6.761	14.23	12.04	16.43	-1.651	61.15	11.43
B / 10³	12.94	45.58	23.97	11.93	14.1	55.62	93.42	-248.2	6.756
C / 10⁵	0	0	0	0	0	0	-14.39	36.81	0

The revised GCVOL model was here extended to high pressures using an approach previously proposed by Gardas and Coutinho²⁶ for ionic liquids and described by Eq. 9.

$$\rho(T, P) = \frac{M_w}{V(T) \cdot (1 + cP)} \quad \text{Eq. 9}$$

where ρ is the density in g/cm^3 , M_w the molecular weight in g/mol , $V(T)$ the molar volume in $\text{cm}^3 \cdot \text{mol}^{-1}$ predicted by GCVOL, P the absolute pressure in MPa and c a fitting parameter. Experimental high pressure densities of three methyl esters (laurate, myristate and oleate) reported by us elsewhere²⁷ were used to estimate the c parameter with a value of $-5.7 \times 10^{-4} \text{ MPa}^{-1}$, describing high pressure densities of the methyl esters with average deviations of 0.3% as reported in Table 8. Equation 9, using this c value, was then used to predict high pressure densities for 7 biodiesel fuels.²⁷ The relative deviations (RDs) between experimental and predicted densities as function of pressure at 293.15 K are presented in Figure 3. The average relative deviations (ARD) for all compounds here studied are presented in Table 8. The overall average deviation (OAAD) of only 0.37 %, confirms that the extension to high pressures of the GCVOL model here proposed can provide excellent predictions of densities of different biodiesel fuels at high pressure.

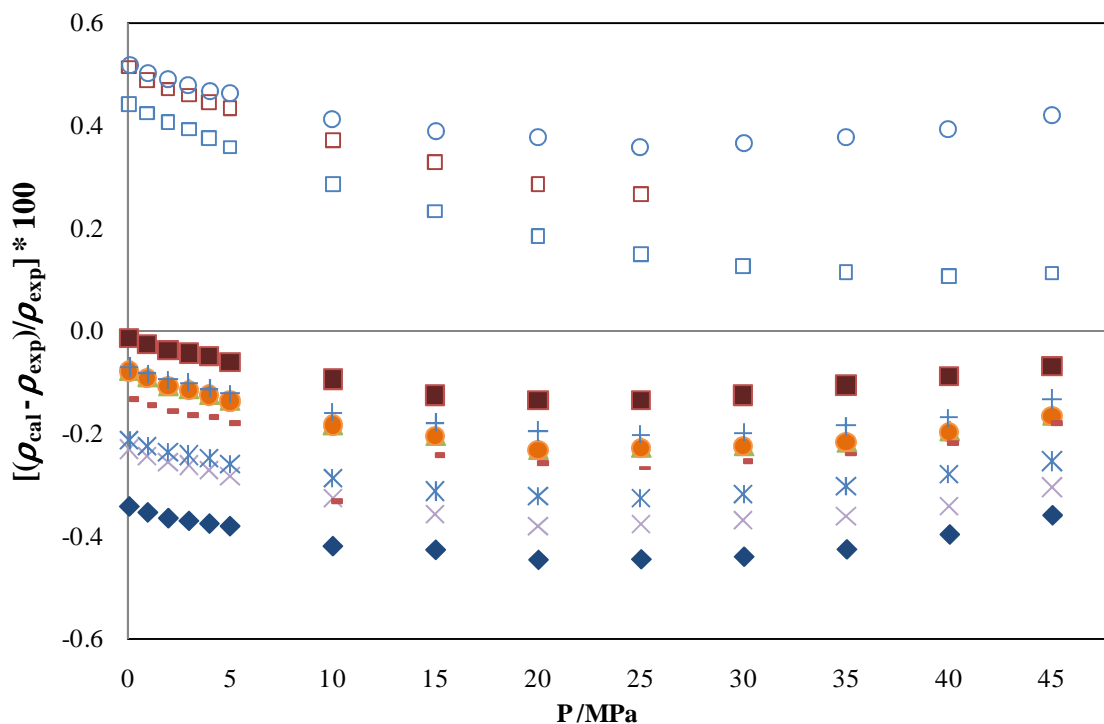


Figure 3. Relative deviations between experimental and predicted densities as function of pressure at 293.15 K using an extension of GCVOL model for 3 methyl esters and 7 biodiesel fuels ²⁷. Legend: \times P, \blacklozenge S, \blacktriangle R, \ast SR, \bullet PR, $+$ SP, $-$ SRP, \blacksquare Sf, \square MEC12, \square MEC14 and \circ MEC18:1

Table 8. Average relative deviations (ARD) for biodiesels and methyl esters densities at high pressures calculated with the GCVOL extension to high pressures.

Compounds	ARD (%)
MEC12	0.27
MEC14	0.28
MEC18:1	0.29
P	0.47
S	0.52
R	0.74
Sf	0.23
RP	0.30
SP	0.29
SR	0.40
SRP	0.32
OARD (%)	0.37

It may be argued that the requirement of knowing the biodiesel detailed composition to predict biodiesel densities requires too much effort when there are plenty of density data in the literature for biodiesels from a large number of vegetable oils. A comparison between the data reported by different authors for the densities of biodiesels produced from soybean oil, presented in Figure 2, shows large differences that cannot be assigned to experimental errors but to the differences in the oil compositions. These results clearly support the idea that a detailed characterization of the biodiesel composition is required even for estimating a simple property such as density.

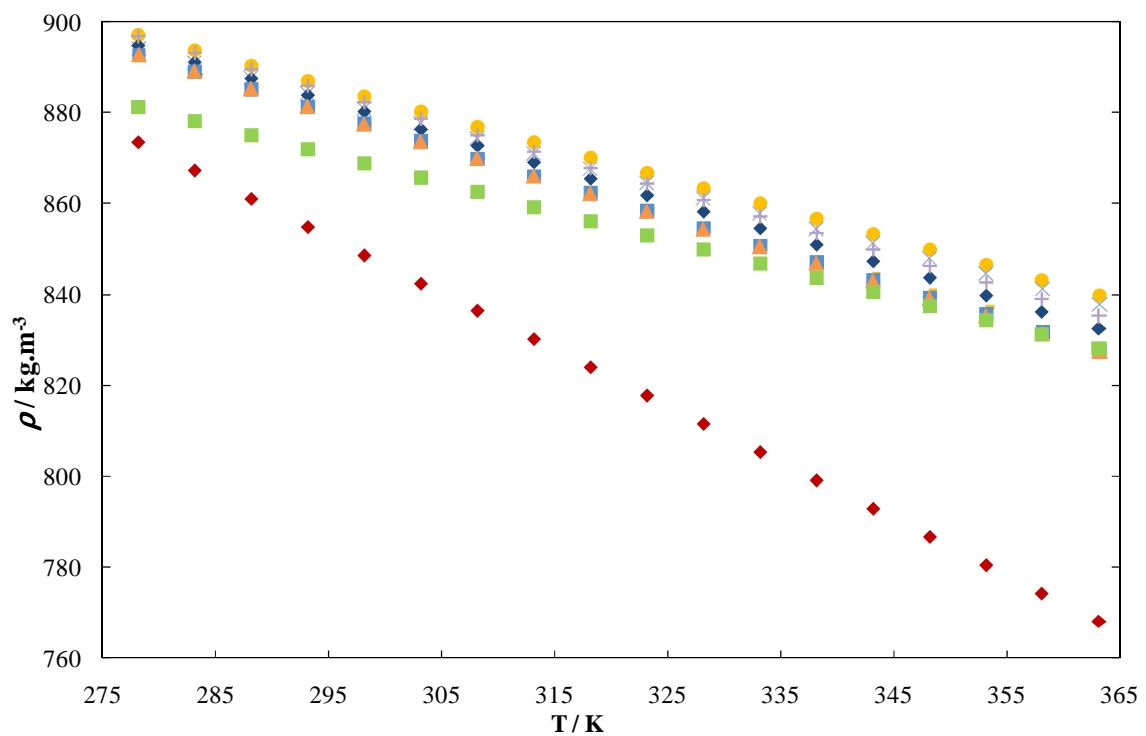


Figure 2. Density values in function of temperature for different soybean biodiesel samples. Legend: ● Blangino and Romano¹¹, × Tat and Van Gerpen¹⁸, ◆ Tate et al.³¹, ■ Yoon et al.³², ■ SoyBA²⁸, ▲ SoyBB²⁸, + SoyC²⁹, ◆ S, and - SoyA.

5. Conclusions

New experimental data for the density of ten biodiesels in the temperature range 273 to 363 K and at atmospheric pressure are reported.

The experimental data here measured were used to test predictive models for biodiesels densities. Three versions of the Kay's mixing rule and two versions of the GCVOL model were investigated. With exception of the Extended GCVOL model all approaches seem to be able to describe the biodiesels densities with deviations smaller than 1%. The various approaches to the Kay's mixing rules studied produce similar results and the revised version of the GCVOL model here proposed predicts the biodiesels densities with deviations of only 0.25%.

An extension of the GCVOL model to high pressures is here proposed based on correlated data for three methyl esters. It was tested in the 7 biodiesel fuels studied and it is shown that it can predict densities in a wide range of pressures and temperatures with an overall average absolute deviation (OAAD) of 0.37 %, being these deviations not sensible to the pressure.

Literature Cited

- [1] Shahid, E. M.; Jamal, Y., A review of biodiesel as vehicular fuel *Renewable and Sustainable Energy Reviews* 2008, *12*, 2484.
- [2] Atadashi, I. M.; Aroua, M. K.; Aziz, A. A., High quality biodiesel and its diesel engine application: A review *Renewable and Sustainable Energy Reviews* 2010, *14*, 1999.
- [3] Kralova, I.; Sjöblom, J., Biofuels–Renewable Energy Sources: A Review *Journal of Dispersion Science and Technology* 2010, *31*, 409
- [4] BS EN 14214 Automotive fuels - Fatty acid methyl esters (FAME) for diesel engines - Requirements and test methods 2009.
- [5] ASTM D6751 - 09 Standard Specification for Biodiesel Fuel Blend Stock (B100) for Middle Distillate Fuels 2009.
- [6] Dzida, M.; Prusakiewicz, P., The effect of temperature and pressure on the physicochemical properties of petroleum diesel oil and biodiesel fuel *Fuel* 2008, *87*, 1941.
- [7] Boudy, F.; Seers, P., Impact of physical properties of biodiesel on the injection process in a common-rail direct injection system *Energy Conversion and Management* 2009, *50*, 2905.
- [8] Baroutian, S.; Aroua, M. K.; Raman, A. A. A.; Sulaiman, N. M. N., Density of Palm Oil-Based Methyl Ester *Journal of Chemical & Engineering Data* 2008, *53*, 877.
- [9] Veny, H.; Baroutian, S.; Aroua, M.; Hasan, M.; Raman, A.; Sulaiman, N., Density of Jatropha curcas Seed Oil and its Methyl Esters: Measurement and Estimations *International Journal of Thermophysics* 2009, *30*, 529.
- [10] Nouredini, H.; Teoh, B.; Davis Clements, L., Densities of vegetable oils and fatty acids *Journal of the American Oil Chemists' Society* 1992, *69*, 1184.
- [11] Blangino, E.; Riveros, A. F.; Romano, S. D., Numerical expressions for viscosity, surface tension and density of biodiesel: analysis and experimental validation *Physics and Chemistry of Liquids: An International Journal* 2008, *46*, 527
- [12] Freitas, S. V. D.; Pratas, M. J.; Ceriani, R.; Lima, A. I. S.; Coutinho, J. A. P., Evaluation of Predictive Models for the Viscosity of Biodiesel *Energy & Fuels* 2010.
- [13] Pratas, M. J.; Freitas, S.; Oliveira, M. B.; Monteiro, S.C.; Lima, A. S.; Coutinho, J. A. P., Densities and Viscosities of Fatty Acid Methyl and Ethyl Esters *Journal of Chemical & Engineering Data* 2010, *55*, 3983.
- [14] Pratas, M. J.; Freitas, S.; Oliveira, M. B.; Monteiro, S. I. C.; Lima, A. I. S.; Coutinho, J. A. P., Densities and Viscosities of Minority Fatty Acid Methyl and Ethyl Esters Present in Biodiesel *Journal of Chemical & Engineering Data*. 2010. Accepted
- [15] Yuan, W.; Hansen, A. C.; Zhang, Q., Predicting the physical properties of biodiesel for combustion modeling *American Society of Agricultural and Biological Engineers* 2003, *46*, 1487.
- [16] Anand, K.; Ranjan, A.; Mehta, P. S., Predicting the Density of Straight and Processed Vegetable Oils from Fatty Acid Composition *Energy & Fuels* 2010, *24*, 3262.
- [17] Feitosa, F. X.; Rodrigues, M. d. L.; Veloso, C. B.; Cavalcante, C. L.; Albuquerque, M. C. G.; de Sant' Ana, H. B., Viscosities and Densities of Binary Mixtures of Coconut + Colza and Coconut + Soybean Biodiesel at Various Temperatures *Journal of Chemical & Engineering Data*.
- [18] Tat, M.; Van Gerpen, J., The specific gravity of biodiesel and its blends with diesel fuel *Journal of the American Oil Chemists' Society* 2000, *77*, 115.
- [19] Baroutian, S.; Aroua, M. K.; Raman, A. A. A.; Sulaiman, N. M. N., Densities of Ethyl Esters Produced from Different Vegetable Oils *Journal of Chemical & Engineering Data* 2008, *53*, 2222.
- [20] Kay, W., Density of Hydrocarbon Gases and Vapors At High Temperature and Pressure *Industrial & Engineering Chemistry* 1936, *28*, 1014.
- [21] Benmekki, E.; Mansoori, G., Pseudoization technique and heavy fraction characterization with equation of state models *Adv. Thermodyn.* 1989, *1*, 57.
- [22] Elbro, H. S.; Fredenslund, A.; Rasmussen, P., Group contribution method for the prediction of liquid densities as a function of temperature for solvents, oligomers, and polymers *Industrial & Engineering Chemistry Research* 1991, *30*, 2576.
- [23] Carvalho, P. J.; Regueira, T.; Santos, L. M. N. B. F.; Fernandez, J.; Coutinho, J. A. P., Effect of Water on the Viscosities and Densities of 1-Butyl-3-methylimidazolium Dicyanamide and 1-Butyl-3-

methylimidazolium Tricyanomethane at Atmospheric Pressure† *Journal of Chemical & Engineering Data* 2009, 55, 645.

[24] Clements, L. D., In Liquid Fuels and Industrial Products from Renewable Resources—Proceedings of the Third Liquid Fuel Conference Nashville TN 1996.

[25] Ihmels, E. C.; Gmehling, J., Extension and Revision of the Group Contribution Method GCVOL for the Prediction of Pure Compound Liquid Densities *Industrial & Engineering Chemistry Research* 2002, 42, 408.

[26] Gardas, R. L.; Coutinho, J. A. P., Extension of the Ye and Shreeve group contribution method for density estimation of ionic liquids in a wide range of temperatures and pressures *Fluid Phase Equilibria* 2008, 263, 26.

[27] Pratas, M. J.; Gallego, M. J. P.-.; Oliveira, M. B.; Queimada, A.; Piñeiro, M. M.; Coutinho, J. A. P., High-Pressure Biodiesel Density: Experimental Measurements, Correlations and Modeling with the Cubic-Plus-Association (CPA) Equation of State 2011. Submitted to Fluid Phase Equilibria

[28] Huber, M. L.; Lemmon, E. W.; Kazakov, A.; Ott, L. S.; Bruno, T. J., Model for the Thermodynamic Properties of a Biodiesel Fuel *Energy & Fuels* 2009, 23, 3790.

[29] Nogueira, C. A.; Feitosa, F. X.; Fernandes, F. A. N.; Santiago, R. I. S.; de Sant'Ana, H. B., Densities and Viscosities of Binary Mixtures of Babassu Biodiesel + Cotton Seed or Soybean Biodiesel at Different Temperatures *Journal of Chemical & Engineering Data* 2010, 55, 5305.

[30] Benjumea, P.; Agudelo, J.; Agudelo, A., Basic properties of palm oil biodiesel-diesel blends *Fuel* 2008, 87, 2069.

[31] Tate, R. E.; Watts, K. C.; Allen, C. A. W.; Wilkie, K. L., The densities of three biodiesel fuels at temperatures up to 300 degrees C *Fuel* 2006, 85, 1004.

[32] Yoon, S. H.; Park, S. H.; Lee, C. S., Experimental Investigation on the Fuel Properties of Biodiesel and Its Blends at Various Temperatures *Energy & Fuels* 2007, 22, 652.

***High-Pressure Biodiesel Density: Experimental Measurements,
Correlation and CPA EoS Modeling***

Energy & Fuels, 2011, 25, 3806–3814.

DOI: 10.1021/ef200807m

High-Pressure Biodiesel Density: Experimental Measurements, Correlation and CPA EoS Modeling

**Maria Jorge Pratas ^a, Mariana B. Oliveira ^a, Maria José Pastoriza-Gallego ^b,
António J. Queimada ^c, Manuel M. Piñeiro ^b and João A.P. Coutinho ^a**

^aCICECO, Chemistry Department, University of Aveiro, Campus de Santiago, 3810–
193 Aveiro, Portugal

^bDepartamento de Física Aplicada, Faculdade de Ciencias, Universidade de Vigo,
E36310, Vigo, Spain

^cLSRE, Laboratory of Separation and Reaction Engineering, Faculdade de Engenharia,
Universidade do Porto, 4200 – 465 Porto, Portugal

Abstract

Density is one of the most important biodiesel properties, since engine injection systems (pumps and injectors) must deliver an amount of fuel precisely adjusted to provide a proper combustion while minimizing greenhouse gases emissions. Pressure influence in fuel density has becoming particularly important with the increase use of modern common rail systems where pressure can reach 250MPa.

Nevertheless, besides its importance, little attention has been given to biodiesels high pressure densities. In fact, there are almost no reports in literature about experimental high pressure biodiesel density data.

To overcome this lack of information, in this work, new experimental measurements, from 283 to 333 K and from atmospheric pressure to 45MPa, were performed for methyl laurate, methyl myristate and methyl oleate and for methyl biodiesels from Palm, Soybean and Rapeseed oils and from three binary and one ternary mixtures of these oils.

Following previous works, were the Cubic-Plus-Association equation of state (CPA EoS) was shown to be the most appropriate model to be applied to biodiesel production and purification processes, the new high pressure experimental data here reported was also successfully predicted with the CPA EoS, with a maximum deviation of 2.5 %. A discussion about the most appropriate CPA pure compound parameters for fatty acid methyl esters is also presented.

Keywords: Fatty Acid Methyl Esters, Biodiesels, High-Pressure Density, Experimental measurements, modified Tait-Tammann equation, CPA EoS.

1. Introduction

Biodiesel has recently been the focus of increasing attention from researchers due to its rising use as a new energy solution to replace petroleum based fuels. Its production has increased exponentially in the last decade, from worldwide negligible productions in 1990 its production reached over 2500 million tons in 2008. Biodiesel is the most used biofuel in Europe, reaching the 9.6 million tons of consumption¹.

Besides its well known environmental advantages over petroleum fuels², biodiesel can be mixed in all proportions with regular diesel with no motor changes, it's easier to store and transport and has a more favorable combustion profile³⁻⁴. It consists on a blend of fatty acid esters that are industrially produced through the transesterification reaction of a vegetable oil or a fat with an alcohol, usually using a basic catalyst to increase reaction speed and yield³. Rapeseed, Soybean and Palm oils are the most commonly used oils to produce biodiesel⁵.

Nowadays, most new vehicles operate with common rail diesel engines, which use high injection pressures to allow a rapid fuel atomization and combustion with consequent higher engine efficiencies and lower emissions⁶. Modern ultra-high-pressure injection systems can approach pressures of 250MPa⁷.

Considering the predictable increase of biodiesel use, with Europe aiming to replace 20% of fossil fuels for alternative renewable fuels such as biofuels until 2020¹, and the introduction of common rail engines in new vehicles, it is expected that these engines will work with biodiesel-fuel blends with high biodiesel content and eventually even with pure biodiesels.

As Boudy and Seers⁸ explained, from the evaluation of the effect of different fuel properties on the injection process of common rail direct injection systems, density is the main property controlling the pressure wave in common rail systems and subsequently the total mass injected. NOx emissions increase from biodiesel use is partly related to advancing of injection timing caused by the more rapid pressure wave transfer from the fuel injection pump to the fuel injector causing it to open earlier.⁹⁻¹⁰

The European Committee for Standardization (CEN) has established quality standards specifying minimum requirements and test methods for biodiesels, the DIN EN 14214:2010¹¹, including density specifications. However, these standards at ambient

conditions can hardly be applied for common rail engines since densities suffer strong oscillations under high pressures.

Knowledge and description of biodiesel densities as a function of pressure and temperature are therefore required for a correct biodiesel formulation and for a proper design and optimization of common rail engines injection systems, in order to a precisely adjusted amount of fuel be delivered to provide a proper combustion while minimizing NO_x emissions⁷. However, in spite of its importance, little attention has been given to high pressure densities of biodiesels and measurements and predictions of that property have been restricted to ambient conditions. Only Aparicio et al.¹²⁻¹³ reported density measurements, in the temperature range 288.15 to 328.15 K and pressure range 0.1 to 350 MPa, for the Rapeseed and Sunflower oil methyl esters. Their experimental results were correlated with the modified Tait-Tammann equation.

After reporting experimental data for the atmospheric pressure temperature dependence of density for several fatty acid methyl and ethyl esters (from the most commonly found in biodiesels samples¹⁴ to the less common¹⁵), for different biodiesels¹⁶, and studying the best models to predict the densities of biodiesel¹⁶, we carried out here experimental high pressure density measurements for several of these pure compounds and biodiesels.

New high pressure density data is reported in this work for three fatty acid methyl esters and seven biodiesels, in the temperature range 283 to 333 K and from atmospheric pressure to 45MPa. Experimental densities were correlated using the modified Tait-Tammann equation¹⁷ and thermodynamic properties such as isothermal compressibilities and isobaric expansion coefficients were as well calculated and evaluated, on the temperature and pressure ranges studied.

Empirical models, like the modified Tait-Tammann equation, are the most commonly used to correlate high pressure density experimental data. In this work, a different and completely predictive approach was also applied, that consisted on the use of the Cubic-Plus-Association equation of state (CPA EoS) to describe the experimental data. In previous works¹⁸⁻²⁰, the CPA EoS was shown to be the most appropriate model to be applied to biodiesel production and purification processes. A discussion about the most appropriate CPA pure compound parameters for esters is also presented.

2. Experimental Section

2.1. Materials

Experimental densities were measured for three pure methyl esters, for methyl laurate and methyl myristate supplied by SAFC with purity 98% and for methyl oleate at 99% purity from Aldrich, and for seven different biodiesels samples. Biodiesels were synthesized by the transesterification reaction with methanol of the vegetal oils: Soybean (S), Rapeseed (R) and Palm (P) and their respective binary and ternary mixtures: Soybean + Rapeseed (SR), Rapeseed + Palm (RP), Soybean + Palm (SP) and Soybean + Rapeseed + Palm (SRP). The molar ratio of oil/methanol used was 1:5 using 0.5% sodium hydroxide by weight of oil as a catalyst. The reaction was performed at 55 °C during 24 h under methanol reflux. The reaction time chosen was adopted for convenience and to guarantee a complete reaction conversion. Raw glycerol was removed in two steps, the first after 3h reaction and then after 24h reaction in a separating funnel. Biodiesel was purified trough washing with hot distilled water until a neutral pH was achieved. The biodiesel was then dried until the EN ISO 14214 limit for water was reached (less than 500 mg/kg of water¹¹).

Biodiesels were characterized by GC-FID following the British Standard EN14103 from EN 14214¹¹ to know their methyl esters composition. Capillary gas chromatography was used to determine the methyl ester composition of the biodiesel samples. A Varian CP-3800 with a flame ionization detector in a split injection system with a Select™ Biodiesel for FAME Column, (30 m x 0.32 mm x 0.25 µm), was used to differentiate all methyl esters in analysis inclusively the poli-unsaturated ones. The column temperature was set at 120°C and then programmed to increase up to 250 °C, at 4 °C/min. Detector and injector were set at 250°C. The carrier gas was helium with a flow rate of 2 mL/min.

2.2. Experimental Procedure

Experimental high pressure densities were determined using an Anton Paar 512P vibrating tube densimeter, connected to an Anton Paar DMA 4500 data acquisition unit. This device determines the vibration period of a metallic U-shape cell filled with the studied fluid, which is directly linked to the sample fluid density. The calibration procedure used in this case has been described previously in detail²¹⁻²² using water and vacuum as calibrating references. This method enables the highest accuracy in density determination over wide ranges of pressure, and even reliable density extrapolation can be performed. The repeatability in the density values determined from the vibration period measured by the DMA 4500 unit is $10^{-5} \text{ g cm}^{-3}$.

Temperature stability is ensured with a PolyScience 9510 circulating fluid bath, and the temperature value is determined with a CKT100 platinum probe placed in the immediacy of the density measuring cell, with an uncertainty that has been determined to be lower than $5 \cdot 10^{-2} \text{ K}$.

Pressure is generated and controlled using a Ruska 7610 pressure controller, whose pressure stability is $2 \cdot 10^{-3} \text{ MPa}$. The pumping hydraulic fluid (dioctylsebacate fluid) is in direct contact with the fluid sample inside the $1.59 \cdot 10^{-3} \text{ m}$ diameter steel pressure line conduction, with a coil designed to keep a distance (around 1m) from the fluid contact interface to the measuring cell, avoiding any diffusion effect. The combinations of density determination repeatability, and the accuracies in temperature and pressure measurement, lead to an overall experimental density uncertainty value that is lower than 0.1 Kg m^{-3} for the whole pressure and temperature range studied in this work.

3. Density models

3.1. Modified Tait-Tammann equation.

Liquid densities were correlated using the modified Tait-Tammann equation¹⁷. Other thermodynamic properties were also derived from this equation, such as the isothermal compressibility coefficient, k_T , and the isobaric expansion coefficient, α_p .

The following form of the modified Tait-Tammann equation¹⁷ is used in this work:

$$\rho = \frac{\rho(T, P = 0.1 \text{MPa})}{\left[1 - C \ln \frac{(B + P)}{(B + 0.1)} \right]} \quad \text{Eq. 1}$$

Where

$$\rho(T, P = 0.1 \text{MPa}) = a_1 + a_2 T + a_3 T^2 \quad \text{Eq. 2}$$

In equation 2, a_1 , a_2 and a_3 are found by fitting to the experimental $\rho(T, P = 0.1 \text{MPa})$.

Coefficient B is defined as:

$$B = b_1 + b_2 T + b_3 T^2 \quad \text{Eq. 3}$$

coefficients C , b_1 , b_2 and b_3 are also obtained by fitting the modified Tait-Tammann equation to the experimental data.

The Tait equation is an integrated form of an empirical equation representative of the isothermal compressibility coefficient behavior versus pressure. The effect of pressure in density can be best described by the isothermal compressibility, k_T , which is calculated according to the following expression:

$$k_T = -\frac{1}{V_m} \left(\frac{\partial V_m}{\partial P} \right)_T = \frac{1}{\rho} \left(\frac{\partial \rho}{\partial P} \right)_T = \left(\frac{\partial \ln \rho}{\partial P} \right)_T \quad \text{Eq. 4}$$

where ρ is the density and P the pressure at constant temperature, T . Isothermal compressibilities can be calculated using equations (1) and (4):

$$k_T = \left(\frac{C}{B + P} \right) \left(\frac{\rho}{\rho(T, P = 0.1 \text{MPa})} \right) \quad \text{Eq. 5}$$

The isobaric expansion coefficient, α_p , is defined as:

$$\alpha_p = \frac{1}{V_m} \left(\frac{\partial V_m}{\partial T} \right)_p = -\frac{1}{\rho} \left(\frac{\partial \rho}{\partial T} \right)_p = -\left(\frac{\partial \ln \rho}{\partial T} \right)_p \quad \text{Eq. 6}$$

and the following expression is derived from the modified Tait-Tammann equation (equation 1):

$$\alpha_p = -\frac{[d\rho(T, P = 0.1 \text{MPa})/dT]}{\rho(T, P = 0.1 \text{MPa})} + C \left\{ \frac{\frac{dB}{dT}(P - 0.1)}{\left[1 - C \ln \left(\frac{B + P}{B + 0.1} \right) \right] (B + 0.1)(B + P)} \right\} \quad \text{Eq. 7}$$

where $d\rho(T, P = 0.1 \text{MPa})/dT = a_2 + 2a_3$ and $dB/dT = b_2 + 2b_3$.

3.2. CPA Equation-of-State.

The Cubic–Plus–Association (CPA) equation of state²³⁻²⁵ combines a physical contribution from a cubic equation of state, in this work the Soave–Redlich–Kwong (SRK), with an association term accounting for intermolecular hydrogen bonding and solvation effects²⁶⁻²⁷, originally proposed by Wertheim and used in other association equations of state such as SAFT²⁸. The association term included in the CPA EoS allowed, in previous works from ours, to correctly describe the water solubility in fatty acid esters and biodiesels²⁰, the atmospheric²⁹ and near/supercritical³⁰ VLE of fatty acid esters + alcohols systems and the LLE of multicomponent systems containing fatty acid esters, alcohols, glycerol and water^{18-19, 31}, since it can explicitly take into account the solvation phenomena found in these systems containing non-self-associating compounds (esters) that can associate with self-associating compounds like water, alcohols and glycerol. As, in this work, we are dealing with esters mixtures and as esters are known to not self-associate, the association term disappears from the CPA EoS and it can be expressed in terms of the compressibility factor as:

$$Z = \frac{1}{1-b\rho} - \frac{a\rho}{RT(1+b\rho)} \quad \text{Eq. 8}$$

where a is the energy parameter, b the co–volume parameter, ρ is the molar density, g a simplified hard–sphere radial distribution function.

The pure component energy parameter, a , is obtained from a Soave–type temperature dependency:

$$a(T) = a_0 \left[1 + c_1 \left(1 - \sqrt{T_r} \right) \right]^2 \quad \text{Eq. 9}$$

For mixtures, the energy and co–volume parameters are calculated employing the conventional van der Waals one–fluid mixing rules:

$$a = \sum_i \sum_j x_i x_j a_{ij} \quad a_{ij} = \sqrt{a_i a_j} (1 - k_{ij}) \quad \text{Eq. 10}$$

And

$$b = \sum_i x_i b_i \quad \text{Eq. 11}$$

As explained above, for non-associating components, such as esters, the association term disappears and CPA has only three pure component parameters in the cubic term (a_0 , c_1 and b). These parameters are regressed simultaneously from vapor pressure and liquid density data. The objective function to be minimized is the following:

$$OF = \sum_i^{NP} \left(\frac{P_i^{\text{exptl}} - P_i^{\text{calcd}}}{P_i^{\text{exptl}}} \right)^2 + \sum_i^{NP} \left(\frac{\rho_i^{\text{exptl}} - \rho_i^{\text{calcd}}}{\rho_i^{\text{exptl}}} \right)^2 \quad \text{Eq. 12}$$

With this procedure, better density estimates are provided overcoming SRK deficiencies in liquid phase density estimates, while leaving the possibility for future modeling in associating systems.

4. Results and Discussion

Density measurements were carried at temperatures ranging from 283.15 to 333.15 K and pressures from 0.10 to 45.0 MPa, for methyl laurate, methyl myristate, methyl oleate, Rapeseed, Soybean, and Palm biodiesel, Soybean + Rapeseed biodiesel, Rapeseed + Palm biodiesel, Soybean + Palm biodiesel and for Soybean + Rapeseed + Palm biodiesel.

Table 1 reports methyl esters compositions for the biodiesels selected for this work. This information is of major importance since biodiesels fatty acid esters profile determine their chemical and physical properties, such as densities³². In addition, in a previous work of ours¹⁶, we showed the importance of knowing the detailed composition of biodiesels to compute their densities even with simple empirical models based on mixing rules and group contribution schemes.

Table 1. Compositions of the biodiesels studied, in mass percentage.

Methyl esters	S	R	P	SR	PR	SP	SRP
C10		0.01	0.03		0.02	0.01	0.01
C12		0.04	0.24	0.03	0.2	0.18	0.14
C14	0.07	0.07	0.57	0.09	0.54	0.01	0.38
C16	10.76	5.22	42.45	8.9	23.09	25.56	18.97
C16:1	0.07	0.2	0.13	0.15	0.17	0.11	0.14
C18	3.94	1.62	4.02	2.76	3.02	4.04	3.28
C18:1	22.96	62.11	41.92	41.82	52.92	33.13	42.51
C18:2	53.53	21.07	9.8	37.51	15.47	31.72	27.93
C18:3	7.02	6.95	0.09	7.02	3.08	3.58	4.66
C20	0.38	0.6	0.36	0.46	0.49	0.39	0.45
C20:1	0.23	1.35	0.15	0.68	0.67	0.2	0.52
C22	0.8	0.35	0.09	0.46	0.24	0.32	0.33
C22:1	0.24	0.19	0	0.12	0.09	0.12	0.14
C24		0.22	0.15			0.63	0.53

The experimental pressure-volume-temperature (PVT) data obtained are reported in Tables 2 to 4 for the pure fatty acid methyl esters and biodiesels.

Table 2. Experimental density data for the fatty acid methyl esters.

	$(\rho \pm 0.1)/(\text{kg}\cdot\text{m}^{-3})$ at $(T \pm 5 \cdot 10^{-2})/\text{K}$					
$(p \pm 2 \cdot 10^{-3})/\text{MPa}$	283.15	293.15	303.15	313.15	323.15	333.15
methyl laurate						
0.10	877.1	869.3	861.4	853.5	845.8	837.6
1.00	877.7	869.9	862.0	854.2	846.5	838.4
2.00	878.4	870.6	862.7	854.9	847.2	839.2
3.00	879.1	871.2	863.4	855.7	848.0	840.0
4.00	879.7	871.8	864.0	856.3	848.7	840.7
5.00	880.3	872.5	864.7	857.1	849.5	841.5
10.0	883.3	875.6	867.9	860.4	853.0	845.3
15.0	886.2	878.5	871.1	863.7	856.4	848.7
20.0	889.0	881.5	874.2	866.9	859.8	852.2
25.0	891.6	884.3	877.1	870.0	863.0	855.8
30.0	894.3	887.1	879.9	872.9	866.1	859.0
35.0	896.9	889.7	882.7	875.9	869.1	862.1
40.0	899.3	892.4	885.4	878.7	872.0	865.1
45.0	901.7	894.9	888.1	881.4	874.8	868.0
methyl myristate						
0.10		867.2	859.6	851.9	844.2	836.4
1.00		867.8	860.1	852.5	844.8	837.1
2.00		868.4	860.8	853.2	845.6	837.9
3.00		869.0	861.5	853.9	846.3	838.6
4.00		869.6	862.1	854.6	847.0	839.4
5.00		870.2	862.7	855.2	847.7	840.1
10.00		873.2	865.9	858.5	851.1	843.7
15.00		876.1	868.9	861.7	854.5	847.2
20.00		878.9	871.9	864.8	857.7	850.5
25.00		881.6	874.7	867.8	860.8	853.8
30.00		884.3	877.5	870.6	863.8	856.9
35.00		886.9	880.2	873.4	866.7	859.9
40.00		889.4	882.8	876.2	869.5	862.8
45.00		891.8	885.3	878.8	872.2	865.6
methyl oleate						
0.10		873.8	866.6	859.3	852.0	844.8
1.00		874.4	867.2	859.9	852.7	845.5
2.00		875.0	867.8	860.6	853.4	846.2
3.00		875.6	868.4	861.2	854.1	846.9
4.00		876.2	869.0	861.9	854.7	847.6
5.00		876.7	869.6	862.5	855.5	848.3
10.0		879.7	872.6	865.6	858.7	851.7
15.0		882.4	875.5	868.7	861.8	855.0
20.0		885.0	878.3	871.6	864.9	858.3
25.0		887.7	881.1	874.4	867.9	861.3
30.0		890.2	883.7	877.2	870.7	864.4
35.0		892.7	886.2	879.8	873.6	867.2
40.0		895.1	888.8	882.5	876.3	869.9
45.0		897.5	891.2	885.0	878.8	872.7

Table 3. Experimental density data for the methyl biodiesels.

	$(\rho \pm 0.1)/(\text{kg}\cdot\text{m}^{-3})$ at $(T \pm 5 \cdot 10^{-2})/\text{K}$					
$(p \pm 2 \cdot 10^{-3})/\text{MPa}$	283.15	293.15	303.15	313.15	323.15	333.15
R						
0.10	885.0	877.6	870.3	862.9	855.6	848.2
1.00	885.5	878.2	870.8	863.5	856.2	848.9
2.00	886.1	878.8	871.4	864.1	856.8	849.6
3.00	886.6	879.3	872.0	864.8	857.5	850.3
4.00	887.2	879.9	872.7	865.4	858.2	851.0
5.00	887.7	880.5	873.3	866.1	858.8	851.7
10.0	890.4	883.3	876.2	869.2	862.1	855.0
15.0	893.0	886.1	879.1	872.2	865.2	858.3
20.0	895.6	888.7	881.9	875.1	868.3	861.4
25.0	898.0	891.3	884.6	877.9	871.2	864.5
30.0	900.5	893.8	887.3	880.7	874.1	867.4
35.0	902.8	896.3	889.8	883.3	876.8	870.3
40.0	905.1	898.7	892.3	885.9	879.5	873.0
45.0	907.4	901.1	894.8	888.5	882.1	875.7
P						
0.10	885.0	877.6	870.3	862.9	855.6	848.2
1.00	885.5	878.2	870.8	863.5	856.2	848.9
2.00	886.1	878.8	871.4	864.1	856.8	849.6
3.00	886.6	879.3	872.0	864.8	857.5	850.3
4.00	887.2	879.9	872.7	865.4	858.2	851.0
5.00	887.7	880.5	873.3	866.1	858.8	851.7
10.0	890.4	883.3	876.2	869.2	862.1	855.0
15.0	893.0	886.1	879.1	872.2	865.2	858.3
20.0	895.6	888.7	881.9	875.1	868.3	861.4
25.0	898.0	891.3	884.6	877.9	871.2	864.5
30.0	900.5	893.8	887.3	880.7	874.1	867.4
35.0	902.8	896.3	889.8	883.3	876.8	870.3
40.0	905.1	898.7	892.3	885.9	879.5	873.0
45.0	907.4	901.1	894.8	888.5	882.1	875.7
S						
0.10	893.6	886.3	879.0	871.8	864.6	857.1
1.00	894.1	886.8	879.5	872.4	865.1	857.7
2.00	894.7	887.4	880.1	873.0	865.8	858.4
3.00	895.3	888.0	880.7	873.6	866.5	859.1
4.00	895.8	888.5	881.3	874.3	867.1	859.8
5.00	896.3	889.1	881.9	874.9	867.8	860.5
10.0	899.0	892.0	884.9	878.0	871.0	863.8
15.0	901.6	894.6	887.8	880.9	874.1	866.8
20.0	904.3	897.3	890.5	883.8	877.1	870.0
25.0	906.7	899.9	893.2	886.6	880.0	873.2
30.0	909.1	902.4	895.8	889.2	882.8	876.1
35.0	911.5	904.9	898.3	891.9	885.5	879.0
40.0	913.7	907.2	900.8	894.5	888.2	881.6
45.0	916.0	909.5	903.3	897.1	890.7	884.3

Table 4. Experimental density data for the methyl biodiesels obtained from oil binary and ternary mixtures.

	$(\rho \pm 0.1)/(\text{kg}\cdot\text{m}^{-3})$ at $(T \pm 5 \cdot 10^{-2})/\text{K}$					
$(p \pm 2 \cdot 10^{-3})/\text{MPa}$	283.15	293.15	303.15	313.15	323.15	333.15
SR						
0.10	891.2	883.9	876.7	869.4	862.5	854.9
1.00	891.7	884.5	877.2	870.0	863.0	855.5
2.00	892.3	885.1	877.8	870.7	863.7	856.2
3.00	892.8	885.6	878.4	871.3	864.3	856.9
4.00	893.4	886.2	879.0	872.0	865.0	857.6
5.00	893.9	886.8	879.6	872.6	865.6	858.3
10.0	896.6	889.6	882.6	875.7	868.8	861.7
15.0	899.3	892.3	885.5	878.6	871.9	864.7
20.0	901.8	894.9	888.2	881.5	875.0	867.9
25.0	904.3	897.6	890.9	884.3	877.9	871.1
30.0	906.7	900.1	893.5	887.0	880.8	874.0
35.0	909.2	902.5	896.1	889.7	883.4	876.8
40.0	911.3	904.9	898.6	892.3	886.2	879.5
45.0	913.6	907.3	901.0	894.8	888.7	882.3
RP						
0.10	886.3	879.0	871.7	864.3	857.0	849.7
1.00	886.8	879.5	872.2	864.9	857.6	850.3
2.00	887.4	880.1	872.8	865.6	858.3	851.1
3.00	888.0	880.7	873.4	866.2	859.0	851.8
4.00	888.5	881.3	874.1	866.8	859.6	852.4
5.00	889.1	881.9	874.7	867.5	860.3	853.1
10.0	891.8	884.7	877.6	870.6	863.5	856.5
15.0	894.5	887.5	880.5	873.6	866.7	859.8
20.0	897.1	890.2	883.3	876.5	869.7	862.9
25.0	899.6	892.8	886.0	879.3	872.6	866.0
30.0	902.1	895.4	888.7	882.0	875.4	868.9
35.0	904.5	897.8	891.2	884.7	878.2	871.8
40.0	906.9	900.3	893.7	887.3	880.9	874.6
45.0	909.1	902.6	896.2	889.8	883.5	877.3
SP						
0.10	887.4	880.1	872.8	865.5	858.2	850.8
1.00	887.9	880.6	873.3	866.1	858.8	851.5
2.00	888.5	881.2	874.0	866.7	859.5	852.2
3.00	889.0	881.8	874.6	867.3	860.1	852.9
4.00	889.6	882.4	875.2	868.0	860.8	853.6
5.00	890.1	882.9	875.8	868.6	861.5	854.3
10.0	892.8	885.8	878.8	871.7	864.7	857.7
15.0	895.5	888.5	881.6	874.8	867.9	861.0
20.0	898.0	891.2	884.4	877.7	870.9	864.1
25.0	900.5	893.8	887.2	880.5	873.8	867.2
30.0	902.9	896.4	889.8	883.2	876.7	870.1
35.0	905.3	898.8	892.4	885.9	879.5	873.0
40.0	907.6	901.2	894.9	888.5	882.1	875.8
45.0	909.9	903.6	897.3	891.0	884.8	878.5

SRP						
0.10	888.4	881.1	873.7	866.4	859.2	851.6
1.00	888.9	881.6	874.3	867.0	859.8	852.3
2.00	889.5	882.2	874.9	867.6	860.4	853.0
3.00	890.1	882.8	875.4	868.3	861.1	853.7
4.00	890.6	883.3	876.0	868.9	861.7	854.4
5.00	891.2	883.9	876.7	869.6	862.5	855.1
10.0	893.9	887.8	879.6	872.6	865.7	858.5
15.0	896.6	889.5	882.6	875.6	868.8	861.6
20.0	899.2	892.2	885.3	878.5	871.9	864.8
25.0	901.6	894.9	888.0	881.3	874.8	868.1
30.0	903.9	897.3	890.7	884.1	877.7	870.9
35.0	906.4	899.8	893.1	886.8	880.4	873.7
40.0	908.7	902.2	895.7	889.3	883.0	876.5
45.0	911.0	904.5	898.1	891.8	885.6	879.2

Considering high pressure experimental measurements, only Aparicio et al.¹² reported previously data for the Rapeseed methyl ester biodiesel. In the pressure range considered in this work, experimental Rapeseed density values are in good agreement with the data reported by Aparicio and co-workers as seen in Figure 1. It should be recalled, however, that no detailed biodiesel composition is reported by Aparicio et al.¹² which limits the validity of a comparison since the compositions of the two fluids are not the same as discussed elsewhere¹⁶. From the experimental results it is possible to observe, for all the pure compounds and mixtures studied, that density decreases both when temperature increases and pressure drops. As expected, since a similar behavior was previously observed for pure unsaturated fatty acid esters¹⁴, biodiesel densities also increase with increasing content on unsaturated FAMEs and their unsaturation level.

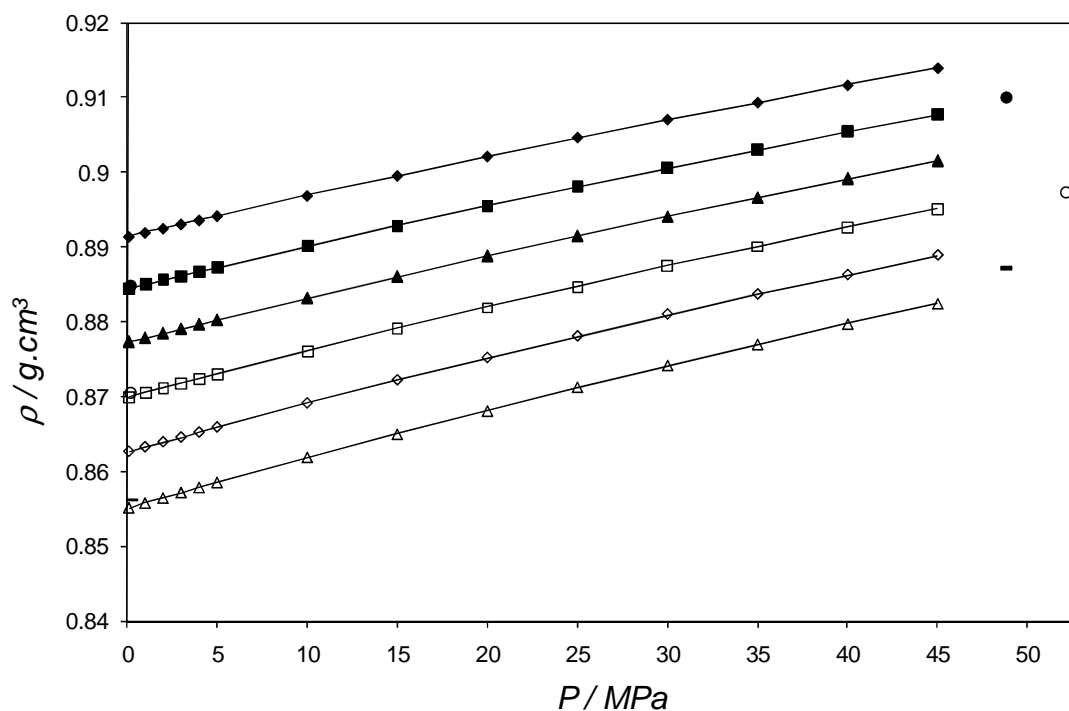


Figure 1. Density isotherms for Rapeseed biodiesel. Experimental data from this work (\blacklozenge , 283.15 K; \blacksquare , 293.15 K; \blacktriangle , 303.15 K; \square , 313.15 K; \diamond , 323.15 K; \triangle , 333.15 K) and from the work of Aparicio et al.¹² (\bullet , 288 K; \circ , 308 K; $-$, 328 K) and modified Tait-Tammann equation results (solid lines).

The modified Tait-Tammann equation was applied to correlate the experimental data. Coefficients a_1 , a_2 and a_3 of equation 2 are presented at Table 5 and coefficients C , b_1 , b_2 , and b_3 for equation 3 at Table 6. It provides a good correlation for the experimental data for pure methyl esters and for biodiesels, with a maximum deviation of 0.009% (Table 6). A graphical illustration is given in Figure 1 for the case of Rapeseed biodiesel.

Table 5. Equation 2 coefficients.

	a_1 kg·m ⁻³	a_2 kg·m ⁻³ ·K ⁻¹	$a_3 \cdot 10^7$ kg·m ⁻³ ·K ⁻²
methyl laurate	1085.250	-0.69015	-1.5872
methyl myristate	1076.212	-0.66388	-1.6758
methyl oleate	1092.999	-0.76617	0.6345
biodiesel R	1041.175	-0.36141	-5.9128
biodiesel P	1099.823	-0.77774	0.6757
biodiesel S	1085.338	-0.63419	-1.5251
biodiesel SR	1089.542	-0.68230	-0.6505
biodiesel RP	1095.181	-0.74229	0.1636
biodiesel SP	1093.702	-0.72685	-0.0637
biodiesel SRP	1088.614	-0.68473	-0.7922

Table 6. Coefficients of equations 1 and 3, along with Average Absolute Deviation (AAD) from modified Tait-Tammann equation.

	C	b_1	b_2	$b_3 \cdot 10^{-4}$	AAD
			MPa	MPa·K	%
methyl laurate	0.08803	466.39	-1.6886	16.9517	0.008
methyl myristate	0.08715	580.56	-2.3911	28.0143	0.006
methyl oleate	0.08486	510.32	-1.9231	20.5896	0.003
biodiesel R	0.08698	414.00	-1.2517	9.7351	0.006
biodiesel P	0.08776	683.20	-2.9750	37.1266	0.009
biodiesel S	0.08787	520.22	-1.9201	20.3902	0.007
biodiesel SR	0.08973	595.81	-2.3825	27.6369	0.008
biodiesel RP	0.08760	351.31	-0.8827	4.2086	0.005
biodiesel SP	0.08589	576.64	-2.3249	26.9757	0.007
biodiesel SRP	0.08280	496.92	-1.8604	19.8567	0.008
* global AAD %					0.007

$$\text{global AAD \%} = \frac{\sum AAD}{N_s} \times 100$$

where N_s is the number of systems studied.

From the modified Tait-Tammann equation it was also possible to compute isothermal compressibility coefficients, k_T , and isobaric expansion coefficients, α_p . These properties are partial derivatives of the specific volume as a function of pressure or temperature, respectively. Examples of both properties in the temperature and pressure ranges studied are presented for Rapeseed biodiesel in Figures 2 and 3, respectively.

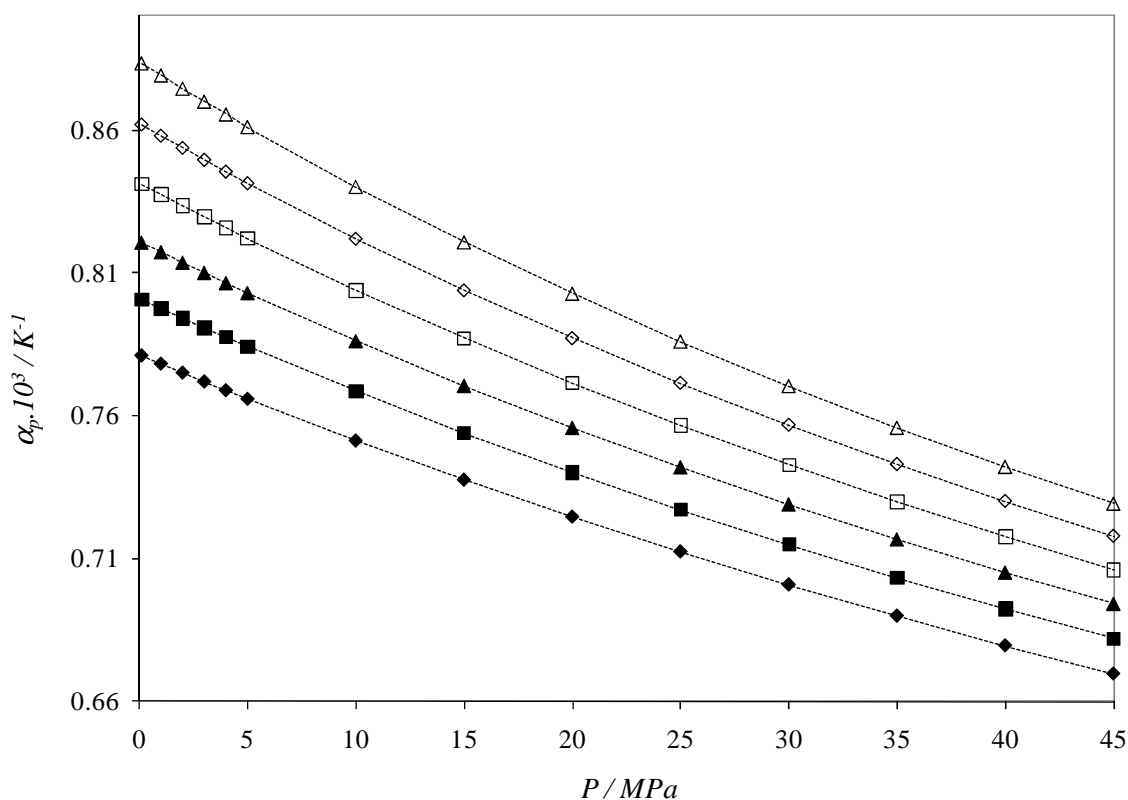


Figure 2. Isotherms for the isobaric expansion coefficient, α_p , of Rapeseed biodiesel (\blacklozenge , 283.15 K; \blacksquare , 293.15 K; \blacktriangle , 303.15 K; \square , 313.15 K; \diamond , 323.15 K; \triangle , 333.15 K).

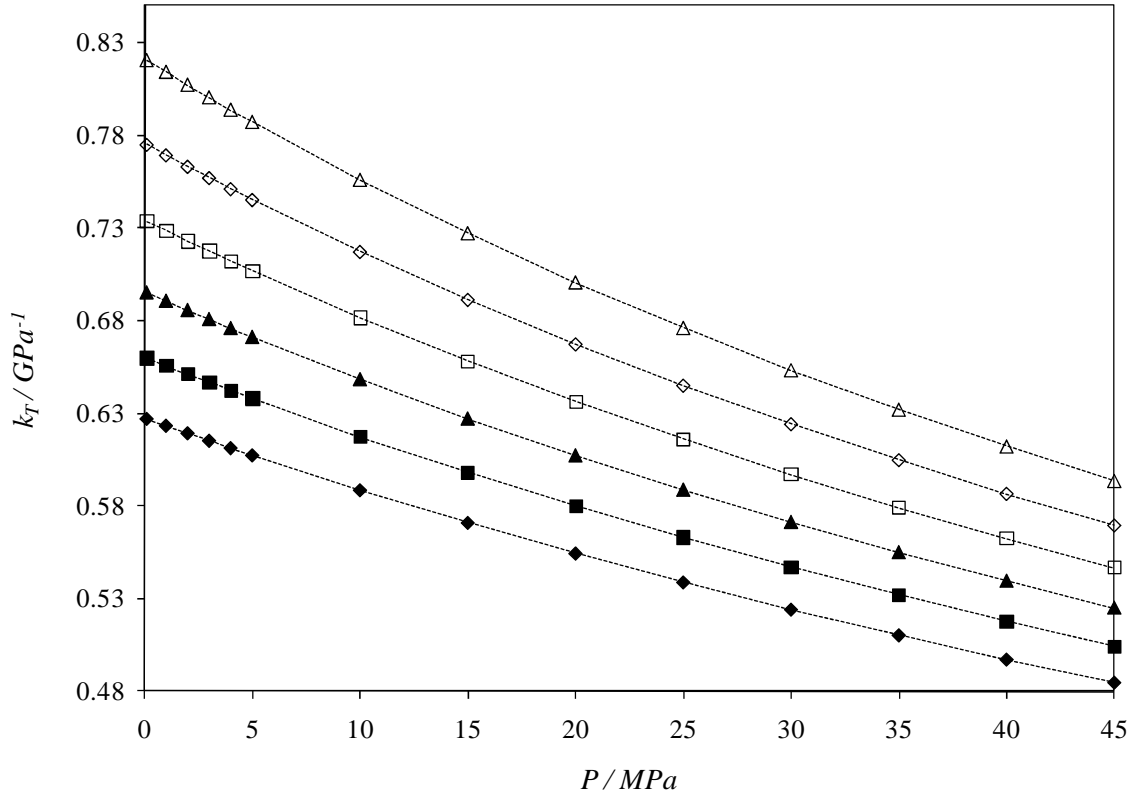


Figure 3. Isotherms for the isothermal compressibility coefficient, k_T , of Rapeseed biodiesel (◆, 283.15 K; ■, 293.15 K; ▲, 303.15 K; □, 313.15 K; ◇, 323.15 K; △, 333.15 K).

By applying the propagation law of errors at equations (5) and (7) and taking into account the uncertainties in the density, temperature, pressure and coefficients involved in equations (5) and (7), we obtained an uncertainty of the order of $\pm 0.05 \text{ GPa}^{-1}$ for k_T and $\pm 5 \cdot 10^{-4} \text{ K}^{-1}$ for α_p .

For the compounds here investigated, fatty acid methyl esters and biodiesels, isobaric expansion coefficient values decrease with increasing ester chain length and pressure and, as previously observed^{14, 16}, increase with increasing temperature. Expansion coefficients values are similar between them for the considered fatty acid methyl esters and biodiesels, and also similar to other values reported in literature for fatty acid esters and biodiesels¹²⁻¹⁶. Colza biodiesel has the highest and the lowest α_p values, at the lowest pressure and highest temperature and at the highest pressure and lowest temperature, of 0.88 and 0.67, respectively. A larger isobaric expansion coefficient means a larger engine power loss due to fuel heating.

Isothermal compressibility coefficients, k_T , decrease when pressure increases and when temperature decreases. The selected fatty acid methyl esters and biodiesels present similar values for the isothermal compressibility coefficients, values ranging from 0.67 and 0.88 in the temperature and pressure ranges here selected. Again, similar values were also found in literature for the Soybean¹³ and Rapeseed¹² biodiesels compressibility coefficients.

The experimental data here reported was also used to evaluate the predictive character of the Cubic-Plus-Association equation of state (CPA EoS) in describing high pressure density data. Fatty acid esters are non-self-associating compounds and so only the three CPA pure compound parameters of the physical term (a_0 , c_1 and b) are required to describe these compounds. CPA EoS parameters for several esters families were proposed in a previous work²⁰ where it was also showed that the a_0 , c_1 and b parameters follow trends with the ester carbon number. Correlations to compute these parameters were proposed enabling to estimate them for new compounds when pure compound data are scarce, as happened at the time for liquid densities of the higher carbon number fatty acid esters. Parameters calculated from the proposed correlations are presented, for all the esters found in the biodiesels studied, in Table 7.

Table 7. Fatty acid methyl esters CPA pure compound parameters and modeling results.

Methyl ester	a_0 (J.m ³ .mol ⁻²)	c_1	$b \times 10^4$ (m ³ .mol ⁻¹)	AAD %		T (K) range
				P	ρ	
C12	6.7139	1.5340	2.3010	0.83	0.60	283.15 - 353.15
C14:0	8.0272	1.6089	2.6361	0.45	0.52	298.15 - 353.15
C16	7.4198	2.2873	2.9749	1.46	0.62	308.15 - 363.15
C16:1	9.2554	1.7805	2.9564	2.38	1.21	287.15 - 363.15
C18	10.1303	1.9196	3.3111	0.39	0.68	313.1 - 363.15
C18:1	10.5075	1.8212	3.2485	0.81	0.74	283.15 - 353.15
C18:2	8.9943	2.1597	3.1714	1.37	0.66	278.15 - 363.15
C18:3	8.6712	2.1722	3.0949	1.18	1.03	278.15 - 373.15
C20	13.4696	1.6123	3.7121	0.78	0.85	323.15 - 373.15
C20:1	12.5293	1.7143	3.5792	5.98	1.22	278.15 - 373.15
C22	16.2713	1.4963	4.0503	0.34	0.71	333.15 - 373.15
C22:1	15.3112	1.5933	3.9168	4.73	1.86	278.15 - 363.15
C24	19.3150	1.4045	4.3953	0.13	0.65	338.15 - 373.15
* global AAD %				1.60	0.87	

$$*\text{global AAD \%} = \frac{\sum AAD}{N_s} \times 100$$

where N_s is the number of systems studied.

Using our recently published density data for several fatty acid esters that can be found in biodiesels¹⁴⁻¹⁵, it was also possible in this work to estimate CPA pure compound parameters for all the fatty acid methyl esters found in the biodiesels samples, compounds ranging from 15 to 25 carbon atoms and with up to three unsaturated bonds (Table 4), by a simultaneous regression of pure component data. Critical temperatures (T_c) for these esters were determined from the group contribution method of Wilson and Jasperson³³ that was previously assessed to be the best one to compute this property for methyl esters³⁴, and vapor pressures were taken from Chickos et al.³⁵, Lipkind et al.³⁶ and Yuan et al.³⁷. Parameters values are presented at Table 7, along with liquid densities and vapor pressures deviations. An excellent description of

vapor pressures and liquid densities for all the fatty acid methyl esters is achieved with the CPA EoS, with global average deviations of 1.6 % and of 0.9 %, respectively.

Having the CPA pure compound parameters for all the pure fatty acid methyl esters that compose the selected biodiesels, the CPA EoS was applied to predict the experimental high pressure density data. First, both set of parameters obtained from the correlations and from pure compound data regression were used to predict the pure fatty acid methyl ester high pressure density data. Higher deviations are obtained when using pure compound parameters computed from correlations, as presented at Table 8, with deviations below 6 %.

Table 8. CPA EoS modeling results for high pressure densities.

	AAD %	AAD %
	ρ (0.1 - 45 MPa)*	ρ (0.1 - 45 MPa)**
methyl laurate	4.47	0.59
methyl myristate	5.86	0.99
methyl oleate	3.24	0.84
biodiesel S		0.79
biodiesel R		2.51
biodiesel P		1.13
biodiesel RP		1.07
biodiesel SR		0.82
biodiesel SP		1.25
biodiesel SRP		0.89
global AAD %		1.09

* With fatty acid methyl esters CPA pure compound parameters from correlations.

** With fatty acid methyl esters CPA pure compound parameters correlated from pure component data.

Results improved when using the regressed fatty acid methyl esters CPA pure compound parameters, being the high pressure experimental data for methyl laurate, myristate and oleate predicted with global average deviations inferior to 0.8%.

Experimental and modeling results are depicted in Figure 4 for methyl laurate. The experimental data slope and range differs from the ones provided by the CPA EoS due to the characteristic inability of analytic EoSs to match the shape of the density temperature dependence. It is also worthy to stand out that higher deviations are obtained with the CPA EoS in comparison with the results obtained with the modified Tait-Tammann equation as expected, since the EoS approach is applied in a totally predictive way and using a considerable inferior number of parameters.

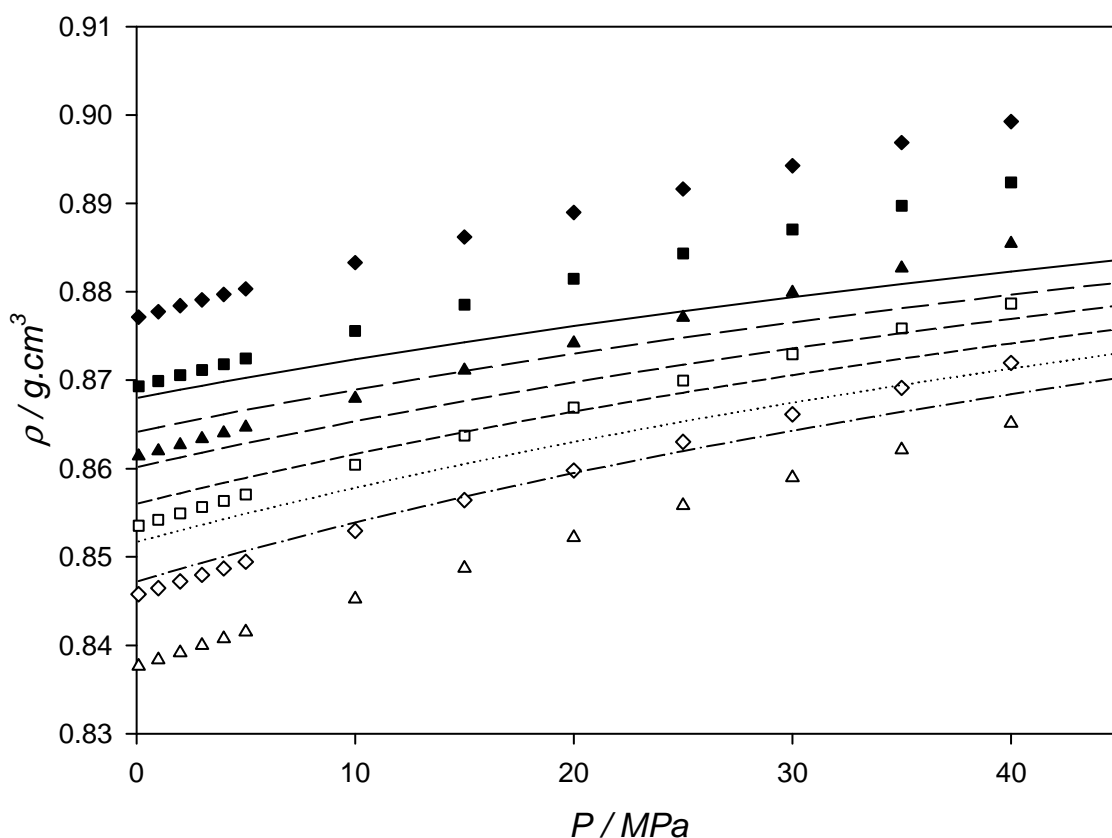


Figure 4. Density isotherms for methyl laurate. Experimental data (\blacklozenge , 283.15 K; \blacksquare , 293.15 K; \blacktriangle , 303.15 K; \square , 313.15 K; \diamond , 323.15 K; \triangle , 333.15 K) and CPA EoS results using pure compound parameters regressed from component data (solid line, 283.15 K; long dash line, 293.15 K; medium dash line, 303.15 K; short dash line, 313.15 K; dotted line, 323.15 K; dash-dot line, 333.15 K).

The new CPA pure compound parameters for fatty acid methyl esters proposed in this work were then applied to successfully predict the experimental high pressure density data for the methyl biodiesels from Palm, Soybean and Rapeseed oils and from their

binary and ternary mixtures. The CPA EoS is able to predict high pressure density data for biodiesels with a maximum deviation of 2.5 %. Results are depicted in **Figure 5** for Soybean biodiesel.

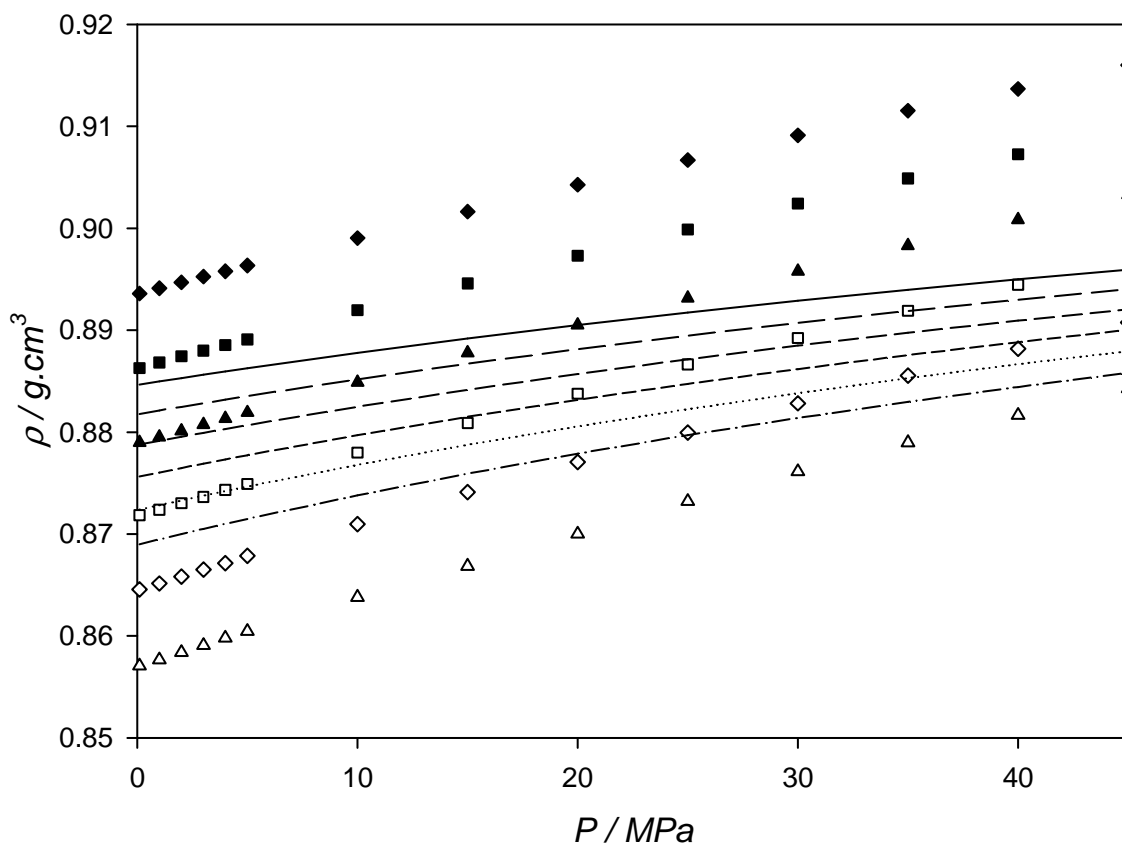


Figure 5. Density isotherms for Soybean biodiesel. Experimental data (\blacklozenge , 283.15 K; \blacksquare , 293.15 K; \blacktriangle , 303.15 K; \square , 313.15 K; \diamond , 323.15 K; \triangle , 333.15 K) and CPA EoS results (solid line, 283.15 K; long dash line, 293.15 K; medium dash line, 303.15 K; short dash line, 313.15 K; dotted line, 323.15 K; dash-dot line, 333.15 K).

5. Conclusions

Europe aims to replace 20% of fossil fuels for alternative renewable fuels such as biofuels until 2020¹. For the introduction of common rail engines in new vehicles, the description of biodiesel high pressure densities is of primary importance to the fuel and automotive industries. New experimental high pressure density measurements were

performed for three fatty acid methyl esters and for seven biodiesels, overcoming the lack of available experimental data.

The experimental data was correlated with the modified Tait-Tammann equation and predicted by the CPA EoS. New CPA EoS parameters were computed in this work for the 13 different fatty acid esters that constitute the biodiesel samples selected for this work, from C₁₅ to C₂₅ and with up to three unsaturated bonds.

The CPA EoS can predict the high pressure density data of pure fatty acid methyl esters and biodiesels with a maximum deviation of 2.5 % showing to be an adequate model to predict properties of relevance for biodiesel fuels.

Supporting Information Available

Values for the isothermal compressibility coefficients, k_T , and isobaric expansion coefficients, α_p , in the selected temperature and pressure ranges, for all the pure compounds and mixtures studied, and CPA pure compound parameters for esters obtained from ester carbon number correlations. This information is available free of charge via the Internet at <http://pubs.acs.org/>.

Nomenclature

Abbreviations

$$\text{AAD} = \text{average absolute deviation} \quad \text{AAD} = \frac{\sum_{i=1}^{N_p} |(\text{exp}_i - \text{calc}_i) / \text{exp}_i|}{N_p}$$

CPA = Cubic-Plus-Association

EoS = equation of state

FAME = fatty acid methyl ester

LLE = liquid-liquid equilibria

S = Soybean

R = Rapeseed

P = Palm

SR = Soybean + Rapeseed

RP = Rapeseed + Palm

SP = Soybean + Palm

SRP = Soybean + Rapeseed + Palm

VLE = vapor-liquid equilibria

List of Symbols

a = energy parameter in the physical term of the CPA EoS ($\text{J.m}^3.\text{mol}^{-2}$)

a_0 = parameter for calculating a ($\text{J.m}^3.\text{mol}^{-2}$)

a_1 = equation 2 coefficients (kg.m^{-3})

a_2, a_3 = equation 2 coefficients ($\text{kg.m}^{-3}\text{K}^{-1}, \text{kg.m}^{-3}\text{K}^{-2}$)

A_i = site A in molecule i

b = co-volume parameter in the physical term of the CPA EoS ($\text{m}^3.\text{mol}^{-1}$)

b_1, C = Equation 3 coefficients (b_1 in MPa)

b_2 = Equation 3 coefficients (MPaK^{-1})

b_3 = Equation 3 coefficients (MPaK^{-1})

g = radial distribution function

k_{ij} = binary interaction parameter

K_T = isothermal compressibility coefficient (GPa^{-1})

P = vapor pressure (Pa)

R = gas constant ($\text{J.mol}^{-1}.\text{K}^{-1}$)

T = temperature (K)

V_m = molar volume ($\text{m}^3.\text{kg}^{-1}$)

x = mole fraction

X_{A_i} = fraction of molecule i not bonded at site A

w = mass fraction

Z = compressibility factor

Greek Symbols

α_P = isobaric expansion coefficient (K^{-1})

β = association volume in the association part of the CPA EoS

$\Delta^{A_i B_j}$ = association strength between site A in molecule i and site B in molecule j in the association part of the CPA EoS ($\text{m}^3.\text{mol}^{-1}$)

ε = association energy in the association part of the CPA EoS (J.mol^{-1})

η = reduced fluid density

ρ = density (kg.m^{-3})

Subscripts

c = critical

$calcd$ = calculated

$exptl$ = experimental

i, j = pure component indexes

r = reduced

Superscripts

$assoc.$ = association

$phys.$ = physical

Literature Cited

- (1) Malca, J.; Freire, F. *Renew. Sust. Energ. Rev.* **2011**, *15*, 338-351.
- (2) Demirbas, A. *Applied. Energy* **2009**, *86*, S108-S117.
- (3) Ma, F. R.; Hanna, M. A. *Bioresour. Technol.* **1999**, *70*, 1-15.
- (4) Van Gerpen, J. *Fuel Process. Technol.* **2005**, *86*, 1097-1107.
- (5) Demirbas, A. *Energ. Policy* **2007**, *35*, 4661-4670.
- (6) Lee, S. W.; Tanaka, D.; Kusaka, J.; Daisho, Y. *Jsae. Rev.* **2002**, *23*, 407-414.
- (7) Dzida, M.; Prusakiewicz, P. *Fuel* **2008**, *87*, 1941-1948.
- (8) Boudy, F.; Seers, P. *Energ. Convers. Manage.* **2009**, *50*, 2905-2912.
- (9) Bora, D. K. *J Sci Ind. Res. India* **2009**, *68*, 960-963.
- (10) Boehman, A. L.; Morris, D.; Szybist, J.; Esen, E. *Energ. Fuel* **2004**, *18*, 1877-1882.
- (11) *European Standard EN 14214, 2010. Automotive fuels – Fatty acid methyl esters (FAME) for diesel engine – Requirements and test methods. CEN – European Committee for Standardization, Brussels, Belgium. Available from: <http://www.din.de>,*
- (12) Aparicio, C.; Guignon, B.; Rodriguez-Anton, L. M.; Sanz, P. D. *J. Therm. Anal. Calorim.* **2007**, *89*, 13-19.
- (13) Aparicio, C.; Guignon, B.; Rodríguez-Antón, L. M.; Sanz, P. D. *J. Agric. Food Chem.* **2007**, *55*, 7394-7398.
- (14) Pratas, M. J.; Freitas, S.; Oliveira, M. B.; Monteiro, S. C.; Lima, A. S.; Coutinho, J. A. P. *J. Chem. Eng. Data* **2010**, *55*, 3983-3990.
- (15) Pratas, M. J.; Freitas, S.; Oliveira, M. B.; Monteiro, S. I. C.; Lima, A. I. S.; Coutinho, J. A. P. *Ind. Eng. Chem. Res.* **2011**, *56*, 2175-2180.
- (16) Pratas, M. J.; Freitas, S. V. D.; Oliveira, M. B.; Monteiro, S. I. C.; Lima, A. I. S.; Coutinho, J. A. P. *Energ. Fuel* **2011**, in press.
- (17) Dymond, J. H.; Malhotra, R. *Int. J. Thermophys* **1988**, *9*, 941-951.
- (18) Oliveira, M. B.; Ribeiro, V.; Queimada, A. J.; Coutinho, J. A. P. *Ind. Eng. Chem. Res.* **2011**, *50*, 2348-2358.
- (19) Oliveira, M. B.; Queimada, A. J.; Coutinho, J. A. P. *Ind. Eng. Chem. Res.* **2010**, *49*, 1419-1427.
- (20) Oliveira, M. B.; Varanda, F. R.; Marrucho, I. M.; Queimada, A. J.; Coutinho, J. A. P. *Ind. Eng. Chem. Res.* **2008**, *47*, 4278-4285.
- (21) Pineiro, M. M.; Bessieres, D.; Gacio, J. M.; Saint-Guirons, H.; Legido, J. L. *Fluid Phase Equilib.* **2004**, *220*, 127-136.
- (22) Pineiro, M. M.; Bessieres, D.; Legido, J. L.; Saint-Guirons, H. *Int. J. Thermophys.* **2003**, *24*, 1265-1276.
- (23) Kontogeorgis, G. M.; Michelsen, M. L.; Folas, G. K.; Derawi, S.; von Solms, N.; Stenby, E. H. *Ind. Eng. Chem. Res.* **2006**, *45*, 4855-4868.
- (24) Kontogeorgis, G. M.; Michelsen, M. L.; Folas, G. K.; Derawi, S.; von Solms, N.; Stenby, E. H. *Ind. Eng. Chem. Res.* **2006**, *45*, 4869-4878.
- (25) Oliveira, M. B.; Coutinho, J. A. P.; Queimada, A. J. *Fluid Phase Equilib.* **2007**, *258*, 58-66.
- (26) Michelsen, M. L.; Hendriks, E. M. *Fluid Phase Equilib.* **2001**, *180*, 165-174.
- (27) Wu, J. Z.; Prausnitz, J. M. *Ind. Eng. Chem. Res.* **1998**, *37*, 1634-1643.
- (28) Muller, E. A.; Gubbins, K. E. *Ind. Eng. Chem. Res.* **2001**, *40*, 2193-2211.
- (29) Oliveira, M. B.; Miguel, S. I.; Queimada, A. J.; Coutinho, J. A. P. *Ind. Eng. Chem. Res.* **2010**, *49*, 3452-3458.

- (30) Oliveira, M. B.; Queimada, A. J.; Coutinho, J. A. P. *J. Supercrit. Fluids* **2010**, *52*, 241-248.
- (31) Follegatti-Romero, L. A.; Lanza, M.; Batista, F. R. M.; Batista, E. A. C.; Oliveira, M. B.; Coutinho, J. o. A. P.; Meirelles, A. J. A. *Ind. Eng. Chem. Res.* **2010**, *49*, 12613-12619.
- (32) Rodrigues, J.; Cardoso, F.; Lachter, E.; Estevão, L.; Lima, E.; Nascimento, R. *J. Am. Oil Chem. Soc.* **2006**, *83*, 353-357.
- (33) Poling, B.; Prausnitz, J.; O'Connel, J. *Mc-Graw Hill*, **2001**,
- (34) Lopes, J. C. A.; Boros, L.; Krahenbuhl, M. A.; Meirelles, A. J. A.; Daridon, J. L.; Pauly, J.; Marrucho, I. M.; Coutinho, J. A. P. *Energ. Fuel* **2008**, *22*, 747-752.
- (35) Chickos, J. S.; Zhao, H.; Nichols, G. *Thermochim. Acta* **2004**, *424*, 111-121.
- (36) Lipkind, D.; Kapustin, Y.; Umnahanant, P.; Chickos, J. S. *Thermochim. Acta* **2007**, *456*, 94-101.
- (37) Yuan, W.; Hansen, A. C.; Zhang, Q. *Fuel* **2005**, *84*, 943-950.

Evaluation of predictive models for the Viscosity of biodiesel

Energy & Fuels **2011**, 25, 352-358.

DOI: 10.1021/ef101299d

Evaluation of predictive models for the viscosity of biodiesel

Samuel V.D. Freitas, Maria Jorge Pratas, Roberta Ceriani[◇], Álvaro S. Lima[§], João

A.P. Coutinho

CICECO, Chemistry Department, University of Aveiro, Campus de Santiago, 3810–193
Aveiro, Portugal;

[◇] Department of Chemical Processes, University of Campinas, 13083-852, Campinas,
São Paulo, Brasil.

[§] Programa de Pós-Graduação em Engenharia de Processos, Universidade Tiradentes,
Av. Murilo Dantas 300, Farolândia, Aracaju-SE, Brasil.

Abstract

Viscosity is an important biodiesel parameter, subject to specifications, and with an impact on the fuel quality. A model that could predict the value of viscosity of a biodiesel based on the knowledge of its composition would be useful in the optimization of biodiesel production processes, and the planning of blending of raw materials and refined products. This work aims at evaluating the predictive capability of several models previously proposed in the literature for the description of the viscosities of biodiesels and their blend with other fuels. The models here evaluated are the Ceriani's, Krisnangkura's and Yuan's models, along with a revised version of the Yuan's model here proposed. The results for several biodiesel systems show that the revised Yuan model proposed provides the best description of the experimental data with an average deviation of 4.65 %, compared to 5.34 % for Yuan's, 8.07 % for Ceriani's and 7.25 % of Krisnangkura's models. The same conclusions were obtained when applying these models to predict the viscosity of blends of biodiesel with petrodiesel.

Keywords: Biodiesel, Viscosity, Modeling.

1. Introduction

Biodiesel refers to a fuel derived from renewable sources that consists of a mixture of methyl or ethyl esters of long-chain fatty acids which is obtained by transesterification of vegetable oils or other feedstocks largely comprised of triacylglycerols with a simple alcohol, such as methanol or ethanol in the presence of a catalyst¹⁻². It is nonflammable and nonexplosive, with a flash point of 423 K compared to 337 K for petrodiesel³. As a fuel it offers many benefits such as ready availability, portability, renewability, domestic origin, lower sulfur and aromatic content, biodegradability, better ignition quality, inherent lubricity, higher cetane number, positive energy balance, higher density, greater safety, nontoxic character of their exhaust emissions and cleaner burning⁴⁻⁷.

It has expanded into the existing markets and infrastructures of gasoline and diesel and has undergone rapid development and acceptance as an alternative diesel fuel. Its worldwide production exceeded 2500 million tons in 2008⁸. It can be blended with diesel fuel to be used in conventional engines⁹ and is able to reduce the carbon dioxide emissions by 78 %¹⁰. Although most commercially available biodiesel is still between 5 and 20 % biodiesel blended with petroleum diesel due to the higher prices of feedstocks for biodiesel production the tendency of increasing production is expected to continue in the coming decades with the development and the growth of non-food feedstocks¹¹.

One of the major problems associated with biodiesel is that its viscosity may be higher than that for diesel fuel. A fuel of high viscosity tends to form larger droplets on injection, leading to poorer atomization during the spray and creating operation problems, such as increased carbon deposits¹², and may enhance the polymerization reaction especially for oils of high degree of unsaturation¹³. It also leads to poor combustion and increased exhaust smoke and emissions, beyond the problems in cold weather due to the increase of viscosity with decreasing temperature. On the other hand, a fuel with low viscosity may not provide sufficient lubrication for the precision fit of fuel injection pumps, resulting in leakage or increased wear¹⁴. Thus the kinematic viscosity of biodiesel at 40 °C, must be in the range of 3.5-5.0 mm²/s according to EN-14214 specifications in Europe and of 1.9-6.0 mm²/s in accordance with American

Society of Testing and Materials (ASTM) D-6751 specifications in the USA¹⁵ while the limit for diesel fuel is 2.0-4.5 mm²/s¹⁴.

There is still a lack of viscosity data of biodiesel blends and biodiesel-diesel over the whole composition range at different operational conditions of pressure and temperature. In this regard, the use of theoretical approaches to estimate the viscosity of biodiesel systems is of great practical interest.

A number of works has presented predictive models and empirical equations with adjustable parameters for the viscosity of fatty acid esters, of which biodiesel is comprised. By knowing the viscosity of fatty acid esters, it is possible to determine the viscosity of biodiesel using the mixture models suggested by Grunberg-Nissan or Hind¹². Moreover there is a possibility to realize biodiesel maximum potential by simply changing the composition of fatty acid esters.

This paper aims at comparing the predictive capabilities of three models developed respectively by Ceriani *et al.*¹⁶, Krisnangkura *et al.*¹³ and Yuan *et al.*¹⁷ for the estimation of the viscosity of several biodiesel and their blends with diesel fuels. A revised version of the Yuan model is also proposed and evaluated.

2 Experimental Section

2.1 Samples

In this work the viscosities of seven biodiesel samples were measured. Two of these samples were obtained from Portuguese biodiesel producers, namely Soy A and GP (mix of soy and rapeseed methyl esters at 50 % w/w). B1 is methyl oleate of technical grade, 70 %, supplied by Sigma.

The other four biodiesel samples: Sunflower, Soy B, Palm and Rapeseed were synthesized in our laboratory by a transesterification reaction of the respective vegetal oils. The molar ratio of oil/methanol used was 1:5 with 0.5 % sodium hydroxide by weight of oil as catalyst. The reaction was performed at 55 °C during 24 h under methanol reflux. The reaction time chosen was adopted for convenience and to guarantee a complete reaction conversion. Raw glycerol was removed in two steps, the first after 3 h reaction and then after 24 h reaction in a separating funnel. Biodiesel was purified by washing with hot distilled water until a neutral pH was achieved. Then

biodiesel was dried until the EN ISO 12937 limit for water was reached (less than 500 mg/kg of water). Some properties of produced biodiesel are presented in Table 1.

Table 1. Properties of biodiesel synthesized on this work.

		Sunflower	Soy B	Palm	Rapeseed
Density / kg/m ³	@ 15 °C	887.2	887.3	877.9	886
Viscosity / mPa.s	@ 40 °C	3.636	3.548	3.961	3.942
Ester content %		98.5	99.4	96.5	98.8

2.2 Experimental Measurements

Measurements of viscosity were performed in the temperature range of (278.15 to 363.15) K at atmospheric pressure using an automated SVM 3000 Anton Paar rotational Stabinger Viscometer. The temperature uncertainty is 0.02 K from (288.15 to 378.15) K. The relative uncertainty of the dynamic viscosity obtained is less than 0.5 % for the standard fluid SHL120 (SH Calibration Service GmbH), in the range of the studied temperatures. This viscometer was previously tested for other compounds and presented a very good reproducibility^{18,19}.

3. Viscosity models

The models here described are valid for the estimation viscosity of mixtures of fatty acid alkyl esters. The viscosities of biodiesel are calculated by using the equation of Grunberg-Nissan which is known to be the most suitable equation for computing the viscosity of liquid mixtures^{12,17}. Given that biodiesel fuels are non-associated liquids, i.e., they have essentially dispersive interaction between the individual components, their dynamic viscosity can be estimated using the following equation:

$$\ln \eta_m = \sum_{i=1}^n x_i \ln \eta_i \quad (1)$$

where η_i is the dynamic viscosity of individual compound, η_m the dynamic viscosity of the mixture and x_i the mole fraction.

The ester nomenclature adopted on this work is based on the fatty acid chain length. A C_{x,y} ester means the methyl ester of fatty acid with x carbons and y unsaturation.

3.1- Ceriani's Model

Ceriani *et al.*¹⁶ proposed a model to predict the viscosity of fatty acid esters based on a group contribution method, i.e., a compound or a mixture of compounds is considered as a solution of groups and its properties are the sum of the contributions of each group¹⁶. The model for the pure compounds is described in Equations (2) – (4):

$$\ln(\eta_i/mPa.s) = \sum_k N_k \left(A_{1k} + \frac{B_{1k}}{T/K} - C_{1k} \ln T/K - D_{1k} T/K \right) + \left[M_i \sum_k N_k \left(A_{2k} + \frac{B_{2k}}{T/K} - C_{2k} \ln T/K - D_{2k} T/K \right) \right] + Q \quad (2)$$

with

$$Q = (f_0 + N_c f_1)q + (s_0 + N_{cs} s_1) \quad (3)$$

and

$$q = \alpha + \frac{\beta}{T/K} - \gamma \ln (T/K) - \delta T/K \quad (4)$$

where N_k is the number of groups k in the molecule i ; M is the component molecular weight that multiplies the “perturbation term”; A_{1k} , B_{1k} , C_{1k} , D_{1k} , A_{2k} , B_{2k} , C_{2k} , and D_{2k} are parameters obtained from the regression of the experimental data; k represents the groups of component i ; Q is a correction term. f_0 , f_1 , s_0 and s_1 are optimized constants; α , β , γ and δ are optimized parameters obtained by regression of databank as whole; N_c is the total number of carbon atoms in the molecule and N_{cs} is the number of carbons of the alcohol side chain. The parameter values can be found at Ceriani *et al.*¹⁶.

3.2- Krisnangkura's Model

Krisnangkura *et al.*¹³ fitted Equation 5 to an experimental viscosity data bank and provided a set of parameters for the description of the viscosity of pure fatty acid methyl esters (FAMES)¹³.

$$\ln(\mu) = \alpha + bz + \frac{c}{T} + \frac{zd}{T} \quad (5)$$

This equation was developed by considering the viscosity as the integral of the interaction forces of molecules. Based on this approach the temperature dependency of the viscosity for short chain methyl esters (C₆-C₁₂) can be estimated by Equation 6:

$$\ln(\mu) = -2.915 - 0.158z + \frac{492.12}{T} + \frac{108.35z}{T} \quad (6)$$

while for longer chain esters (C_{12:0}-C_{18:0}) the viscosity obeys the Equation 7:

$$\ln(\mu) = -2.177 - 0.202z + \frac{403.66}{T} + \frac{109.77z}{T} \quad (7)$$

The viscosity of unsaturated FAMES is estimated by Equations (8) - (11).

$$\ln(\mu)_{18:1} = -5.03 + \frac{2051.5}{T} \quad (8)$$

$$\ln(\mu)_{18:2} = -4.51 + \frac{1822.5}{T} \quad (9)$$

$$\ln(\mu)_{18:3} = -4.18 + \frac{1685.5}{T} \quad (10)$$

$$\ln(\mu)_{22:1} = -5.42 + \frac{2326.2}{T} \quad (11)$$

In all these equations μ is kinematic viscosity expressed in mm²/s and T is absolute temperature in K.

Since Krisnangkura's model does not provide equations for several unsaturated FAMES such as C_{16:1}, C_{20:0}, C_{20:1} and C_{22:1}, to predict the viscosity of biodiesel containing these compounds, it was necessary to resort to a pseudo-component approach where the biodiesel composition was modified by adding C_{16:1} to C_{16:0}, C_{20:0} and C_{20:1} to C_{18:3} and C_{22:0} to C_{22:1}.

Beyond that, given that Krisnangkura's model provides only kinematic viscosities, their conversion into dynamic viscosities was done by considering the density data for pure FAMES reported by Pratas *et al.*^{18,20}

3.3- Yuan's Model

Yuan *et al.*¹⁷ applied the Vogel-Tammann-Fulcher (VTF) equation to describe the viscosity-temperature relationship of pure FAME commonly present in biodiesel fuels

$$\ln \eta / mPa \cdot s = A + \frac{B}{T/K + T_0} \quad (12)$$

and then estimate the viscosity of biodiesel fuels based on their FAME composition through the mixture model. In Equation (12) A , B and T_0 are parameters with values

were determined by fitting experimental viscosity data available and are reported by Yuan *et al.*¹⁷

3.4- Revised Yuan's Model

In previous works Pratas *et al.*^{18,20} reported new and more accurate data for the viscosities of fatty acid methyl and ethyl esters. The revised Yuan's model consists of a version of the Yuan's model where the parameters of the VTF model were refitted to the new data. The new parameters for FAME are presented in Table 2.

Table 2. VTF parameters for the revised Yuan's model.

FAME	A	B	T0
C8	-3.476	859.303	68.948
C10	-3.316	814.674	93.317
C12	-3.089	767.388	112.267
C14	-3.124	837.282	112.358
C16	-2.808	746.528	132.676
C16:1	-2.867	748.275	118.441
C18	-2.985	876.221	122.303
C18:1	-2.700	748.184	129.249
C18:2	-2.618	733.236	119.641
C18:3	-2.997	904.378	91.882
C20	-3.074	967.596	115.000
C20:1	-2.545	733.804	137.194
C22	-2.528	768.640	145.057
C22:1	-2.409	715.397	143.268
C24	-2.870	951.526	127.000

3.5- Database of biodiesel viscosities

Although values for the biodiesel viscosity are common in the open literature, information concerning the biodiesel composition that is more detailed than the information about the oil used for the biodiesel synthesis is scarce. To apply the models here studied detailed information about the biodiesel composition is required. The database used in this work was collected from the literature and supplemented with a

data for seven new biodiesel measured in our laboratory. The compositions in terms of FAMES of all biodiesel used in this work are reported in Table 3. The biodiesels used in this study cover the most important oils used in biodiesel production such as soy, palm, canola, rapeseed and sunflower, but also other oils such as cotton seed, coconut and babassu, relevant due to their singular compositions. In terms of fatty acid methyl ester distributions it addresses both oils rich in short chain and saturated fatty acids such as coconut, in saturated fractions such as palm, and rich in unsaturated compounds such as soy and sunflower.

Table 3. Composition of the biodiesel studied, in mass fraction.

References	Biodiesel	Fatty acids methyl esters (FAME), 100.w														
		C8	C10	C12	C14	C16	C16:1	C18	C18:1	C18:2	C18:3	C20:0	C20:1	C22:0	C22:1	C24:0
Yuan <i>et al.</i> ¹⁷	Soy	0.02			0.08	10.61		4.27	24.2	51.36	7.48	0.36	0.28	0.4	0.07	0.14
	Palm					40.60		5.10	42.80	11.00	0.50					
	Canola					4.20		1.20	56.80	21.70	15.70					
	Coconut	9.20	6.40	48.70	17.00	7.70		2.20	5.40	2.20						
	YGME ^a					1.70	19.47		14.38	54.67	7.96	0.69	0.25	0.52	0.21	
Yuan <i>et al.</i> ²¹	SMEA ^b				0.08	10.49	0.12	4.27	24.2	51.36	7.48	0.36	0.28	0.40	0.07	0.14
	SMEB ^b					10.81	0.11	4.54	24.96	50.66	7.27	0.37	0.32	0.42		0.12
	GMSME ^c					3.97	0.13	2.99	82.54	4.98	3.7	0.30	0.50	0.36		0.12
	YGME* ^s				1.27	13.44	2.03	12.38	54.67	7.96	0.69	0.25	0.52	0.21		
Blangino <i>et al.</i> ²³	Soy					9.27		3.77	22.83	57.46	6.67					
Krisnangkura <i>et al.</i> ¹³	Palm ^d			0.40	1.06	40.05		5.83	42.21	10.46						
	Coconut ^d	4.80	6.20	52.70	17.50	7.40		2.40	7.60	1.40						
This work	Soy A					16.18		3.82	28.80	50.46						
	Soy B				0.07	10.78	0.07	3.95	23.02	53.66	7.03	0.38	0.23	0.80		
	B1 ^e				1.80	4.70	4.70	1.90	71.13	9.89		5.89				
	Sunflower			0.02	0.07	6.41	0.09	4.23	23.93	64.25	0.12		0.03	0.77	0.08	
	Rapeseed		0.01	0.04	0.07	5.26	0.20	1.63	62.49	20.94	6.99	0.60	1.23	1.35	0.19	
	Palm		0.03	0.25	0.57	42.52	0.13	4.03	41.99	9.81	0.09	0.36	0.15	0.09		
	GP ^f			0.02	0.13	10.57	0.13	2.66	41.05	36.67	7.10	0.44	0.67	0.45	0.12	
Knothe <i>et al.</i> ¹	B ^g +Petroleum (B10 to B90)					10.79		4.21	24.41	53.38	7.21					
Feitosa <i>et al.</i> ²⁴	Coconut	4.08	3.65	35.35	19.84	13.83		3.94	14.30	4.73						
Nogueira <i>et al.</i> ²⁵	Babassu		5.10	28.11	25.56	15.41		5.04	20.79							
	Cotton Seed				0.62	24.09		2.56	15.74	56.99						

^a YGME=yellow grease methyl ester. ^b SMEA and SMEB = soybean oil methyl esters. ^c GMSME = genetically modified soy oil methyl ester. ^d Mol fraction (100.X), ^e B1 = biodiesel composed by 71% of methyl oleate, ^f GP – blending of soy and rapeseed. ^g B =biodiesel.

The database of blends analyzed in this work was collected from Knothe *et al.*¹ and Yuan *et al.*²¹. The first author measured the low-temperature kinematic viscosity data of binary blends between methyl oleate, methyl linoleate and commercial biodiesel and petrodiesel in different mixing ratios while the last author reported the kinematic viscosity of blending of yellow grease methyl esters (YGME) and of soy methyl esters (SMEA and SMEB) and a genetically modified soy methyl esters (MGSME) with no. 2 Diesel. The kinematic viscosity of the commercial petrodiesel and the no.2 Diesel are listed in Table 4.

Table 4. Experimental viscosity, in mm²/s, for petrodiesel and No 2 Diesel used in this work.

T, K	Petrodiesel ¹	No. 2 Diesel ²¹
273.15	8.58	
278.15	7.23	
283.15	6.21	
288.15	5.31	
293.15	4.55	3.94
298.15	4.08	
303.15	3.64	
308.15	3.25	
313.15	2.90	2.56
333.15		1.82
353.15		1.35
373.15		1.09

4. Results and Discussion

The viscosities of the seven biodiesel samples measured in this work as function of temperature are reported in Table 5. The magnitude of the viscosities is in good agreement with other data previously reported in the literature for biodiesel produced from the same oils.^{13,17,21,22}

Table 5. Experimental viscosity, in mPa.s, for biodiesel measured in our laboratory.

T, K	Biodiesel						
	Soy A	Soy B	B1	Sunflower	Rapeseed	Palm	GP
278.15		8.812			10.33		9.315
283.15	8.016	7.555	9.359	7.940	8.763		7.958
288.15	6.916	6.535	7.998	6.844	7.518	7.814	6.856
293.15	6.021	5.711	6.894	5.965	6.517	6.748	5.971
298.15	5.286	5.033	6.000	5.243	5.701	5.883	5.244
303.15	4.679	4.478	5.271	4.658	5.034	5.152	4.655
308.15	4.170	3.995	4.663	4.143	4.467	4.550	4.137
313.15	3.740	3.548	4.154	3.636	3.942	3.961	3.630
318.15	3.372	3.249	3.722	3.356	3.594	3.632	3.349
323.15	3.057	2.922	3.354	2.988	3.217	3.214	2.981
328.15	2.784	2.697	3.037	2.776	2.955	2.968	2.769
333.15	2.546	2.473	2.767	2.542	2.699	2.702	2.534
338.15	2.338	2.276	2.529	2.337	2.475	2.471	2.329
343.15	2.154	2.102	2.321	2.156	2.278	2.269	2.148
348.15	1.992	1.948	2.138	1.996	2.104	2.091	1.988
353.15	1.848	1.794	1.976	1.831	1.933	1.911	1.823
358.15		1.686		1.726	1.811	1.794	1.718
363.15		1.575		1.612	1.688	1.669	1.604

To study the predictive ability of the various models studied in this work the relative deviations of the predicted viscosities for each biodiesel were estimated according to

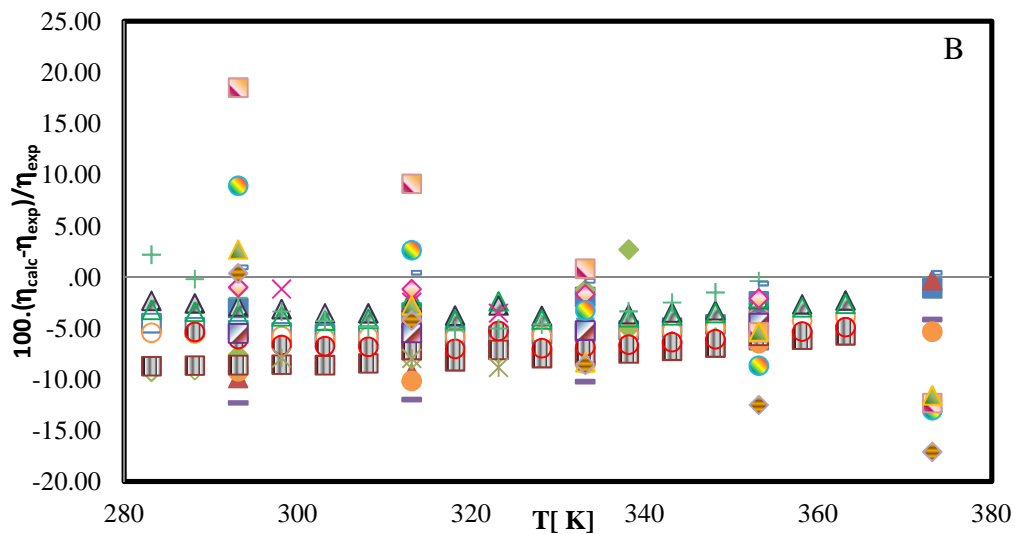
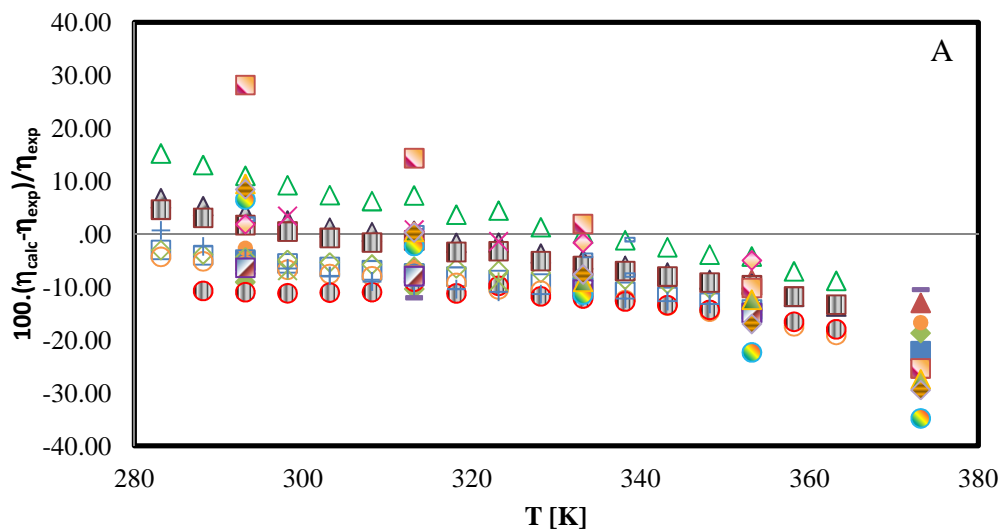
$$RD(\%) = 100. \frac{\eta_{calc} - \eta_{exp}}{\eta_{exp}} \quad (13)$$

where η is the dynamic viscosity in $mPa.s$. The average value (ARD) was calculated as a somatory of the modulus of RD over N experimental data points. The overall deviation was calculated by

$$OARD(\%) = \frac{\sum n ARD}{N_s} \quad (14)$$

where N_s is the number of systems studied.

The average relative deviations for each biodiesel and biodiesel blend studied are reported in Table 6 while the relative deviations of the individual data points for the 23 biodiesel samples are shown in Figures 1 A-D.



(continued in next page)

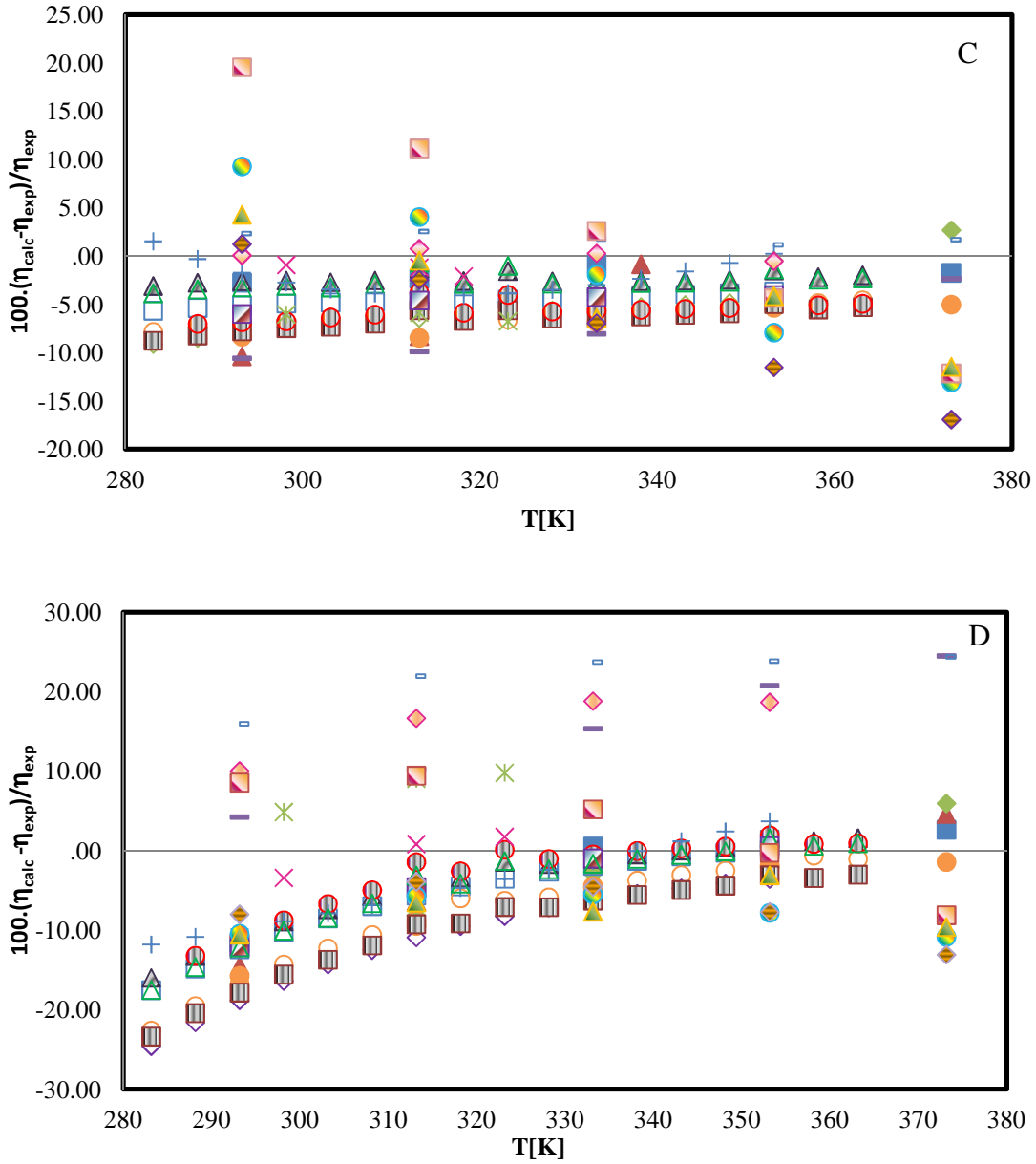


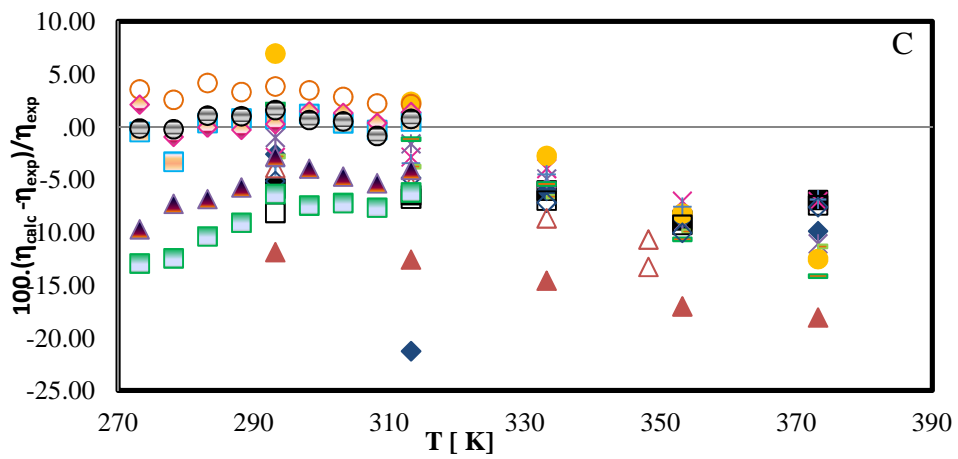
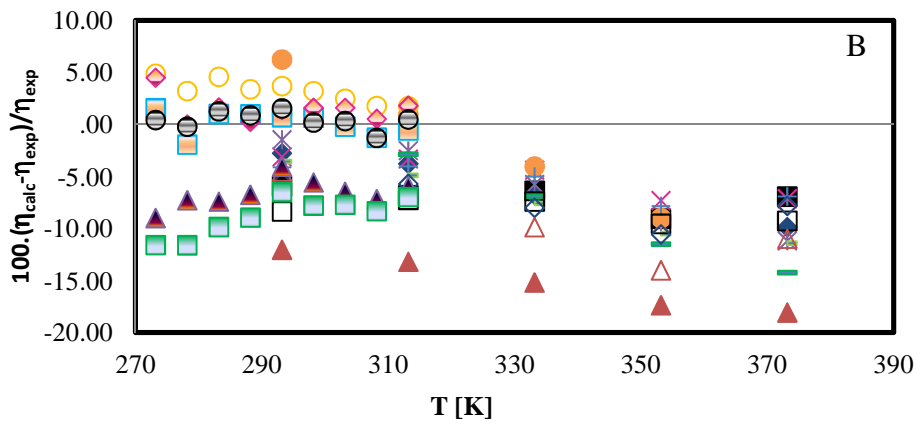
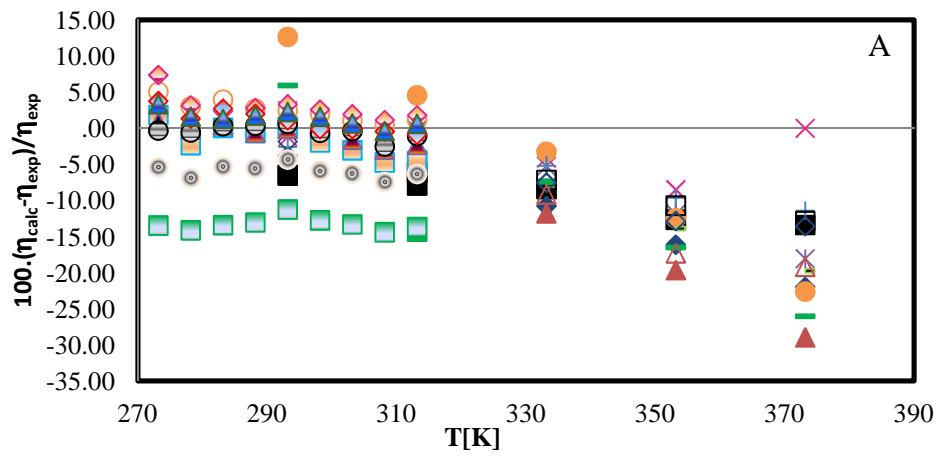
Figure 1 A-D. Relative deviation between experimental and predicted dynamic viscosity using (A) Ceriani's Model, (B) Yuan's Model, (C) revised Yuan's Model and (D) Krisnangkura's Model for 22 types of pure biodiesel ■ Yuan Soy; ▲ Yuan Palm; ◆ Yuan Canola; — Yuan Coconut; ● Yuan YGME; □ This work Soy A; ◇ This work B1; ○ This work Sunflower; ▲ This work Soy C; ● This work Palm; ■ This work Rapeseed; ▲ This work GP; × Krisnangkura Palm; ✱ Krisnangkura Coconut; + Blangino Soy; — Feitosa Coconut; ◇ Nogueira Babassu and ■ Nogueira Cotton seed, ● Yuan SMEA, ■ Yuan SMEB, ▲ Yuan GMSME and ◆ Yuan YGME*.

Table 6: Average relative deviations for viscosity of several biodiesel systems.

References	Biodiesel	Average relative deviation, %			
		Ceriani	Yuan	Revised Yuan	Krisnangkura
Yuan <i>et al.</i> ¹⁷	Soy	11.55	2.38	1.71	4.28
	Palm	8.05	6.22	5.85	6.55
	Canola	12.48	4.69	3.66	7.22
	Coconut	10.93	9.10	7.14	13.61
	YGME	8.45	7.92	6.77	7.44
Yuan <i>et al.</i> ²¹	SMEA	11.22	8.66	7.91	7.82
	SMEB	14.59	9.12	11.18	8.12
	GMSME	9.76	5.31	4.35	7.67
	YGME*	8.72	8.56	6.93	7.72
Blangino <i>et al.</i> ²³	Soy	9.01	3.25	2.39	5.73
Krisnangkura <i>et al.</i> ¹³	Palm	1.93	2.38	1.39	2.49
	Coconut	7.72	8.24	6.21	5.88
This work	Soy A	8.12	5.25	4.57	7.00
	Soy B	8.17	2.99	2.48	3.12
	B1	5.41	7.75	6.55	10.84
	Sunflower	9.64	5.48	5.64	7.60
	Palm	4.77	6.21	5.59	2.61
	Rapeseed	8.93	7.81	6.34	9.07
	GP	6.39	3.58	2.77	3.61
Knothe <i>et al.</i> ¹	Blending FAME (14 systems)	6.03	2.44	2.84	8.64
Feitosa <i>et al.</i> ²⁴	Coconut	3.34	0.56	1.91	15.49
Nogueira <i>et al.</i> ²⁵	Babassu	1.74	1.44	0.40	11.94
	Cotton seed	9.06	5.35	4.42	3.53
	Cotton seed+Babassu	7.69	3.48	2.49	6.06
Overall average relative deviation (OARD), %		8.07	5.34	4.65	7.25

The results suggest that all the models tend to underpredict the experimental viscosities. As one can see in Figures 1a and 1d, the predictions of Ceriani's and Krisnangkura's model are systematically larger than the Yuan type models (Figures 1b and 1c) and temperature dependent. Note, however, this dependency is opposite in the two cases: while Ceriani's deviations tend to increase with temperature, the reverse effect is observed for Krisnangkura's model, i.e., the deviations are lower at the higher temperatures, where the viscosities have lower values. In both cases, the deviations at the temperature extremes tend to be very large (up to 25 %). The temperature dependency of Ceriani's model seems to be related with the poor description of the viscosity of unsaturated fatty acid esters as discussed in previous works.^{18,20} A reestimation of the parameters for these compounds should allow a better description of the experimental viscosities. The temperature dependency of the fatty acid esters is better described in large temperature ranges by a Vogel-Tammann-Fulcher (VTF) equation, as suggested by Yuan's *et al.*¹⁷ than by the Arrhenius type adopted by Krisnangkura. The poor temperature dependency of this model is due to the equation used to describe temperature dependency of the viscosity of the pure components of the mixture.

Figures 1b and 1c reveals that the relative deviations obtained with the two versions of the Yuan model are temperature independent and the maximum deviation observed are in general lower than 10 %. They are thus more robust and reliable, producing suitable average deviations in comparison with other models available in the literature. In numbers, both Ceriani's and Krisnangkura's models have global average relative deviations around 8 %, Yuan's original model of 5.3 % and the revised version of Yuan's model here proposed of just 4.7 % that must be close to the experimental uncertainty of many of the experimental data.



(continued in next page)

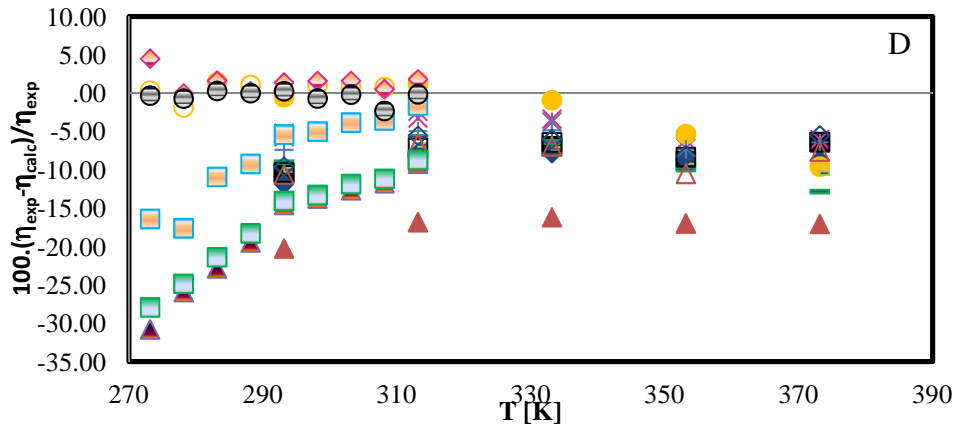


Figure 2a. Deviation between experimental and predicted dynamic viscosity using (A) Ceriani’s Model, (B) Yuan’s Model, (C) revised Yuan’s Model and (D) Krisnangkura’s Model for biodiesel blends with diesel fuel ■ SMEA 25, ◆ SMEA 50, ▲ SMEA 75, × SMEB 25, * SMEB 50, ● SMEB 75, + GMSME 25, - GMSME 50, - GMSME 75, □ YGME 25, ◇ YGME 50, △ YGME 75, ○ B10-B90 Max, ◻ B10-B90 Min, ◊ MO10-MO90 Max, ▲ MO10-MO90 Min, ⊖ ML10-ML90 Max, ◻ ML10-ML90 Min, (for panel A only, ◊ B10-B90 Med, ▲ MO10-MO90 Med and ⊖ ML10-ML90 Med).

The prediction of the viscosities of mixtures of biodiesel with petroleum diesel was also studied here by using Equation (1) where the biodiesel viscosity is estimated using the models here studied and the petroleum diesel viscosity used was the experimental value (panel A-D of Figure 2). The relative deviations were estimated using Equations (13) and (14) and are reported in Table 7. It was found that the deviations observed for the individual mixtures and the global deviations are in good agreement with those observed for the pure biodiesel, showing that their predictive capabilities of the approach here used is not affected by the presence of hydrocarbons in the mixture. Ceriani’s model shows an overall deviation of 6.47 %, Yuan’s and Krisnangkura’s models presented 5.59 % and 7.10 % respectively, while the revised Yuan’s model had the lowest global deviation of just 5.21 %, suggesting that the Yuan type models are also suitable to predict the viscosity data of biodiesel blends with petrodiesel.

Table 7. Average relative deviations for viscosity of several biodiesel blends with diesel fuel.

References	Biodiesel+Diesel	Average relative deviation, %			
		Ceriani	Yuan	Revised Yuan	Krisnangkura
Knothe <i>et al.</i> ¹	B+Petroleum (B10-B90)	1.75	1.97	1.79	2.19
	MO+petroleum (MO10-MO90)	1.88	3.23	2.46	9.07
	ML+petroleum (ML10-ML90)	7.05	3.80	3.75	7.78
Yuan <i>et al.</i> ²¹	SMEA (25, 50, 75 %)	10.20	9.56	9.90	11.45
	SMEB (25, 50, 75 %)	7.18	5.46	5.29	4.02
	GMSME (25, 50, 75 %)	9.40	6.47	5.49	8.26
	YGME (25, 50, 75 %)	7.84	8.67	7.75	6.91
Overall average relative deviation (OARD), %		6.47	5.59	5.21	7.10

MO -Methyl Oleate; ML – Methyl Linoleate

5. Conclusions

Viscosity data for seven well characterized biodiesel samples in terms of its FAME composition was measured and reported. Along with a database compiled from the literature, they were used to evaluate four models able to predict biodiesel viscosities based on information of their FAME compositions. It is shown that although all the models studied are able to predict the viscosities of both pure biodiesels and blends of biodiesel with petrodiesel with less than 10 % deviation in general, the models of Krisnangkura *et al.*¹³ and Ceriani *et al.*¹⁶ present deviations that are temperature dependent and that at the extremes of the temperature range studied can have deviations as high as 25 %. The deviations presented by the Yuan type models are more robust over temperature and also lower than those obtained with the two previous models. In particular the revised version of the Yuan's model here proposed based on new and more accurate data for the fatty acid methyl esters produces predictions with uncertainties that are close to the experimental uncertainties of the experimental data and can thus be an interesting tool to the design of biofuels or biofuel blends with viscosities that comply with legal specifications.

References

- [1] Knothe, G.; Steidley, K. R., Kinematic viscosity of biodiesel components (fatty acid alkyl esters) and related compounds at low temperatures *Fuel* 2007, 86, 2560.
- [2] Robert, O. D., Antioxidants for improving storage stability of biodiesel *Biofuels, Bioproducts and Biorefining* 2008, 2, 304.
- [3] Kralova, I.; Sjöblom, J., Biofuels–Renewable Energy Sources: A Review *Journal of Dispersion Science and Technology* 2010, 31, 409.
- [4] Knothe, G., Biodiesel Derived from a Model Oil Enriched in Palmitoleic Acid, Macadamia Nut Oil *Energy & Fuels* 2010, 24, 2098.
- [5] Anand, K.; Ranjan, A.; Mehta, P. S., Estimating the Viscosity of Vegetable Oil and Biodiesel Fuels *Energy & Fuels* 2009, 24, 664.
- [6] Demirbas, A., New Biorenewable Fuels from Vegetable Oils *Energy Sources, Part A: Recovery, Utilization, and Environmental Effects* 2010, 32, 628.
- [7] Kerschbaum, S.; Rinke, G., Measurement of the temperature dependent viscosity of biodiesel fuels *Fuel* 2004, 83, 287.
- [8] Paton, J. M.; Schaschke, C. J., Viscosity measurement of biodiesel at high pressure with a falling sinker viscometer *Chemical Engineering Research and Design* 2009, 87, 1520.
- [9] Benjumea, P.; Agudelo, J.; Agudelo, A., Basic properties of palm oil biodiesel-diesel blends *Fuel* 2008, 87, 2069.
- [10] Gerpen, J. V., Biodiesel processing and production *Fuel Processing Technology* 2005, 86, 1097.
- [11] Wagner, E.; Koehle, M.; Moyle, T.; Lambert, P., Predicting Temperature Dependent Viscosity for Unaltered Waste Soybean Oil Blended with Petroleum Fuels *Journal of the American Oil Chemists' Society* 2010, 87, 453.
- [12] Shu, Q.; Yang, B.; Yang, J.; Qing, S., Predicting the viscosity of biodiesel fuels based on the mixture topological index method *Fuel* 2007, 86, 1849.
- [13] Krisnangkura, K.; Yimsuwan, T.; Pairintra, R., An empirical approach in predicting biodiesel viscosity at various temperatures *Fuel* 2006, 85, 107.
- [14] Refaat, A. A., Correlation between the chemical structure of biodiesel and its physical properties *International Journal of Environmental Science and Technology* 2009, 6, 677.
- [15] Alptekin, E.; Canakci, M., Determination of the density and the viscosities of biodiesel-diesel fuel blends *Renewable Energy* 2008, 33, 2623.
- [16] Ceriani, R.; Goncalves, C. B.; Rabelo, J.; Caruso, M.; Cunha, A. C. C.; Cavaleri, F. W.; Batista, E. A. C.; Meirelles, A. J. A., Group Contribution Model for Predicting Viscosity of Fatty Compounds *Journal of Chemical & Engineering Data* 2007, 52, 965.
- [17] Yuan, W.; Hansen, A. C.; Zhang, Q., Predicting the temperature dependent viscosity of biodiesel fuels *Fuel* 2009, 88, 1120.
- [18] Pratas, M. J.; Freitas, S.; Oliveira, M. B.; Monteiro, S. I. C.; Lima, A. S.; Coutinho, J. A. P., Densities and Viscosities of Fatty Acid Methyl and Ethyl Esters *Journal of Chemical & Engineering Data* 2010, 55, 3983.
- [19] Carvalho, P. J.; Regueira, T.; Santos, L. M. N. B. F.; Fernandez, J.; Coutinho, J. A. P., Effect of Water on the Viscosities and Densities of 1-Butyl-3-methylimidazolium

- Dicyanamide and 1-Butyl-3-methylimidazolium Tricyanomethane at Atmospheric Pressure *Journal of Chemical & Engineering Data* 2009, 55, 645.
- [20] Pratas, M. J.; Freitas, S.; Oliveira, M. B.; Monteiro, S. I. C.; Lima, A. S.; Coutinho, J. A. P., Densities and Viscosities of Fatty Acid Methyl and Ethyl Esters of Minority Present in Biodiesel *Journal of Chemical & Engineering Data* 2010.
- [21] Yuan, W.; Hansen, A.; Zhang, Q.; Tan, Z., Temperature-dependent kinematic viscosity of selected biodiesel fuels and blends with diesel fuel *Journal of the American Oil Chemists' Society* 2005, 82, 195.
- [22] Duncan, A. M.; Ahosseini, A.; McHenry, R.; Depcik, C. D.; Stagg-Williams, S. M.; Scurto, A. M., High-Pressure Viscosity of Biodiesel from Soybean, Canola, and Coconut Oils *Energy & Fuels* 2010, 24, 5708.
- [23] Blangino, E.; Riveros, A. F.; Romano, S. D., Numerical expressions for viscosity, surface tension and density of biodiesel: analysis and experimental validation *Physics and Chemistry of Liquids: An International Journal* 2008, 46, 527.
- [24] Feitosa, F. X.; Rodrigues, M. d. L.; Veloso, C. B.; Cavalcante, C. I. L.; Albuquerque, M. n. C. G.; de Sant' Ana, H. B., Viscosities and Densities of Binary Mixtures of Coconut + Colza and Coconut + Soybean Biodiesel at Various Temperatures *Journal of Chemical & Engineering Data*, 55, 3909.
- [25] Nogueira, C. A.; Feitosa, F. X.; Fernandes, F. A. N.; Santiago, R. I. S.; de Sant'Ana, H. B., Densities and Viscosities of Binary Mixtures of Babassu Biodiesel + Cotton Seed or Soybean Biodiesel at Different Temperatures *Journal of Chemical & Engineering Data* 2010, 55, 5305.

- **Chapter 2**

**Low temperature
behaviour**

My direct contribution for Published Paper

This Chapter presents a study on the low temperature behaviour of biodiesels. The experimental work here reported was carried out by me in collaboration with Mariana Gonçalves.

Measurement and Modelling of Biodiesel Cold Flow Properties

Energy & Fuel, **2010**, 24, 2667-2674

DOI: 10.1021/ef901427g.

Measurement and Modelling of Biodiesel Cold Flow Properties

João A. P. Coutinho, M. Gonçalves, M.J. Pratas, M. L. S. Batista, V. F. S. Fernandes

CICECO, Departamento de Química, Universidade de Aveiro, 3810-193, Aveiro,
Portugal

J. Pauly, J.L. Daridon

Laboratoire des Fluides Complexes, Centre Universitaire de Recherche Scientifique,
Université de Pau, Avenue de l'Université, BP 1155, 64013 Pau, France

ABSTRACT

In spite of their interest for the understanding of the low temperature behavior of biodiesel, data on the phase equilibria of biodiesels at temperatures below the cloud point are not available in the literature. To overcome this limitation the liquid and solid phase compositions and fractions at temperatures below the cloud point were studied for three commercial diesels at temperatures ranging from 260 to 275 K.

A thermodynamic framework able to describe these multiphase systems is presented. Two versions of the Predictive UNIQUAC model along with an approach assuming complete immiscibility of the compounds in the solid phase are evaluated with success against the experimental phase equilibrium data measured in this work

KEYWORDS Biodiesel; Fatty acid methyl ester (FAME); Solid-liquid equilibrium; Modelling; Predictive UNIQUAC.

1. INTRODUCTION

Biodiesel production and consumption has been increasing steadily in the last few years thanks to the environmental benefits that result from its utilization. The cost of the raw materials and the competition with food for oils or soils are the main limitations to a more widespread use of biodiesel. The use of waste oil or cheap and non-edible oils and fats can help minimize this problem but the formulation of a biodiesel must conform to a number of standards before approval for commercialization.

The main biodiesel properties are dependent on the oils or fats used on its production. This biofuel is much less complex than conventional diesels. It consists on a liquid blend of, non toxic, biodegradable fatty acid esters, yellow coloured and immiscible with water. Its cold flow performance depends both on the oil and the alcohol used in the transesterification. A biodiesel with a large concentration of saturated fatty acid esters, although less vulnerable to oxidation and displaying better combustion properties, has a worst performance at low temperatures because of its tendency to crystallize¹. There are a number of specifications for the biodiesel performance at low temperatures. The most important are the Cloud Point, CP, the Pour Point, PP, the Cold Filter Plugging Point, CFPP, and the Low Temperature Filterability Test, LTFT². Dunn and co-workers have produced a large body of work that provides a comprehensive picture of the influence of the saturated fatty esters and various alcohols on the low temperature behaviour of biodiesel^{1, 3-8}. What currently lacks is a good and reliable model that, from the knowledge of the biodiesel composition, could predict the low temperature behavior of the fuel⁸. This model would be an essential tool for a quick evaluation of the biodiesel characteristics, design of a biodiesel to meet the requirements for low temperature utilization, and design and operation of winterization processes for biodiesels⁹.

Our previous work has addressed the low temperature behavior of conventional fuels. A thermodynamic model, Predictive UNIQUAC¹⁰⁻¹⁵, was developed and extensively tested in diesels¹⁶⁻¹⁸, jet fuels and other refined products^{17, 19-21} and unrefined oils²²⁻²⁵ with success. Lately we have been addressing the application of this model to the description of the cloud points of fatty acid mixtures²⁶, and fatty acid methyl²⁷ and ethyl ester²⁸ mixtures. The Predictive UNIQUAC model was shown to be able to successfully

describe the cloud point of the mixtures studied but presented limited advantages compared to a simpler model where no solid solution formation was considered as discussed in a previous work²⁸.

The cloud point provides, however, a limited information about the low temperature behavior of a fuel. Both the CFPP and the LTFT are related to what happens below the cloud point, i.e. the composition of the material that precipitates and the amount of crystals formed. This last issue is particularly relevant as the gelling of the fluid and the plugging of filters is essentially dependent on the amount of solids crystallizing at low temperatures. The adequate design and operation of winterization processes to produce biodiesel that can conform to low temperature specifications also requires the capability to predict the composition of the liquid phase after partial crystallization of a biodiesel and the prediction of its new low temperature characteristics^{9, 29-31}. To learn more about the behavior of a biodiesel below its cloud point an approach successfully used previously for the study of conventional diesels^{16, 18} and other complex synthetic mixtures^{12, 32-36} was here applied to biodiesels. It consists in separating by filtration the liquid and solid phases at various temperatures below the cloud point and study their composition and relative amounts.

In this work experimental data for the solid liquid phase equilibria of three commercial non-additivate biodiesels at temperatures ranging from 260 to 275 K are reported. A thermodynamic framework able to describe these multiphase systems is presented. Two versions of the Predictive UNIQUAC model along with a model assuming complete immiscibility of the compounds on the solid phase are evaluated with success against the experimental data as shown below.

2. EXPERIMENTAL

The three commercial biodiesels here studied, BDA, BDB and BDC, were obtained from Portuguese biodiesel producing companies. They were collected at the end of the production line before additivation and their composition was measured by gas chromatography on a Varian 3800CP chromatograph equipped with a split/splitless injector at 250°C (split ratio of 1:20) and a FID detector at 220°C. A DB1-HT column (length: 15m, internal diameter: 0.32mm and film thickness: 0.1µm) coated with a film of dimethylpolysiloxane, with a temperature program of 5 °C/min from 80 °C to 200 °C

was used. The carrier gas was helium with a flow rate of 2mL/min. The compositions of the fatty acid esters present in concentrations above 0.5 wt% are reported in Table 1. The total concentration of other esters was less than 2 wt%.

Table 1. Composition (wt%) and Cloud Points of the biodiesel studied.

	BDA	BDB	BDC
C16:0	16.18	5.59	11.04
C18:0	3.82	2.39	4.07
C18:1	28.80	55.20	22.92
C18:2	50.46	34.89	61.03
Cloud Point / K	280	271	276

The low temperature behavior of the biodiesels was studied using a methodology previously developed by us to measure solid liquid phase equilibria in hydrocarbon fluids^{12, 32} and widely used to the study of both synthetic mixtures^{12, 33-36} and diesels^{16, 18}. It consists in separating the liquid phase from the precipitate by filtration at controlled temperature and analyzing the phases by gas chromatography. The phase separation is achieved using UniPrep syringeless filters from Whatman of 5 mL capacity with filters of 0.2 μ m porosity. The biodiesel is distributed in 1 mL samples by the UniPrep that are introduced on a thermostatic bath where the samples are equilibrated for 24 hours before separation. When the separation is completed, the two phases recovered are analyzed using the gas chromatography analytical procedure described above. The liquid and solid phase composition and fractions are estimated by mass balances from the results of these analysis according to a procedure proposed previously^{12, 32} and detailed below. No multiple measurements were carried for each point so a correct value of reproducibility of the experimental data cannot be assigned. Based on our previous experience^{12, 32-36} and on the results for the points that were duplicated the estimated reproducibility is of 1% on the liquid phase composition, 5% on the solid phase composition and 5-10% on the solid fraction.

The precipitate (P) recovered is composed by the solid phase (S) and important quantities of liquid (L) that remain entrapped in the crystals after the filtration. It is thus impossible to assess directly the composition of the solid phase after the filtration. Only the composition of the liquid phase (L) and the precipitate (P) can be determined

directly. Since the unsaturated fatty acid esters have melting points much lower than the corresponding saturated fatty acid esters they will not crystallize at the temperatures used on this study and thus the portion of liquid entrapped in the crystals of the precipitate can be determined from the quantity of unsaturated fatty esters present in the precipitate. Since the exact composition of the liquid phase is known from chromatography it is possible to calculate the fraction of entrapped liquid, c , as:

$$c = \frac{W_{C18:1}^P + W_{C18:2}^P}{W_{C18:1}^L + W_{C18:2}^L} \quad (1)$$

where W are the mass fraction of the compounds obtained from the chromatographic analysis and P and L stand for the precipitate and the liquid fractions. Using the value of this fraction c it is possible to estimate the composition of the various compounds i present in the solid phase, S, as

$$W_i^S = \frac{W_i^P - cW_i^L}{1 - c} \quad (2)$$

The fraction of the initial biodiesel sample that crystallized, X^S , can be obtained from a mass balance to any of the compounds present but is ideally estimated from the concentration of any of the unsaturated fatty acid esters on both the original biodiesel, BD, and the concentration in the liquid phase, L, under the conditions studied as

$$X^S = \frac{W_i^L - W_i^{BD}}{W_i^L} \quad (3)$$

This experimental methodology allows an easy measurement of the composition of the liquid, W^L , and solid phases, W^S , as well as the fraction of crystallized material, X^S , as function of the temperature.

3. THERMODYNAMIC MODEL

The precipitation of solids in biodiesel at low temperatures is described using an approach previously proposed by us for alkane mixtures¹⁰⁻²⁵ and also applied to fatty acids²⁶, and fatty acids methyl and ethyl esters^{27,28} with success.

The solid-liquid equilibrium can be described by an equation relating the composition of component i in the solid and liquid phases with their non ideality, and the thermophysical properties of the pure component³⁷

$$\ln \frac{x_i^s \gamma_i^s}{x_i^l \gamma_i^l} = \frac{\Delta_{fus} H_i}{RT_{fus,i}} \left(\frac{T_{fus,i}}{T} - 1 \right) - \frac{\Delta_{fus} C_{p,i}(T_{fus,i})}{R} \left(1 - \frac{T_{fus,i}}{T} + \ln \frac{T_{fus,i}}{T} \right) \quad (4)$$

where γ_i is the activity coefficient of the compound, x_i its mole fraction, $\Delta_{fus} H(T_{fus})$ the molar enthalpy of fusion of the pure solute at the melting temperature T_{fus} , and $\Delta_{fus} C_{p,i}(T_{fus,i})$ the molar heat capacity change upon fusion, at fusion temperature T_{fus} . The heat capacity change upon fusion is usually regarded as being independent of the temperature and the bracketed term multiplied with $\Delta_{fus} C_{p,m}$ is often considered as being small, as the opposite signs inside the bracket lead to near cancellation³⁸. This term was thus neglected on the calculations. The thermophysical properties of the crystallizing saturated fatty acid esters used were obtained from correlations developed in a previous work²⁷ and are reported in Table 2.

Table 2. Thermophysical properties of saturated fatty acid methyl esters.

	$T_{fus} /$ K	$\Delta_{fus} H /$ kJ mol ⁻¹	$\Delta_{vap} H /$ kJ mol ⁻¹
C16:0	302.59	56.85	96.58
C18:0	311.45	64.84	105.92

Since the major compounds of a biodiesel are fatty acid esters of similar size and nature, the liquid phase may be treated as an ideal solution. Using Eq. (1), along with a multiphase flash algorithm, the composition and amount of the phases in equilibrium can be calculated if a model for the non-ideality of the solid phases is available. Due to its simplicity and robustness the algorithm of resolution of the Rachford-Rice equations proposed by Leivobici and Neoschil³⁹ was used in the calculations.

The solid phase non-ideality is described by the most recent version of the Predictive UNIQUAC model¹⁵. The UNIQUAC model can be written as

$$\frac{g^E}{RT} = \sum_{i=1}^n x_i \ln \left(\frac{\Phi_i}{x_i} \right) + \frac{Z}{2} \sum_{i=1}^n q_i x_i \ln \frac{\theta_i}{\Phi_i} - \sum_{i=1}^n x_i q_i \ln \left[\sum_{j=1}^n \theta_j \exp \left(- \frac{\lambda_{ij} - \lambda_{ii}}{q_i RT} \right) \right] \quad (5)$$

with

$$\Phi_i = \frac{x_i r_i}{\sum_j x_j r_j} \quad \text{and} \quad \theta_i = \frac{x_i q_i}{\sum_j x_j q_j} \quad (6)$$

On this version of Predictive UNIQUAC the structural parameters, r_i and q_i are obtained from the UNIFAC parameter table⁴⁰.

The predictive local composition concept¹⁰⁻¹⁵ allows the estimation of the interaction energies, λ_{ij} , used by these models without fitting to experimental data. The pair interaction energies between two identical molecules are estimated from the heat of sublimation of the pure component,

$$\lambda_{ii} = -\frac{2}{Z}(\Delta_{sub}H_i - RT) \quad (7)$$

where Z is the coordination number with a value of 10 as in the original UNIQUAC model^{15, 41}. The heats of sublimation are calculated at the melting temperature of the pure component as

$$\Delta_{sub}H = \Delta_{vap}H + \Delta_{fus}H \quad (8)$$

The pair interaction energy between two non-identical molecules is given by

$$\lambda_{ij} = \lambda_{ji} = \lambda_{jj}(1 + \alpha_{ij}) \quad (9)$$

where j is the ester with the shorter chain of the pair ij . The interaction parameter α_{ij} allows the tuning of the non ideality of the solid solution. In this work three approaches to the solid phase non ideality will be evaluated: assuming $\alpha_{ij}=0$ (*UNIQUAC*) as was previously done for alkanes¹⁰⁻²⁵; using $\alpha_{ij}=-0.05$ (*UNIQUAC -0.05*), a value similar to that used on the description of the phase diagrams of fatty acids²⁶ and fatty acid esters²⁷; and finally assuming that there is no solid solution formation and each compound crystallizes as a pure crystal (*No solution*). This last situation corresponds to an infinite value of the solid phase activity coefficient that within the framework of Predictive UNIQUAC can be achieved with a value of α_{ij} larger than -0.25.

The solid-liquid equilibrium model used in this work is thus a purely predictive model that uses only pure component properties for the calculation of the phase equilibria. The three versions here evaluated will be used to predict the low temperature behavior of the three biodiesels studied in this work⁴².

3. RESULTS AND DISCUSSION

The experimental methodology used on this work provides direct information about the composition of the liquid phase. The compositions of the solid phase are estimated from the composition of the liquid phase and the precipitate according to Eqs. (1) and (2). The fraction of solids crystallizing from the biodiesel at each temperature is obtained from the differences between the concentrations of the unsaturated fatty acid esters on the original biodiesel and on the liquid phase according to Eq. (3). It follows that the uncertainty associated to the solid phase compositions and the solid fractions is consequently larger than that of the liquid phase, which is just the uncertainty associated to the GC analysis. The compositions of the liquid and solid phases along with the solid fraction formed are reported on Tables 3 to 5 at the various temperatures studied for each of the biodiesels used on this work. These values along with the predictions achieved by the three studied models are presented in Figures 1 to 9.

Table 3. Composition (wt %) of the solid and liquid phases in equilibrium as function of temperature for BDA.

Temperature / K	Liquid phase				Solid phase		Solid fraction
	C16:0	C18:0	C18:1	C18:2	C16:0	C18:0	
265.65	4.57	1.05	33.82	59.54	81.08	18.92	15.28
268.15	5.23	1.06	33.84	59.1	80.23	19.77	14.95
270.65	6.6	1.43	33.19	57.95	80.21	19.79	13.47
273.15	8.34	1.86	31.98	56.77	80.91	19.09	11.15
275.65	10.91	2.75	30.91	54.42	82.61	17.39	7.47

Table 4. Composition (wt %) of the solid and liquid phases in equilibrium as function of temperature for BDB.

Temperature / K	Liquid phase				Solid phase		Solid fraction
	C16:0	C18:0	C18:1	C18:2	C16:0	C18:0	
260.65	2.63	0.87	58.45	37.06	65.9	34.1	5.62
263.15	3.58	1.21	57.33	36.39	62.04	37.96	3.83
265.65	4.11	1.58	57.04	36.29	64.54	35.46	3.44
268.15	5.52	2.22	55.6	35.02	36.45	63.55	2.45
270.15	5.32	2.19	56.39	34.76	10.97	89.03	2.11

Table 5. Composition (wt %) of the solid and liquid phases in equilibrium as function of temperature for BDC.

Temperature / K	Liquid phase				Solid phase		Solid fraction
	C16:0	C18:0	C18:1	C18:2	C16:0	C18:0	
260.65	4.2	1.23	25.86	68.71	71.86	28.14	11.05
263.15	5.61	1.84	25.32	66.87	71.92	28.08	9.14
265.65	6	1.98	25.07	66.34	70.98	29.02	8.23
268.15	6.73	2.35	24.94	65.46	72.18	27.82	7.19
270.65	10.7	3.95	22.97	61.4	71.27	28.73	0.5

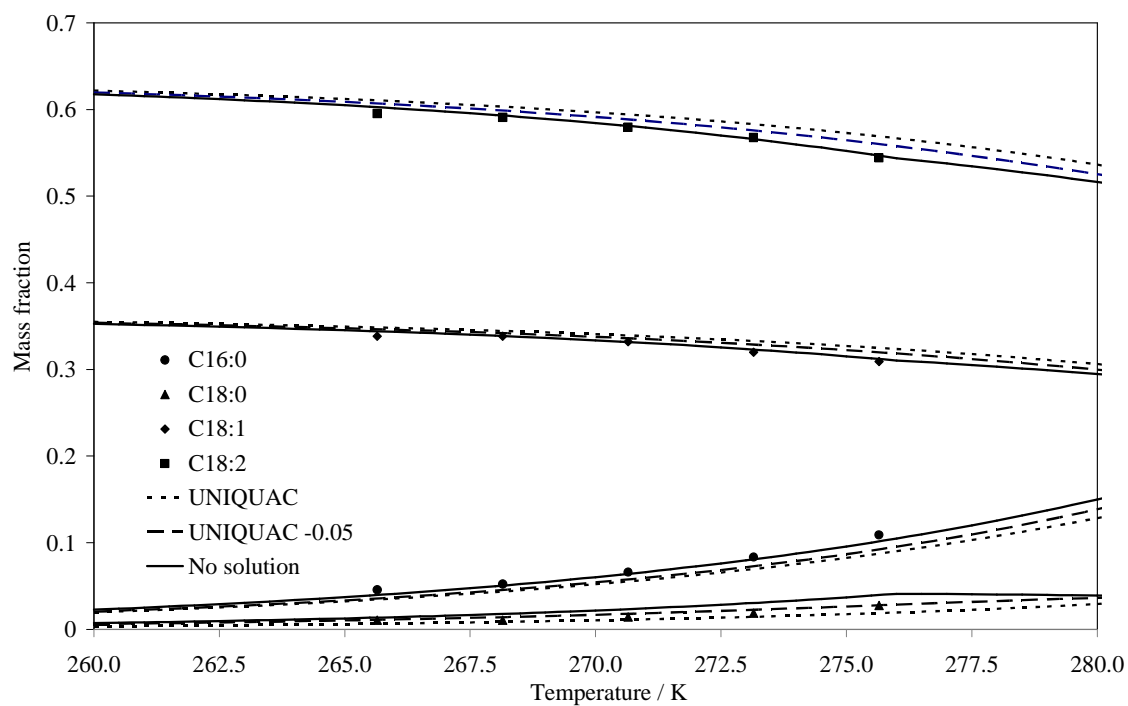


Figure 1. Liquid phase composition for BDA.

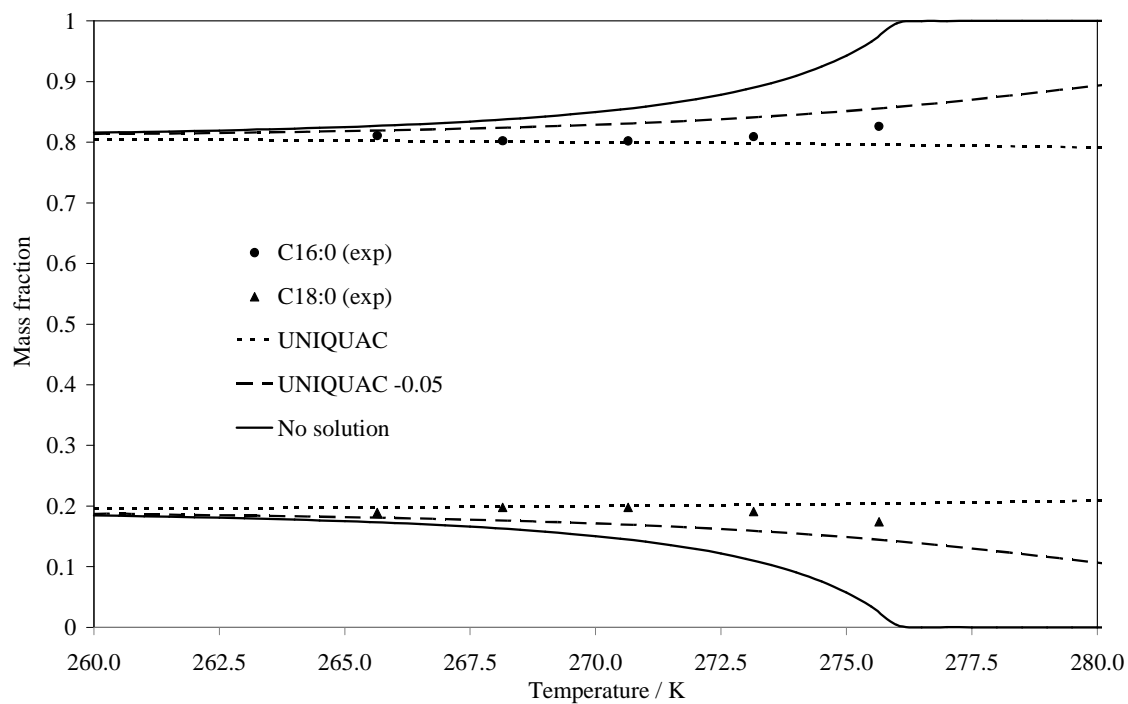


Figure 2. Solid phase composition for BDA.

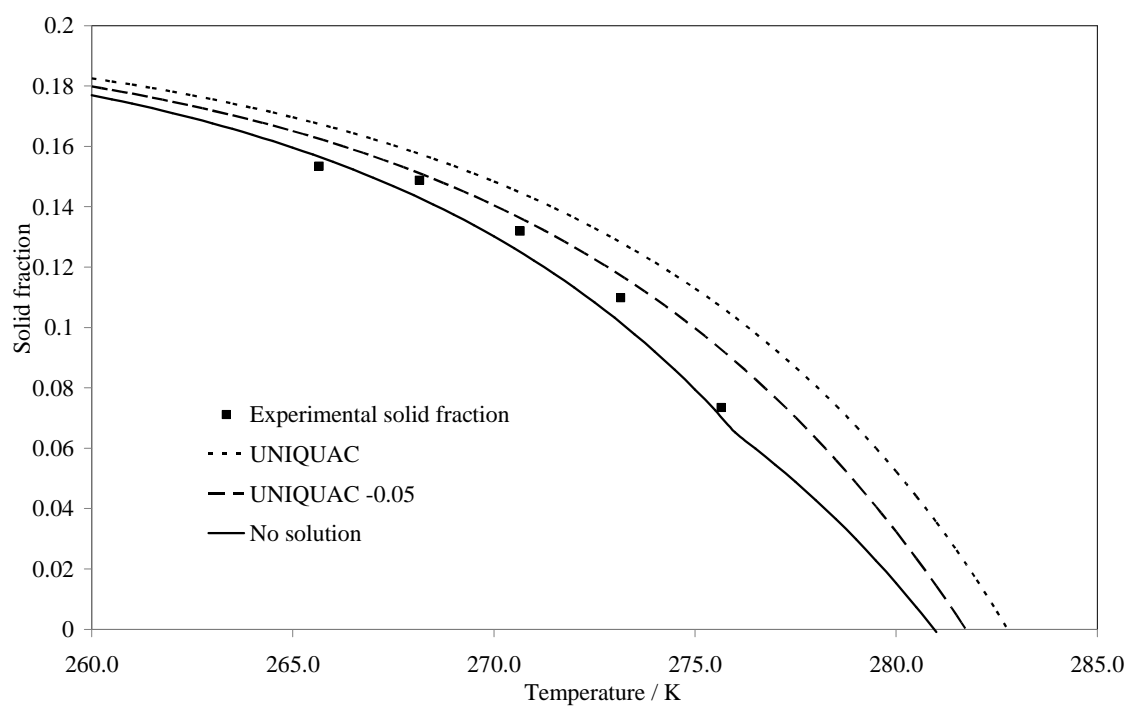


Figure 3. Dependence with the temperature of the fraction of precipitated solid material for BDA.

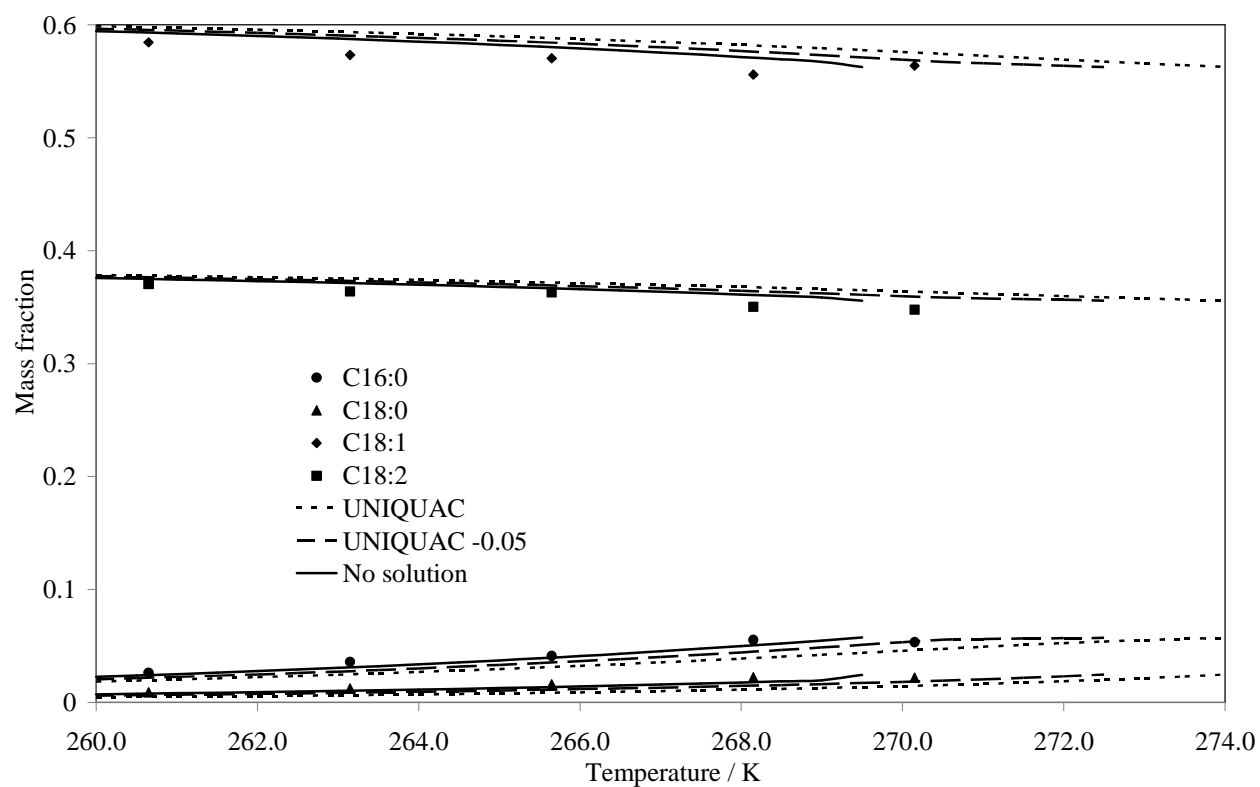


Figure 4. Liquid phase composition for BDB.

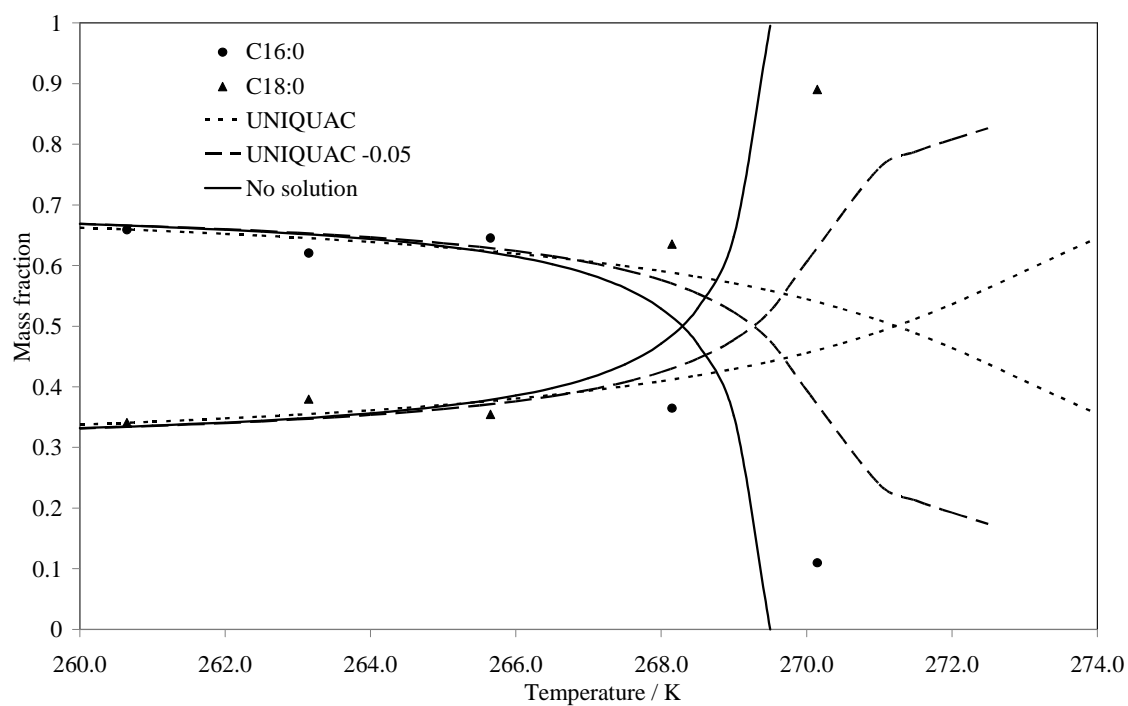


Figure 5. Solid phase composition for BDB.

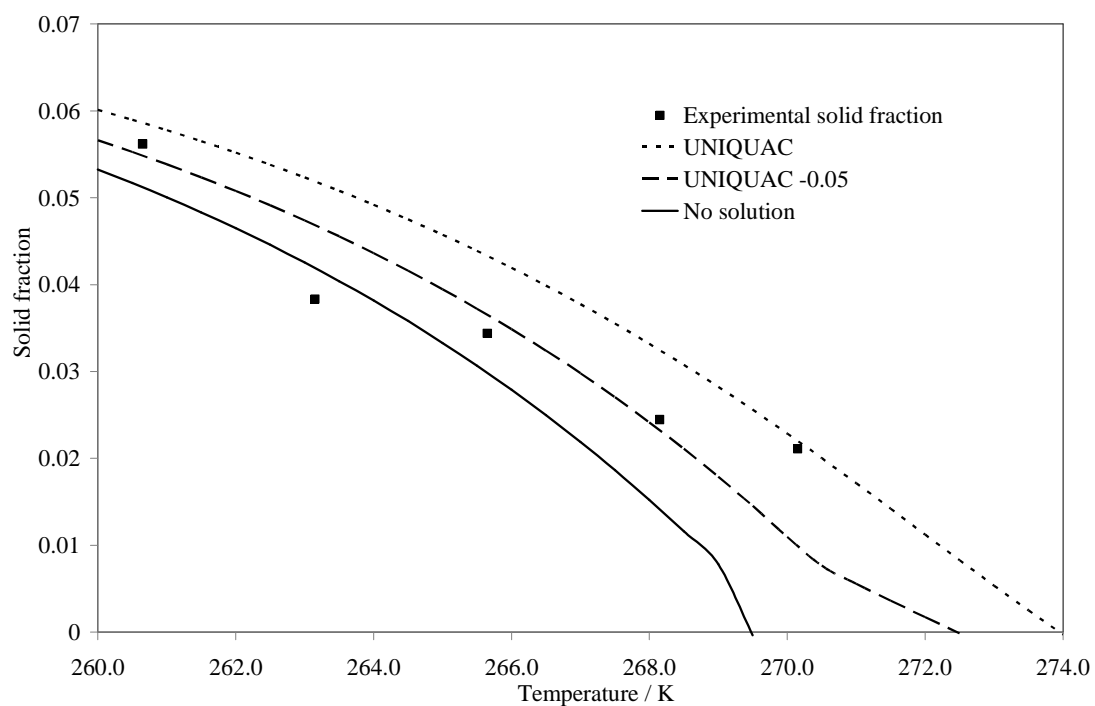


Figure 6. Dependence with the temperature of the fraction of precipitated solid material for BDB.

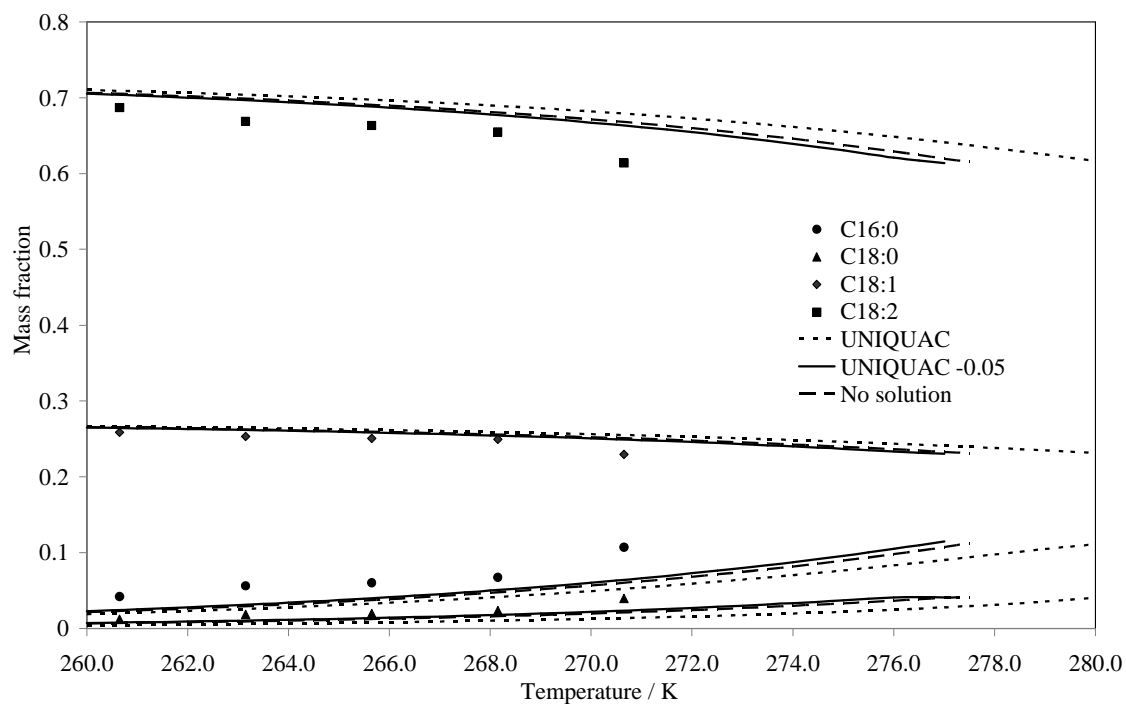


Figure 7. Liquid phase composition for BDC.

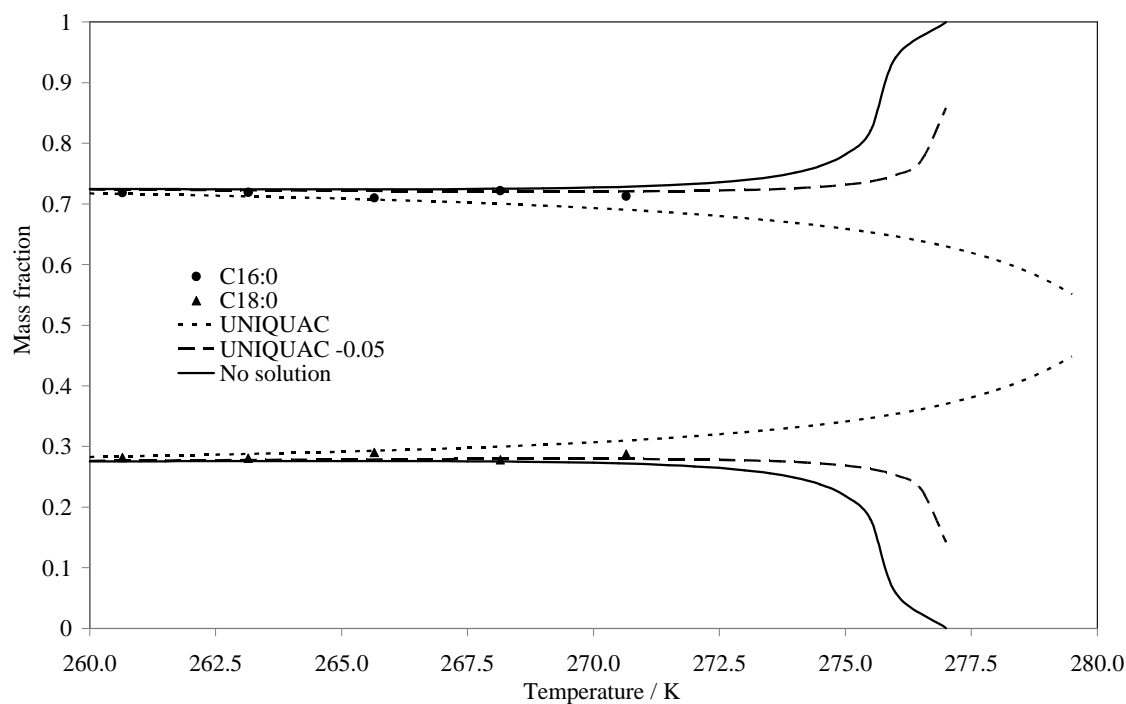


Figure 8. Solid phase composition for BDC.

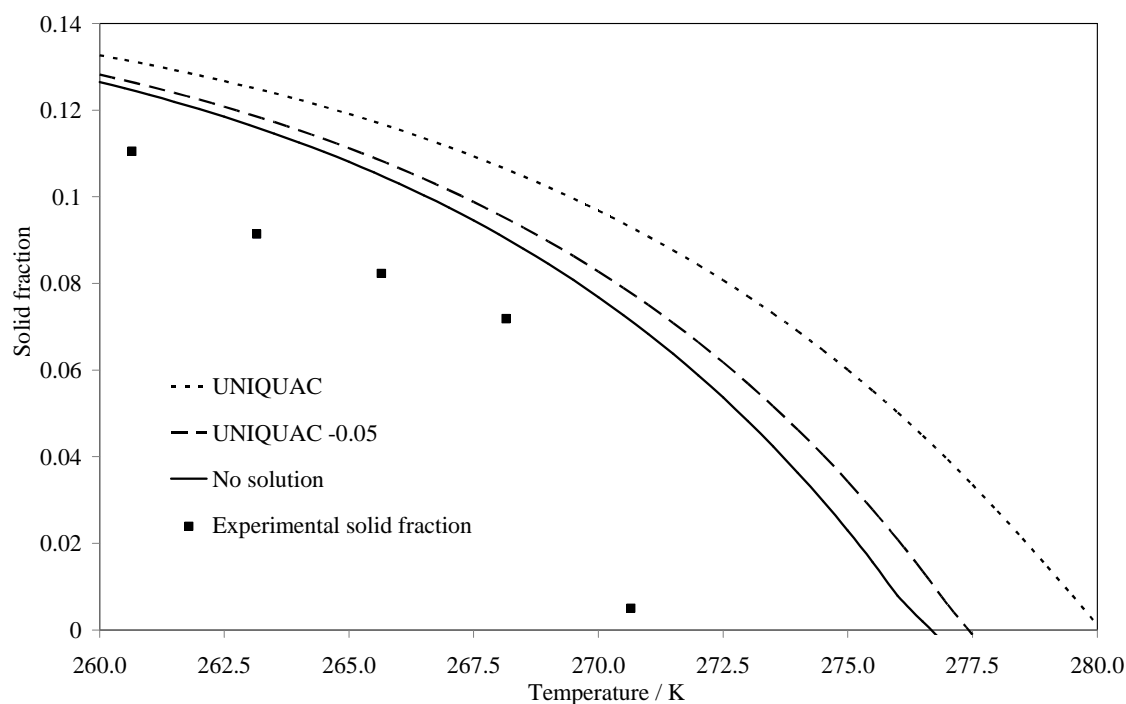


Figure 9. Dependence with the temperature of the fraction of precipitated solid material for BDC.

Since the lowest temperature studied was 260.65 K and the melting points of the unsaturated fatty acid esters present on the biodiesel are lower than this value it was admitted that these compounds did not crystallize under the conditions used in this work. The solid phase is thus composed solely by the saturated fatty acid methyl esters, methyl palmitate (C16:0) and methyl stearate (C18:0). The temperature dependency of the liquid phase compositions observed for all the biodiesels is similar as shown in Figures 1, 4 and 7. As the temperature decreases the saturated esters crystallize and then the liquid phase becomes depleted on the saturated esters and enriched on the unsaturated esters. This results on an increase of the unsaturated esters concentration at low temperatures while the saturated esters show the opposite behavior with a decrease in concentration with temperature. In what concerns the description of the liquid phase compositions the three models adopted have quite similar performances providing a description of the data that is essentially within their experimental uncertainty.

The solid phase compositions presented in Figures 2, 5 and 8 display a richer and more complex behavior becoming a more stringent test to the models. Although the models predict a similar solid phase composition at temperatures 5 to 10 K lower than the cloud point, close to it they display a very different behavior. While the Predictive

UNIQUAC model with $\alpha_{ij}=0$ (*UNIQUAC*) predicts that both saturated esters crystallize simultaneously, as expected from the formation of a solid solution, the model assuming that each ester crystallizes independently (*No solution*) starts with the crystallization of just one of the esters and, as the temperature decreases and the ratio between the stearate and palmitate esters reaches the eutectic point of the mixture, they start both to crystallize although as independent solid phases. This produces some interesting features on the phase equilibria predicted by the *No solution* model such as a small increase on the concentration of the methyl stearate on the liquid phase below the cloud point and down to 276 K for BDA while the methyl palmitate crystallizes alone.

The kinks observed on the solid fraction lines predicted by this model and reported in Figures 3, 6 and 9 can also be assigned to the change of regimen of crystallization of a single ester to the simultaneous crystallization of two esters. In any case these behaviors would be too subtle to be observed on the experimental data to test the model validity. The Predictive UNIQUAC model with $\alpha_{ij}=-0.05$ (*UNIQUAC -0.05*) presents an intermediate behavior between these two extremes. While it clearly favors the crystallization of one of the esters over the other at the cloud point it still predicts nevertheless that there is always some degree of co-crystallization. This allows the correct description of the decrease in methyl palmitate and increase in methyl stearate concentrations as the temperature decreases observed in BDA. The *UNIQUAC* model predicts the opposite behavior for all the studied biofuels, while the *No solution* model, although qualitatively correct, overestimates this composition change. This change in the solid phase composition is particularly visible for BDB shown in Figure 5. Because in BDB the methyl palmitate to methyl stearate ratio is much lower than in the two other fuels the crystallization will start on the opposite side of the eutectic point than the observed in BDA and BDC. This originates that at the cloud point it will be the methyl stearate, rather than the methyl palmitate that dominates in the solid phase. This peculiar behavior is rather clear in the experimental data with an inversion of the dominant ester in the solid phase as the temperature decreases.

Although all the models can qualitatively describe the change in the dominant ester present in the solid phase the *UNIQUAC* model fails to adequately describe it while the two other models provide a fair description of the concentration inversion. On BDC, presented on Figure 8, the *UNIQUAC* model again fails to provide a description of the

qualitative trend observed in the solid phase compositions. The two other models show no differences within the experimental temperature range studied.

The crystallization differences around the cloud point, along with the differences on the estimation of the cloud point itself, generate important differences on the solid fractions predicted by the three models studied on this work reported on Figures 3, 6 and 9. The solid fraction, as well as the cloud point estimation, decreases with the increasing non ideality of the solid phase. In all cases the solid fractions predicted by the *UNIQUAC* model are larger than those estimated by the *UNIQUAC -0.05* and these larger than those obtained from the *No solution* model. It is clear that the *UNIQUAC* model overestimates the solid fractions measured. Given the quality of the experimental data measured for the solid fractions it is not possible to clearly identify which of the two other models is the best since both describe the data within its experimental uncertainty.

A global analysis of the data suggests that both the *UNIQUAC -0.05* and the *No solution* model can provide an adequate description of the phase equilibrium data of biodiesels below the cloud point of the fuel. The *UNIQUAC -0.05* model is probably superior with a better description of the cloud point and of the solid phase composition. A more extensive set of data and of higher quality seems to be required to reach a final conclusion.

5. CONCLUSIONS

This work reports experimental data for the solid liquid phase equilibria of three commercial, non-additive, biodiesels at temperatures ranging from 260 to 275 K. A thermodynamic framework able to describe these multiphase systems is presented. Two versions of the Predictive *UNIQUAC* model along with a model assuming complete immiscibility of the compounds in the solid phase are evaluated against the experimental data measured. It is shown that both the Predictive *UNIQUAC* model with $\alpha_{ij}=-0.05$ (*UNIQUAC -0.05*) and a model assuming complete immiscibility on the solid phase are capable of providing an adequate representation of the phase equilibria for these systems below their cloud points.

REFERENCES

- [1] Dunn, R.O.; Bagby, M.O. *JAOCs* **1995**, 72, 895-904.
- [2] *Annual Book of ASTM Standards*, Vol. 05.01, **1999**.
- [3] Dunn, R.O.; Shockley, M.W.; Bagby, M.O. *JAOCs* **1996**, 73, 1719-1728.
- [4] Foglia, T.A.; Nelson, L.A.; Dunn, R.O. *JAOCs* **1997**, 74, 951-955.
- [5] Dunn, R.O.; Bagby, M.O. *JAOCs* **2000**, 77, 1315-1323.
- [6] Dunn, R.O. *JAOCs* **2002**, 79, 709-715.
- [7] Dunn, R.O. *JAOCs* **2008**, 85, 961-972.
- [8] Dunn, R.O. *Energy & Fuels* **2009**, 23, 4082-4091.
- [9] Knothe, G. *Energy & Fuels* **2008**, 22, 1358-1364.
- [10] Coutinho, J.A.P.; Knudsen, K.; Andersen, S.I.; Stenby, E.H. *Chem. Eng. Sci.* **1996**, 51, 3273-3282.
- [11] Coutinho, J.A.P.; Stenby, E.H. *Ind. Eng. Chem. Res.* **1996**, 35, 918-925.
- [12] Coutinho, J.A.P.; Ruffier-Meray, V. *Ind. Eng. Chem. Res.* **1997**, 36, 4977-4983.
- [13] Coutinho, J.A.P. *Ind. Eng. Chem. Res.* **1998**, 37, 4870-4875.
- [14] Coutinho, J.A.P. *Fluid Phase Equilib.* **1999**, 158-160, 447-457.
- [15] Coutinho, J.A.P.; Mirante, F.; Pauly, J. *Fluid Phase Equilib.* **2006**, 247, 8-17.
- [16] Coutinho, J.A.P.; Dauphin C.; Daridon, J.L. *Fuel* **2000**, 79, 607-616.
- [17] Coutinho, J.A.P. *Energy & Fuels* **2000**, 14, 625-631.
- [18] Pauly, J.; Daridon, J.L.; Sansot, J.M.; Coutinho, J.A.P. *Fuel* **2003**, 82, 595-601.
- [19] Mirante F.I.C.; Coutinho, J.A.P. *Fluid Phase Equilib.* **2001**, 180, 247-255.
- [20] Coutinho, J.A.P.; Mirante F.; Ribeiro J.C.; Sansot, J.M.; Daridon, J.L. *Fuel* **2002**, 81, 963-967
- [21] Queimada, A.J.N.; Dauphin, C.; Marrucho, I.M.; Coutinho, J.A.P. *Thermochim Acta* **2001**, 372, 93-101.
- [22] Coutinho, J.A.P.; Daridon, J.L. *Energy & Fuels* **2001**, 15, 1454-1460.
- [23] Daridon, J.L.; Pauly, J.; Coutinho, J.A.P.; Montel, F. *Energy & Fuels* **2001**, 15, 730-735.
- [24] Sansot, J.M.; Pauly, J.; Daridon, J.L.; Coutinho, J.A.P. *AIChE J.* **2005**, 51, 2089-2097.
- [25] Coutinho, J.A.P.; Edmonds, B.; Morwood, T.; Szczepanski, B.; Zhang, X. *Energy & Fuels* **2006**, 20, 1081-1088.
- [26] Costa, M.C.; Krahenbuhl, M.A.; Meirelles, A.J.A.; Daridon, J.L.; Pauly, J.; Coutinho, J.A.P. *Fluid Phase Equilib.* **2007**, 253, 118-123.
- [27] Lopes, J.C.A.; Boros, L.; Krähenbühl, M. A.; Meirelles, A.J.A.; Daridon, J.L.; Pauly, J.; Marrucho, I.M.; Coutinho, J.A.P. *Energy & Fuels* **2008**, 22, 747-752.
- [28] Boros, L.; Batista, M.L.S.; Vaz, R.V.; Figueiredo, B.R.; Fernandes, V.F.S.; Costa, M.C.; Krahenbuhl, M.A.; Meirelles, A.J.A.; Coutinho, J.A.P. *Energy & Fuels* **2009**, 23, 4625-4629.

- [29] Kerschbaum, S.; Rinke, G.; Schubert, K. *Fuel* **2008**, 87, 2590-2597.
- [30] Lee, I.; Johnson, L.A.; Hammond, E.G. *JAOCs* **1996**, 73, 631-636.
- [31] Dunn, R.O.; Schockley, M.W.; Bagby, M.O. *SAE Technol. Pap. Ser.* 971682, **1997**.
- [32] Dauphin, C.; Daridon, J.L.; Coutinho, J.A.P.; Baylere, P.; Pontin-Gautier, M. *Fluid Phase Equilib.* **1999**, 161, 135-151.
- [33] Pauly, J.; Daridon, J.L.; Coutinho, J.A.P. *Fluid Phase Equilib.* **2001**, 187, 71-82
- [34] Pauly, J.; Daridon, J.L.; Coutinho, J.A.P. *Fluid Phase Equilib.* **2004**, 224, 237-244.
- [35] Pauly, J.; Daridon, J.L.; Coutinho, J.A.P.; Dirand, M. *Fuel* **2005** 84, 453-459.
- [36] Coutinho, J.A.P.; Gonçalves, C.; Marrucho, I.M.; Pauly, J.; Daridon, J.L. *Fluid Phase Equilib.* **2005**, 233, 29-34.
- [37] Prausnitz, J.M.; Lichtenthaler, R.N.; Azevedo, E.G. *Molecular Thermodynamics of Fluid-Phase Equilibria*. 3rd ed., Prentice-Hall, Englewood Cliffs, NJ, (**1999**).
- [38] Coutinho, J.A.P.; Andersen, S.I.; Stenby, E.H. *Fluid Phase Equilibria* **1995**, 103, 23-29.
- [39] C. F. Leibovici, and J. Neoschil, *Fluid Phase Equilib.* **1995**, 112, 217-221.
- [40] Larsen, B.L.; Rasmussen, P.; Fredenslund, A. *Ind. Eng. Chem. Res.* **1987**, 26, 2274-2286.
- [41] Abrams, D.S.; Prausnitz, J.M. *AIChE J.* **1975**, 21, 116-128.
- [42] The program used to perform the calculations reported on this work can be obtained from the authors.

- **Chapter 3**

Biodiesel

Properties vs

Composition

Dependency of the Biodiesel Properties on its Composition

In preparation

My direct contribution for Published Paper

This Chapter presents a paper that joins together a lot of biodiesel properties and relates them to the composition on fatty acid methyl esters. Biodiesel used was identified in *Biodiesel Synthesis* and characterized as *Biodiesel Characterization*.

Experimental measurements of quality parameters of my biodiesels productions were made by Sovena accredited laboratory in Caparica – Almada that follows the BS EN 14214:2008 norm (Automotive fuels. Fatty acid methyl esters (FAME) for diesel engines. Requirements and test methods (British Standard)).



Figure 11- Aspect of Sovena Biodiesel factory in Caparica, Almada, Portugal.

Dependency of the Biodiesel Properties on its Composition

Maria Jorge Pratas, Mariana B. Oliveira, Sílvia C. Monteiro[#], João A.P. Coutinho

CICECO, Chemistry Department, University of Aveiro, Campus de Santiago, 3810–193
Aveiro, Portugal.

[#]Environment Department, ESTG, Polytechnic Institute of Leiria, Leiria, Morro do
Lena – Alto Vieiro, 2411-901 Leiria, Portugal

Abstract

European and American governments are targeting the incorporation of 10% and 20%, respectively of biofuels in transportation fuels by 2020. A number of important properties of the biodiesel can be directly related to the chemical composition of the raw material. It is therefore possible to predict these properties for each biodiesel based on their fatty acid profile.

The aim of this work is to study the biodiesel properties dependence with composition. To have a database to perform this study we synthesized methyl esters of rapeseed, soybean and palm as also their binary mixtures and ternary mixture, and also sunflower biodiesel. The properties evaluated were density, viscosity, iodine index, and CFPP. The objective of this study is to evaluate the properties of biodiesel oils obtained from different feedstock (soybean, rapeseed, palm, sunflower) and also their mixtures.

KEYWORDS: Biodiesel, Properties, Composition dependence, Density, Viscosity, CFPP, Iodine Value.

INTRODUCTION

The fossil fuel resources are dwindling day by day. Oil is becoming increasingly scarce and soon will not be able to meet the numerous demands, arising mainly from the transport sector. Faced with the energy crisis and environmental degradation, due to the massive use of fossil energy sources, biodiesel became an attractive alternative to diesel fuel. Biodiesel can reduce the environmental impacts of transportation, reduce the dependence on crude oil imports and thus on related political and economic factors, they offer business possibilities to agricultural enterprises.¹

A substitute diesel fuel derived from vegetable oils or animal fats, biodiesel is a mixture of saturated and unsaturated long-chain fatty acid alkyl esters. It is the final product of a transesterification reaction of vegetal oil, with a short alcohol in a presence of a catalyst. Industrially the most used process is the alkaline-catalyzed reaction.

The biodiesel fuel has to fulfill a number of quality standards. In Europe the biodiesel fuel standards are compiled in the norm CEN EN 14214², and in USA in the norm ASTM D6751³. The norms specify the requirements and test methods for biodiesel fuel to be used in diesel engines, in order to increase the biodiesel fuel quality and its acceptance among consumers. According to the European legislation, there are 25 parameters that have to be analyzed to certify biodiesel quality. Most of these analytical parameters provide indications of the quality of the production process. Some others reflect the properties of the raw materials that are used to produce the biodiesel. The transesterification does not alter the fatty acid composition of the feedstock and this composition plays an important role in some critical parameters of the biodiesel.⁴ Properties such as density, viscosity, low temperature performance, flash point, cetane number, iodine index, or oxidative stability depend on the fatty acid esters profile.

The biodiesel has a poor cold-temperature performance and a low oxidative stability, increased NO_x and exhausts emissions. Solutions to one of these problems often entail increasing the problematic behavior of another property and require the use of additives or modifying the fatty acid composition, either through physical processes, such as winterization, or through changes in the raw materials.^{5 6} In this regard, the generation of transgenic soybean lines with high oleic acid content represents one way in which plant biotechnology has already contributed to the improvement of biodiesel.⁶ Viable

strategies for increasing oil production in seeds have also been demonstrated, although additional work is necessary to translate these to yield increases in the field. In addition, research at an early stage has also suggested ways of producing oil in vegetative tissue rather than in seeds. Combining these approaches to develop high-yielding energy crops will increase the production of plant oils suitable for biodiesel.⁶

In order to test several fatty acid ester profile different biodiesels were synthesis and evaluated in this work. Fatty acid methyl esters of soybean, rapeseed, palm oils and their mixtures (binary and ternary) and also, sunflower were synthesized. The quality of biodiesel was tested for some parameters according to the European Standard EN 14214:2003².

A special importance is here given to critical properties that depend on fatty acid profile of raw material as density, viscosity, iodine value, and cold filter plugging point (CFPP).

MATERIALS AND METHODS

Materials. The eight biodiesel samples studied in this work were synthesized at our laboratory by a transesterification reaction of the vegetal oils: Soybean (S), Rapeseed (R), and Palm (P), and their respective binary and ternary mixtures: Soybean+Rapeseed (SR), Rapeseed+Palm (RP), Soybean+Palm (SP), and Soybean+Rapeseed +Palm (SRP) and Sunflower (Sf). Methanol (99.9% m/m) was purchased from Lab-scan, and all other chemicals used were obtained commercially and were of analytical grade.

Transesterification process

The transesterification reaction for all biodiesel samples was performed under specific conditions: the molar ratio of oil/methanol used was 1:5 with 0.5% sodium hydroxide by weight of oil as catalyst. The reaction was performed at 55 °C during 24 h under methanol reflux. The reaction time chosen was adopted for convenience and to guarantee a complete reaction conversion of one liter of oil. Raw glycerol was removed in two steps, the first after 3 h reaction and then after 24 h reaction in a separating funnel. Biodiesel was purified by washing with hot distilled water until a neutral pH was achieved. The biodiesel was then dried until the EN ISO 12937 limit for water was reached (less than 500 ppm of water). The water content was checked by Karl- Fischer titration.

There are a lot of publications that report biodiesel productions in shorter times (3-4 hours of synthesis). But in these conditions biodiesels did not possess a good quality level, as the yield was less than 90%. The presence of intermediate species in biodiesel influences dramatically their thermodynamic properties. Conditions to produce biodiesel were optimized until conversion reaction obtained has yields of more than 96.5% (EN14103). Therefore the reaction time was increased to a limit value (24h) to guarantee a complete conversion at the reaction.

In fact many author produce and test biodiesel considering the optimization procedures developed by other works, as a generic recipe.⁷ This could be acceptable where the target is to produce biodiesel from different raw materials, but yield needs to be always evaluated as esters content, in order to produce reliable data for scientific community.

After production the biodiesel fuels were stored under a nitrogen inert atmosphere until analysis of biodiesel quality.

Biodiesel Characterization.

Biodiesel was characterized following the EN14214:2003 and the results are presented in Tables 1. Detailed description of biodiesel composition is reported in Table 2, showing qualitative and quantitative information. Figure 1 presents the quantity of saturated and unsaturated components of each biodiesel.

RESULTS AND DISCUSSION

As presented in Table 1 and Figure 1 all biodiesel have different fatty acids profile. Palm oil has the higher quantity of saturated long chain such as palmitic (C16:0) and stearic (C18:0) acid. It has three times more saturated compounds than other raw materials studied. In the other hand soybean, rapeseed and sunflower oils are rich in esters of unsaturated fatty acids, namely oleate (C18:1), linoleate (C18:2) and linolenate (C18:3) acid. However they differ in the relative percentages. Sunflower and soybean present a similar fatty acid profile but in the first linolenate acid (C18:3) doesn't appear. Rapeseed oil has the higher percentage of monounsaturated compounds, especially oleate acid (C18:1).

With such unique profiles of fatty acid esters the various biodiesel fuels, as reported in Table1 and presented in Figure 1, are expected to present different properties.

Table 6 - Compositions in mass percentage of the studied biodiesels.

Methyl Esters	Sf	S	R	P	SR	RP	SP	SRP
C10			0.01	0.03		0.02	0.01	0.01
C12	0.02		0.04	0.24	0.03	0.20	0.18	0.14
C14	0.07	0.07	0.07	0.57	0.09	0.54	0.01	0.38
C16	6.40	10.76	5.22	42.45	8.90	23.09	25.56	18.97
C16:1	0.09	0.07	0.20	0.13	0.15	0.17	0.11	0.14
C18	4.22	3.94	1.62	4.02	2.76	3.02	4.04	3.28
C18:1	23.90	22.96	62.11	41.92	41.82	52.92	33.13	42.51
C18:2	64.16	53.53	21.07	9.80	37.51	15.47	31.72	27.93
C18:3	0.12	7.02	6.95	0.09	7.02	3.08	3.58	4.66
C20	0.03	0.38	0.60	0.36	0.46	0.49	0.39	0.45
C20:1	0.15	0.23	1.35	0.15	0.68	0.67	0.20	0.52
C22	0.76	0.80	0.35	0.09	0.46	0.24	0.32	0.33
C22:1	0.08	0.24	0.19		0.12	0.09	0.12	0.14
C24			0.22	0.15			0.63	0.53

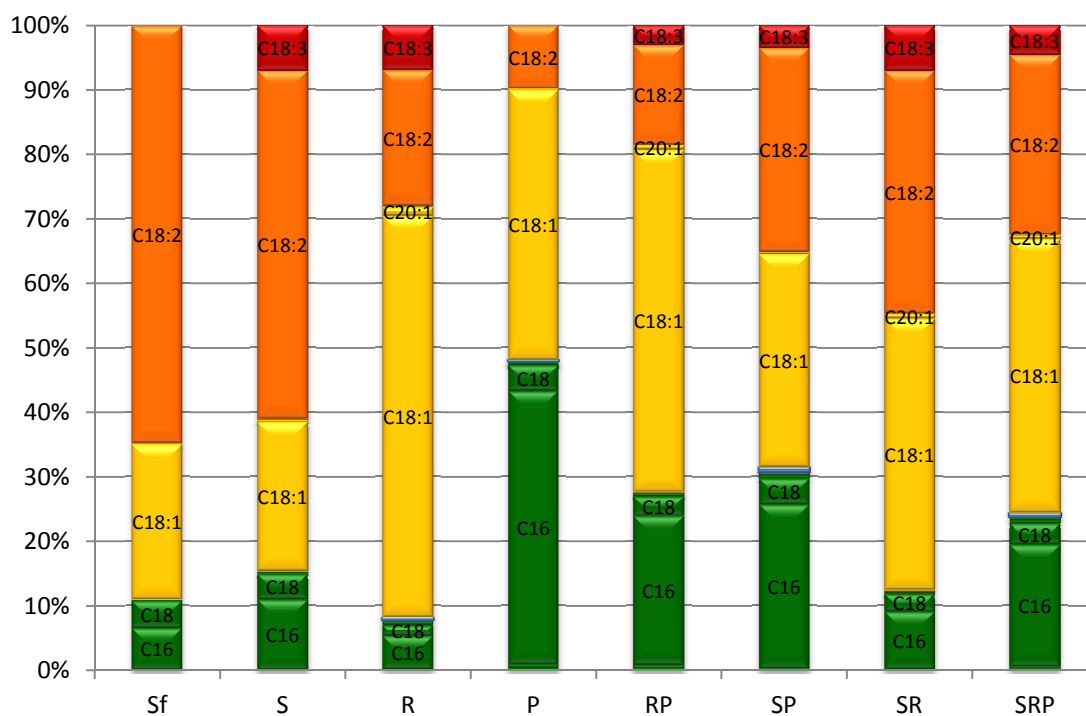


Figure 1 - Saturation level of fatty acid profile of vegetal oils used. ■ Saturate, ■ Monounsaturate, ■ Diunsaturate, and ■ Triunsaturate components.

Table 7- Characteristics of biodiesel followed EN 14214:2003.

Property	unit	limits		Biodiesel Methyl Esters							
		min.	max.	Sf	S	R	P	RP	SP	SR	SRP
Ester content	% m/m	96.5		98.5	99.4	98.8	96.5	98.9	97.1	97.2	97.3
Density @ 15°C ^a	kg/m ³	860	900	887.2	887.3	886.0	877.9	882.1	882.0	885.7	883.0
Viscosity @ 40°C	mm ² /s	3.5	5	4.18 ^b	4.08 ^b	4.54 ^b	4.61 ^b	4.53	4.30	4.28	4.36
Water content	mg/kg		500	<300	<300	<300	<300	<300	<300	<300	<300
Acid Value	mgKOH/g		0.5	0.18	0.26	0.23	0.17	0.28	0.2	0.16	0.2
Iodine value	g iodine /100g		120	132.2	131.2	109.5	55.7	79.5	93.1	120.1	97.8
Linolenic acid methyl ester	% (m/m)		12	0.12	7.02	6.95	0.13	3.08	3.58	7.02	4.66
Methanol Content	%(m/m)		0.2	<0.01	<0.01	<0.01	<0.01	<0.01	<0.01	<0.01	<0.01
Monoglyceride content	%(m/m)		0.8	0.66	0.4	0.86	0.95	0.48	0.75	0.85	0.79
Diglyceride content	%(m/m)		0.2	0.05	0.02	0.05	0.4	0.06	0.14	0.09	0.12
Triglyceride content	%(m/m)		0.2	0.01	0.01	0.01	0.08	0.01	0.07	0.07	0.08
Free glycerol	%(m/m)		0.02	0	0	0	0.02	0	0	0	0
Total Glycerol	%(m/m)		0.25	0.18	0.11	0.23	0.33	0.13	0.22	0.24	0.23
Group I metals (Na ⁺ ,K ⁺)	mg/kg		5	10.2	5.9	0.95	1.03	1.3	3.1	<0.7	2.1
Group II metals (Ca ⁺ ,Mg ⁺)	mg/kg		5	4.7	25.8	<0.3	<0.3	<0.3	9.6	4.1	4.6
Phosphorus content	ppm		10	<0.4	11.6	<0.4	<0.4	<0.4	3.5	0.6	0.8
CFPP	°C			-3	-5	-17	11	4	5	-10	1
CP	°C			0	0	-4	>5	3	5	-2	4

^a reference 8; ^b reference 9

The best way to evaluate properties is compared them involving the standards limits present in the European norms. American norm has opened standard limitation for almost properties. The studied properties are density, viscosity, iodine value, and CFPP.

Atomization and vaporization of fuel in engines are greatly influenced by the viscosity and density of the fuel and these properties are temperature and pressure dependents. The viscosity is defined as the resistance offered by one portion of a material moving over another portion of the same material.⁸ The viscosity is required for the design of pipes, fittings and equipment to be used in industry of oil and fuel⁹. A viscous fuel, causing a poorer atomization, which is the first step of combustion, is responsible for premature injector cooking and poor fuel combustion.^{10 11} The biodiesel standard EN 14214 sets the viscosity at 40°C measured with viscometer Stabinger in a range of 3.5 – 5 mm²/s. American limits lies in the range 1.9 - 6 mm²/s. It was shown¹²⁻¹³ that viscosity decreases with decreasing of the length chain and with the alcohol length, and with increasing of unsaturation level.

Figure 2 presents results of kinematic viscosity of all biodiesel samples at 40 °C. In a general way it's seen that biodiesel with great content of saturated compounds, as palm, presents higher viscosity, and soybean with more than 80% of unsaturated compounds presents the lower viscosity. The viscosity has almost no correlation with percentage of total saturated or total unsaturated compounds (0.50), but presents a high correlation coefficient of 0.94 with the percentage of polyunsaturated esters.

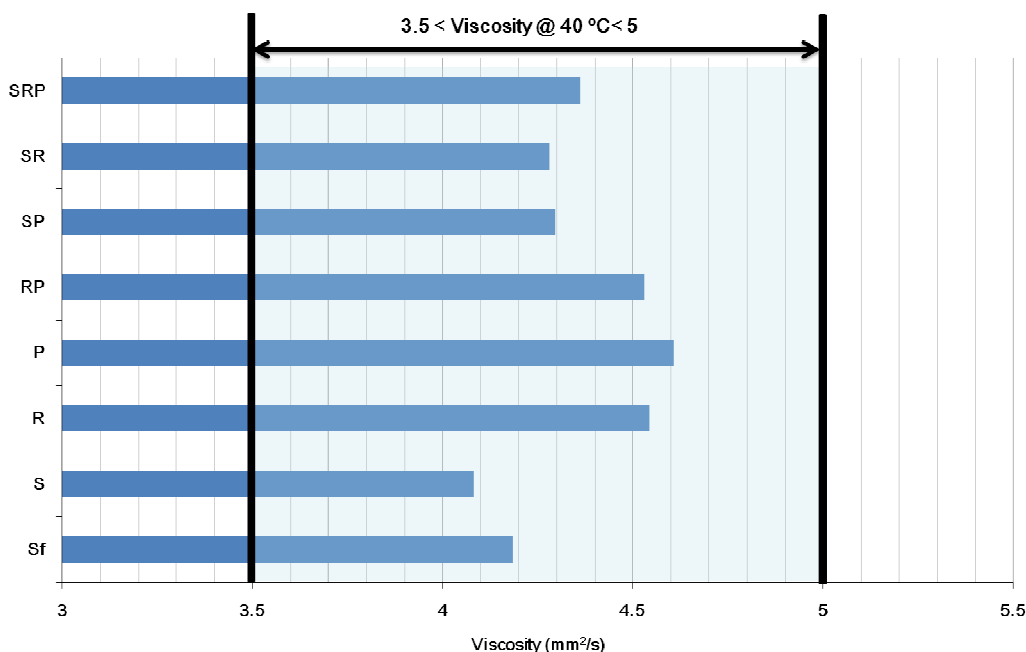


Figure 2 – Viscosity of methyl esters of studied biodiesels and EN14214 limits.

The density is of special importance for diesel engines because fuel is metered to the engine volumetrically. The higher density of biodiesel, compared to petrodiesel, compensates their lower energy content on a weight basis. Biodiesel density data are relevant because injection systems, pumps and injectors must deliver the amount of fuel precisely adjusted to provide proper combustion.¹⁴ In biodiesel standard EN 14214 the density was measured at 15°C with viscometro Stabinger in a range of 860 – 900 kg/m³.

It is shown¹²⁻¹³ that density increase with decreasing of the length chain and the alcohol length, and with the increasing of unsaturation level

Figure 3 presents measured density of produced biodiesel at 15°C. All biodiesel fuels fall within the limits imposed by the norm and present very similar densities ranging from 878 and 887 kg/m³. Overall, palm biodiesel with great content of saturated compounds presents lower density, and with more than 90% of unsaturated compounds soybean, sunflower and rapeseed presents the higher densities. Density property has a coefficient correlation of 0.96 with percentage of total saturated or unsaturated compounds.

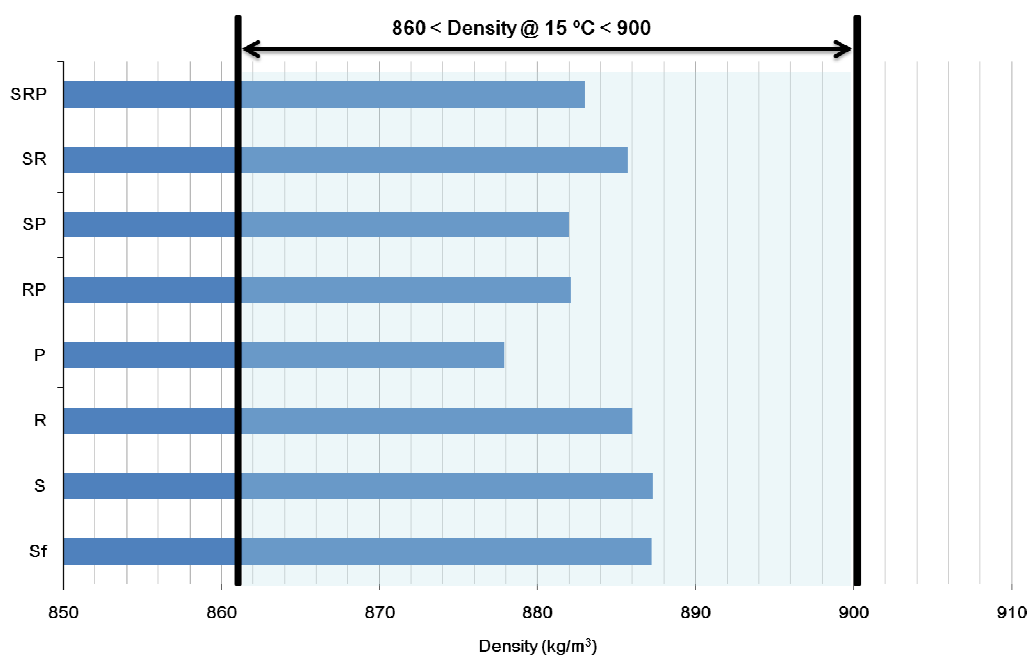


Figure 3 – Density of methyl esters of studied biodiesels and EN14214 limits.

Iodine value is a measure of total unsaturation of a fatty material measured in g iodine/100 g of sample when formally adding iodine to the double bonds. The iodine value of a vegetable oil or animal fat is almost identical to that of the corresponding methyl esters. The idea behind the use this property to evaluate biodiesel is that it would indicate the propensity of an oil or fat to oxidize, but it may also indicate the propensity of the oil or fat to polymerize and form engine deposits.⁸ Thus, an iodine value of 120 was specified in EN 14214 that would largely exclude vegetable oils such as soybean and sunflower as biodiesel feedstock, whereas in the United States iodine value was not included in biodiesel standards ASTM D6751³. Palm oil, rich in esters of saturated fatty esters, was the oil with a lower iodine value and higher saturated methyl esters content.⁸ On the other extreme limit are soybean and sunflower with the higher percentage of polyunsaturated compounds (C18:2 and C18:3) with an iodine value that came out of European limitation of 120 g iodine/100 g of sample. Iodine value presents a correlation coefficient of 0.93 with total of polyunsaturated esters.

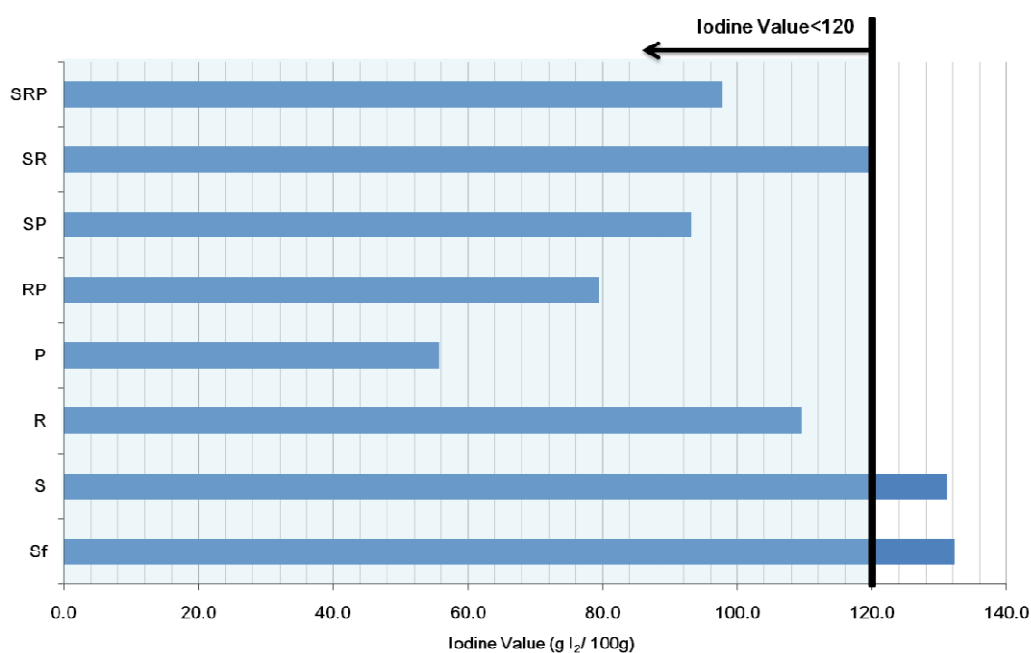


Figure 4 – Iodine Value of methyl esters of studied biodiesels and EN14214 limits.

The low-temperature behavior of fuels is evaluated by different properties: cloud point (CP), cloud point (PP) and cold filter plugging point (CFPP). All of them are related to the temperature of crystallization wax process. The fuel contains small amounts of long-chain hydrocarbons, called waxes, which crystallize at temperatures within the normal engine operating range. Initially, cooling temperatures cause the formation of solid wax crystal nuclei that are submicron in scale and invisible to the human eye. A further decrease in temperature causes these crystals to grow. The temperature at which crystals become visible [diameter (d) $\geq 0.5 \mu\text{m}$] is defined as the cloud point (CP) because the crystals usually form a cloudy or hazy suspension. Due to the orthorhombic crystalline structure, unchecked crystalline growth continues rapidly in two dimensions forming large platelet lamellae. If temperatures are low enough, larger crystals ($d \sim 0.5\text{--}1 \text{ mm} \times 0.01 \text{ mm}$ thick) fuse together and form large agglomerates that can restrict or cut off the flow through fuel lines and filters and cause start-up and performance problems. This is the temperature of cold filter plugging point (CFPP). The temperature at which crystal agglomeration is extensive enough to prevent free pouring of fluid is determined by measurement of its pour point (PP). This

phenomenon occurs with both biodiesel and petrodiesel. These cold flow properties are associated to chemical structure profile of a fuel. The higher the content of long chain saturated hydrocarbons the higher the temperature at which crystallization occurs and worse the fuel quality. Unsaturated compounds have a better performance at low temperature. European standard used CFPP to evaluate biodiesel low temperature behavior while American standard uses CP. For both the limits are climate-dependent. The options are given to allow for seasonal grades to be set nationally (summer and winter season) or classes for arctic climates. CFPP presents a correlation coefficient of 0.91 with the percentage of total saturated or total unsaturated esters. Rapeseed and palm biodiesel presents opposite extremes behavior. The first is the most unsaturated (with 92% of unsaturated compounds) and the better behavior at low temperature. Palm biodiesel is the most saturated one (with 45% of saturated esters) and shows the worst low temperature performance, that also affects as all biodiesels produced with palm oil. CP of biodiesel samples were also measured and exhibit the higher coefficient correlation of all correlated properties 0.97, with total saturated or total unsaturated esters.

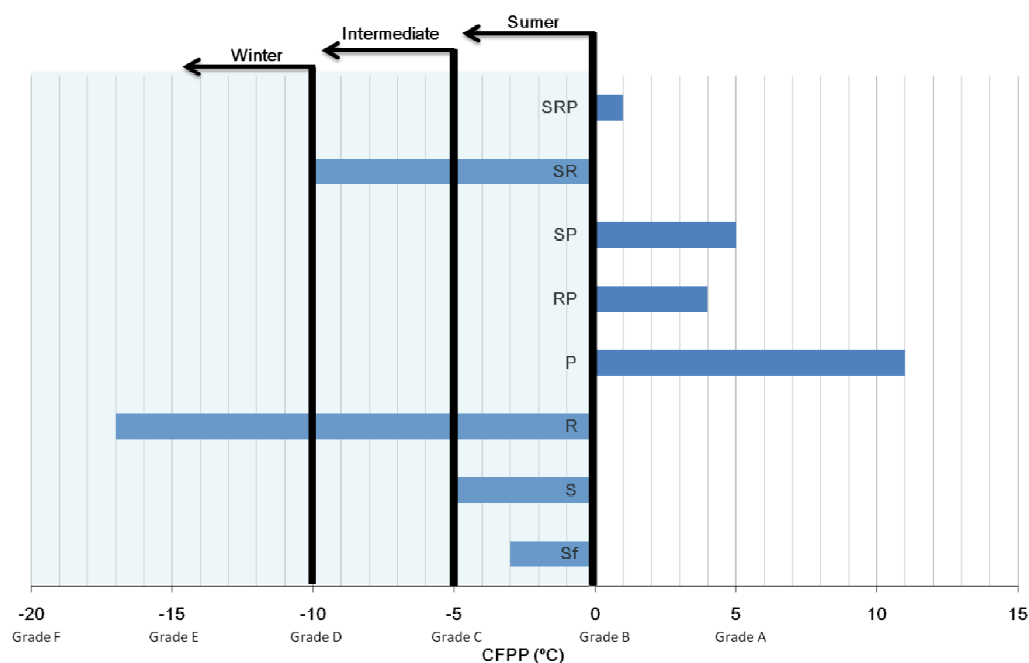


Figure 5 – CFPP of methyl esters of studied biodiesels and EN14214 limits for Portugal.

Correlation matrix of the properties, in Figure 6, shows us a small correlation between studied properties. Nevertheless CP and CFPP have the higher correlation coefficient, 0.95. Density presents a better correlation with CP than with CFPP. Viscosity presents the best correlation with iodine value.

Figure 6 - Correlation matrix of properties.

	CFPP	CP	Density	Viscosity	Iodine Value
CFPP	-	-	-	-	-
CP	0.96	-	-	-	-
Density	0.81	0.90	-	-	-
Viscosity	0.23	0.36	0.36	-	-
Iodine Value	0.72	0.81	0.81	0.81	-

CONCLUSIONS

New experimental data are presented for several biodiesel fuels produced in our laboratory with methyl esters profile information available. It was possible to evaluate the influence of unsaturation level in the properties measured and also correlate them.

Studied properties were density, viscosity, iodine value, and CFPP (and CP). All properties related with original raw material composition. No correlation between the density and viscosity was observed, as in another investigation on biodiesel⁸ but all biodiesel compliances the European and American Standard for density and viscosity properties.

Biodiesels made from feedstock containing higher concentrations of high-melting point saturated long-chain fatty acids tends to have poor cold flow properties. It was observed that the biodiesel from palm oil presents problems for cold flow properties with specification outside the European limits. Blends of it with other biodiesel fuels can improve these properties in order to comply with European specifications.

The ideal biodiesel fuel profile presents a limited quantity of saturated esters for improving his cold behavior. Likewise a small quantity of polyunsaturated esters will reduce iodine value and increase stability.

ACKNOWLEDGMENTS

Maria Jorge Pratas acknowledges the financial support from Fundação para a Ciência e a Tecnologia through her Ph.D. grant (SFRH/BD/28258/2006). The authors acknowledge Marina Reis from Sovena Company for experimental collaboration.

LITERATURE CITED

1. Cvangros, J.; Povazanec, F., Production and treatment of rapeseed oil methyl esters as alternative fuels for diesel engines. *Bioresource Technology* **1996**, *55* (2), 145-150.
2. European Standard EN 14214, 2003. Automotive fuels - Fatty acid methyl esters (FAME) for diesel engines - Requirements and test methods. CEN – European Committee for Standardization, Brussels, Belgium. Available from: <http://www.din.de>.
3. ASTM, D6751 - 09 Standard Specification for Biodiesel Fuel Blend Stock (B100) for Middle Distillate Fuels. 2009.
4. Ramos, M. J.; Fernandez, C. M.; Casas, A.; Rodriguez, L.; Perez, A., Influence of fatty acid composition of raw materials on biodiesel properties. *Bioresource Technology* **2009**, *100* (1), 261-268.
5. Knothe, G., "Designer" biodiesel: Optimizing fatty ester (composition to improve fuel properties. *Energ Fuel* **2008**, *22* (2), 1358-1364.
6. Durrett, T. P.; Benning, C.; Ohlrogge, J., Plant triacylglycerols as feedstocks for the production of biofuels. *Plant Journal* **2008**, *54* (4), 593-607.
7. Pinzi, S.; Garcia, I. L.; Lopez-Gimenez, F. J.; de Castro, M. D. L.; Dorado, G.; Dorado, M. P., The Ideal Vegetable Oil-based Biodiesel Composition: A Review of Social, Economical and Technical Implications. *Energ Fuel* **2009**, *23*, 2325-2341.
8. Knothe, G.; Gerpen, J. V.; Krahl, J., *The Biodiesel Handbook*. AOCS Press, Champaign, Illinois: **2005**.
9. Goncalves, C. B.; Ceriani, R.; Rabelo, J.; Maffia, M. C.; Meirelles, A. J. A., Viscosities of Fatty Mixtures: Experimental Data and Prediction. *J Chem Eng Data* **2007**, *52* (5), 2000-2006.
10. Ejim, C. E.; Fleck, B. A.; Amirfazli, A., Analytical study for atomization of biodiesels and their blends in a typical injector: Surface tension and viscosity effects. *Fuel* **2007**, *86* (10-11), 1534-1544.
11. Frederic Boudy; Seers, P., Impact of physical properties of biodiesel on the injection process in a common-rail direct injection system. *Energy Convers. Manage.* **2009**, *50*, 2905-2912.
12. Pratas, M. J.; Freitas, S.; Oliveira, M. B.; Monteiro, S. C.; Lima, A. S.; Coutinho, J. A. P., Densities and Viscosities of Fatty Acid Methyl and Ethyl Esters. *J Chem Eng Data* **2010**, *55* (9), 3983-3990.

13. Pratas, M. J.; Freitas, S.; Oliveira, M. B.; Monteiro, S. C.; Lima, A. S.; Coutinho, J. A. P., Densities and Viscosities of Minority Fatty Acid Methyl and Ethyl Esters Present in Biodiesel. *J Chem Eng Data* **2011**, *56* (5), 2175-2180.
14. Dzida, M.; Prusakiewicz, P., The effect of temperature and pressure on the physicochemical properties of petroleum diesel oil and biodiesel fuel. *Fuel* **2008**, *87* (10-11), 1941-1948.

- **Chapter 4**

**Water solubility in
biodiesels and
fatty acids**

My direct contribution for Published Paper

This work takes a look at the mutual solubilities of water and fatty acids, and solubilities of water in biodiesel. Both are important to industrial biodiesel production and their scarcity on open literature motivated this study. I have made all experimental part, namely measurements on equilibrium phases: water solubility determined by Karl Fisher and solubility in water by turbidimetry in close glass ampoules. The biodiesel used was identified in *Biodiesel Synthesis* and characterized as described in *Biodiesel Characterization*.

***Description of the mutual solubilities of fatty acids and water with
the CPA EoS***

AICHE Journal, **2009**, 55, 1604-1613

DOI: 10.1002/aic.11766.

Description of the mutual solubilities of fatty acids and water with the CPA EoS

**M. B. Oliveira, M. J. P. de Melo, I. M. Marrucho, A. J. Queimada*,
J. A. P. Coutinho**

CICECO, Chemistry Department, University of Aveiro, 3810-193 Aveiro, Portugal

*LSRE - Laboratory of Separation and Reaction Engineering, Faculdade de Engenharia,
Universidade do Porto, Rua do Doutor Roberto Frias, 4200 - 465 Porto, Portugal

Abstract

Data for the mutual solubilities of fatty acid + water mixtures are scarce and so measurements for seven fatty acid (C₅-C₁₀, C₁₂) + water systems were carried out. This new experimental data was successfully modelled with the CPA EoS. Using data from C₆ to C₁₀ and the Elliot's cross-associating combining rule a correlation for the k_{ij} binary interaction parameter, as a function of the acid chain length, is proposed. The mutual solubilities of water and fatty acids can be adequately described with average deviations inferior to 6 % for the water rich phase and 30 % for the acid rich phase. Furthermore, satisfactory predictions of solid-liquid equilibria of seven fatty acids (C₁₂-C₁₈) + water systems were achieved based only on the k_{ij} correlation obtained from LLE data.

Keywords: Biodiesel, CPA EoS, Fatty acids, Mutual solubilities, Water

Introduction

Fatty acids are important commodities with an increasing wide range of industrial applications¹. Widespread use can be found in different products, such as: household and industrial cleaners, coatings and adhesives, paints, personal care products, pharmaceuticals, cosmetics, industrial lubricants, corrosion inhibitors, polymers, textiles, foods, paper, crayons, candles and waxes. Particular applications of some specific fatty acids can be found elsewhere¹. Fatty acids can also be used as raw materials for fatty alcohols and biodiesel production^{1,2}.

Although the chain length limits used to define fatty acids are not strict, these are typically higher chain length aliphatic carboxylic acids with 6-24 carbon atoms. According to literature, the worldwide production capacity for fatty acids in 2001 was around 4×10^6 metric tons¹.

Although shorter chain length carboxylic acids are usually produced synthetically, most of the fatty acids are obtained from natural oils and fats by hydrolysis (chemical or enzymatic). Hydrolysis converts the oil or fat (a triglyceride) into three fatty acid molecules and glycerol, usually at high temperature and high pressure conditions, using about 30-60 % water in a fatty acid weight basis. In some cases, acid washing is performed before the hydrolysis reaction in order to remove impurities. Following hydrolysis, different purification processes can be employed, among them crystallization (typically with methanol or acetone), solvent extraction (either liquid-liquid or supercritical fluid extraction) distillation and adsorption. Distillation removes colour and odour bodies³, low boiling unsaponifiable materials, polymerized materials, triglycerides and heavy decomposition products. Other separation processes include hydrophilization, panning and pressing and formation of solid urea complexes¹.

Although fatty acids may be used for biodiesel production, transesterification is the most frequently used⁴ method for producing biodiesel from vegetable oils, tallow or waste cooking oils⁵. It consists on the reaction of an oil or fat with an alcohol to form fatty esters with glycerol as a byproduct. A catalyst is necessary to increase reactions rate and yield and basic catalysts are preferred due to higher reaction rates and lower process temperatures⁶. Methanol and ethanol can be used as alcohols in the reaction, but

methanol is preferred due to its low cost and physical and chemical advantages in the process^{4,7}.

In the biodiesel production process the fatty esters rich current coming from the reactor is saturated with glycerol, alcohol, catalyst and unreacted soaps. This current is washed in a liquid-liquid extractor in counter current with acidified water to neutralize the catalyst and to convert soaps to free fatty acids. The raffinate current is composed of water saturated biodiesel while the extract is a low pH aqueous solution containing the polar compounds⁸. The design and optimization of the purification of biodiesel with water requires a model that can describe this phase equilibria.

In spite of the importance of the phase equilibria of fatty acid + water systems, there is a lack of experimental data for their mutual solubilities. To overcome this limitation, measurements were carried out for the water solubility in six fatty acids and the complete phase diagrams were established for pentanoic, hexanoic and dodecanoic acids.

Several models have been previously applied to systems containing fatty acids with different degrees of success. Carboxylic acids can form dimers in the vapour phase as well as dimers, trimers or even oligomers in the liquid phase, which make acid mixtures highly non-ideal, requiring a model able to take into account these interactions, in order to correctly describe their phase equilibria.

One of those approaches is the UNIFAC model. Yet, this model does not perform well when dealing with polar compounds with association, such as the water + acid systems⁹⁻¹², because it does not take explicitly into account the association interactions present in these systems. Moreover it does not take into account the dimerization in the vapour phase. Improvements with respect to the original UNIFAC model were achieved by the addition of an association term so as to take into account the association effects. The A-UNIFAC model was satisfactorily applied to predict vapor-liquid and liquid-liquid equilibria and to compute infinite dilution activity coefficients for mixtures containing alcohols, carboxylic acids, water, esters, aromatic hydrocarbons and alkanes¹³. Applying the A-UNIFAC model to associating systems is quite demanding since it is necessary to analyze every UNIFAC functional group in order to recognize the presence of associating sites.

Another thermodynamic model proposed for acid systems is the group contribution equation of state, GC-EoS developed by Skjold-Jørgensen¹⁴ that was extended by Gros

et al.¹⁵ to mixtures of fatty oils and their derivatives (fatty acids, fatty acid esters, mono- and di-glycerides) with supercritical solvents like carbon dioxide or propane. The association model proposed by Gros et al. provided results in better agreement with the experimental data than the GC-EoS.

The coupling of a cubic equation of state (SRK) with a model that expresses the dimerization of the acid molecules was also used to correlate experimental VLE for gases in acetic acid^{16, 17}.

The Statistical Associating Fluid Theory (SAFT) model was used to compute phase equilibria of formic, acetic and propanoic acid binary systems with aromatic hydrocarbons¹⁸. The same approach was followed by Fu and Sandler¹⁹ and its results compared to those of the simplified SAFT EoS. These two models were also used, in the same work, to correlate cross-associating systems containing acids, alcohols and water. The original SAFT model performed better than the simplified one, but none of them was able to produce a good description of aqueous systems.

The Cubic plus Association (CPA) EoS was used to correlate VLE and LLE for short chain acids + aliphatic hydrocarbons, in agreement with the experimental data²⁰. The extension of the application of this model to binary aqueous mixtures was only made up to acetic acid systems, with satisfactory results²¹.

As a result of our ongoing effort to develop an equation of state model for the description of the phase equilibria, relevant for the biodiesel production, in a previous work, the CPA EoS was shown to be an accurate model to describe the water solubility in fatty acid esters and commercial biodiesels²².

In this subsequent study, which scope is also of interest for the biodiesel industry, the CPA EoS is applied for the first time to carboxylic acids heavier than propanoic acid (up to C₂₀ for pure component properties and up to C₁₈ for mixtures), and to the description of LLE and SLE of their binary mixtures with water.

In the mentioned preceding paper, the CPA EoS was applied to mixtures of fatty acid esters (non-self-associating compounds) and water, while in this paper mixtures of acids (self-associating compounds) and water are studied. Systems with carboxylic acids are usually strongly non-ideal and considerably more difficult to model than ester mixtures.

Two different associating combining rules are here evaluated on the basis of their ability to correlate these water + fatty acid systems.

It will be shown that short chain and long chain carboxylic acids have different behaviour requiring different cross-associating combining rules and that the dissociation of the acids smaller than pentanoic acid will have a major impact on their mutual solubilities with water. To correlate the mutual solubilities of water and carboxylic acids studied in this work, only binary interaction parameters (k_{ij}) in the physical part of CPA were used, and these were found to be linearly dependent on the acid chain length.

Using this dependency for the interaction parameters, SLE predictions for seven fatty acids in water will also be presented in this work.

Experimental Section

Water solubility measurements were carried in: pentanoic acid (SIGMA, $\geq 99\%$), hexanoic acid (SIGMA, $\geq 99.5\%$), heptanoic acid (FLUKA, $\geq 99\%$), octanoic acid (SIGMA, $\geq 99\%$), nonanoic acid (SIGMA, $\geq 99.5\%$) and decanoic acid (SIGMA, $\geq 98\%$), at temperatures from 288.15 to 323.15 K and at atmospheric pressure. The methodology used in this work, has previously been successfully used for other organic compounds at our laboratory²²⁻²⁵. The acid and the water phases were initially agitated vigorously and allowed to reach equilibrium by separation of both phases in 20 mL glass vials for at least 48 h. This period proved to be the time required to guarantee a complete separation of the two phases and that no further variations in mole fraction solubilities occurred.

The temperature was maintained by keeping the glass vials containing the phases in equilibrium inside an aluminium block specially designed for this purpose, which is placed in an isolated air bath capable of maintaining the temperature within (± 0.01 K).

The temperature control was achieved with a PID temperature controller driven by a calibrated Pt100 (class 1/10) temperature sensor inserted in the aluminium block. In order to reach temperatures below room temperature, a Julabo circulator, model F25-HD, was coupled to the overall oven system allowing the passage of a thermostated fluid flux around the aluminium block. The solubility of water in the acid rich phase was determined using a Metrohm 831 Karl Fischer (KF) coulometer.

The acid rich phase was sampled at each temperature from the equilibrium vials using glass syringes kept dry and at the same temperature of the measurements. Samples of 0.1 to 0.2 g were injected directly into the KF coulometric titrator.

For pentanoic, hexanoic and dodecanoic (SIGMA, $\geq 99\%$) acids, measurements of the phase envelope for the two phase region were made by turbidimetry. Several samples covering the entire concentration range were prepared. The mixture was heated inside a closed glass tube in a thermostatic bath up to the one phase region. On slowly cooling, the phase separation temperature was registered. The temperature assigned to the phase envelope is an average of five measurements.

For heavier acids, melting temperatures are significantly higher, what therefore prevents the measurements of solubilities in a temperature range adequate to the experimental techniques used in this work.

Model

The CPA equation of state can be described as the sum of two contributions: one accounting for physical interactions, that in the current work is taken as the SRK EoS, and another accounting for association, the Wertheim association term^{26, 27}.

$$Z = Z^{phys.} + Z^{assoc.} = \frac{1}{1 - b\rho} - \frac{a\rho}{RT(1 + b\rho)} - \frac{1}{2} \left(1 + \rho \frac{\partial \ln g}{\partial \rho} \right) \sum_i x_i \sum_{A_i} (1 - X_{A_i}) \quad (1)$$

where a is the energy parameter, b the co-volume parameter, ρ is the density, g a simplified hard-sphere radial distribution function, X_{A_i} the mole fraction of pure component i not bonded at site A and x_i is the mole fraction of component i .

The pure component energy parameter of CPA has a Soave-type temperature dependency:

$$a(T) = a_0 \left[1 + c_1 \left(1 - \sqrt{T_r} \right) \right]^2 \quad (2)$$

where a_0 and c_1 are regressed from pure component vapour pressure and liquid density data.

X_{A_i} is related to the association strength $\Delta^{A_i B_j}$ between sites belonging to two different molecules and is calculated by solving the following set of equations:

$$X_{Ai} = \frac{1}{1 + \rho \sum_j x_j \sum_{B_j} X_{B_j} \Delta^{A_i B_j}} \quad (3)$$

where

$$\Delta^{A_i B_j} = g(\rho) \left[\exp\left(\frac{\varepsilon^{A_i B_j}}{RT}\right) - 1 \right] b_{ij} \beta^{A_i B_j} \quad (4)$$

where $\varepsilon^{A_i B_j}$ and $\beta^{A_i B_j}$ are the association energy and the association volume, respectively.

The simplified radial distribution function, $g(\rho)$ is given by :

$$g(\rho) = \frac{1}{1 - 1.9\eta} \quad \text{where} \quad \eta = \frac{1}{4} b\rho \quad (5)$$

For non-associating components, such as n-alkanes, CPA has three pure component parameters (a_0 , c_1 and b) while for associating components like organic acids it has five (a_0 , c_1 , b , ε , β). In both cases, these parameters are regressed simultaneously from pure component experimental data. The objective function used is:

$$OF = \sum_i^{NP} \left(\frac{P_i^{\text{exp.}} - P_i^{\text{calc.}}}{P_i^{\text{exp.}}} \right)^2 + \sum_i^{NP} \left(\frac{\rho_i^{\text{exp.}} - \rho_i^{\text{calc.}}}{\rho_i^{\text{exp.}}} \right)^2 \quad (6)$$

When CPA is extended to mixtures, the energy and co-volume parameters of the physical term are calculated by employing the conventional van der Waals one-fluid mixing rules:

$$a = \sum_i \sum_j x_i x_j a_{ij} \quad a_{ij} = \sqrt{a_i a_j} (1 - k_{ij}) \quad (7)$$

and

$$b = \sum_i x_i b_i \quad (8)$$

For a binary mixture composed by a self-associating and a non-associating compound, as for example water + n-alkane systems, the binary interaction parameter k_{ij} is the only adjustable parameter.

For cross-associating systems, combining rules for the cross-association energy, ε_{ij} , and cross-association volume, β_{ij} (or the cross-association strength, $\Delta^{A_i B_j}$) are required. Different sets of combining rules have been proposed by several authors^{19, 28-30}:

$$\text{i) } \varepsilon^{A_i B_j} = \frac{\varepsilon^{A_i} + \varepsilon^{B_j}}{2}, \quad \beta^{A_i B_j} = \frac{\beta^{A_i} + \beta^{B_j}}{2} \quad (9) \quad , \text{ which is referred as the CR-1 set}^{30}$$

$$\text{ii) } \varepsilon^{A_i B_j} = \frac{\varepsilon^{A_i} + \varepsilon^{B_j}}{2}, \quad \beta^{A_i B_j} = \sqrt{\beta^{A_i} \beta^{B_j}} \quad (10) \quad , \text{ which is referred as the CR- 2 set}^{30}$$

$$\text{iii) } \varepsilon^{A_i B_j} = \sqrt{\varepsilon^{A_i} \varepsilon^{B_j}}, \quad \beta^{A_i B_j} = \sqrt{\beta^{A_i} \beta^{B_j}} \quad (11) \quad , \text{ which is referred as the CR- 3 set}^{30}$$

$$\text{iv) } \Delta^{A_i B_j} = \sqrt{\Delta^{A_i B_i} \Delta^{A_j B_j}} \quad (12) \quad , \text{ which is referred as the CR- 4 set (or Elliot rule)}^{30}$$

CR-2 and CR-4 are the most commonly used. Only these combining rules have been found to be successful in previous applications^{27, 31}. CR-2 provided very good results in the modelling of the VLE of glycol + water systems³¹, the LLE and VLE of water + heavy alcohol systems³⁰ and the LLE of the water + amine systems³²; on the other hand, the CR-4 approach performed better in predicting the VLE and SLE of water + small alcohols systems³⁰, the VLE of small acids + water or small acids + alcohol systems²⁰, the VLE of amine + alcohol³² systems and the SLE of the MEG + water systems³³. In this work, the CR-2 and the CR-4 were evaluated on the basis of their ability to describe LLE and SLE of water and fatty acids binary mixtures.

For the estimation of the k_{ij} parameter the objective function employed was:

$$OF = \sum_i^{NP} \left(\frac{x_i^{calc.} - x_i^{exp.}}{x_i^{exp.}} \right)^2 \quad (13)$$

where single phase or both phase data can be selected for the parameter optimization.

The association term depends on the number and type of association sites. For water a four-site (4C) association scheme was adopted³⁴, and for acids the carboxylic group is treated as a single association site (1A).

Carboxylic acids can form dimers in the vapor phase as well as dimers, trimers or even oligomers in the liquid phase. Several previous works with the CPA EoS or with some variants of the SAFT EoS had already discussed the best association scheme for organic acids¹⁶⁻²⁰. Several association schemes were evaluated for both the gas and liquid phases (1A, 2B and 4C). It was showed that when using the CPA EoS, the 1A scheme performs globally better than the two-site (2B) model (VLE, LLE, second virial coefficients and equilibrium constants²⁰). Huang and Radosz using SAFT¹⁸ also used the one site model for carboxylic acids such as formic, acetic and n-propanoic. The same associating scheme for carboxylic acids (1A) can also be found in the paper of Fu and Sandler¹⁹. Therefore this association scheme was adopted in this work.

Results and discussion

Experimental Results

The data for the water solubility in 6 fatty acids, in the temperature range 288.15 - 323.15 K, are listed in **Table 1** as well as their respective standard deviations. Results are presented at temperatures above the melting point of each compound. The water solubility results at each individual temperature are an average of at least five independent measurements.

Table 1. Water Solubility in Fatty Acids by Karl Fisher Coulometry.

	Pentanoic Acid	Hexanoic Acid	Heptanoic Acid	Octanoic Acid	Nonanoic Acid	Decanoic Acid
T/K	($x_{H_2O} \pm \sigma^a$)					
288.15	0.4566 ± 0.0006	0.252 ± 0.001	0.171 ± 0.001		0.1008 ± 0.0004	
293.15	0.4791 ± 0.0008	0.268 ± 0.003	0.1863 ± 0.0003	0.136 ± 0.002	0.1111 ± 0.0004	
298.15	0.4995 ± 0.0006	0.284 ± 0.002	0.196 ± 0.001	0.151 ± 0.001	0.1205 ± 0.0005	
303.15	0.508 ± 0.004	0.307 ± 0.003	0.2132 ± 0.0007	0.167 ± 0.004	0.133 ± 0.002	
308.15	0.536 ± 0.003	0.338 ± 0.003	0.2470 ± 0.0003	0.1852 ± 0.0006	0.1502 ± 0.0003	0.123 ± 0.002
313.15	0.547 ± 0.006	0.342 ± 0.006	0.240 ± 0.002	0.199 ± 0.004	0.1546 ± 0.0007	0.138 ± 0.005
318.15	0.562 ± 0.002	0.364 ± 0.003	0.265 ± 0.005	0.210 ± 0.004	0.171 ± 0.006	0.154 ± 0.007
323.15	0.588 ± 0.005	0.389 ± 0.003		0.229 ± 0.017		0.1686 ± 0.004

a- Standard Deviation

The experimental liquid-liquid phase envelopes for pentanoic, hexanoic and dodecanoic acids, obtained by turbidimetry, are presented in **Table 2**.

Table 2. LLE data for pentanoic acid + water, hexanoic acid + water and dodecanoic acid + water determined by turbidimetry.

X Pentanoic Acid	(T ± σ^a)/K	X Hexanoic Acid	(T ± σ^a)/K	X Dodecanoic Acid	(T ± σ^a)/K
0.3025	352.13 ± 0.43	0.0091	425.04 ± 0.57	0.1613	336.93 ± 0.91
0.4019	323.33 ± 0.17	0.0190	439.31 ± 0.30	0.1770	344.64 ± 0.01
0.4756	304.44 ± 0.04	0.0415	440.12 ± 0.22	0.1848	349.09 ± 0.06
0.0452	385.49 ± 0.03	0.0724	439.70 ± 0.21	0.2960	380.46 ± 0.14
0.0693	385.62 ± 0.03	0.1059	438.77 ± 0.122	0.3960	409.24 ± 0.08
0.1426	382.87 ± 0.16	0.1498	435.96 ± 0.14	0.5717	434.55 ± 0.62
0.2787	358.22 ± 0.08	0.2143	426.94 ± 0.23	0.5141	444.85 ± 0.08
0.0202	380.27 ± 0.03	0.2965	410.61 ± 0.37		
0.0306	384.38 ± 0.08	0.4346	376.35 ± 0.65		
0.2113	372.91 ± 0.13	0.4952	357.49 ± 0.07		
		0.6108	327.15 ± 0.34		

a- Standard Deviation

The results show that the water solubilities increase with temperature and decrease with chain length. The differences in water solubility between consecutive chain length acids also tend to become smaller as the chain length increases.

Data concerning the water solubility in fatty acids are scarce but can still be found for the smaller pentanoic and hexanoic acids in the temperature range 293.15-343.15 K³⁵. The data measured in this work are in good agreement with the few and old available literature data, as seen in **Figure 1**, showing the ability of the experimental methodology used for measuring the water solubility in heavier acids.

The two experimental techniques used in this work provided very similar results for the water solubility.

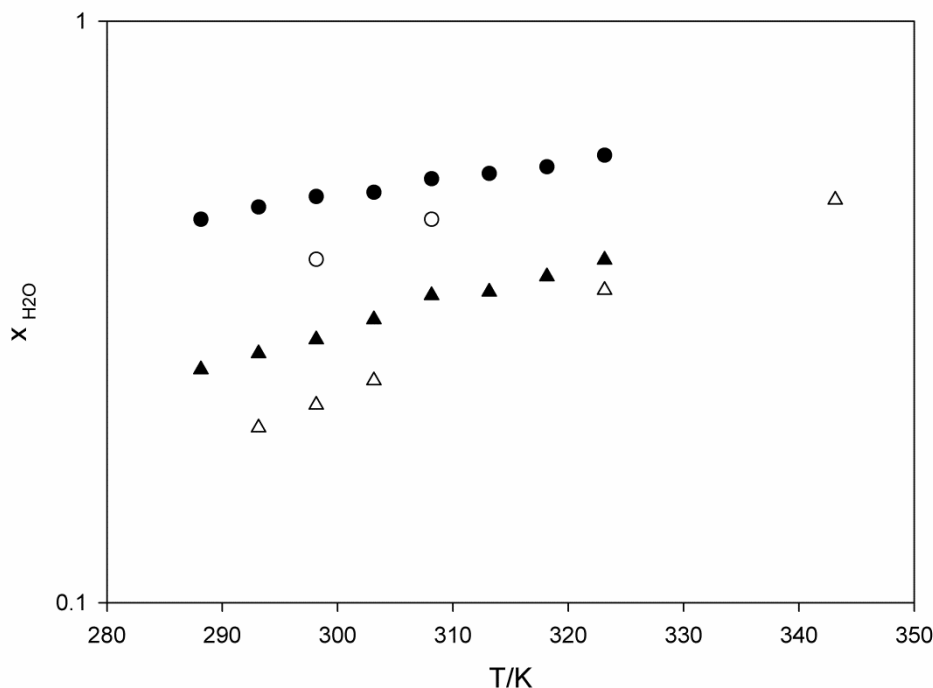


Figure 1. Experimental water solubility from this work (full symbols) and reported in the literature (empty symbols), in pentanoic acid (circles), and in hexanoic acid (triangles).

Correlation of the CPA pure compound parameters

The organic acids studied in this work are all self-associating and so the five CPA parameters must be estimated for each compound. This was done by a simultaneous regression of vapour pressure and saturated liquid density data, collected from the DIPPR database³⁶, covering the range of reduced temperatures from 0.45-0.85, for linear saturated carboxylic acids from 1 up to 20 carbons atoms and the unsaturated oleic acid, an important natural product with 18 carbon atoms and a double bound at carbon 9, usually referred as 18:1. The reasonability of the application of DIPPR correlations in a broad temperature range is questionable when actual experimental data is missing, and extrapolation was required in some cases, as can be seen in **Table 3**, where the reduced temperature ranges for which experimental data for vapor pressures and liquid densities are available from DIPPR are presented for the organic acids studied. The results reported in **Table 4**, show that it is possible with CPA to achieve an excellent description of the experimental (correlated) vapour pressure and liquid densities for all the studied acids, with global average deviations of about 2 % for both properties.

Table 3. Temperature limits for the experimental data available in DIPPR³⁶ for vapor pressures and liquid densities for the organic acids studied.

n.º Carbons	P ^σ		ρ	
	T _r min	T _r max	T _r min	T _r max
1	0.45	0.75	0.47	0.96
2	0.46	1.00	0.46	1.00
3	0.46	0.99	0.38	1.01
4	0.47	1.00	0.44	1.01
5	0.46	0.89	0.36	0.83
6	0.43	0.81	0.41	0.84
7	0.44	0.77	0.40	0.52
8	0.52	0.78	0.42	0.83
9	0.42	0.79	0.41	0.50
10	0.55	0.79	0.42	0.77
11	0.42	0.80	0.40	0.48
12	0.51	0.81	0.39	0.63
13	0.54	0.81	0.39	0.56
14	0.43	0.84	0.38	0.75
15	0.42	0.83	0.38	0.55
16	0.43	0.84	0.37	0.73
17	0.42	0.84	0.37	0.52
18	0.43	0.99	0.36	0.71
18:01	0.37	1.00	0.37	0.58
19	0.63	0.86	0.36	0.42
20	0.44	0.86	0.35	0.45

Table 4. Critical temperatures for acids, CPA pure compounds parameters and average absolute deviations of vapour pressure and liquid densities from the CPA EoS. The “4C” association scheme is considered for water and for acids the “1A” scheme.

n.° Carbons	T _c (K) ³⁶	a ₀ (J.m ³ .mol ⁻²)	c ₁	b×10 ⁵ (m ³ .mol ⁻¹)	ε (J.mol ⁻¹)	β	AAD %	
							P ^σ	ρ
1	605.9	0.6749	0.5466	3.24	20724.7	3.06E-01	0.47	0.97
2	594	0.8312	0.7101	4.69	33709.5	3.96E-02	2.06	1.17
3	606.9	1.4631	0.7913	6.33	30121.7	6.38E-03	0.76	0.47
4	625	2.3128	0.8554	8.50	31665.2	6.44E-04	1.05	1.6
5	645.8	2.8564	0.917	9.77	30738.5	5.58E-04	2.77	4.66
6	660.4	3.41	1.0001	11.50	37909	1.31E-04	2.56	3.02
7	677.9	4.0657	1.0333	13.40	39224.5	1.21E-04	3.52	3
8	693.5	4.8206	1.0883	15.30	41221.2	4.23E-05	1.42	1.68
9	708.6	5.55	1.1414	17.30	38553.3	7.71E-05	1.51	2.47
10	721.7	5.9482	1.1927	18.80	40685.3	1.34E-04	1.06	1.38
11	734.9	6.8717	1.2423	20.70	39467.1	6.97E-05	2.3	2.85
12	746	7.4908	1.2904	22.40	44385.4	3.77E-05	2.75	1.87
13	761	8.1444	1.3447	24.10	44431	3.77E-05	3.77	2.22
14	763.7	9.097	1.3822	26.00	43772.2	3.14E-05	2.57	1.95
15	778.3	9.8006	1.4419	27.80	45888.3	1.54E-05	3.78	2.29
16	788.3	10.9279	1.4689	30.70	44729.7	2.54E-05	1.98	2.04
17	801.5	11.4163	1.5105	31.50	44943.9	1.60E-05	1.3	2.7
18	808.3	12.336	1.5597	33.70	44506.6	1.99E-05	2.88	2.16
18:01	781	11.7378	1.2303	32.90	55646.4	4.71E-05	1.84	3.05
19	817.7	13.2612	1.5921	35.90	43926.7	2.54E-05	3.81	2.83
20	830	14.1516	1.6348	38.20	41738.4	4.51E-05	3.54	2.93
Water ³⁹	647.29	0.1228	0.6736	1.45	16655	6.92E-02	1.72	0.82
Global AAD %							2.27	2.25

$$(\% \text{AAD} = \frac{1}{NP} \sum_{i=1}^{NP} \text{ABS} \left[\frac{\text{exp}_i - \text{calc}_i}{\text{exp}_i} \right] \times 100)$$

Once again, as was observed previously for several families of other compounds (n-alkanes, n-alcohols, n-FCs and esters)^{22, 37}, the CPA pure component parameters for the acid series also seem to follow a smooth trend with the carbon number.

Having estimated the pure component parameters it was possible to model binary mixtures of water with several acids (pentanoic acid, hexanoic acid, heptanoic acid, octanoic acid, nonanoic acid and decanoic acid). Although the solubility of these acids in water was available in the literature³⁸ between 298.15 – 373.15 K, little information was found for the water solubility on the acids³⁵ prompting the measurement of these data in this work.

Correlation of the mutual solubilities

To obtain a good description of the mutual solubilities of water and fatty acids the fitting of the binary interaction parameter k_{ij} of Eq. 7 is required. Data from both the organic and aqueous phases were used for the binary interaction parameter optimization. Values for the binary interaction parameters obtained using both combining rules under study are presented at **Table 5**.

Table 5. CPA modelling results for the mutual solubilities and binary interactions parameters.

n. Carbons	CR-2			CR-4		
	k_{ij}	AAD %		k_{ij}	AAD %	
		acid rich phase	water rich phase		acid rich phase	water rich phase
5	-0.0903	39.01	10.4	-0.0951	56.17	9.19
6	-0.0833	11.87	4.24	-0.0894	42.40	4.67
7	-0.0918	21.14	2.70	-0.0987	29.51	2.08
8	-0.0967	40.49	2.38	-0.1033	24.78	2.63
9	-0.1151	84.39	6.93	-0.1217	11.14	8.11
10	-0.1333	78.5	8.83	-0.1430	9.05	3.88
AAD						
Global %		45.90	5.92		28.84	5.09

In order to improve the predictive character of the CPA EoS, linear correlations for the k_{ij} values with the carbon number were previously proposed for alkanes + water³⁹ and ester + water²² mixtures. For the heavier acids the trends of the k_{ij} values with the carbon number are also close to a linear tendency, as seen in **Figure 2**. The k_{ij} values for the smaller acids are somewhat off the linear tendency, particularly for pentanoic acid. Nevertheless, in order to increase the predictive character of the model, linear correlations of the k_{ij} with the chain length of the acid, C_n , for the two combining rules evaluated, were proposed, and described by equations (14) and (15) for CR-2 and CR-4, respectively, in order to allow the applicability of the model for heavier acids when equilibria data are not available. The extrapolation of the linear correlation will further be shown to be successful for the description of fatty acids + water systems from C_{12} to C_{18} .

$$k_{ij} = -0.0140 \times C_n + 0.0070 \quad (14)$$

$$k_{ij} = -0.0142 \times C_n + 0.0020 \quad (15)$$

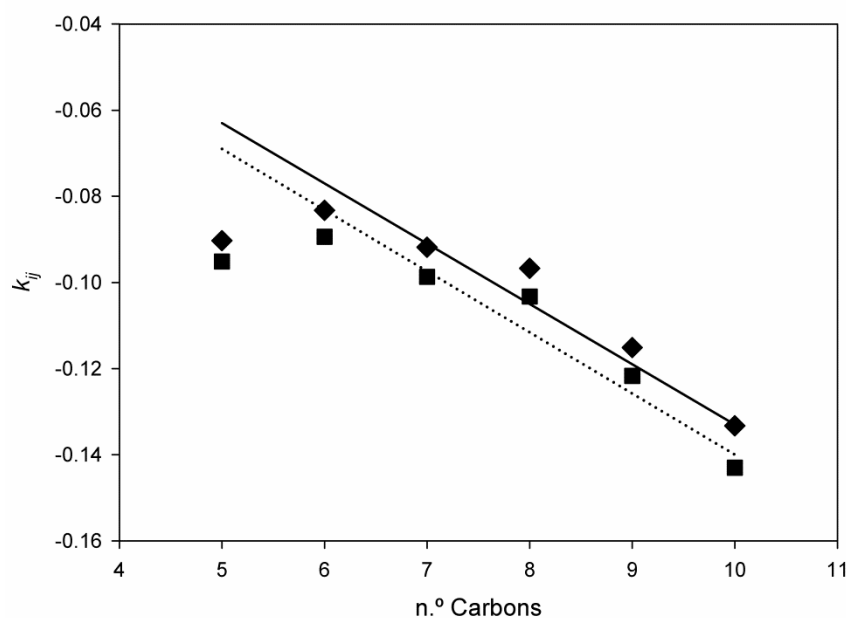


Figure 2. k_{ij} trend with the acid carbon number (◆, CR-2; ■, CR-4) and linear correlations (—, CR-2; ···, CR-4).

Results on the water rich phase are more dependent on the binary interaction parameter than the acid rich phase. Small variations in the k_{ij} 's values result in significant deviations in the description of the water rich phase with almost no impact in the acid rich phase. In fact, and for both association combining rules, the values for the k_{ij} 's optimized using both phases follow the same dependency as the k_{ij} 's evaluated solely from the water rich phase. The results obtained indicate that it is possible to predict the behaviour of the acid rich phase from the binary interaction parameters optimized using only data from the water rich phase.

The estimated k_{ij} 's are small, indicating that the CPA EoS is able to take adequately into account the cross-association interactions that occur in water + fatty acid systems, with any of the combining rules studied.

As shown in **Figure 2**, for the pentanoic acid + water system, the k_{ij} value was considerably off the linear tendency observed for the other compounds, indicating that different interactions may be present on this system. This deviation of the pentanoic acid from the behaviour of the other acids may be due to a higher degree of dissociation of the pentanoic acid in water, that the CPA EoS does not take into account. This may also be related to the unexpected behaviour of butanoic acid. From the analysis of the mutual solubilities of the higher acids, the phase envelopes of pentanoic and hexanoic acids, and the CPA predictions using the k_{ij} correlations, it would be expected that butanoic acid would only be partially miscible with water at room temperature. Yet, full miscibility of butanoic acid and water is observed under these conditions. The enhanced solubility of the lower acids in water results from new favourable interactions between the two compounds, not fully represented by the approach used in this work.

Evaluation of the Combining rule

The two combining rules studied produce very different descriptions of the acid rich phase but have no impact on the water rich phase, showing very similar global average deviations.

As shown in **Table 5** the CR-2 combining rule produces better results for smaller acids up to C₇. An increase in global average deviations with the chain length of the acid is observed for the heavier compounds of the homologous series.

The opposite behaviour was observed for the CR-4 rule, producing very good results for the heavier acids. The CR-4 combining rule performs globally better than the CR-2 with the advantage of increasing the calculation speed. With this combining rule, the water solubility in acids is described with a global average deviation below 30 %. The acid solubility in water is estimated with a global average deviation below 6 %, as reported in **Table 5**. Phase equilibria results for water + fatty acid systems are depicted in **Figures 3 and 4**.

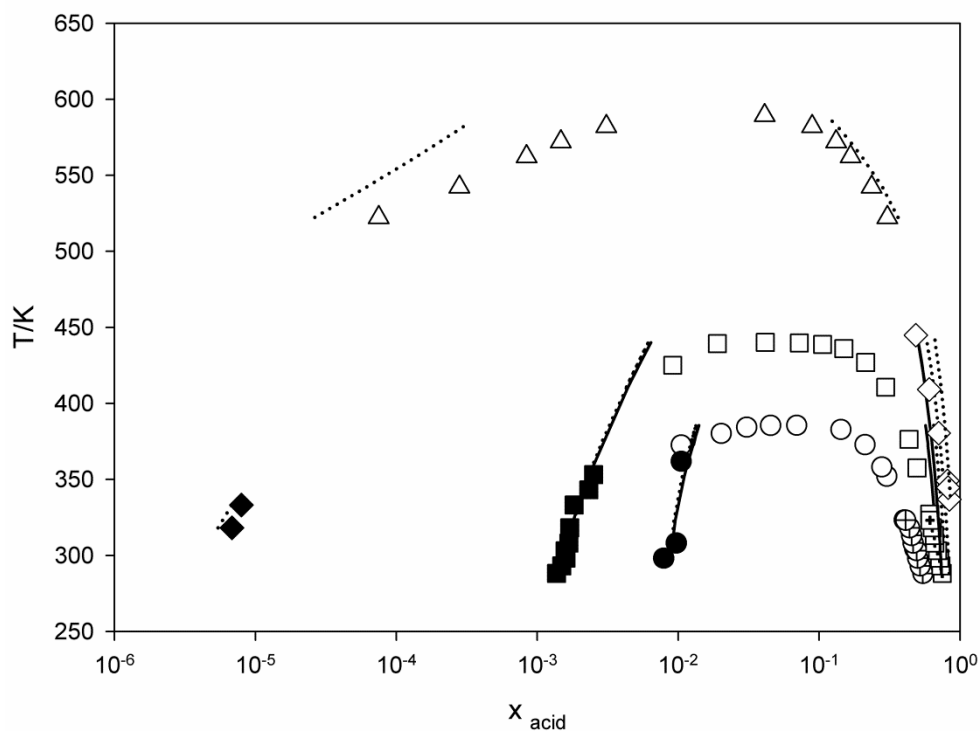


Figure 3. LLE for three water + acid systems. Experimental values for pentanoic acid (\circ , turbidimetry; \oplus , Karl Fisher; \bullet , literature data), for hexanoic acid (\square , turbidimetry; \boxplus , Karl Fisher; \blacksquare , literature data), for dodecanoic acid (\diamond , turbidimetry; \blacklozenge , literature data), and for oleic acid (Δ ; literature data), and CPA results ($—$, CR-2; \cdots , CR-4).

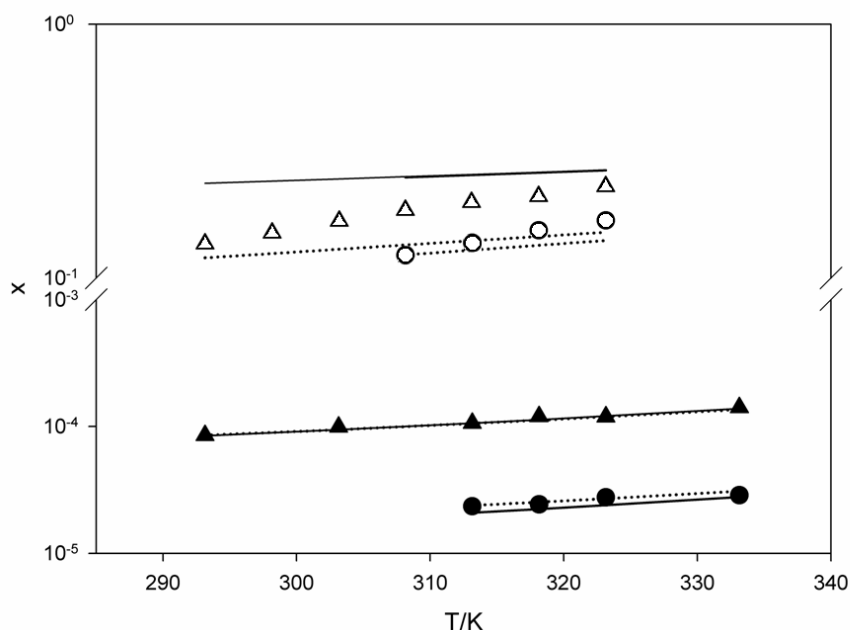


Figure 4. Mutual solubilities for two water + acid systems. Experimental results for water + octanoic acid (\blacktriangle , aqueous phase; \triangle , acid phase), and for water + octanoic acid (\bullet , aqueous phase; \circ , acid phase) and CPA results using two different combining rules (— , CR-2; \cdots , CR-4).

The results clearly indicate that the CPA-EoS provides a good description of the phase equilibria for water-fatty acid binary systems. The proposed model and the linear correlation for the binary interaction parameters can be used as a predictive tool to the description of systems of interest in industrial processes where organic and aqueous phases are present. For instance, for the oleic acid + water system, for which LLE data at higher temperatures and pressures were available in the literature⁴⁰. The CR-4 combining rule and the k_{ij} predicted through the linear correlation were used. As seen in **Figure 3** very good results were obtained for the water solubility with a global average deviation inferior to 6 %. The same prediction was made for the dodecanoic acid + water system with global average deviations inferior to 22 % for the water solubility.

Prediction of the solubility of solid fatty acids in water

Saturated fatty acids above decanoic acid are solid at room temperature and their solubilities in water are solid – liquid equilibria.

The CPA EoS has been previously applied to the description of the SLE of alcohol – alkanes, glycol – water and alcohol – water²⁶ mixtures, but never to the SLE of fatty acids and water systems. The purpose here is to investigate the predictive performance of the CPA EoS with the interaction parameter correlations obtained from LLE data and for each combining rule selected.

Equations to describe the SLE for binary systems are well established in the literature⁴¹.

Considering the formation of a pure solid phase and neglecting the effect of pressure, the solubility of a solute s can be calculated from the following generalized expression that relates the reference state fugacities:

$$\ln \frac{f_s^{liq}(T, P)}{f_s^{sol}(T, P)} = \frac{\Delta_{fus} H_s}{R} \left(\frac{1}{T} - \frac{1}{T_{m,s}} \right) - \frac{\Delta C_p}{R} \left[\frac{T_m}{T} - \ln \left(\frac{T_m}{T} \right) - 1 \right] \quad (16)$$

where $\Delta_{fus} H$ is the enthalpy of fusion, T is the absolute temperature, T_m is the melting temperature, ΔC_p is the difference of the liquid and solid molar heat capacities and R the gas constant.

The heat capacity contribution can be neglected with respect to the enthalpic term, as already observed for fatty acid systems in the work from Costa et al⁴² where the high pressure solid-liquid equilibria of fatty acids was studied. Complete immiscibility in the solid phase and absence of a solid–complex phase were also assumed.

The following expression for the solubility is considered,

$$x_s = \frac{\varphi_s^{L_0}}{\varphi_s^L} \exp \left[- \frac{\Delta_{fus} H_s}{R} \left(\frac{1}{T} - \frac{1}{T_{m,s}} \right) \right] \quad (17)$$

where φ is the fugacity coefficient and subscript 0 refer to pure component.

Few experimental SLE data are available in the literature and only for 7 fatty acids (from C₁₂ to C₁₈)^{38, 40}.

The values for the thermophysical properties needed to perform SLE calculations, melting temperature (T_m) and heat of fusion ($\Delta_{fus}H$), found in literature for the pure compounds (from C₁₂ to C₁₈)³⁶ are presented at **Table 6**.

These properties increase with the organic acid carbon number and a parity effect can be observed due to differences in the molecular packing of these compounds in the solid state.

The CR-2 combining rule performed better than CR-4 with global average deviations of 51 % and 63 %, respectively, as seen in **Table 6** and **Figure 5**.

Table 6. Values of T_m and Δh_m and CPA SLE modelling results.

n. Carbons	$\Delta h_m(\text{J.mol}^{-1})$	$T_m(\text{K})$	CR-2	CR-4
			AAD %	
12	36650	317.15	33.00	45.44
13	33729	314.65	28.51	47.81
14	45100	327.15	54.12	66.73
15	41520	325.68	30.05	48.62
16	54894	335.73	90.97	93.50
17	51342	334.25	55.13	66.53
18	61209	343.15	64.03	73.97
AAD Global %			50.83	63.23

Part of these deviations may be attributed to the low accuracy of the experimental data available. However, very satisfactory SLE predictions were achieved with the proposed model and using a single interaction parameter correlated from LLE data.

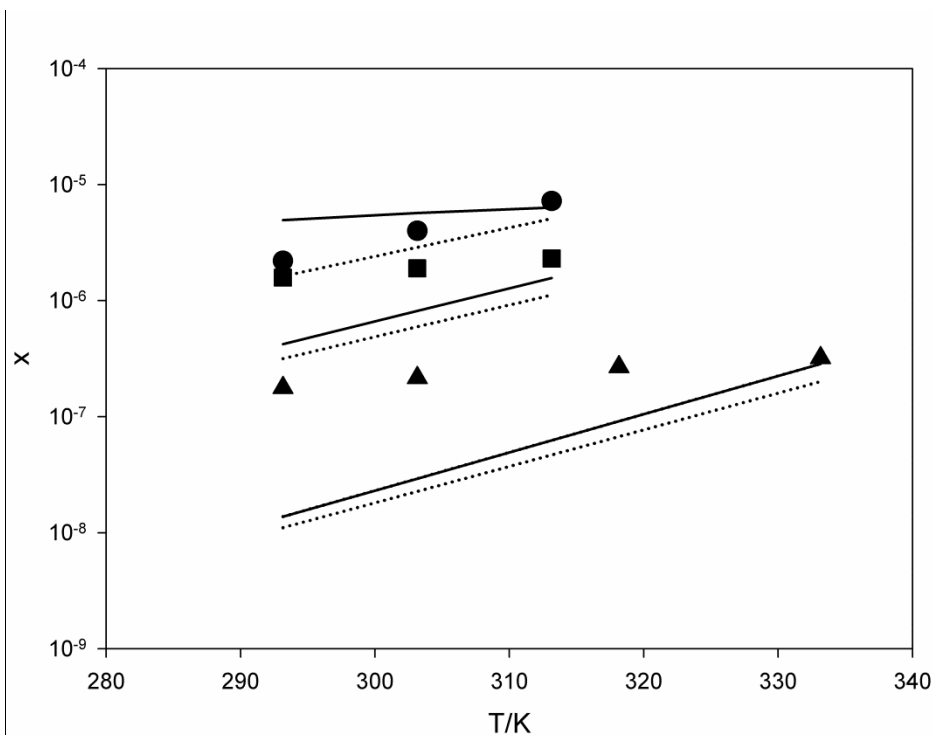


Figure 5. SLE prediction for three water + acid systems. Experimental values for dodecanoic acid (●), for tetradecanoic acid (■) and for octadecanoic acid (▲), and CPA results (—, CR-2; ···, CR-4).

Conclusions

Water solubilities in six fatty acids and LLE phase envelopes for three fatty acid + water systems were determined, using respectively Karl-Fisher coulometry and turbidimetry. The measured data are in good agreement with previously available measurements.

The CPA EoS was here extended to long chain carboxylic acids and their binary aqueous mixtures. Two different combining rules were tested.

A single, small, temperature independent and chain length dependent binary interaction parameter was enough to describe the mutual solubilities. A correlation for the binary interaction parameters was proposed.

For small acids, from C₅ to C₇, the CR-2 combining rule produced somewhat better results for the mutual solubilities, while the Elliot combining rule (CR-4) performed

better for the heavier fatty acids up to C_{10} . Using the CPA EoS and the CR-4 combining rule, global average deviations lower than 30 % were obtained for the water solubility and than 6% for the acid solubility.

The k_{ij} correlation was successfully extrapolated to model the LLE of the oleic acid + water and dodecanoic + water systems and to predict, SLE of binary aqueous mixtures with fatty acids from C_{12} to C_{18} , supporting the use of a linear correlation with the acid carbon number for the binary interaction parameters.

The good results obtained for the different types of equilibria of water + fatty acid mixtures and for the mutual solubilities of water + ester binary systems encourage the application of the CPA EoS for the design of extraction units for fatty acid and biodiesel production.

Notation

a = energy parameter in the physical term

a_0, c_1 = parameters for calculating a

A_i = site A in molecule i

b = co-volume

C_p = heat capacity

g = simplified hard-sphere radial distribution function

H = enthalpy

k_{ij} = binary interaction parameter

P = vapor pressure

R = gas constant

s = solubility

T = temperature

x = mole fraction

X_{A_i} = fraction of molecule i not bonded at site A

Z = compressibility factor

Greek Symbols

β = association volume

ε = association energy

η = reduced fluid density
 ρ = mole density
 Δ = association strength
 Δ = variation
 σ = vapour
 γ = activity coefficient
 ϕ = the fugacity coefficient

Subscripts

c = critical
fus = fusion
i,j = pure component indexes
liq. = liquid
m = melting
r = reduced

Superscripts

assoc. = association
phys. = physical

List of Abbreviations

AAD = average absolute deviation
CPA = cubic-plus-association
CR = combining rule
EoS = equation of state
LLE = liquid - liquid equilibria
VLE = vapor - liquid equilibria
SLE = solid - liquid equilibria
SAFT = statistical associating fluid theory
SRK = Soave-Redlich-Kwong

Literature Cited

1. Kirk RE, Othmer DF. Encyclopedia of Chemical Technology: Carboxylic Acids, Economic Aspects (4th edition). Boston: John Wiley & Sons, Inc., 1997.
2. Aranda DAG, Santos RTP, Tapanes NCO, Ramos ALD, Antunes OAC. Acid-catalyzed homogeneous esterification reaction for biodiesel production from palm fatty acids. *Catal. Lett.* 2008;122:20-25.
3. Prieto MM, Bada JC, Camacho ML, Constante EG. Deacidification and recovery of distillates in the physical refining of edible oils. *Eur. J. Lipid Sci. Technol.* 2008;110:101-110.
4. Ma FR, Hanna MA. Biodiesel production: a review. *Bioresour. Technol.* 1999; 70:1-15.
5. Encinar JM, Gonzalez JF, Rodriguez-Reinares A. Biodiesel from used frying oil. Variables affecting the yields and characteristics of the biodiesel. *Ind. Eng. Chem. Res.* 2005;44:5491-5499.
6. Freedman B, Butterfield RO, Pryde EH. Transesterification Kinetics of Soybean Oil. *J. Am. Soc. Brew. Chem.* 1986;63:1375-1380.
7. van Kasteren JMN, Nisworo AP. A process model to estimate the cost of industrial scale biodiesel production from waste cooking oil by supercritical transesterification. *Resources Conservation and Recycling.* 2007;50: 442-458.
8. Haas MJ, McAloon AJ, Yee WC, Foglia TA. A process model to estimate biodiesel production costs. *Bioresour. Technol.* 2006;97:671-678.
9. Ince E, Kirbaslar SI, Sahin S. Liquid-liquid equilibria for ternary systems of water plus formic acid plus dibasic esters. *J. Chem. Eng. Data.* 2007;52:1889-1893.
10. Bilgin M, Kirbaslar SI, Ozcan O, Dramur U. (Liquid plus liquid) equilibria of (water plus butyric acid plus isoamyl alcohol) ternary system. *J. Chem. Thermodyn.* 2005;37:297-303.
11. Kirbaslar SI, Bilgin M, Batr D. (Liquid plus liquid) equilibria of (water plus butyric acid plus cyclohexyl acetate) ternary system. *J. Chem. Thermodyn.* 2005;37:175-180.
12. Kirbaslar SI, Sahin S, Bilgin M. (Liquid plus liquid) equilibria of (water plus butyric acid plus dibasic esters) ternary systems. *J. Chem. Thermodyn.* 2007;39: 284-290.
13. Ferreira O, Macedo EA, Bottini SB. Extension of the A-UNIFAC model to mixtures of cross- and self-associating compounds. *Fluid Phase Equilib.* 2005;227:165-176.
14. Skjoldjorgensen S. Group Contribution Equation of State (Gc-Eos) - a Predictive Method for Phase-Equilibrium Computations over Wide Ranges of Temperature and Pressures up to 30 Mpa. *Ind. Eng. Chem. Res.* 1988;27:110-118.
15. Gros HP, Bottini S, Brignole EA. A group contribution equation of state for associating mixtures. *Fluid Phase Equilibria.* 1996;116:537-544.
16. Twu CH, Coon JE, Cunningham JR. An Equation of State for Carboxylic-Acids. *Fluid Phase Equilib.* 1993;82:379-388.
17. Jonasson A, Persson O, Rasmussen P, Soave GS. Vapor-liquid equilibria of systems containing acetic acid and gaseous components. Measurements and calculations by a cubic equation of state. *Fluid Phase Equilib.* 1998;152:67-94.

18. Huang SH, Radosz M. Equation of State for Small, Large, Polydisperse, and Associating Molecules - Extension to Fluid Mixtures. *Ind. Eng. Chem. Res.* 1991;30:1994-2005.
19. Fu YH, Sandler SI. A Simplified Saft Equation of State for Associating Compounds and Mixtures. *Ind. Eng. Chem. Res.* 1995;34:1897-1909.
20. Derawi SO, Zeuthen J, Michelsen ML, Stenby EH, Kontogeorgis GM. Application of the CPA equation of state to organic acids. *Fluid Phase Equilib.* 2004;225:107-113.
21. Zeuthen J, Extension of the CPA EoS to systems containing organic acids, Master Thesis, in Center for Phase Equilibria and Separation Processes (IVC-SEP), Department of Chemical Engineering. 2003, DTU: Lyngby, Denmark. p. 120.
22. Oliveira MB, Varanda FR, Marrucho IM, Queimada AJ, Coutinho JAP. Prediction of water solubility in biodiesel with the CPA EoS. *Ind. Eng. Chem. Res.* 2008;47:4278-4285.
23. Freire MG, Neves CMSS, Carvalho PJ, Gardas RL, Fernandes AM, Marrucho IM, Santos LMNBF, Coutinho JAP. Mutual Solubilities of water and hydrophobic ionic liquids. *J. Phys. Chem. B.* 2007;111:13082-13089.
24. Freire MG, Santos LMNBF, Fernandes AM, Coutinho JAP, Marrucho IM. An overview of the mutual solubilities of water-imidazolium-based ionic liquids systems. *Fluid Phase Equilib.* 2007;261:449-454.
25. Freire MG, Gomes L, Santos LMNBF, Marrucho IM, Coutinho JAP. Water solubility in linear fluoroalkanes used in blood substitute formulations. *J. Phys. Chem. B.* 2006;110:22923-22929.
26. Kontogeorgis GM, Michelsen ML, Folas GK, Derawi S, von Solms N, Stenby EH. Ten years with the CPA (Cubic-Plus-Association) equation of state. Part 1. Pure compounds and self-associating systems. *Ind. Eng. Chem. Res.* 2006;45:4855-4868.
27. Kontogeorgis GM, Michelsen ML, Folas GK, Derawi S, von Solms N, Stenby EH. Ten years with the CPA (Cubic-Plus-Association) equation of state. Part 2. Cross-associating and multicomponent systems. *Ind. Eng. Chem. Res.* 2006;45:4869-4878.
28. Suresh SJ, Elliott JR. Multiphase Equilibrium-Analysis Via a Generalized Equation of State for Associating Mixtures. *Ind. Eng. Chem. Res.* 1992;31:2783-2794.
29. Suresh J, Beckman EJ. Prediction of Liquid-Liquid Equilibria in Ternary Mixtures from Binary Data. *Fluid Phase Equilib.* 1994;99:219-240.
30. Voutsas EC, Yakoumis IV, Tassios DP. Prediction of phase equilibria in water/alcohol/alkane systems. *Fluid Phase Equilib.* 1999;160:151-163.
31. Folas GK, Gabrielsen J, Michelsen ML, Stenby EH, Kontogeorgis GM. Application of the cubic-plus-association (CPA) equation of state to cross-associating systems. I *Ind. Eng. Chem. Res.* 2005;44:3823-3833.
32. Kaarsholm M, Derawi SO, Michelsen ML, Kontogeorgis GM. Extension of the cubic-plus-association (CPA) equation of state to amines. *Ind. Eng. Chem. Res.* 2005;44:4406-4413.
33. Folas GK, Derawi SO, Michelsen ML, Stenby EH, Kontogeorgis GM. Recent applications of the cubic-plus-association (CPA) equation of state to industrially important systems. *Fluid Phase Equilib.* 2005;228:121-126.

34. Huang SH, Radosz M. Equation of State for Small, Large, Polydisperse, and Associating Molecules. *Ind. Eng. Chem. Res.* 1990;29:2284-2294.
35. Sorensen JM, Arlt W *Liquid-liquid equilibrium data collection*; DECHEMA: Frankfurt, 1980.
36. DIPPR, Thermophysical Properties Database, (1998).
37. Oliveira MB, Marrucho IM, Coutinho JAP, Queimada AJ. Surface tension of chain molecules through a combination of the gradient theory with the CPA EoS. *Fluid Phase Equilib.* 2008;267:83-91.
38. Yalkowsky SH, Yan H. *Handbook of Aqueous Solubility Data*; CRC Press, 2003.
39. Oliveira MB, Coutinho JAP, Queimada AJ. Mutual solubilities of hydrocarbons and water with the CPA EoS. *Fluid Phase Equilib.* 2007; 258: 58-66.
40. Ralston AW, Hoerr CW. The solubilities of the normal saturated fatty acids. *J. Org. Chem.* 1942;7:546-555.
41. Prausnitz JM, Lichtenthaler RN, Azevedo EGD. *Molecular Thermodynamics and Fluid Phase Equilibria* Prentice-Hall, 1999.
42. Costa MC, Krahenbuhl MA, Meirelles AJA, Daridon JL, Pauly J, Coutinho JAP. High pressure solid-liquid equilibria of fatty acids. *Fluid Phase Equilib.* 2007;253:118-123.

***Another look at the water solubility in biodiesels: Further
experimental measurements and prediction with the CPA EoS***

Fuel, 97, 843-847, 2012

DOI: 10.1016/j.fuel.2012.03.022

Another look at the water solubility in
biodiesels: Further experimental measurements
and prediction with the CPA EoS

M. B. Oliveira¹, M.J. Pratas¹, A. J. Queimada², J. A. P. Coutinho^{1,*}

¹CICECO, Chemistry Department, University of Aveiro, 3810-193 Aveiro, Portugal

²LSRE – Laboratory of Separation and Reaction Engineering, Faculdade de Engenharia,
Universidade do Porto, Rua do Doutor Roberto Frias, 4200 - 465 Porto, Portugal

Abstract

In a previous work we addressed the importance of knowing and describing the water solubility in biodiesels, for producing high quality biodiesel using the most suitable feedstock and operating the processing plants at the optimal conditions. The lack of information on the water solubility in methyl linoleate limited the quality of the results then reported. To overcome the identified limitations new water solubility measurements were carried out for methyl linoleate and four methylic biodiesels synthesized at our laboratory from the main oil feedstock currently used for biodiesel production (soybean, palm, rapeseed and sunflower oils).

The new experimental data presented here for the water solubility in methyl linoleate allowed to obtain the information about the binary system water/methyl linoleate (specifically the binary interaction parameter, k_{ij}) to be used in the modelling of multicomponent systems (biodiesels) with the CPA EoS. With this new interaction parameter the new experimental water solubilities reported in this work for four biodiesels were predicted with the CPA EoS with global average deviations inferior to 7%.

Keywords: Biodiesel, Methyl linoleate, CPA EoS, Water solubility, Prediction

1. Introduction

The large number of recent research works addressing the production, characterization and use of biodiesel clearly demonstrate the increasing worldwide importance of this biofuel. Offering the various advantages known to characterize biofuels, sustainability, reduction of greenhouse gases emissions, regional development and secure supply [1], biodiesel is actually the most promising alternative for petroleum based fuels for compressed ignition (diesel) engines. Due to its similarity in chemical structure and energy content with conventional diesel, it can be used in existing engines as pure or blended with regular diesel [2]. In fact, biodiesel, a blend of fatty acid alkyl esters, along with bioethanol, already represents 1.6% of the transport fuel used worldwide [3].

Although most research activities have been addressing different methods to produce biodiesel, involving new feedstock (such as cooking waste oil and microalgae oils [4]), novel catalysts (heterogeneous catalyst and enzymes) [4] and process conditions (supercritical [4]), the actual industrial way to produce biodiesel consists on the transesterification reaction of a vegetable oil with an alcohol (usually methanol [5] or ethanol in countries where this alcohol is easily produced and available [6]) with a basic catalyst, using mild operation conditions. The produced fatty acid esters cannot be labeled as biodiesel until they meet the EN 14214 [7] quality specifications in Europe, and the ASTM D6751 in the USA. As a consequence, after the transesterification reaction, the fatty acid methyl esters undergo several purification processes in order not to overcome the minimum contents in free glycerol, soap, metals, alcohol, free fatty acids, catalyst, water and glyceride established by the European and American standards. A high presence of these compounds in the biodiesel strongly affects the fuel properties and performance and consequently the engine life.

One of these purification steps is the fatty acid esters washing with hot water. This is the most common method of purification as it is efficient in removing methanol glycerol, sodium compounds, free fatty acid esters and soaps [8].

However, one of the requirements of the European and American quality standards is the biodiesel water content, since water affects the calorific value of the biodiesel, can cause the esters to react to produce soaps and can cause blocking and wearing of the

engine injection system. Water in biodiesel also diminishes the shelf life of the fuel, since it decreases the biodiesel oxidation stability and promotes biological growth [[9, 10]]. Consequently, after being washed with water, the fatty acid esters are dried in order to produce biodiesel with a water content not overcoming the maximum value of 0.05% (w/w) imposed in Europe by the EN 14214.

In the last few years, our research group has been addressing the measurement of phase equilibria and the development of thermodynamic models for the description of biodiesel production and purification processes [11-17]. Being able to predict the different phase equilibria of the binary and multicomponent systems found during the biodiesel production and purification, in a wide range of thermodynamic conditions, is essential for a correct design and optimization of these industrial processes, through the correct selection of suitable solvents, the most advantageous unit operations and separation sequence and their optimal size and operating conditions.

Two of these studies were focused on the measurement and prediction of the water solubility in pure fatty acid alkyl esters and biodiesels [15, 17]. Knowing the water solubility in biodiesels is essential for the biodiesel production and purification processes, allowing tuning the more favorable raw materials and correctly designing and optimizing the biodiesel washing and drying units in order to produce high quality biodiesel in agreement with the European and American quality specifications.

While assessing the poor performance of commonly used thermodynamic models, namely cubic equations of state and activity coefficient models, to describe the water solubility in fatty acid esters and their mixtures [15], the authors also developed and applied a more theoretical sound model, the Cubic-Plus-Association equation of state (CPA EoS), that explicitly describes the specific interactions between like molecules (in this case water) and unlike molecules (cross-association, in this case between esters and water). In an accurate, predictive and simple way, this model proved to be the most appropriate to describe the water solubility in biodiesels [15, 17].

Following these studies, in this work, new experimental water solubility measurements were carried out for methyl linoleate and four biodiesels synthesized at our laboratory from edible oils commonly used for producing biodiesel [4]: rapeseed, soybean, palm and sunflower, and the CPA EoS was applied to predict these new experimental data.

As the CPA EoS prediction of the water solubility in biodiesels is performed using interaction parameters obtained from binary phase equilibria data, it was possible, using the new data for methyl linoleate, to evaluate the contribution of this binary system to the improvement of the model prediction capability for the water solubility in biodiesels, by reassessing the results presented before for the water solubility in six commercial biodiesels [17].

2. Experimental Section

Materials

The water solubility was measured in the biodiesels synthesized by the transesterification reaction with methanol of the vegetable oils: soybean, rapeseed, palm and sunflower. The molar ratio of oil/methanol used was 1:5 using 0.5% sodium hydroxide by weight of oil as a catalyst. The reaction was performed at 55 °C during 24 h under methanol reflux. The reaction time chosen was adopted for convenience and to guarantee a complete reaction conversion. Raw glycerol was removed in two steps, the first after 3h reaction and then after 24h reaction in a separating funnel. Biodiesel was purified through washing with hot distilled water until a neutral pH was achieved. The biodiesel was then dried until the EN ISO 14214 limit for water was reached [7].

Biodiesels were characterized by GC-FID following the British Standard EN14103 from EN 14214 [7] to know their methyl esters composition. Capillary gas chromatography was used to determine the methyl ester composition of the biodiesel samples. A Varian CP-3800 with a flame ionization detector in a split injection system with a Select™ Biodiesel for FAME Column, (30 m x 0.32 mm x 0.25 µm), was used to differentiate all methyl esters in analysis inclusively the poli-unsaturated ones. The column temperature was set at 120°C and then programmed to increase up to 250 °C, at 4 °C/min. Detector and injector were set at 250 °C. The carrier gas was helium with a flow rate of 2 mL/min.

The water solubility was also measured in methyl linoleate (Aldrich, 99%).

Experimental Procedure

The water solubility measurements were carried out at temperatures from 288.15 to 318.15 K and at atmospheric pressure. The methodology used in this work, has already been successfully used for measuring the water solubility in fatty acid esters, biodiesels [17] and fatty acids [12]. The ester and the water phases were initially agitated vigorously and allowed to reach the saturation equilibrium by the separation of both phases in 20 mL glass vials for at least 48 h. This period proved to be the minimum time required to guarantee a complete separation of the two phases and that no further variations in mole fraction solubilities occurred.

The temperature was maintained by keeping the glass vials containing the phases in equilibrium inside an aluminium block specially designed for this purpose, which is placed in an isolated air bath capable of maintaining the temperature within (± 0.01 K).

The temperature control was achieved with a PID temperature controller driven by a calibrated Pt100 (class 1/10) temperature sensor inserted in the aluminium block. In order to reach temperatures below room temperature, a Julabo circulator, model F25-HD, was coupled to the overall oven system allowing the passage of a thermostated fluid flux around the aluminium block. The solubility of water in the ester rich phase was determined using a Metrohm 831 Karl Fischer (KF) coulometer.

The esters rich phase was sampled at each temperature from the equilibrium vials using glass syringes maintained dry and at the same temperature of the measurements. Samples of 0.1 to 0.2 g were taken and injected directly into the KF coulometric titrator.

The water solubility results at each individual temperature are an average of at least five independent measurements.

3. Model

The Cubic-Plus-Association equation of state (CPA EoS) has been extensively described in the literature and no further details will be explained in this work. For further information please see related works [18-20].

4. Results and discussion

Table 1 reports the methyl ester composition of the four synthesized biodiesels. The methyl esters are presented as CX or as CX:Y where X is the acid chain carbon number and Y is the number of double bonds in the fatty acid chain.

Table 1. Compositions of the biodiesels studied, in mass percentage.

methyl ester	soybean	rapeseed	palm	sunflower
C10		0.01	0.03	
C12		0.04	0.24	0.02
C14	0.07	0.07	0.57	0.07
C16	10.76	5.22	42.45	6.40
C16:1	0.07	0.20	0.13	0.09
C18	3.94	1.62	4.02	4.22
C18:1	22.96	62.11	41.92	23.90
C18:2	53.53	21.07	9.80	64.16
C18:3	7.02	6.95	0.09	0.12
C20	0.38	0.60	0.36	0.03
C20:1	0.23	1.35	0.15	0.15
C22	0.80	0.35	0.09	0.76
C22:1	0.24	0.19	0.00	0.08
C24		0.22	0.15	

The water solubility results in soybean, rapeseed, palm and sunflower biodiesels and in methyl linoleate, in the temperature range 288.15-318.15 K are listed in **Table 2**, as well as their respective standard deviations.

Table 2. Experimental results, in molar fractions, for the water solubility in biodiesels and in methyl linoleate.

T/K	($x_{H_2O} \pm \sigma^a$)
rapeseed biodiesel	
303.15	0.0303 ± 0.0030
308.15	0.0330 ± 0.0005
313.15	0.0365 ± 0.0002
318.15	0.040 ± 0.001
soybean biodiesel	
303.15	0.0284 ± 0.0002
308.15	0.0313 ± 0.0005
313.15	0.0351 ± 0.0005
318.15	0.0402 ± 0.0003
palm biodiesel	
298.15	0.022 ± 0.003
303.15	0.0246 ± 0.0005
308.15	0.0273 ± 0.0005
313.15	0.030 ± 0.008
318.15	0.0322 ± 0.0007
sunflower biodiesel	
298.15	0.024 ± 0.002
303.15	0.0317 ± 0.0009
308.15	0.0345 ± 0.0002
313.15	0.0369 ± 0.0002
318.15	0.0397 ± 0.0006
methyl linoleate	
303.15	0.0277 ± 0.0001
308.15	0.0333 ± 0.0007
313.15	0.037 ± 0.001
318.15	0.0420 ± 0.0007

^a Standard deviation

The values presented for the water solubility in the biodiesels and in methyl linoleate are in agreement with the results previously presented [17]. As expected, since the water solubility in fatty acid esters increases with the ester insaturation [17], palm biodiesel presents the lowest water solubility, in agreement with its higher content in the saturated ester methyl palmitate. The other biodiesels present quite similar water

solubility values, as expected due to their analogous fatty acid ester composition, with the sunflower biodiesel presenting the highest water solubility.

As explained at the introduction section, we have previously applied the CPA EoS to describe the water solubility in fatty acid esters and to predict it in biodiesels [17]. The information gathered in that work will be applied here, as subsequently shown, to predict the experimental results.

Modeling with the CPA EoS starts with the definition of the CPA pure compounds parameters. Esters are non-self-associating compounds and consequently there are only three pure compound parameters from the physical term to be determined: a_0 , c_1 and b . These parameters are usually determined from a simultaneous regression of vapour pressure and liquid density data. In a previous work [17] these parameters were estimated for the methyl esters $C_{16:0}$, $C_{18:0}$, $C_{18:1}$, $C_{18:2}$, which are the major components of commercial biodiesels. Due to the lack of reliable liquid density data for the unsaturated esters at the time, preference was given to the vapour pressure description.

Recently, using density data for several fatty acid esters and biodiesels [21, 22], measured by us, it was possible to re-estimate the CPA pure compound parameters for all the fatty acid methyl esters found in the biodiesel samples considered in this work, compounds ranging from 15 to 25 carbon atoms and with up to three unsaturated bonds (**Table 3**), by a simultaneous regression of pure component data. Vapor pressures and liquid densities were described with global average deviations inferior to 2 % (**Table 3**).

Table 3. Fatty acid methyl esters critical temperatures computed from the Wilson and Jasperson group contribution method for saturated methyl esters and from the Ambrose method for unsaturated methyl esters, CPA pure compound parameters and modeling results [23].

Methyl ester	$T_c(K)$	$a_0(J.m^3.mol^{-2})$	c_1	$b \times 10^4 (m^3.mol^{-1})$	AAD %	
					P	ρ
C12	710.41	6.7139	1.5340	2.3010	0.83	0.60
C14:0	740.97	8.0272	1.6089	2.6361	0.45	0.52
C16	765.92	7.4198	2.2873	2.9749	1.46	0.62
C16:1	749.63	9.2554	1.7805	2.9564	2.38	1.21
C18	788.63	10.1303	1.9196	3.3111	0.39	0.68
C18:1	772.34	10.5075	1.8212	3.2485	0.81	0.74
C18:2	786.37	8.9943	2.1597	3.1714	1.37	0.66
C18:3	797.26	8.6712	2.1722	3.0949	1.18	1.03
C20	803.28	13.4696	1.6123	3.7121	0.78	0.85
C20:1	786.99	12.5293	1.7143	3.5792	5.98	1.22
C22	817.47	16.2713	1.4963	4.0503	0.34	0.71
C22:1	801.18	15.3112	1.5933	3.9168	4.73	1.86
C24	830.41	19.3150	1.4045	4.3953	0.13	0.65
*global AAD %					1.60	0.87

$$\text{global AAD \%} = \frac{\sum AAD}{N_s} \times 100$$

where N_s is the number of data points studied.

Having the CPA pure compound parameters it was then possible to predict the water solubility in the ester multicomponent systems considered here. The k_{ij} 's for ester/ester were set to zero and, as already stated above, the solvation phenomena between the non-self-associating ester and the self-associating water was considered as a cross-association within the framework of the CPA EoS, where the cross-association energy

(ε_{ij}) was considered to be half the value of the association energy for the self-associating component (in this case water) and the cross-association volume (β_{ij}) was left as an adjustable parameter, fitted to the equilibrium data along with the k_{ij} .

When describing the water solubility in different fatty acid esters [17], a constant value for the cross-association volume, β_{ij} , was established (of 0.201), as well as a linear correlation for calculating the k_{ij} 's between esters and water was found with the chain length of the ester, C_n :

$$k_{ij}=0.0136 C_n - 0.3322 \quad (1)$$

This correlation, and the constant value for the cross-association volume, allowed predicting the water solubility in six commercial biodiesels from GALP, with global average deviations inferior to 15% [17]. Only for the k_{ij} between water and methyl oleate it was used the regressed value from phase equilibria data since it did not fit in the linear dependency with the carbon number determined for the saturated methyl esters. In addition, as phase equilibria data for the water/methyl linoleate system wasn't available at that time, the k_{ij} value for this sub-binary system was made equal to the one established for the water/methyl oleate system.

In this work, having measured the water solubility in methyl linoleate, the corresponding k_{ij} interaction parameter was determined, using the same constant value for the cross-association volume referred before. A k_{ij} value of -0.13 was obtained, describing the water solubility with global average deviations inferior to 3% (**Table 4** and **Figure 1**).

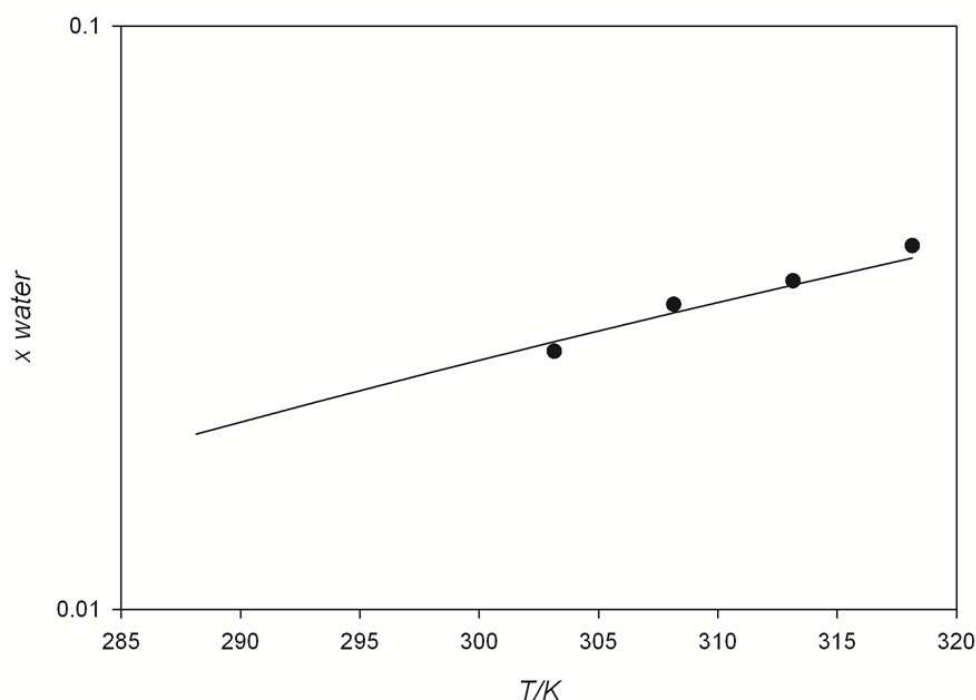


Figure 1. Water solubility in methyl linoleate: symbols experimental results and solid line CPA EoS results ($k_{ij} = -0.130$).

The experimental water solubility in the soybean, rapeseed, palm and sunflower biodiesels were then predicted using the recently assessed CPA pure compound parameters for esters and the previously proposed linear correlation to estimate the interaction parameters between the different saturated fatty acid methyl esters constituting the biodiesels and water, with global average deviations inferior to 7 % for these four biodiesels. (**Table 4**). For the binary sub-systems containing water and methyl oleate and linoleate the interaction parameter values regressed from phase equilibria data were used (from an earlier work for methyl oleate [17] ($k_{ij} = -0.100$) and from the present study for methyl linoleate ($k_{ij} = -0.130$)), as they didn't fit in the linear correlation proposed for saturated methyl esters. For methyl linolenate, the unsaturated fatty ester in less percentage in the selected biodiesels, the same k_{ij} value used for methyl linoleate was applied.

Prediction results are depicted in **Figure 2** for the palm and soybean biodiesels.

The strength of the solvation phenomena between water and esters is clearly showed by the relatively high values of the binary interaction parameters needed. In fact, as previously showed [17], the model must explicitly take into account the cross-

association between esters and water, since without it, the calculated water solubilities are much lower than the experimental values.

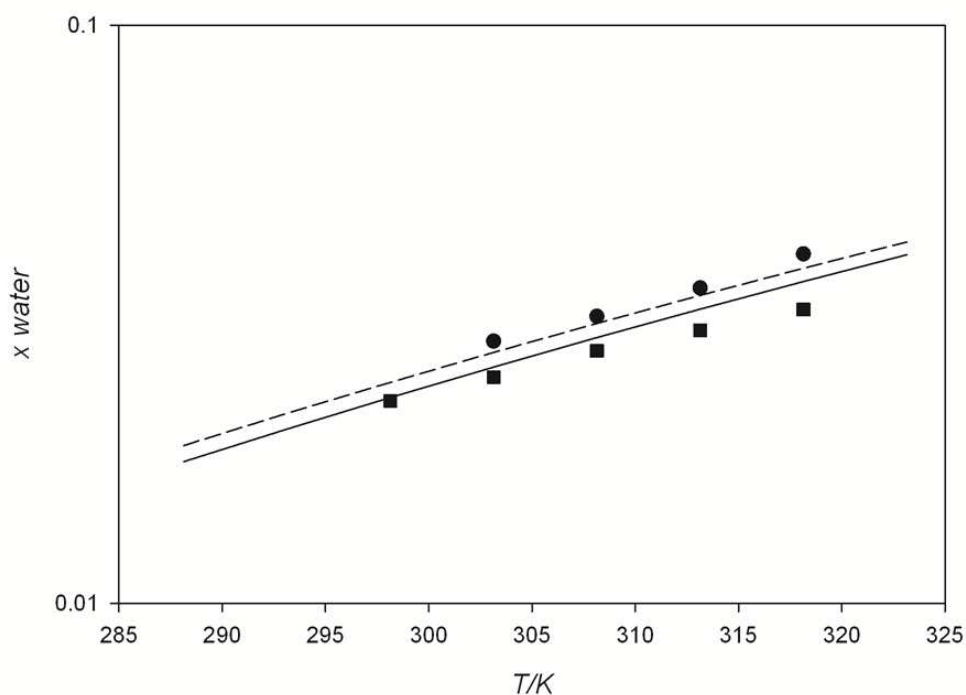


Figure 2. Water solubility in palm biodiesel (■, experimental results; solid line CPA EoS results), and in soybean biodiesel (●, experimental results; dashed line CPA EoS results).

These set of pure and binary parameters were also applied in this work to predict the water solubility in the GALP biodiesels addressed previously (Biodiesel A to F in **Table 4**). The global average deviations for the water solubility in these 6 biodiesels previously estimated to be 15 % [[17]] were reduced in this work to 11 % (biodiesels A to F in **Table 4**). It must be pointed out that the improvement on these results is mainly due to the use of a regressed k_{ij} value for the binary sub-system water/methyl linoleate, instead of using the same value obtained for the methyl oleate/water sub-system as previously done [[17]], and not as much due to the use of new CPA pure compound parameters for esters, since it was verified that the regressed binary interaction parameters obtained are quite independent of the CPA pure compound parameters used for esters, leading to the same global average deviations for the water solubility in biodiesels obtained before if no specific k_{ij} value is used for the water/methyl linoleate sub-system.

This demonstrates the importance that the right description of unsaturated ester systems can have on the modeling of the water solubility in biodiesels.

Table 4. Deviations in the mole fraction water solubility from CPA (the first column represents deviations using the recently assessed pure compounds and binary parameters and the second column previous results from reference [17]).

Compound	Former results [17]	
	<i>AAD %</i>	<i>AAD %</i>
methyl linolenate	3.4	
rapeseed biodiesel	10.5	
soybean biodiesel	3.9	
palm biodiesel	6.3	
sunflower biodiesel	9.4	
<i>Global AAD %</i>	6.7	
Biodiesel A	11.0	18.6
Biodiesel B	11.9	15.8
Biodiesel C	15.4	18.4
Biodiesel D	11.4	13.3
Biodiesel E	12.5	16.9
Biodiesel F	5.3	9.8
<i>Global AAD %</i>	11.3	15.5

$$\text{global AAD \%} = \frac{\sum AAD}{N_s} \times 100$$

where N_s is the number of data points studied.

5. Conclusions

Biodiesel is seen as one of the most important alternatives to conventional fuels since its use can solve the range of environmental, economic and political problems related to the use of conventional petroleum based fuels.

The water content in biodiesel have significant effects on the fuel quality and performance and so the ability to predict this property is essential for dimensioning biodiesel production and purification processes and optimizing their operation within product specifications.

Here new experimental measurements were performed for the water solubility in methyl linoleate and four methylic biodiesels synthetized from oils constituting the principal feedstock currently used for biodiesel production.

The water solubility in the soybean, palm, rapeseed and sunflower biodiesels was predicted with the CPA EoS with global average deviations inferior to 7%.

Acknowledgements

M. B. Oliveira acknowledges the financial support from Fundação para a Ciência e a Tecnologia for her Post-Doctoral grant (SFRH/BPD/71200/2010) and M. J. Pratas her Ph.D. grant (SFRH/BD/28258/2006).

The program used to perform the calculations with the CPA EoS is available at: <http://path.web.ua.pt/biodiesel.asp>

List of symbols

a = energy parameter in the physical term

a_0, c_1 = parameters for calculating a

A_i = site A in molecule i

b = co-volume

g = radial distribution function

k_{ij} = binary interaction parameters
 P = vapor pressure
 R = gas constant
 T = temperature
 x = mole fraction
 X_A = fraction of molecule not bonded at site A
 Z = compressibility factor

Greek Symbols

β = association volume
 ε = association energy
 η = reduced fluid density
 ρ = mole density
 Δ = association strength

Subscripts

i, j = pure component indexes
 $liq.$ = liquid
 r = reduced

Superscripts

$assoc.$ = association
 $phys.$ = physical

List of Abbreviations

AAD = average absolute deviation
CPA = cubic-plus-association
EoS = equation of state
SRK = Soave-Redlich-Kwong

Literature Cited

- [1] Reijnders L. Conditions for the sustainability of biomass based fuel use. *Energy Policy* 2006;34: 863-876.
- [2] Kamarudin SK, Yusuf NNAN, Yaakub Z. Overview on the current trends in biodiesel production. *Energy Conversion and Management* 2011;52: 2741-2751.
- [3] OECD/FAO. *Agricultural outlook 2008-2017*. Paris: Organization for Economic Co-operation & Development and Food and Agriculture Organization of the United Nations, OECD Publishing; 2008.
- [4] Cheng JJ, Timilsina GR. Status and barriers of advanced biofuel technologies: A review. *Renewable Energy* 2011;36: 3541-3549.
- [5] Van Gerpen J. Biodiesel processing and production. *Fuel Process Technology* 2005;86: 1097-1107.
- [6] Moser BR. Biodiesel production, properties, and feedstocks. *In Vitro Cell Dev-Biotechnol* 2009;45: 229-266.
- [7] EN 14214:2008. Automotive fuels. Fatty acid methyl esters (FAME) for diesel engines. Requirements and test methods.
- [8] Martin MA, Berrios M, Chica AF, Martin A. Purification of biodiesel from used cooking oils. *Applied Energy* 2011;88: 3625-3631.
- [9] Hanna MA, Ma FR. Biodiesel production: a review. *Bioresource Technology* 1999;70: 1-15.
- [10] Correia MJN, Felizardo P, Baptista P, Menezes JC. Multivariate near infrared spectroscopy models for predicting methanol and water content in biodiesel. *Anal Chim Acta* 2007;595: 107-113.
- [11] Oliveira MB, Miguel SI, Queimada AJ, Coutinho JAP. Phase Equilibria of Ester plus Alcohol Systems and Their Description with the Cubic-Plus-Association Equation of State. *Ind Eng Chem Res* 2010;49: 3452-3458.
- [12] Oliveira MB, Pratas MJ, Marrucho IM, Queimada AJ, Coutinho JAP. Description of the Mutual Solubilities of Fatty Acids and Water With the CPA EoS. *AIChE J* 2009;55: 1604-1613.

- [13] Oliveira MB, Queimada AJ, Coutinho JAP. Prediction of near and supercritical fatty acid ester plus alcohol systems with the CPA EoS. *J Supercrit Fluid* 2010;52: 241-248.
- [14] Oliveira MB, Queimada AJ, Coutinho JAP. Modeling of Biodiesel Multicomponent Systems with the Cubic-Plus-Association (CPA) Equation of State. *Ind Eng Chem Res* 2010;49: 1419-1427.
- [15] Oliveira MB, Ribeiro V, Queimada AJ, Coutinho JAP. Modeling Phase Equilibria Relevant to Biodiesel Production: A Comparison of g(E) Models, Cubic EoS, EoS-g(E) and Association EoS. *Ind Eng Chem Res* 2011;50: 2348-2358.
- [16] Oliveira MB, Teles ARR, Queimada AJ, Coutinho JAP. Phase equilibria of glycerol containing systems and their description with the Cubic-Plus-Association (CPA) Equation of State. *Fluid Phase Equilib* 2009;280: 22-29.
- [17] Oliveira MB, Varanda FR, Marrucho IM, Queimada AJ, Coutinho JAP. Prediction of water solubility in biodiesel with the CPA equation of state. *Ind Eng Chem Res* 2008;47: 4278-4285.
- [18] Kontogeorgis GM, Michelsen ML, Folas GK, Drawai S, von Solms N, Stenby EH. Ten Years with the CPA (Cubic-Plus-Association) Equation of State. Part 1. Pure Compounds and Self-Associating Systems. *Ind Eng Chem Res* 2006;45: 4855-4868.
- [19] Kontogeorgis GM, Michelsen ML, Folas GK, Drawai S, von Solms N, Stenby EH. Ten Years with the CPA (Cubic-Plus-Association) Equation of State. Part 2. Cross-Associating and Multicomponent Systems. *Ind Eng Chem Res* 2006;45: 4869-4878.
- [20] Oliveira MB, Coutinho JAP, Queimada AJ. Mutual solubilities of hydrocarbons and water with the CPA EoS. *Fluid Phase Equilib* 2007;258: 58-66.
- [21] Pratas MJ, Freitas S, Oliveira MB, Monteiro SC, Lima AS, Coutinho JAP. Densities and Viscosities of Fatty Acid Methyl and Ethyl Esters. *J Chem Eng Data* 2010;55: 3983-3990.
- [22] Pratas MJ, Freitas S, Oliveira MB, Monteiro SC, Lima AS, Coutinho JAP. Densities and Viscosities of Minority Fatty Acid Methyl and Ethyl Esters Present in Biodiesel. *J Chem Eng Data* 2011;56: 2175-2180.
- [23] Pratas MJ, Oliveira MB, Pastoriza-Gallego MJ, Queimada AJ, Pineiro MM, Coutinho JAP. High-Pressure Biodiesel Density: Experimental Measurements, Correlation, and Cubic-Plus-Association Equation of State (CPA EoS) Modeling. *Energy Fuel* 2011;25: 3806-3814.

Section 2

Enzymatic

Synthesis of

Biodiesel

My direct contribution for Published Paper

This Session presents a paper related to enzymatic production of biodiesel from FFA with methanol and ethanol. The yield of both reactions was evaluated by Response Surface Methodology with an experimental design with five levels. Where molar ratio acid / alcohol, enzyme quantity were studied. Other variables as time of reaction, temperature and pressure were also evaluated.

Experimental work was carried in collaboration with Marise Afonso, Ricardo Gomes and Rui Queirós, related to those MsC Thesis and final graduation project for last both.

Enzymatic Biodiesel Production using Novozyme 435 as a catalyst

In preparation

Enzymatic Biodiesel Production using Novozyme 435 as a catalyst

Maria Jorge Pratas, Marise Afonso, Sílvia C. Monteiro[#], João A.P. Coutinho

CICECO, Chemistry Department, University of Aveiro, Campus de Santiago, 3810-193
Aveiro, Portugal;

[#]Polytechnic Institute of Leiria, Leiria, Morro do Lena – Alto Vieiro, 2411-901 Leiria,
Portugal;

Abstract

Free Fatty Acids (FFA) are a by-product in edible oil refining, that are removed in the deodorizing step on oil purification. The deodorization is carried not just in edible oils but also in some cases before alkaline catalysis in biodiesel production. Enzymatic catalysis is here studied as an alternative to convert this by-product into biodiesel.

As the oleic acid is one of the main components recovered in the deodorization step it was used in this work as model. The optimal esterification conditions of oleic acid with methanol and ethanol were evaluated by their influence in reaction yield. An experimental design 2^2 was followed to study the influence of the dependent variables in percentage of conversion, namely the alcohol / oleic acid molar ratio (R) and enzyme concentration (E).

The optimal conditions obtained were R=6.3 and E=6.6% for methanol (100% conversion), and R=4.9 and E=5.7% for ethanol (95.5% of conversion).

The influence of temperature on the reaction was also studied, in a range between 30 and 60 °C for methanol, and between 30 and 70 °C for ethanol; with a molar ratio of 6 and an enzyme concentration of 2%. It was found that the conversion increases monotonously with increasing temperature for ethanol. For methanol, the conversion has a maximum at 50 °C and then decreases.

Another investigated variable was the pressure in the methanol esterification reaction, at constant temperature of 40°C, in the same conditions as temperature study, and was observed that the yield increases 38% just with 90 bar of nitrogen in the vessel.

The same enzyme was shown to be reusable up to 10 times in the esterification of oleic acid with ethanol, without significant loss of enzyme activity.

KEYWORDS: Enzymatic Catalyze, Esterification, Biodiesel, Oleic Acid, Novozyme
435.

INTRODUCTION

The energy used nowadays comes mostly from fossil fuels like coal, natural gas or oil. The fact that the reserves of fossil fuels are finite and the environmental problems associated with their use need a change in mindset and the use of alternative forms of energy production.^{1,2}

In these scenario vegetable oils, become more attractive, because of their renewable nature and environmental benefits. However, vegetable oils have some disadvantages to be used as a combustible.^{3,4} First of all, the direct use in internal combustion engines is problematic. Due to their high viscosity (about 5–10 times greater than diesel fuel)⁵ and low volatility, they do not burn completely and form deposits in the fuel injectors of diesel engine.⁶ An improvement on viscosity can be obtained with transesterification, which seems to be the process that assures best results in terms of lowering viscosity and improving other characteristics.⁷⁻⁸

The final product of a transesterification reaction of vegetal oil, with an alcohol in a presence of a catalyst, is a mixture of alkyl esters that is known as biodiesel. It is highly biodegradable in fresh water as well as in soil.⁹ Furthermore, the use of biodiesel in diesel engines reduces the emissions of hydrocarbons, carbon monoxide, particulate matter and sulphur dioxide.^{5,10,11} Biodiesel is said to be carbon neutral, it means that CO₂ produced from their combustion is being put back into the atmosphere, as recently has been removed from there by photosynthesis during the growth of the feedstock crops.

The transesterification process, used in biodiesel production, can be carried out in different ways such as alkali, acid or bio-catalysis. Of all these methods, the alkali process is the most used in industrial scale but it presents problems of separation of catalyst and unreacted methanol from biodiesel.^{4,12} Biocatalysis eliminates these disadvantages producing biodiesel with a very high purity. Nevertheless enzyme catalyzed process offers several additional benefits:¹³

- compatibility with variations in quality of the raw the raw materials,
- few process steps,
- higher quality glycerol,
- improved phase separation (no emulsification from soaps)
- reduce energy consumption and wastewater volumes.

However, the enzymatic process has not been implemented in an industrial scale due to enzymes high cost, lipase low activity or enzyme inhibition by methanol.^{14,15}

The raw material costs and limited availability of raw vegetable oil are being recently critical issues for the biodiesel production.¹⁶ Therefore, it has been necessary to look for another raw material to produce biodiesel. Acid oils or raw materials with high levels of available free fatty acids could be an alternative. In these cases the alkaline catalysis has serious limitations, and the enzymatic production of biodiesel is a good alternative.

In this work the performance of lipase Novozym® 435 was tested as a biocatalyst in the enzymatic esterification reaction of oleic acid with an alcohol, to produce biodiesel in a solvent-free system, shown in Figure 1. It was also tested the effect of reactions factors, as enzyme quantity and alcohol / oil molar ratio. Another studied variable was pressure of an inert gas in the vessel reaction.

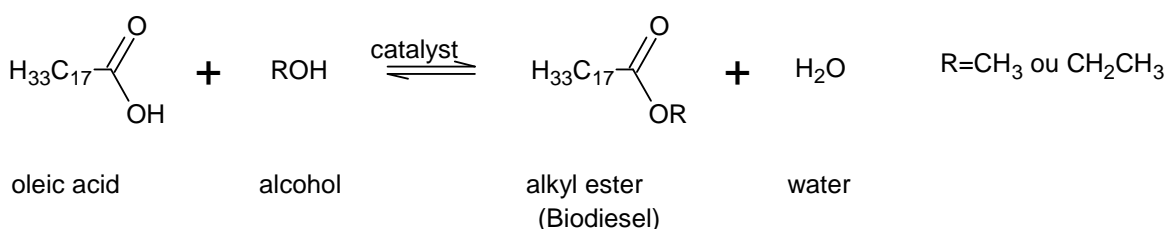


Figure 1 - Esterification reaction of oleic acid with an alcohol.

The process of biodiesel production was optimized by application of the experimental design and Response Surface Methodology (RSM). Using a factorial planning with three levels, the influence of temperature, enzyme/oil ratio and methanol/oil ratio was studied, as well as their interaction. After being verified that the temperature had no statistical significance, on the studied range, a new design factorial 2^2 was defined. In order to improve the response surface another design was defined on the region with higher conversions, central composite 2^2 . The tested variables were methanol/oleic acid molar ratio and enzyme concentration.

The reaction effects were studied to indicate the best stoichiometry conditions to perform the esterification reaction with Novozym 435. The temperature was studied later on a larger range of values under fixed conditions of alcohol/oleic acid molar ratio and enzyme concentration. To study the reuse of the immobilized enzymes was carried out a set of ten consecutive tests of three hours for each alcohol. In order to evaluate

pressure influence on esterification reaction, variable pressures of an inert gas were added in the beginning of the reaction, and then evaluated its effect on the yield.

MATERIALS AND METHODS

Materials. Novozym 435, a commercial Lipase B from *Candida antarctica*, immobilized on macroporous acrylic resin was used as a catalyst in the esterification reaction of oleic acid. It was a kind gift of Novozymes to perform this work.

Oleic acid (90.0% m/m) was supplied by Aldrich. Methanol and Ethanol (99.9% m/m) was purchased from Lab-scan, and all other chemicals used were obtained commercially and were of analytical grade.

Esterification process. The enzymatic esterification reactions were carried out in a closed vase containing oleic acid, the enzyme and alcohol. All reagents and catalyst were weighted in a five digits balance. The reaction was carried out in an orbital stirrer with controlled temperature and stirring. After the reaction two samples were collected from the bottom of the final product. Finally the samples were dried passing through anhydrous sodium sulfate. Variables that could affect the yield, like total volume of vase, and total volume of reagents, were maintained constant in each experiment.

The work was performed in several steps, a previous study was made to define reaction time in order to keep it constant though all experiments, then the influence in the yield of reaction factors, and at last temperature and pressure effects were studied.

Sample derivatization. Before gas chromatography analysis, samples were silylated as follows¹⁷: approximately 30 μL of each dried sample was dissolved in 100 μL of pyridine. At this point compounds containing carboxyl groups were converted into TMS esters, by adding 100 μL of bis(trimethylsilyl)trifluoro-acetamide (BSTFA) and 50 μL of trimethylchlorosilane, and keeping at 70°C for 30 min. Then the derivatized samples were analyzed by gas chromatography.

Analysis of methyl esters. The methyl ester contents were quantified using a capillary gas chromatography. Each silylated sample was injected into a gas

chromatographer with a flame ionization detector (Varian 3800 GC-FID) in a split injection system with the ratio of 1:20. On analysis a DB1-ht column (length: 15 m, internal diameter: 0.32 mm and film thickness: 0.1 µm) coated with 0.1 µm film of dimethylpolysiloxane was used. The column temperature was set at 100 °C and then programmed to increase up to 200 °C, at 8 °C/min with a final landing of 5 min holding the temperature. Detector and injector temperatures were set at 220 °C and 250 °C, respectively. The carrier gas was Helium with a flow rate of 2 mL/min.

Yield quantification. The percentage of conversion (alkyl esters formed) on the reaction was quantified by comparison between the areas from the peaks of alkyl esters and oleic acid on the chromatogram according to Equation 1, where A_{ae} is the area of the peak of alkyl ester and A_{oa} is the area of the peak of oleic acid.

$$\mathbf{Conversion} = \frac{A_{ae}}{A_{ae} + A_{oa}} \times \mathbf{100} \quad (1)$$

Software. All statistical analysis were made using Statistica 8.0 from Statsoft© (ANOVA and pareto chart), Matlab R2009b from The MathWorksTM (response surface and contour plot) and Microsoft Office Excel 2007 from Microsoft©. The confidence level used was 90%.

RESULTS AND DISCUSSION

Study of reaction time. An initial study of the conversion over time was made in order to define a reaction time that could be used though all experiments. Esterification reaction of oleic acid with methanol was followed during 24 hours (Figure 212). The alcohol/oleic acid molar ratio was 6 and the enzyme concentration was 2%. The agitation used was 150 rpm with a temperature of 40 °C. All variables were selected based on available literature.¹³⁻²¹ This reaction was repeated using ethanol, with similar results.

To evaluate the influence of variable in the yield three hours of reaction time was chosen and was used in all experiments.

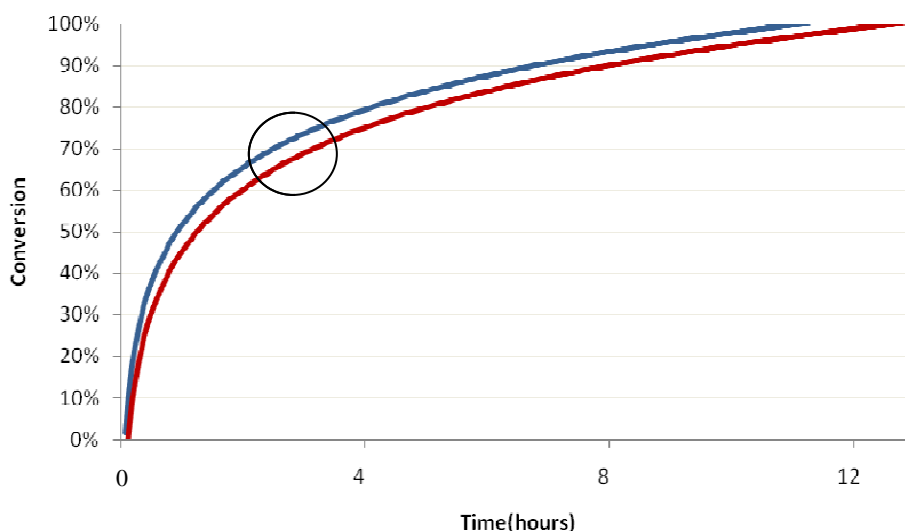


Figure 212: Logarithmic trend line for the time study using (—blue) methanol or (—red) ethanol. Reaction Conditions: 2% Novozym435, R=6, 40°C, 150 rpm.

Effect of temperature, enzyme/oil ratio and methanol/oil ratio

For the enzymatic esterification of oleic acid with methanol three parameters were tested: methanol/oleic acid molar ratio (R), enzyme concentration (E) and temperature (T). A central composite design, 2^3 , with six replications of the central point was used. The conditions were defined for zero level (central point) and one level (+1 and -1, the factorial points), and the design was extended up to +1.682, the axial points.

The data obtained were fitted to the following second order polynomial equation

$$Y = b_0 + b_1x_1 + b_2x_2 + b_{11}x_1^2 + b_{22}x_2^2 + b_{12}x_1x_2 \quad (2)$$

where Y is the dependent variable (conversion in %) and b_0 , b_1 , b_2 , b_{11} , b_{22} , and b_{12} are the regression coefficients for the intercept, linear, quadratic and interaction terms, respectively. x_1 and x_2 are the independent variables.^{6, 22, 23}

The conditions that define each level of the experimental design adopted for the enzymatic esterification of oleic acid with methanol are represented on Table 1.

Table 1: Level of variables for central composite design 2³.

Variables	Levels				
	-1.68	-1	0	+1	+1.68
R	5	7.03	10	12.97	15
E	1	1.81	3	4.19	5
T	35	37.03	40	42.97	45

To carry a statistical analysis with the experimental results of each experimental design a second order mathematical model was generated where, not only the linear effects for each variable, but also the quadratic effects and the interaction between each variable were considered. Were considered as significant parameters those with p under 10% ($p < 0.1$), due to the large variability inherent to bioprocesses.

For the central composite design 2³ the second order mathematical model derived can be described by the following equation:

$$Yield = -5.989 + 1.078E + 0.191T + .283R - 0.018ET - 0.002ER - 0.007TR - 0.032E^2 - 0.001T^2 - 0.003R^2 \quad (2)$$

On the Pareto chart shown on Figure are represented the effects considered for the reaction. The height of the bars shows the absolute value of t calculated and the bars are arranged in descending order of significance. The vertical line gives the t tabulated ($t_{10, 0.1/2} = 1.81$) from which the effects are considered significant for a confidence level of 90%. The parameters with no statistical significance are incorporated to residuals on ANOVA analysis (Table 2).

In agreement with Figure 3 enzyme concentration is the most significant variable. The effects that show statistical significance ($p < 0.10$) are the enzyme concentration (E), methanol/oleic acid molar ratio (R), enzyme concentration-temperature interaction (ExT), temperature-methanol/oleic acid molar ratio interaction (TxR) and quadratic enzyme concentration (E^2).

The proposed method has a very good coefficient of determination ($R^2 = 0.971$) and F calculated is highly significant ($p = 0.000002$), as can be seen on Table 2, which demonstrates a good adjustment of the model to the experimental values.

The statistical analysis of this procedure is not detailed as the following since the experimental design was redefined excluding the temperature variable.

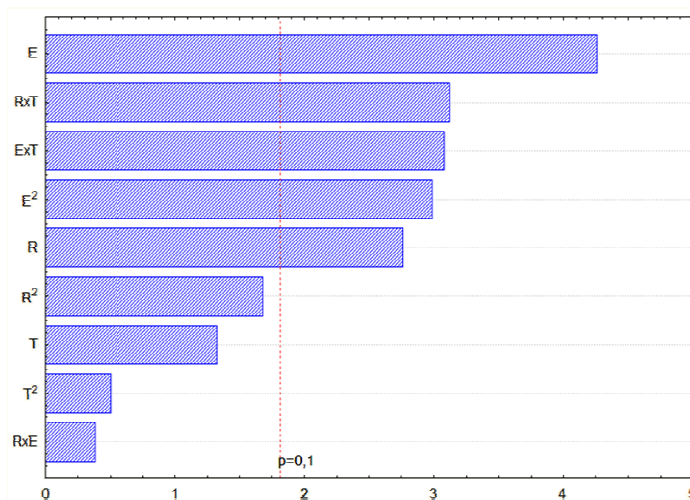


Figure 3: Pareto chart for the effects on conversion rate for esterification with methanol for experimental design with 3 variables.

Table 2: ANOVA table for central composite design 2³ for esterification with methanol

Source	SS	DF	MS	Fcalc	p
Regression	1.154	9	0.128	36.63	0.000002
Residuals	0.035	10	0.004		
Total	1.189	19			

The statistical analysis of the experimental data for the central composite design 2³ showed that the temperature had no statistical significance for the range of values studied. A new experimental design was defined excluding the temperature, this time with only two variables: methanol/oleic acid molar ratio (R) and enzyme concentration (E). The temperature was kept at 40 °C in all experiments.

Effect of enzyme/oil ratio and methanol/oil ratio

Two different designs of experiments were defined. First, a factorial design 2² (Table 3) was used and then a central composite design 2² (Table 4) was defined on the region with the conditions of higher conversion values. The aim of this procedure was to obtain

a good response surface that would allow us to find the optimal conditions of the reaction.

Table 3: Levels of variables for factorial design 2^2 for methanol.

Variables	Levels	
	-1	1
R	0.5	10
E	1	5

Table 4: Levels of variables for central composite design 2^2 for methanol.

Variables	Levels				
	-1.414	-1	0	1	1.414
R	0.78	1.5	3.25	5	5.72
E	2.59	3	4	5	5.41

For the statistical analysis the experimental values obtained from both experimental designs of two variables, factorial and central composite design were considered. Based on these results it was possible to create a second order mathematical model for studied parameters and their interaction, represented on Equation 3.

$$Yield = 0.353 + 0.141R + 0.0933E - 0.0192R^2 + 0.0153RE - 0.0143E^2 \quad (3)$$

By the analysis of the Pareto chart and the table of regression coefficients (Figure 4), it can be seen that that the most significant effects ($p < 0.1$) are methanol/oleic acid molar ratio (R), quadratic methanol/oleic acid molar ratio (R^2) and methanol/oleic acid molar ratio-enzyme concentration interaction (Rx E). The most significant variable is the quadratic methanol/oleic acid molar ratio (R^2).

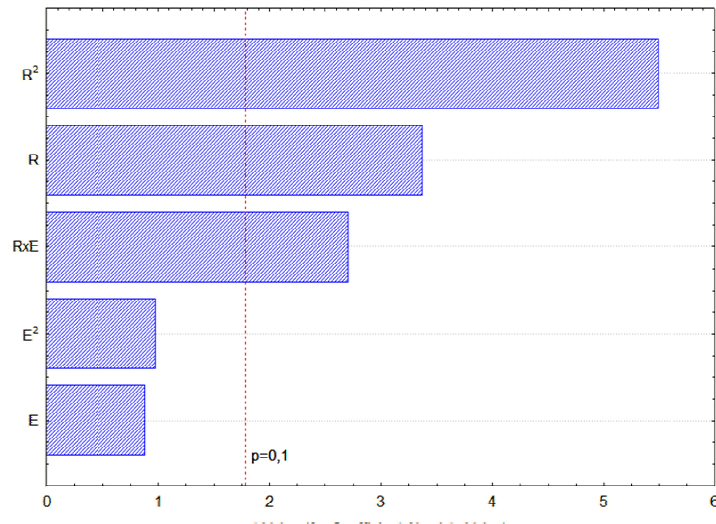


Figure 4: Pareto chart for the effects on conversion rate for experimental designs of 2 variables of esterification with methanol.

The proposed method has a good coefficient of determination ($R^2=0.841$) and by the analysis of variance on ANOVA table it can be observed that F calculated is much larger than F tabulated ($F_{5; 7; 0.1}=2.88$). Those results indicate a good agreement between the experimental values and the predicted by the model as can be seen on Table 5.

Table 5: ANOVA table for experimental designs of 2 variables of esterification with methanol.

Source	SS	DF	MS	F	P
Regression	1.036	5	0.207	15.533	0.00007
Residuals	0.160	12	0.0133		
Total	1.196	17			

Based on the response surface, and contour plot represented on Figure 5 and Figure 6, the conditions that result on a higher conversion of methyl esters can be identified. It is possible to observe that the area with higher conversion ($>80\%$) lies between a molar ratio of 4 and 9 and an enzyme concentration between 4 and 9%.

The response surface and contour plot indicate that the reaction is favored by a methanol/oleic acid molar ratio equal to concentration of enzyme in the range 4 to 9. It is possible to obtain a complete reaction with a molar ratio of 4 and an enzyme concentration of 4%, as also 9 and 9% respectively.

For values of enzyme concentration above 6, an increase of the molar ratio up to about 5 benefits the reaction, but the conversion decrease for higher enzyme concentration values.

The oblique arrangement of curves in contour plot indicates that the interaction is significant in the tested model.

The maximum value of the Equation 3 was over 100%, due to the mathematical extrapolation, which corresponded to the conditions of a molar ratio of 6.32 and an enzyme concentration of 6.64%. This point was tested experimentally and a conversion of 100% was obtained.

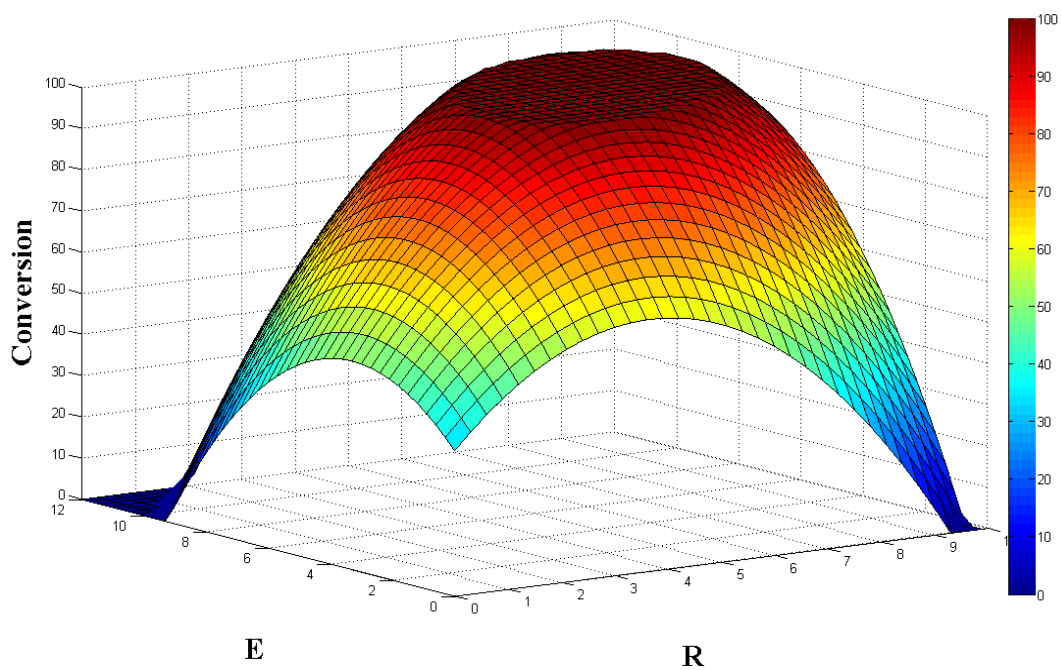


Figure 5: Response surface for experimental designs of 2 variables of esterification with methanol.

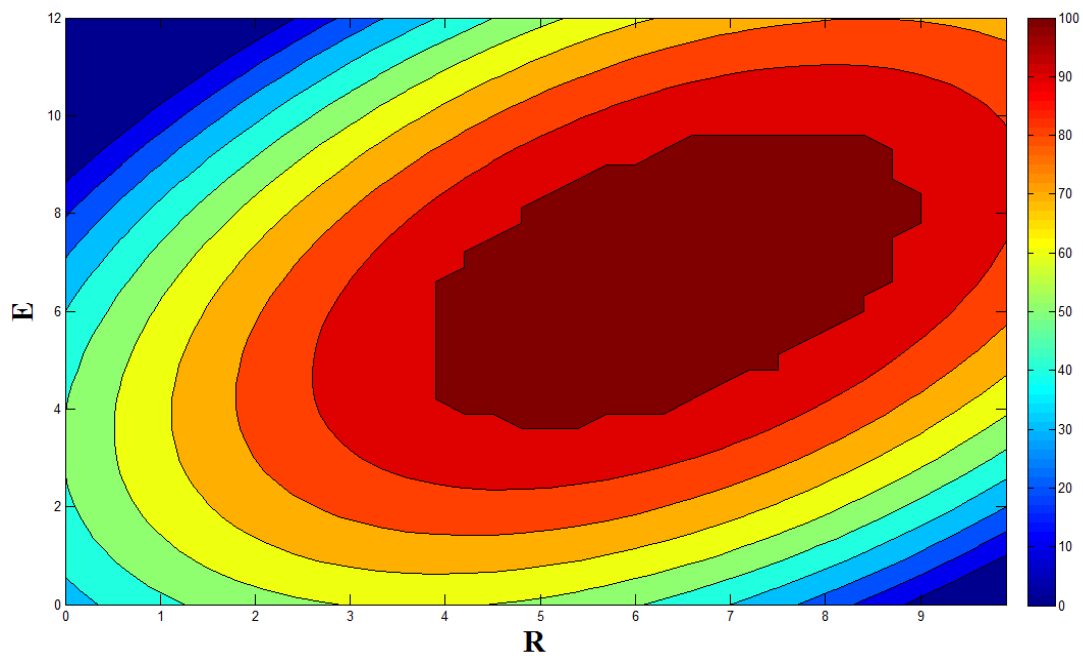


Figure 6 : Contour plot for experimental designs of 2 variables of esterification with methanol.

Effect of enzyme/oil ratio and Ethanol/oil ratio

Two different designs of experiments were defined. First, a central composite design 2^2 (Table 6) was used and then a factorial design 2^2 (Table 7) was defined on the region with the conditions of higher conversion values. The aim of this procedure was to obtain a good response surface that would allow us to find the optimal conditions of the reaction.

Table 6: Levels of variables for central composite design 2^2 for ethanol.

Variables	Levels				
	-1.414	-1	0	1	1.414
R	0.26	1.5	4.5	7.5	8.75
E	0.17	1	3	5	5.83

Table 7: Levels of variables for factorial design 2^2 for ethanol.

Variables	Levels	
	-1	1
R	3	6
E	5	7

For the statistical analysis the experimental values obtained from both experimental designs of two variables, factorial and central composite design were considered. Based on these results it was possible to create a second order mathematical model for studied parameters and their interaction, represented on equation 5.

The equation generated by the second order mathematical model for the experimental designs of two variables for esterification with ethanol is

$$Yield = -4.613 + 12.50R + 23.87E - 1.354R^2 + 0.2381RE - 2.166E^2 \quad (5)$$

From the analysis of Pareto chart and the table of regression coefficients (Figure 7 and Table 8) can be observed that the interaction ethanol/oleic acid molar ratio-enzyme concentration (RxE) is the only factor that has no statistical significance with a confidence level of 90%. The enzyme concentration is the most significant variable.

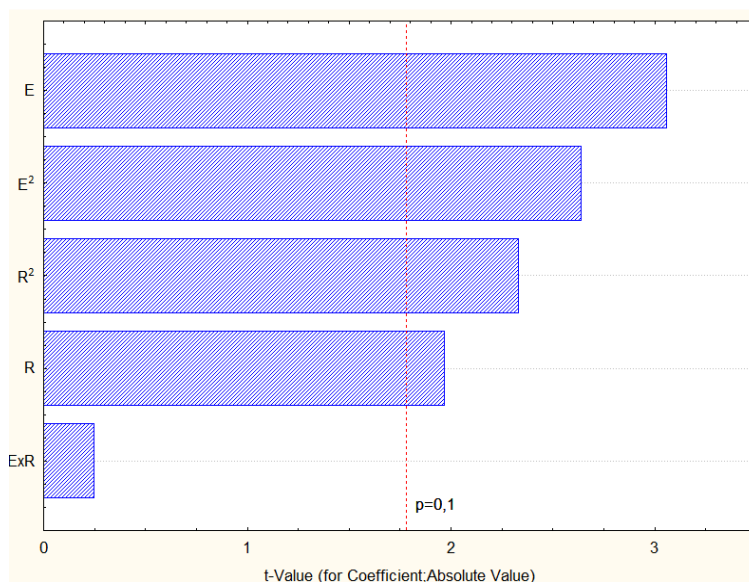


Figure 7 : Pareto chart for experimental designs of 2 variables of esterification with ethanol.

The correlation of the model is 0.760, which can be considered acceptable considering that we are working with biological catalysts. The value of F calculated is good when compared to the tabled ($F_{5;12;0.1}=2.39$) as shown in the ANOVA table.

Table 8 : ANOVA table for experimental designs of 2 variables of esterification with ethanol

Source	SS	DF	MS	F	P
Regression	7814.24	5	1562.85		
Residuals	2464.56	12	205.38	7.610	0.00197
Total	10278.80	17			

Based on the response surface and contour plots represented on Figure 8 and Figure 9 the conditions that result on a higher conversion of ethyl esters can be identified. It is possible to verify that the area with higher conversion (>80%) lies between a molar ratio of 3 and 7 and an enzyme concentration between 4 and 7%. These graphs indicate that the conversion increases with increasing ethanol/oleic acid molar ratio up to about 5 and there is a decrease on the conversion for higher molar ratio values. The increase in enzyme concentration has a positive effect in response up to values of about 6%, and from that value, the conversion decreases.

The maximum value of the Equation 5 was about 93.4%, which corresponded to the conditions of a molar ratio of 4.87 and an enzyme concentration of 5.65%. The result obtained experimentally for these conditions was 95.5%, a value close to expected, confirming the suitability of the model.

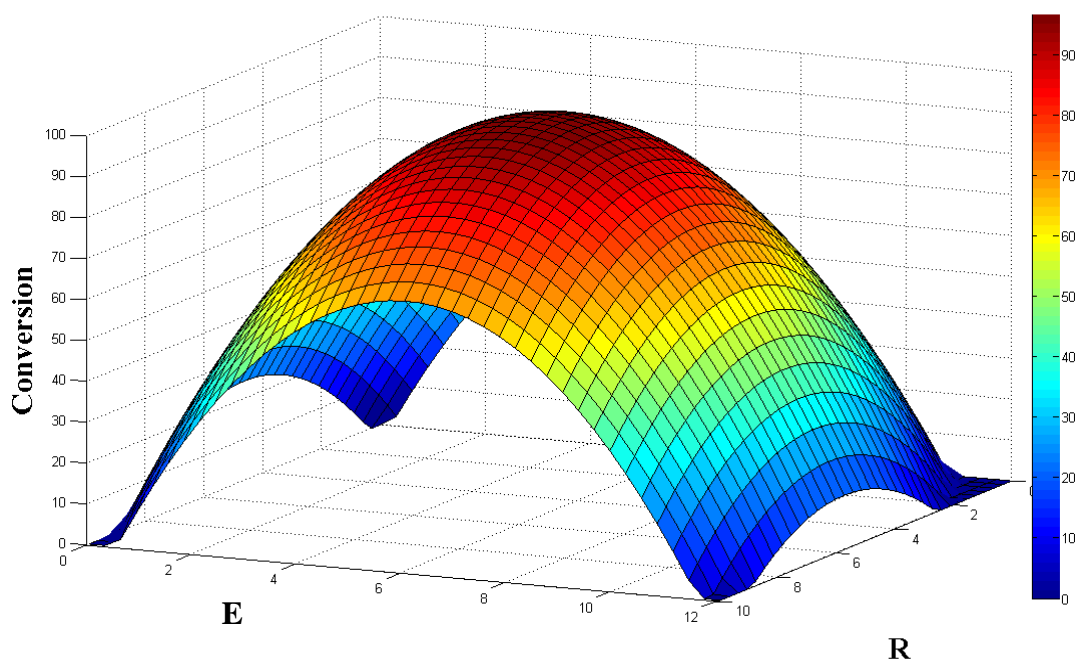


Figure 8 : Response surface for experimental designs of 2 variables of esterification with ethanol.

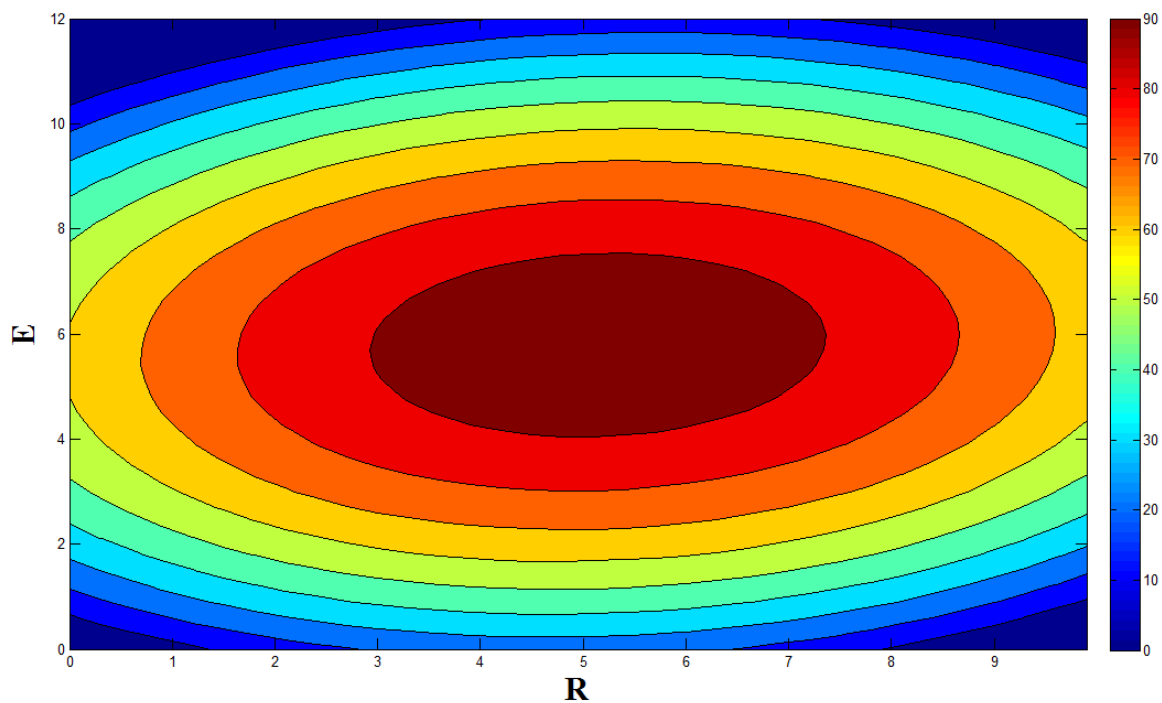


Figure 9 : Contour plot for experimental designs of 2 variables of esterification with ethanol.

Study of the Temperature influence on the reaction

The influence of the temperature on the reaction was presented in Figure 10. As can be seen, the conversion increases monotonously with increasing temperature when ethanol is used for the range of values studied. For methanol the conversion increases up to approximately 50 °C and decreases with increasing temperature for higher temperatures. This behavior can be explained by the fact that methanol is more adverse to the enzyme than ethanol. So, for higher temperatures, the enzyme is deactivated by methanol leading to lower conversions.

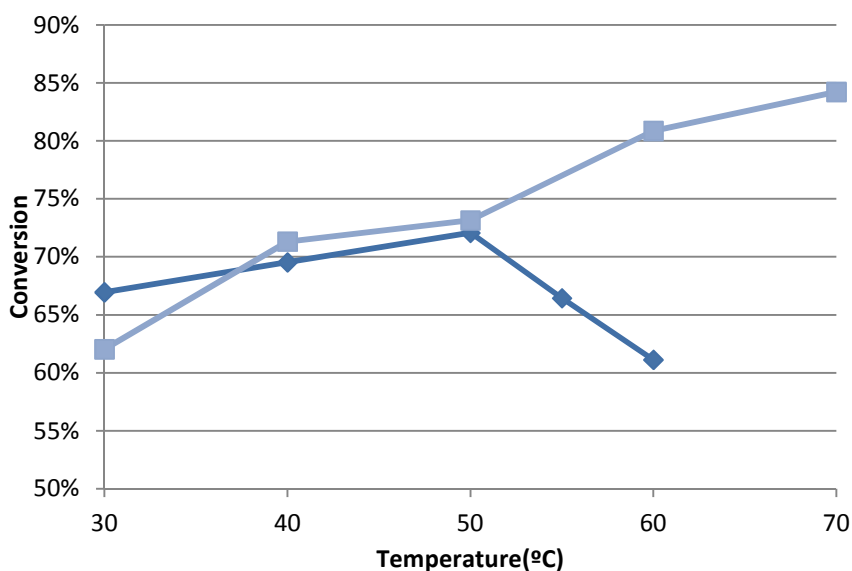


Figure 10: Influence of the temperature on the reaction using (—) methanol or (—) ethanol. Reaction Conditions: 2% Novozym435, R= 6, 150 rpm.

Study of pressure effect

Esterification reaction was carried in a stainless-steel cell in which the pressure is varied, keeping all other parameters constants. A high pressure cell made in stainless steel was especially developed for the effect. The reaction occurs inside the cell that was carried on an incubator with orbital stirring at 40°C, 150 rpm for 3 hours. Molar ratio methanol/oleic acid were 10 and 3% of enzyme percentage. The pressure is induced by

injecting nitrogen directly into the cell, through a flexible high pressure capillary connected to a gas line. The pressure is measured by a Setra pressure transducer, previously calibrated, that managed to the gas line and with accuracy better than 0.5%. Figure 11 shows esterification yield conversion in function of pressure and respectively standard deviation. Each point was obtained by the medium of two experimental tests.

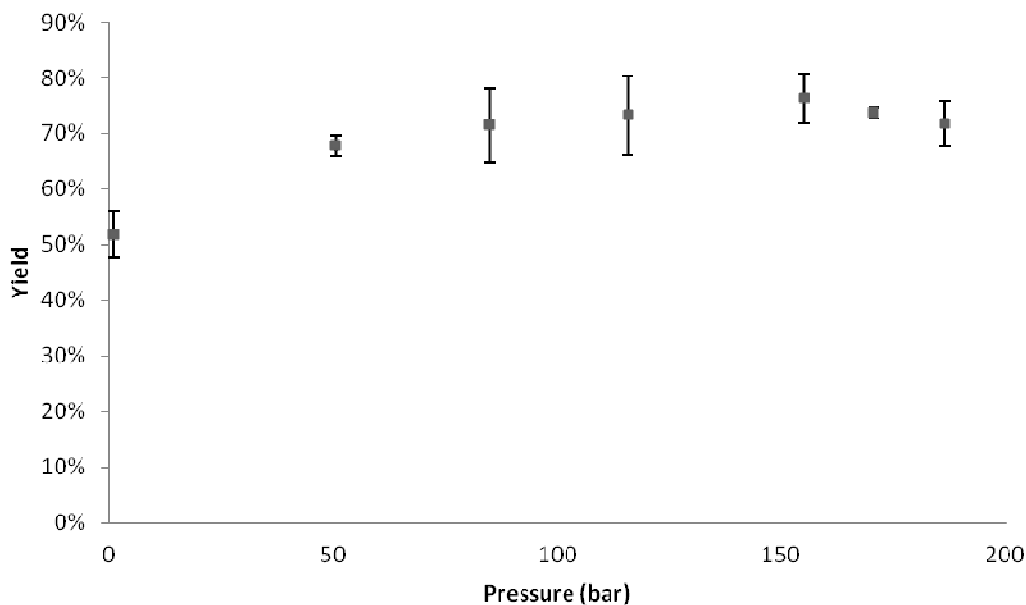


Figure 11: Esterification yield conversion in function of pressure and respectively standard deviation.

Esterification reaction of oleic acid catalyzed by Novozym 435 is benefited by being carried out at a pressure of between 90 and 150 bar. Pressure around 90 bars allows an increase in 38% in the yield of esterification reaction.

Study of the Reusability of the immobilized enzyme

The results obtained for the study of the reusability of the enzyme are shown in Figure 13. Can be verified that, in the case of enzymatic esterification of oleic acid with ethanol, doesn't occur a significant loss of enzyme activity after ten cycles. In the case of methanol there is a significant decrease in conversion caused by a decrease in enzyme activity as a consequence of the deleterious effect of methanol.

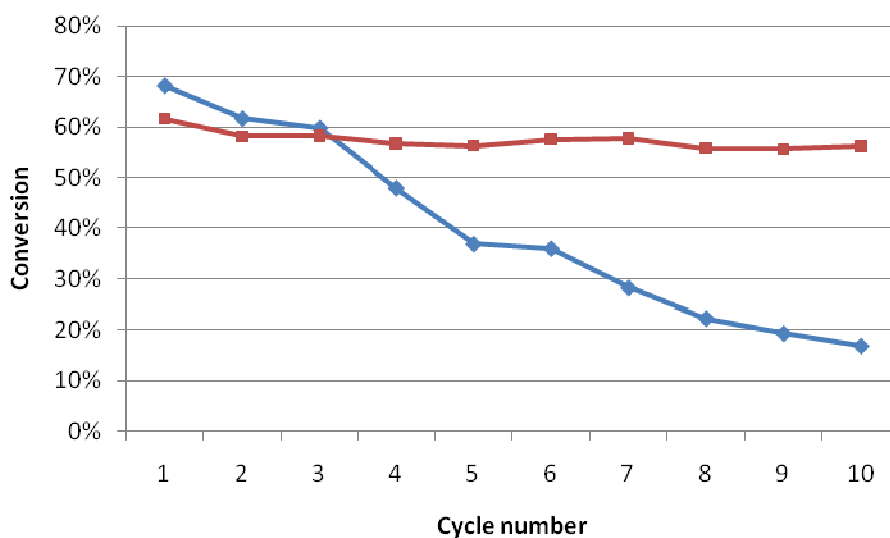


Figure 13: Study of immobilized enzyme reuse using (—) methanol or (—) ethanol.

Reaction Conditions: 2% Novozym435, R=6, 40°C, 150 rpm.

CONCLUSIONS

In the enzymatic esterification of oleic acid with methanol the most significant variable is the methanol/oleic acid molar ratio, but when the methanol is replaced by ethanol it is observed that the variable most significant is the enzyme concentration.

The interaction molar ratio-enzyme concentration is much more significant on the enzymatic esterification with methanol than with ethanol.

According to the second order mathematical equations the conditions with the maximum conversion were R=6.32 and E=6.64% for methanol (>100% of conversion), and R=4.87 and E=5.65% for ethanol (93.4% of conversion). The experimental values were 95.5% and 100% for methanol and ethanol, respectively. For methanolysis reaction with 4% of enzyme and 4 for ratio it's enough conditions to obtain 100% yield.

The conversion increases with increasing temperature when ethanol is used for the range of values studied. For methanol the conversion increases up to approximately 50°C and decreases with increasing temperature for upper values.

Esterification reaction of oleic acid catalyzed by Novozym 435 is benefited by being carried out at a pressure of between 90 and 150 bar of nitrogen, which pressure is obtained a yield 38% higher.

The same enzyme can be used 10 times in the enzymatic esterification of oleic acid with ethanol without significant loss of enzymatic activity by washing the immobilized enzymes resin with distilled hexane at the end of each test.

It was verified by the study of temperature influence, by the fact that the molar ratio between the alcohol and oleic acid is the variable with higher significance on esterification with methanol, contrary to esterification with ethanol, and in the study of enzyme reuse, that methanol is more deleterious to the enzyme than ethanol.

ACKNOWLEDGMENTS

Maria Jorge Pratas acknowledges the financial support from Fundação para a Ciência e a Tecnologia through her Ph.D. grant (SFRH/BD/28258/2006). The authors acknowledge Ricardo Gomes and Rui Queirós for experimental collaboration.

LITERATURE CITED

1. Dale, B., Biofuels: Thinking clearly about the issues. *Journal of Agricultural and Food Chemistry* **2008**, *56* (11), 3885-3891.
2. Kulkarni, M. G.; Dalai, A. K., Waste cooking oil-an economical source for biodiesel: A review. *Industrial & Engineering Chemistry Research* **2006**, *45* (9), 2901-2913.
3. Barnwal, B. K.; Sharma, M. P., Prospects of biodiesel production from vegetables oils in India. *Renewable & Sustainable Energy Reviews* **2005**, *9* (4), 363-378.
4. Sharma, Y. C.; Singh, B.; Upadhyay, S. N., Advancements in development and characterization of biodiesel: A review. *Fuel* **2008**, *87* (12), 2355-2373.
5. Sivaprakasam, S.; Saravanan, C. G., Optimization of the transesterification process for biodiesel production and use of biodiesel in a compression ignition engine. *Energ Fuel* **2007**, *21* (5), 2998-3003.

6. A.P. de A. Vieira, M. A. P. d. S., M.A.P. Langone, Biodiesel Production Via Esterification Reactions catalyzed by lipase. *Latin American Applied Research* **2006**, *36*, 283-288.
7. Pratas, M. J.; Freitas, S.; Oliveira, M. B.; Monteiro, S. C.; Lima, A. S.; Coutinho, J. A. P., Densities and Viscosities of Fatty Acid Methyl and Ethyl Esters. *J Chem Eng Data* **2010**, *55* (9), 3983-3990.
8. Pratas, M. J.; Freitas, S.; Oliveira, M. B.; Monteiro, S. C.; Lima, A. S.; Coutinho, J. A. P., Densities and Viscosities of Minority Fatty Acid Methyl and Ethyl Esters Present in Biodiesel. *J Chem Eng Data* **2011**, *56* (5), 2175-2180.
9. Shaw, J. F.; Chang, S. W.; Lin, S. C.; Wu, T. T.; Ju, H. Y.; Akoh, C. C.; Chang, R. H.; Shieh, C. J., Continuous enzymatic synthesis of biodiesel with Novozym 435. *Energ Fuel* **2008**, *22* (2), 840-844.
10. Knothe, G.; Gerpen, J. V.; Krahl, J., *The Biodiesel Handbook*. AOCS Press, Champaign, Illinois: **2005**.
11. Aranda Moraes, M. S.; Krause, L. C.; da Cunha, M. E.; Faccini, C. S.; de Menezes, E. W.; Veses, R. C.; Alves Rodrigues, M. R.; Caramao, E. B., Tallow biodiesel: Properties evaluation and consumption tests in a diesel engine. *Energ Fuel* **2008**, *22* (3), 1949-1954.
12. Marchetti, J. M.; Miguel, V. U.; Errazu, A. F., Possible methods for biodiesel production. *Renewable & Sustainable Energy Reviews* **2007**, *11* (6), 1300-1311.
13. Nielsen, P. M.; Brask, J.; Fjerbaek, L., Enzymatic biodiesel production: Technical and economical considerations. *European Journal of Lipid Science and Technology* **2008**, *110* (8), 692-700.
14. Rodrigues, R. C.; Volpato, G.; Wada, K.; Zachia Ayub, M. A., Enzymatic synthesis of biodiesel from transesterification reactions of vegetable oils and short chain alcohols. *Journal of the American Oil Chemists Society* **2008**, *85* (10), 925-930.
15. Fjerbaek, L.; Christensen, K. V.; Norddahl, B., A Review of the Current State of Biodiesel Production Using Enzymatic Transesterification. *Biotechnology and Bioengineering* **2009**, *102* (5), 1298-1315.
16. Talukder, M. M. R.; Wu, J. C.; Lau, S. K.; Cui, L. C.; Shimin, G.; Lim, A., Comparison of Novozym 435 and Amberlyst 15 as Heterogeneous Catalyst for

- Production of Biodiesel from Palm Fatty Acid Distillate. *Energ Fuel* **2009**, *23* (1), 1-4.
17. Freire, C. S. R.; Silvestre, A. J. D.; Neto, C. P., Identification of new hydroxy fatty acids and ferulic acid esters in the wood of *Eucalyptus globulus*. *Holzforschung* **2002**, *56* (2), 143-149.
 18. Du, W.; Xu, Y. Y.; Zeng, J.; Liu, D. H., Novozym 435-catalysed transesterification of crude soya bean oils for biodiesel production in a solvent-free medium. *Biotechnol Appl Biochem* **2004**, *40*, 187 - 190.
 19. Chang, H. M.; Liao, H. F.; Lee, C. C.; Shieh, C. J., Optimized synthesis of lipase-catalyzed biodiesel by Novozym 435. *Journal of Chemical Technology and Biotechnology* **2005**, *80* (3), 307-312.
 20. Bouaid, A.; Martinez, M.; Aracil, J., A comparative study of the production of ethyl esters from vegetable oils as a biodiesel fuel optimization by factorial design. *Chemical Engineering Journal* **2007**, *134* (1-3), 93-99.
 21. Akgun, N.; Iscan, E., Effects of process variables for biodiesel production by transesterification. *European Journal of Lipid Science and Technology* **2007**, *109* (5), 486-492.
 22. Rodrigues, M. I. I., António Francisco, *Planejamento de Experimentos e Otimização de processos*. Campinas, **2005**; p 326.
 23. Watanabe, Y.; Shimada, Y.; Sugihara, A.; Noda, H.; Fukuda, H.; Tominaga, Y., Continuous production of biodiesel fuel from vegetable oil using immobilized *Candida antarctica* lipase. *Journal of the American Oil Chemists' Society* **2000**, *77* (4), 355-360.

General Conclusions

First section presents the biodiesel properties which were measured and modelled on this thesis.

Density and Viscosity of biodiesel and its pure components have now new reliable data in a wide range of temperature, as well as in a range of pressure for the density.

New experimental data of density and viscosity of pure saturated and unsaturated methyl and ethyl esters and biodiesel of different raw material in a temperature range of 273K to 363K and atmospheric pressure are presented. Here were studied 15 methyl esters which 6 are unsaturated compounds (with 2 polyunsaturated) and 10 ethyl esters which 3 are unsaturated, as well as 8 different biodiesel samples, fatty acid methyl esters, produced in our laboratory.

An extensive critical review of the data available for these systems was carried out to identify spurious or poor quality data among the often conflicting data previously found in the literature. For biodiesel fuels the lack of information about its composition limited the utility of most data available in the open literature.

The performance of predictive models for these properties was evaluated. GC-VOL model was tested for density as its group contribution methods, it can predict the property directly from their structure. GC-VOL model shows to be able to predict density of pure methyl and ethyl esters with deviations lower than 1% for saturated esters and 2% for unsaturated. In order to improve predictive ability of GC-VOL model to this type of compounds, new coefficients were proposed. Thus deviations of density of pure esters were reduced to 0.25% and for biodiesel to 0.37%.

Group contribution models were evaluated in prediction of pure esters viscosity. Ceriani & Meirelles model provide a fair description of viscosity of fatty acid esters with a global average deviation of 8.8% while Marrero & Gani model presents an average deviation of 20.9% for overall pure esters.

Several models were tested in biodiesel viscosity evaluation. Yuan, Ceriani & Meirelles and Krisnangkura models present average deviation of 5.34%, 8.07% and 7.25%, respectively. A revised Yuan's model was proposed which provides the best description of experimental data with an average deviation of 4.65%.

Density at pressures up to 45 MPa was also measured for 3 pure methyl esters and 8 biodiesels fuels. High pressure experimental data were successfully predicted with the CPA EoS, with a maximum deviation of 2.5%.

To understand the biodiesel cold flow performances data on the phase equilibria of biodiesel below the CP were measured. The UNIQUAC predictive model is shown to be capable of providing an adequate representation of the phase equilibria for these systems below their cloud point.

A large number of properties depend on the esters profile of biodiesel, such as density, viscosity, iodine index, and CFPP. The objective of this study is to evaluate the properties of biodiesel oils obtained from different raw materials. Biodiesels made from feedstock containing higher concentrations of high-melting point saturated long-chain fatty acids tends to have poor cold flow properties. Biodiesel made from raw material with higher concentrations of unsaturated long-chain fatty acids presents low resistance to oxidation as expressed by a high iodine value.

Water solubility data on biodiesels were measured and modelled. The good results obtained for water + fatty acid mixtures, for the mutual solubilities of water + ester binary system, and for the solubility of water in biodiesel encourage the application of the CPA EoS for the design of extraction units for fatty acid an biodiesel production.

In second section the study of enzymatic esterification of oleic acid catalyzed by Novozym 435 was presented. Different results were obtained for reaction with methanol or with ethanol. For the first alcohol, less quantity of enzyme and also less excess of alcohol are necessary to achieve 100% yield. Esterification reaction is benefited being carried out under pressure, obtained a yield 38% higher with just 90 bar.

Ideas to the future

In consequence of environmental, economical and also political turmoil, caused by the excessive use and dependency of conventional petroleum based fuels the attention of several countries has been addressed towards the development of alternative fuels from renewable resources.^{1,2}

The world has got so accustomed to using petrofuels that we never realized that they came with an expiry date. Who can imagine a world without planes, cars and trains? Many scientists have started researching alternatives to the fuels that we use. These alternatives need to be lasting and renewable in nature. Initial attempts at replacing fuels with electricity to run cars have proved successful. However, the performance of these cars does not match that of the conventional petrol or diesel-run engines. So it becomes necessary to replace existing fuels and biodiesel appears as an alternative.

After examining the pros and cons of biofuels, we may be left wondering if they are really worthwhile and right for us. On one hand biofuels could potentially reduce carbon emissions and can help save cash too; but on the other hand biofuels can negatively affect the habitat of many species and aren't necessarily energy efficient at the production stage.

With the increase in global human population, more land may be needed to produce food for human consumption (indirectly via animal feed). The problem already exists in Asia. Vegetal oil prices are relatively higher there. The same trend will eventually happen in the rest of the world. This is the potential challenge to biodiesel. From this point of view, biodiesel can be used most effectively as a supplement to other energy forms, not as a primary source. Biodiesel is particularly useful in mining and marine situations where lower pollution levels are important.

Perhaps the biggest hope for biofuels is that the arrival of second and third generation alternatives should lead to more efficient production and diversify the plants as well as plant wastes used – therefore limiting the effects to any particular habitat. Biofuels are very much a work in progress.

The studies on biofuels are important but even if fossil diesel will not be completely substitute by biofuels, it can reduce our dependence from those kind of non renewable source of energy.

Even though future discoveries and inventions in renewable energy might be surprising, it is nonetheless important for us to start learning how to consume energy more sensibly.

Bibliography

1. *World Energy Outlook 2010*. International Energy Agency, **2010**.
2. *Europe in Figures 2011*. Eurostat, European Union: Luxembourg, **2011**.
3. Prof. P. Capros, D. L. M., N. Tasios, A. De Vita, N. Kouvaritakis, *EU energy trends to 2030*. Publications Office of the European Union: Luxembourg, **2010**.
4. Knothe, G.; Gerpen, J. V.; Krahl, J., *The Biodiesel Handbook*. AOCS Press, Champaign, Illinois: **2005**.
5. *Europe in Figures 2010*. Eurostat, European Union: Luxembourg, **2010**.
6. Malca, J.; Freire, F., Life-cycle studies of biodiesel in Europe: A review addressing the variability of results and modeling issues. *Renew Sust Energ Rev* **2011**, *15* (1), 338-351.
7. Acciona-Energia Ciclo del biodiesel http://www.accion-energia.es/areas_actividad/biodiesel/biodiesel.aspx?id=4.
8. Demirbas, M. F.; Balat, M., Recent advances on the production and utilization trends of bio-fuels: A global perspective. *Energy Conversion and Management* **2006**, *47* (15-16), 2371-2381.
9. Demirbas, A., Political, economic and environmental impacts of biofuels: A review. *Appl. Energy* **2009**, *86*, S108-S117.
10. Demirbas, A., *Biodiesel: A Realistic Fuel Alternative for Diesel Engines*. Springer-Verlag London Limited: Turkey, **2008**.
11. Pinzi, S.; Garcia, I. L.; Lopez-Gimenez, F. J.; de Castro, M. D. L.; Dorado, G.; Dorado, M. P., The Ideal Vegetable Oil-based Biodiesel Composition: A Review of Social, Economical and Technical Implications. *Energ Fuel* **2009**, *23*, 2325-2341.
12. Fukuda, H.; Kondo, A.; Noda, H., Biodiesel fuel production by transesterification of oils. *Journal of Bioscience and Bioengineering* **2001**, *92* (5), 405-416.
13. Karaosmanoglu, F., Vegetable oil fuels: A review. *Energy Sources* **1999**, *21* (3), 221-231.

14. Ashok Pandey, *Handbook of Plant-based Biofuels*. CRC Press Taylor & Francis Group: **2009**.
15. Knothe, G., Biodiesel Derived from a Model Oil Enriched in Palmitoleic Acid, Macadamia Nut Oil. *Energ Fuel* **2010**, *24*, 2098-2103.
16. Anand, K.; Ranjan, A.; Mehta, P. S., Estimating the Viscosity of Vegetable Oil and Biodiesel Fuels. *Energ Fuel* **2010**, *24*, 664-672.
17. Demirbas, A., New Biorenewable Fuels from Vegetable Oils. *Energy Sources Part a-Recovery Utilization and Environmental Effects* **2010**, *32* (7), 628-636.
18. Kerschbaum, S.; Rinke, G., Measurement of the temperature dependent viscosity of biodiesel fuels. *Fuel* **2004**, *83* (3), 287-291.
19. Sharma, Y. C.; Singh, B.; Upadhyay, S. N., Advancements in development and characterization of biodiesel: A review. *Fuel* **2008**, *87* (12), 2355-2373.
20. Hoekman, S. K.; Broch, A.; Robbins, C.; Cenicerros, E.; Natarajan, M., Review of biodiesel composition, properties, and specifications. *Renewable & Sustainable Energy Reviews* **2012**, *16* (1), 143-169.
21. Environmental Protection Agency, *Comprehensive Analysis of Biodiesel Impacts on Exhaust Emissions*. <http://www.epa.gov>, 2002.
22. Pinto, A. C.; Guarieiro, L. L. N.; Rezende, M. J. C.; Ribeiro, N. M.; Torres, E. A.; Lopes, W. A.; Pereira, P. A. D.; de Andrade, J. B., Biodiesel: An overview. *J Braz Chem Soc* **2005**, *16* (6B), 1313-1330.
23. Ma, F. R.; Hanna, M. A., Biodiesel production: a review. *Biores Tech* **1999**, *70* (1), 1-15.
24. Lotero, E.; Liu, Y. J.; Lopez, D. E.; Suwannakarn, K.; Bruce, D. A.; Goodwin, J. G., Synthesis of biodiesel via acid catalysis. *Ind Eng Chem Res* **2005**, *44* (14), 5353-5363.
25. Leung, D. Y. C.; Wu, X.; Leung, M. K. H., A review on biodiesel production using catalyzed transesterification. *Appl. Energy* **2010**, *87* (4), 1083-1095.
26. Saka, S.; Kusdiana, D., Biodiesel fuel from rapeseed oil as prepared in supercritical methanol. *Fuel* **2001**, *80* (2), 225-231.
27. Demirbas, A., Biodiesel Production via Rapid Transesterification. *Energy Sources* **2008**, *30*, 1830-1834.
28. Moser, B. R., Biodiesel production, properties, and feedstocks. *In Vitro Cell Dev Bio: Plant* **2009**, *45* (3), 229-266.

29. Kleinova, A.; Paligova, J.; Vrbova, M.; Mikulec, J.; Cvengros, J., Cold flow properties of fatty esters. *Process Saf Environ* **2007**, *85* (B5), 390-395.
30. Foglia, T. A.; Nelson, L. A.; Dunn, R. O.; Marmer, W. N., Low-temperature properties of alkyl esters of tallow and grease. *JAACS* **1997**, *74* (8), 951-955.
31. Cheirsilp, B.; H-Kittikun, A.; Limkatanyu, S., Impact of transesterification mechanisms on the kinetic modeling of biodiesel production by immobilized lipase. *Biochem Eng J* **2008**, *42* (3), 261-269.
32. Dennis, B. H.; Jin, W.; Cho, J.; Timmons, R. B., Inverse determination of kinetic rate constants for transesterification of vegetable oils. *Inverse Problems in Science and Engineering* **2008**, *16* (6), 693 - 704.
33. Haas, M. J.; McAloon, A. J.; Yee, W. C.; Foglia, T. A., A process model to estimate biodiesel production costs. *Bioresource Technology* **2006**, *97* (4), 671-678.
34. Oliveira, M. B.; Teles, A. R. R.; Queimada, A. J.; Coutinho, J. A. P., Phase equilibria of glycerol containing systems and their description with the Cubic-Plus-Association (CPA) Equation of State. *Fluid Phase Equilib* **2009**, *280* (1-2), 22-29.
35. Knothe, G., "Designer" biodiesel: Optimizing fatty ester (composition to improve fuel properties. *Energ Fuel* **2008**, *22* (2), 1358-1364.
36. Blangino, E.; Riveros, A. F.; Romano, S. D., Numerical expressions for viscosity, surface tension and density of biodiesel: analysis and experimental validation. *Phys. Chem. Liq.* **2008**, *46* (5), 527 - 547.
37. European Standard EN 14214, 2003. Automotive fuels - Fatty acid methyl esters (FAME) for diesel engines - Requirements and test methods. CEN – European Committee for Standardization, Brussels, Belgium. Available from: <http://www.din.de>.
38. ASTM, D6751 - 09 Standard Specification for Biodiesel Fuel Blend Stock (B100) for Middle Distillate Fuels. 2009.
39. Knothe, G., Dependence of biodiesel fuel properties on the structure of fatty acid alkyl esters. *Fuel Process. Technol.* **2005**, *86* (10), 1059-1070.
40. Ramos, M. J.; Fernandez, C. M.; Casas, A.; Rodriguez, L.; Perez, A., Influence of fatty acid composition of raw materials on biodiesel properties. *Bioresource Technology* **2009**, *100* (1), 261-268.
41. Knothe, G., Improving biodiesel fuel properties by modifying fatty ester composition. *Energy & Environmental Science* **2009**, *2* (7), 759-766.

42. Dzida, M.; Prusakiewicz, P., The effect of temperature and pressure on the physicochemical properties of petroleum diesel oil and biodiesel fuel. *Fuel* **2008**, *87* (10-11), 1941-1948.
43. Boudy, F.; Seers, P., Impact of physical properties of biodiesel on the injection process in a common-rail direct injection system. *Energy Conversion and Management* **2009**, *50* (12), 2905-2912.
44. Baroutian, S.; Aroua, M. K.; Raman, A. A. A.; Sulaiman, N. M. N., Density of palm oil-based methyl ester. *J Chem Eng Data* **2008**, *53* (3), 877-880.
45. Goncalves, C. B.; Ceriani, R.; Rabelo, J.; Maffia, M. C.; Meirelles, A. J. A., Viscosities of Fatty Mixtures: Experimental Data and Prediction. *J Chem Eng Data* **2007**, *52* (5), 2000-2006.
46. Ejim, C. E.; Fleck, B. A.; Amirfazli, A., Analytical study for atomization of biodiesels and their blends in a typical injector: Surface tension and viscosity effects. *Fuel* **2007**, *86* (10-11), 1534-1544.
47. Dunn, R. O.; Bagby, M. O., Low-temperature properties of triglyceride-based diesel fuels - transesterified methyl-esters and petroleum middle distillate/ester blends. *JAOCs* **1995**, *72* (8), 895-904.
48. Elbro, H. S.; Fredenslund, A.; Rasmussen, P., Group Contribution Method for the Prediction of Liquid Densities as a Function of Temperature for Solvents, Oligomers, and Polymers. *Ind Eng Chem Res* **1991**, *30* (12), 2576-2582.
49. Ceriani, R.; Goncalves, C. B.; Coutinho, J. A. P., Prediction of Viscosities of Fatty Compounds and Biodiesel by Group Contribution. *Energ Fuel* **2011**, *25* (8), 3712-3717.
50. Marrero, J.; Gani, R., Group-contribution based estimation of pure component properties. *Fluid Phase Equilib.* **2001**, *183*, 183-208.
51. Conte, E.; Martinho, A.; Matos, H. A.; Gani, R., Combined Group-Contribution and Atom Connectivity Index-Based Methods for Estimation of Surface Tension and Viscosity. *Ind Eng Chem Res* **2008**, *47* (20), 7940-7954.
52. Pratas, M. J.; Freitas, S.; Oliveira, M. B.; Monteiro, S. C.; Lima, A. S.; Coutinho, J. A. P., Densities and Viscosities of Fatty Acid Methyl and Ethyl Esters. *J Chem Eng Data* **2010**, *55* (9), 3983-3990.
53. Pratas, M. J.; Freitas, S.; Oliveira, M. B.; Monteiro, S. C.; Lima, A. S.; Coutinho, J. A. P., Densities and Viscosities of Minority Fatty Acid Methyl and Ethyl Esters Present in Biodiesel. *J Chem Eng Data* **2011**, *56* (5), 2175-2180.
54. Veny, H.; Baroutian, S.; Aroua, M. K.; Hasan, M.; Raman, A. A.; Sulaiman, N. M. N., Density of Jatropha curcas Seed Oil and its Methyl Esters: Measurement and Estimations. *International Journal of Thermophysics* **2009**, *30* (2), 529-541.

55. Yuan, W.; Hansen, A. C.; Zhang, Q., Predicting the temperature dependent viscosity of biodiesel fuels. *Fuel* **2009**, 88 (6), 1120-1126.
56. Tat, M. E.; Van Gerpen, J. H., The specific gravity of biodiesel and its blends with diesel fuel. *JAOCs* **2000**, 77 (2), 115-119.
57. Kay, W. B., Density of hydrocarbon gases and vapors at high temperature and pressure. *Ind Eng Chem* **1936**, 28, 1014-1019.
58. Pratas, M. J.; Freitas, S. V. D.; Oliveira, M. B.; Monteiro, S. C.; Lima, A. S.; Coutinho, J. A. P., Biodiesel Density: Experimental Measurements and Prediction Models. *Energ Fuel* **2011**, 25 (5), 2333-2340.
59. Dymond, J. H.; Malhotra, R., The Tait Equation - 100 Years On. *International Journal of Thermophysics* **1988**, 9 (6), 941-951.
60. Oliveira, M. B.; Ribeiro, V.; Queimada, A. J.; Coutinho, J. A. P., Modeling Phase Equilibria Relevant to Biodiesel Production: A Comparison of g(E) Models, Cubic EoS, EoS-g(E) and Association EoS. *Ind Eng Chem Res* **2011**, 50 (4), 2348-2358.
61. Oliveira, M. B.; Varanda, F. R.; Marrucho, I. M.; Queimada, A. J.; Coutinho, J. A. P., Prediction of water solubility in biodiesel with the CPA equation of state. *Ind Eng Chem Res* **2008**, 47 (12), 4278-4285.
62. Oliveira, M. B.; Miguel, S. I.; Queimada, A. J.; Coutinho, J. A. P., Phase Equilibria of Ester plus Alcohol Systems and Their Description with the Cubic-Plus-Association Equation of State. *Ind Eng Chem Res* **2010**, 49 (7), 3452-3458.
63. Shu, Q.; Yang, B.; Yang, J.; Qing, S., Predicting the viscosity of biodiesel fuels based on the mixture topological index method. *Fuel* **2007**, 86 (12-13), 1849-1854.
64. Ceriani, R.; Goncalves, C. B.; Rabelo, J.; Caruso, M.; Cunha, A. C. C.; Cavaleri, F. W.; Batista, E. A. C.; Meirelles, A. J. A., Group Contribution Model for Predicting Viscosity of Fatty Compounds. *J Chem Eng Data* **2007**, 52 (3), 965-972.
65. Krisnangkura, K.; Yimsuwan, T.; Pairintra, R., An empirical approach in predicting biodiesel viscosity at various temperatures. *Fuel* **2006**, 85 (1), 107-113.

Appendix A



SPECIFICATION FOR BIODIESEL (B100) – ASTM D6751-09

Nov. 2008

Biodiesel is defined as the mono alkyl esters of long chain fatty acids derived from vegetable oils or animal fats, for use in compression-ignition (diesel) engines. This specification is for pure (100%) biodiesel prior to use or blending with diesel fuel. #

Property	ASTM Method	Limits	Units
Calcium & Magnesium, combined	EN 14538	5 maximum	ppm (ug/g)
Flash Point (closed cup)	D 93	93 minimum	degrees C
Alcohol Control (One of the following must be met)			
1. Methanol Content	EN14110	0.2 maximum	% mass
2. Flash Point	D93	130 minimum	Degrees C
Water & Sediment	D 2709	0.05 maximum	% vol.
Kinematic Viscosity, 40 C	D 445	1.9 - 6.0	mm ² /sec.
Sulfated Ash	D 874	0.02 maximum	% mass
Sulfur			
\$ 15 Grade	D 5453	0.0015 max. (15)	% mass (ppm)
\$ 500 Grade	D 5453	0.05 max. (500)	% mass (ppm)
Copper Strip Corrosion	D 130	No. 3 maximum	
Cetane	D 613	47 minimum	
Cloud Point	D 2500	report	degrees C
Carbon Residue 100% sample	D 4530*	0.05 maximum	% mass
Acid Number	D 664	0.50 maximum	mg KOH/g
Free Glycerin	D 6584	0.020 maximum	% mass
Total Glycerin	D 6584	0.240 maximum	% mass
Phosphorus Content	D 4951	0.001 maximum	% mass
Distillation, T90 AET	D 1160	360 maximum	degrees C
Sodium/Potassium, combined	EN 14538	5 maximum	ppm
Oxidation Stability	EN 14112	3 minimum	hours
Cold Soak Filtration	Annex to D6751	360 maximum	seconds
For use in temperatures below -12 C	Annex to D6751	200 maximum	seconds

BOLD = 8Q-9000 Critical Specification Testing Once Production Process Under Control

* The carbon residue shall be run on the 100% sample.

A considerable amount of experience exists in the US with a 20% blend of biodiesel with 80% diesel fuel (B20). Although biodiesel (B100) can be used, blends of over 20% biodiesel with diesel fuel should be evaluated on a case-by-case basis until further experience is available.

